Universität Bremen

z m t bremen

The Northern Humboldt Current Ecosystem and its resource dynamics: Insights from a trophic modeling and time series analysis

Doctoral thesis

by

Marc Hollis Taylor

Submitted to Faculty 2 (Biology & Chemistry),

Bremen University

in partial fulfillment of the requirements for the degree of

Doctor rerum naturalium (Doctor of Natural Sciences)

March 2008, Bremen

Advisory Committee:

1. Reviewer: Prof Dr. Matthias Wolff (Center for Tropical Marine Ecology (ZMT), Bremen, Germany)

2. Reviewer: Dr. habil. Thomas Brey (Alfred Wegener Institute for Polar and Marine Research (AWI), Bremerhaven, Germany)

1. Examiner: Prof. Dr. Wolf Arntz (Alfred Wegener Institute for Polar and Marine Research (AWI), Bremerhaven, Germany)

2. Examiner: Dr. Werner Ekau (Center for Tropical Marine Ecology (ZMT), Bremen, Germany)

Abstract

The Northern Humboldt Current Ecosystem (NHCE) is one of the most productive in the world. Wind-driven coastal upwelling brings cool, nutrient-rich water to the photic zone where rich plankton communities develop. This high productivity supports large populations of small plankton-grazing pelagic fish, which are an important food source for many higher predators and support a large fish meal industry. The NHCE is subject to strong interannual environmental variability from the El Niño Southern Oscillation (ENSO), which has direct and indirect effects on the biotic components of the ecosystem. This complex mixture of environmental, trophic, and human influences calls for a holistic approach for management. This thesis contributes to our understanding of the NHCE by shedding light on the changes in energy flow that occur during strong "El Niño" events (warm phase of ENSO) as well as differentiating between the relative importance of environmental, trophic, and human influences in reproducing historical changes in fisheries resources. Methods included the application of time-series and trophic modeling analyses for two NHCE subsystems of different scale: i) the nearshore benthic ecosystems of Independencia Bay and Sechura Bay (2 models, include the area of <30m depth), and ii) the larger coastal upwelling system (4°-16°S with a 110km extension from the coast). Comparisons of steady-state trophic models between a normal upwelling year (~1995/96) and a strong El Niño year (1997/98) describe the changes in energy flow structure. Longer-term dynamics were explored with multivariate analyses for the scallop species *Argopecten purpuratus*, and with dynamic simulations of the trophic model. Results show that during normal upwelling the NHCE is quite efficient on a large scale, with most energy utilized (3.6% of total flows are exports). The nearshore subsystem is much less efficient (~28% of total flows are exports) due to higher primary production and low oxygen concentrations, preventing efficient utilization by primary consumers. During El Niño, both subsystems show increased overall efficiency due primarily to improved usage of the (reduced) primary production. El Niño appears to negatively affect flows at higher trophic levels most, as observed through statistics of flow organization and development (relative ascendancy, A/C) and cycling of energy (predatory cycling index, PCI). Explorations of dynamics revealed a dominance of bottom-up control among predator-prey interactions. The larger coastal upwelling subsystem showed a higher importance of trophic interactions on dynamics than the nearshore benthic system. Fishing-related changes are also more important in the larger upwelling system, while dynamics appear to be dominated by environmental effects in the nearshore subsystem.

The spatial scale of the models affected the ability to reproduce dynamics, as the larger scale of the coastal upwelling model contained a higher degree of closure of flows. Recommendations are given for improving the models for future explorations of management strategies; including the extension and standardization of historical time-series data for a more robust analysis, and further research on the underlying mechanisms of population dynamics for species showing strong environmental mediation.

Zusammenfassung

Das Ökosystem des nördlichen Humboldtstroms (NHCE) ist eines der produktivsten auf der Erde. Der hauptsächlich vom Wind angetriebene küstennahe Auftrieb bringt kühles, nährstoffreiches Wasser in die euphotische Zone, so dass dort reichhaltige Planktongemeinschaften gedeihen können. Die hohe Primärproduktion ist die Grundlage für riesige Bestände kleiner planktonfressender Fische, die eine wichtige Nahrungsquelle für Räuber höherer Trophiestufen und der Rohstoff einer der weltweit grössten Fischmehlindustrien sind. Das NHCE ist starken interannuellen Umweltschwankungen ausgesetzt, die durch El Niño Southern Oscillation (ENSO) verursacht werden und direkte und indirekte Auswirkungen auf die biotischen Komponenten des Ökosystems haben. Neben ENSO sind trophische Interaktionen und die Fischerei wichtige Einflussgrössen für die teils extremen Bestandsschwankungen der Arten im NHCE. Ein holistischer Ansatz scheint angesichts der hohen Verknüpfungsgrades der einzelnen Einflussgrössen am geeignesten, um die Prozesse im NHCE zu verstehen und Managementempfehlungen ableiten zu können. Diese Arbeit trägt zu unserem Verständnis des NHCE bei, indem sie die Veränderungen im Energiefluss aufzeigt, die während El Niño-Ereignissen (warmen ENSO-Phasen) auftreten sowie zwischen dem relativen Einfluss von Umwelt-, trophischen und anthropogenen Einflüssen bei der Wiedergabe historischer Veränderungen in den Ressourcen unterscheidet. Methodisch wurden Zeitreihenanalyse und trophische Modellierung auf zwei Teilsysteme unterschiedlicher räumlicher Ausdehnung des NHCE verwendet: i) das benthische Flachwassersystem in der Independencia Bucht und in der Sechura Bucht (2 Modelle, beinhaltet das Gebiet oberhalb der Sprungschicht: <30m Wassertiefe) und ii) das grössere, küstennahe Auftriebsgebiet (4°-16°S, bis 110km Entfernung vor der Küste). Vergleiche von trophischen steady-state Modellen zwischen Jahren mit normalem Auftrieb (~1995/96) und einem starken El Niño Jahr (1997/98) beschreiben die strukturellen Veränderungen im Energiefluss. Längerfristige Dynamiken wurden mit multivariater Analyse für die Jakobsmuschel *Argopecten purpuratus* sowie mit dynamischen Simulationen des trophischen Models untersucht. Die Ergebnisse zeigen, dass das NHCE während normalem Auftrieb grossräumig sehr effizient arbeitet. Die meiste Energie wird genutzt und nur 3.6% des gesamten Energieflusses werden exportiert. Aufgrund höherer Primärproduktion kommt es zu niedrigeren Sauerstoffkonzentrationen im benthischen Flachwassersystem, die die effiziente Nutzung der Primärproduktion durch die Primärkonsumenten verhindern; das System ist weniger effizient und ~28% des gesamten

Energieflusses werden exportiert. Während El Niño zeigen beide Teilsysteme Abnahmen im Gesamtfluss, hauptsächlich aufgrund der verringerten Primärproduktion. El Niño scheint den Energiefluss höherer Trophiestufen am stärksten zu beeinflussen. Dies legen statistische Analysen der Organisation und der Entwicklung des Energieflusses (relative ascendancy, A/C) nahe sowie der Anteil des nichtexportierten Detritus, der höheren Trophiestufen zur Verfügung steht (predatory cycling index, PCI). Andererseits ermöglichen die verringerte Primärproduktion und erhöhte Sauerstoffkonzentrationen – im Fall des benthischen Flachwasser-Teilsystems – während El Niño eine effizientere Nutzung der Produktion mit geringeren Exporten und Abflüssen in den Detrituspool. Die Untersuchung der Dynamiken zeigte ein Dominanz der bottom-up Kontrolle zwischen den Räuber-Beute-Beziehungen. Im grösseren küstennahen Auftriebssystem waren trophische Interaktionen von grösserer Bedeutung für die Dynamiken als im benthischen Flachwassersystem. Auch der Einfluss der Fischerei auf Veränderungen war im küstennahen Auftriebssystem grösser als im benthischen Flachwassersystem, wohingegen die Dynamiken im benthischen Flachwassersystem durch Umwelteinflüsse dominiert zu sein schienen. Die räumliche Ausdehnung der Modelle beeinflusste ihre Fähigkeit, Dynamiken zu reproduzieren. So scheint die grössere Skala die Simulation der Dynamiken im Modell des küstennahen Auftriebssystems verbessert zu haben, da sie besser die Spanne möglicher ontogenetischer Bewegungen beinhaltet. Es werden Verbesserungen der existierenden Modelle vorgeschlagen, um in Zukunft realistischere Szenarien für das Management entwerfen zu können. Die Empfehlungen beinhalten die Erweiterung und Standartisierung historischer Zeitreihen, um belastbarere Analysen durchführen zu können, sowie die gezielte Erforschung der Populationsdynamiken von Arten, die besonders stark von Umweltschwankungen beeinflusst werden.

Resumen

El Ecosistema Norte de la Corriente de Humboldt (NHCE) es uno de los más productivos del mundo. La surgencia costera inducida por los vientos predominantes lleva agua fría y rico en nutrients a la zona eutrófica, en las que se desarrollan las comunidades plantónicas. Esta alta productividad sostiene grandes poblaciones de pequeños peces pelágicos planctívoros, que son una fuente importante de alimento para muchos predadores de niveles tróficos superiores y apoyan una gran industria de producción de harina de pescado. El NHCE está sujeto a la fuerte variabilidad ambiental interanual de la El Niño Oscilación del Sur (ENSO), que tiene efectos directos e indirectos sobre los componentes bióticos del ecosistema. Esta mezcla compleja que incluye influencias ambientales, tróficas, y humanas hace necesario un enfoque holístico para el manejo pesquero. Esta tesis contribuye a nuestra comprensión del NHCE elucidando acerca de los cambios en los flujos de la energía que ocurren durante eventos fuertes “EL Niño” (fase calida de ENSO) así como distinguir la importancia relativa de las influencias ambientales, tróficas, y humanas en los cambios históricos en los recursos pesqueros. Los métodos incluyeron análisis de series de tiempo y modelaje trófico en dos subsistemas de NHCE de escalas diferentes: i) los ecosistemas bénticos cercanos a la costa de las bahías de Sechura y Independencia (2 modelos que incluyen el área < 30m de profundidad), y ii) el mayor sistema de surgencia costera (extensión entre 4°-16°S y hasta 110 km desde la costa). Se describen los cambios en estructura del flujo de energía a través de comparaciones de modelos tróficos de estado estable entre un año de surgencia normal (~1995/96) y un año fuerte del “El Niño” (1997/98; la fase caliente de ENSO). La dinámica de largo plazo fue explorada con análisis multivariados para la especie de la concha de abanico Argopecten purpuratus, y con simulaciones dinámicas del modelo trófico. Los resultados demuestran que durante periodos de surgencia normal el NHCE es eficiente en gran escala, con la mayoría de la energía siendo utilizada (3.6% de los flujos totales son exportaciones). La escala más pequeña del sistema cercano a la costa es mucho menos eficiente (~28% de los flujos totales son exportaciones) debido a una producción primaria más alta y a bajas concentraciones de oxígeno, impidiendo la utilización eficiente por los consumidores primarios. El Niño parece afectar más negativamente los flujos en niveles tróficos superiores, según lo observado a través de estadístico de la organización y desarrollo de flujos del sistema (ascendencia relativa, A/C) y el ciclaje de energía (índice de ciclaje por predadores, PCI). La exploración de dinámicas mostró un dominio del control bottom-up en las interacciones predador-presa.

El sistema mayor de surgencia costero muestrá una mayor importancia de las interacciones tróficas que las dinámicas en el sistema béntico cercano a la costa. El efecto de la pesquería también es importante en el sistema de surgencia mayor, mientras que la dinámica ambiental parece dominar el subsistema cercano a la costa. La escala espacial de los modelos afectó la capacidad de reproducir las dinámicas, ya que el modelo de surgencia costera de escala mayor contuvo un mayor grado de cierre de flujos. Se dan recomendaciones para el mejoramiento de los modelos para futuras exploraciónes de estrategias de manejo, incluyendo la extensión y la estandardización de los datos históricos de series de tiempo para análisis más robustos, y mas investigación sobre los mecanismos subyacentes de la dinámica poblaciones que tienen demuestran un fuerte control ambiental.

Contents

List of Tables

List of Figures

List of Collaborators (in alphabetical order)

● Center for Tropical Marine Ecology (ZMT)
Fahrenheitstrasse 6
28359 Bremen, Germany

· MSc. Flora Vadas (fl_va@uni-bremen.de)
· Prof. Dr. Matthias Wolff (matthias.wolff@zmt-bremen.de)

● Institute of Research for Development (IRD)
UR097, CRHMT, Avenue Jean Monnet
34203 Sete, France

· MSc. R. Michael Ballón (michballon@googlemail.com)

● Instituto del Mar del Peru (IMARPE)
Esq. Gamarra y Valle s/n, Apartado 22
Callao, Peru

· Patricia Ayón (payon@imarpe.gob.pe)
· Juan Argüelles (jarguelles@imarpe.gob.pe)
· Verónica Blaskovic (vblasko@imarpe.gob.pe)
· Erich Díaz (ediaz@imarpe.gob.pe)
· MSc. (c) Pepe Espinoza (pespinoza@imarpe.gob.pe)
· Elisa Goya (egoya@imarpe.gob.pe)
· Dr. Dimitri Gutiérrez (dgutierrez@imarpe.gob.pe)
· Dr. Sara Purca (spurca@imarpe.gob.pe)
· Dr. Jorge Tam (jtam@imarpe.gob.pe)
· MSc (c) Luis Quipuzcoa (lquipuzcoa@imarpe.gob.pe)
· Dr. Claudia Wosnitza-Mendo (claudiawosnitza@yahoo.de)
· Dr. Carmen Yamashiro (cyamashiro@imarpe.gob.pe)

● **Universidad Agraria La Molina (UNALM)**
Facultad de Pesqueria
Apto. 456
Lima 100, Peru

· Dr. Jaime Mendo (jmendo@lamolina.edu.pe)

● **Universidad Nacional Mayor de San Marcos (UNMSM)**
Facultad de Ciencias Biologicas
Av. Venezuela, Cdra. 34
Lima 100, Peru

· Noemi Ochoa (aochoal@unmsm.edu.pe)

List of Abbreviations

Abbreviation	Description
(Φ/C)	Relative overhead
A/C	Relative ascendency
B	Biomass
B/T	System biomass/throughput ratio
C	Catch
Chl a	Chlorophyll a
EBCS	Eastern Boundary Current System
EE	Ecotrophic efficiency
EwE	Ecopath with Ecosim
F	Fishing mortality
FCI	Finn's cycling index
GE	Gross efficiency
HCLME	Humboldt Current Large Maribe Ecosystem
LME	Large Marine Ecosystem
M	Natural mortality
M0	Non-predatory mortality
M2	Predatory mortality
MSVPA	Multi-Species Virtual Population Analysis
MTI	Mixed trophic impact
NHCE	Northern Humboldt Current Ecosytem
NOAA	National Oceanic and Atmospheric Administration
P	Production
PP/B	System primary production/biomass ratio
PP/R	System primary production/respiration ratio
PPR	Primary production required to sustain all catches
PPR/catch	Primary production required per unit of catch
Q	Consumption
T	Total system throughput
TE	Transfer efficiency
TL	Trophic level
VPA	Virtual Population Analysis

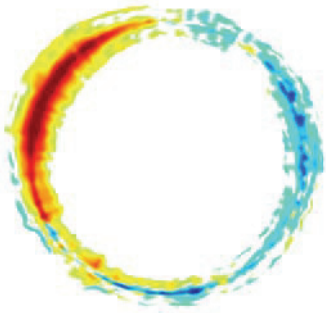

"ENSO circle" by Michael Tippett
(International Research Institute
for Climate and Society)

Preface

This doctoral thesis was supported by the "***CENSOR***" project (**C**limate variability and **E**l **N**iño **S**outhern **O**scillation: implications for natural coastal **r**esources and management), funded within the FP6-INCO Programme of the European Commission.

My hope is that the work presented here will further the case for an ecosystem based approach to fisheries management in Peru. I take away with me a greater understanding of the complexities involved in such work – from the need of integrated research and long-term monitoring, to the value of scientific cooperation and the political hurdles thereof. I wish to thank many people with whom I have had the pleasure to work with during the past three years in Germany and Peru, without which this thesis would not have been realized. Besides those who are mentioned in the acknowledgements at the ends of particular chapters, I wish to thank the following people:

To my doctoral advisor, Matthias Wolff, for his constant support and involvement throughout the thesis. His openness and encouragement to pursue new directions and to expand the scope of the thesis into "rougher waters" has been a great motivation for me. Many thanks for your leadership and continual investment in my development as a scientist. To my field advisor, Jaime Mendo, for being a fantastic working companion and friend, the best guide to Peruvian culture anyone could ask for, and for his passion for the sea and the people who live in constant connection with it. To Claudia Wosnitza-Mendo, who opened doors for me in her home and work, for always making me feel welcome, and for always bringing an open and inquisitive attitude to our work together. To Jorge Tam, for welcoming me into the modeling working group at IMARPE, for his hardworking nature, his investment in our cooperation despite countless other ongoing projects and, of course, his friendship. This work owes so much of its success to you and I am very happy to see that you will continue its development in the future. To Sara Purca, a fantastic collaborator

and friend – thank you for your constant energy. I greatly appreciate your help and guidance in everything from the microscopic world of phytoplankton to the canyons of Peru! To all the other members of CIMOBP, thank you for your assistance and for welcoming into your working group. To my fellow members of WP4, Marie-Caroline Badjeck and Ricardo Chero, for your hard work in the project and as great sources of information on artisanal fisheries in Peru. To Carmen Yamashiro, thank you for your very warm welcome into the Invertebrate biology group of IMARPE, and for opening of so many doors for me. To Juan Argüelles, for his insight into the headache that is the jumbo squid. To him and his wife, Charo, thank you for your friendship and hospitality in Lima. To Gonzalo Olivares, for his friendship and many insights into the Humboldt Current and its oceanography. To Cyril Piou, for his friendship and for allowing me to constantly bounce ideas off him on all subjects thoughout our studies together at the ZMT. To Uwe Krumme for his very helpful and constructive input as well as help with translation of the abstract into German. To Rubén Lara and Jorge Paramo, for their help with translation of the abstract into Spanish. To all of my fellow doctoral students at the ZMT, who have been great sources of support and comradship throughout the past three years. To my parents, for their constant love and support. Finally, to Bettina, for always being a loving partner and confidant. You have kept me happy and healthy, been my fellow explorer in Peru, and helped me "step off" when I needed it.

Chapter I. Overview

Background and scope of thesis

This thesis is comprised by a collection of papers focusing on the functioning of the Northern Humboldt Current Ecosystem (NHCE) and its subsystems. These works attempt to contribute to bridging the gap between our relatively rich knowledge of the physical drivers of environmental variability and their lesser understood consequences to the biological components of the ecosystem.

The Northern Humboldt Current Ecosystem has long been of interest to marine scientists due to its incredible productivity and contribution to world fish catches. Spatially, it includes the northernmost of two main upwelling centers of the Humboldt Current Large Marine Ecosystem, and spans the length of Peru to northern Chile (Fig. I.1). It is by far the most productive of the Eastern Boundary Current Systems (EBCSs) in terms of fish production, mainly due to the landings of the Peruvian anchovy *Engraulis ringens*. Its location near the equator allows for strong upwelling under relatively moderate wind forcing, which occurs throughout the year. Under periods of decreased wind forcing, offshore waters can intrude into the coastal zone due to underlying geostrophic flows directed onshore (Fig. I.1).

EBCSs appear to possess strong trophic links between the components of the ecosystem, making them interesting subjects of trophic flows analyses. One hypothesis is that intense plankton grazing by small pelagic fish ("small pelagics") may exert a major control on trophic dynamics in upwelling systems by funneling energy through mid-trophic levels (referred to as "wasp-waist") (Cury et al., 2000). For example, decreases in anchovy biomass during the mid-1970's to early 1990's has been correlated to lower concentrations of zooplankton prey and subsequent crashes of top-predator populations e.g. seabirds and pinnipeds. The impact of the fishing is also considered to be higher than in other EBCSs due to a strong targeting of lower trophic levels (Moloney et al., 2005) and extreme overcapacitation of fleets, which prevents rapid adaptability to changing conditions and, therefore, long-term sustainability (Fréon, 2006).

These strong trophic connections call for a more holistic approach to managing the resources of the ecosystem. While a large undertaking in itself, the task is further complicated in the NHCE by extremely high interannual environmental variability as affected by the El Niño Southern Oscillation (ENSO). Deciphering some of these

environmental influences on key resource dynamics is a major focus of the project "***CENSOR***" (**C**limate variability and **E**l **N**iño **S**outhern **O**scillation: implications for natural coastal **r**esources and management). In particular, my collaborators and I have employed both time series analysis and trophodynamics models to historical changes of catch and biomass data in order to distinguish between trophic, human (i.e. fishing), and environmental influences on ecosystem dynamics. Our hope is that these results will serve future explorations of resource management; ultimately improving the sustainability of the fisheries and reducing stakeholder vulnerability to environmental variability.

ENSO and its impacts

The El Niño Southern Oscillation (ENSO) affects the ocean-atmosphere system in the tropical Pacific, having important consequences for weather around the globe (NOAA, 2008). Under "normal", non-El Niño conditions, equatorial trade winds blow towards the west across the tropical Pacific, building up warm surface water in the west, so that the sea surface is about 1/2 meter higher at Indonesia than at Ecuador. This accumulation of surface waters in the western Pacific, in effect, pushes down the thermocline (Fig. I.2), while in the east the thermocline is closer to the surface. Off the coast of Peru, along coast wind forcing further pushes coastal waters offshore, allowing for the nutrient-rich water below the thermocline to be upwelled to the surface where it can be used by primary producers. A relaxing of the trade winds can result in the warm "El Niño" phase of ENSO while a strengthening of trade winds can result in the cold "La Niña" phase with increased upwelling.

The effects of ENSO are particularly strong in Peru and affect both terrestrial and marine environments. The term El Niño or "The Christ Child" actually originated in Peru, where fisherman observed that the unusually warm water conditions typically began following Christmas. Strong El Niño warm phases are particularly devastating, causing extreme rainfall and flooding to the normally arid coast and warming of the coastal waters. An El Niño event is usually triggered by the arrival of a Kelvin wave to the coast of Peru, which is reflected southward. This pushes the thermocline further down with the result that cool, nutrient-rich water is no longer in the layer of upwelled water (Fig. I.3a). The east-west sea surface water temperature gradient is reduced and convection becomes more omnipresent and less localized in the east, leading to a disruption of the circulation cell and further slackening of the trade winds (IRI, 2008) (Fig. I.3b). This positive feedback reinforces the development of El Niño events, which, while varying in intensity, show a

similar pattern of development and duration until the trade winds resume and recreate the normal Pacific basin gradient (ca. one year; Fig. I.4).

The impacts to the marine resources vary by species and habitat. Generally, species found along the coastal zone of the NHCE are adapted to the cold, highly productive normal or La Niña upwelling conditions. Species adapted to warmer, more mesotrophic conditions are found further offshore in oceanic waters or to the north in equatorial waters. Under El Niño conditions the upwelling habitat is reduced and both oceanic and equatorial waters intrude into the coastal zone. While some coastal species struggle to find enough food during the period of decreased primary production, others seem to thrive in the more tropical El Niño conditions. Additionally, a strong contrast is observed between the responses of the coastal upwelling and nearshore benthic habitats and, thus, their dynamics are dealt with in separate analyses of the thesis.

Chapters II-IV deal with the dynamics of the coastal upwelling ecosystem. It is this part of the ecosystem that is perhaps most familiar to marine scientists outside of Peru – often used as a case study example for: i) the functioning of an upwelling system, ii) small pelagic fish production (and crashes thereof), iii) bottom-up effects of small pelagic fish on the dynamics of higher predators, and iv) a "regime change" of dominance between small pelagic fish species (i.e. anchovy and sardine). A general hypothesis is that reductions in primary production, associated with periods of reduced upwelling, is a major forcing factor for observed reductions in most groups and trophic levels – from zooplankton to seabirds. In order to outline a framework for adapting previous trophic network models of the NHCE (specifically, those of Jarre et al., 1991; Jarre-Teichmann, 1992) for use in dynamic simulations, a review of the state-of-the-art in modeling of EBCSs was conducted (**Chapter II**). As a result, suggestions of compartmentalization and spatial and temporal considerations helped define the construction of the steady-state models for upwelling and EN periods (**Chapter III**). The model of the normal upwelling period of 1995-96 also provided a starting point for the initiation of dynamic simulations (**Chapter IV**).

Chapters V-VII deal with the dynamics of the nearshore benthic ecosystem. While these subsystems are also subject to the upwelling conditions, they may be less limited by bottom-up fluctuations in primary production. Upwelling fuels intense primary production in the coastal zone, where a high amount of unconsumed organic material ends up settling to the seafloor. This material is mainly broken down by benthic bacterial communities below the thermocline where, due to their intense production and respiration rates, oxygen concentrations are extremely low (<0.5 $ml \cdot l^{-1}$). Only the well-mixed, oxygenated waters of the shallow benthic environment are able to sustain higher benthic biomass. Nevertheless, even in these shallower depths, oxygen levels are quite low and may limit the biomass of some benthic groups. This is supported by the observed increases in

faunal density, biomass, species richness, and diversity under the reduced upwelling conditions of El Niño, when the thermocline deepens and oxygen concentration increases. Building on previous community analysis studies of other authors (Tarazona et al., 1988b, 1988a), the second series of chapters address dynamics through both single species, process-oriented explorations of population dynamics (**Chapters V and VII**) and holistic, energy flow structure analyses using trophic models (**Chapters VI and VII**). Furthermore, a focus on two separate bay systems of differing latitude – Independence Bay (**Chapters V and VI**, ~14°S) and Sechura Bay (**Chapter VII**, ~6°S) (Fig. I.5) – allowed for a comparison of the degree of susceptibility to ENSO variability and impacts thereof.

Main methods employed

Three approaches have been used to assess the impact of environmental variability on the dynamics of the NHCE and its subsystems. These include: i) time series analysis of catch dynamics by multiple regression analysis, ii) comparison of steady-state models between normal upwelling and El Niño periods, and iii) fitting ecosystem dynamics using trophodynamic simulations (Table I.1).

Multiple regression analyses were used to explore the catch dynamics of scallop *Argopecten purpuratus* populations in the bays of Independencia and Sechura. The dependant variable was yearly catch and independent variables were "Spawning stock size" and "Settlement factor", with the additional factor, "Riverine input", in the case of Sechura Bay. Settlement factor was an index of larval survival to metamorphosis and was calculated from known relationships of temperature-mediated larval development time, which were assumed to affect accumulated mortality during the pelagic phase. Riverine discharge was incorporated for the Sechura Bay exploration due to a hypothesized impact of changing salinities affecting mortality of the recruited scallop population.

Both comparison of steady-state models and explorations of ecosystem dynamics were conducted with the program *Ecopath with Ecosim* (EwE) (Christensen and Pauly, 1992; Walters et al., 1997). The program allows for the construction of mass-balanced models of trophic flows using input parameters commonly estimated in fisheries management, e.g. biomass, total mortality, and diet. This compatibility with ready available data has made EwE the most widely used trophic modeling package worldwide. Its predecessor, *Ecopath*, was recently listed as one of the ten most significant breakthroughs of the National Oceanographic and Atmospheric Administration (NOAA) during their 200th anniversary in 2007. The EwE package includes three main modeling

tools: i) the original steady state modeling routine, Ecopath, allowing for the estimation of indices of ecosystem energetics and developmental indices as calculated from a network analysis, ii) the temporal dynamic modeling routine, Ecosim, allowing for the exploration of fishery impacts and predator-prey dynamics, and iii) the spatial dynamic modeling routine, Ecospace, most often used in zoning management scenarios (e.g. marine protected areas). The first two routines were utilized in the following works.

Specifically, holistic comparisons of steady state trophic flows and ecosystem development indices between normal upwelling (1995/96) and El Niño (1997/98) periods were conducted using Ecopath for the coastal upwelling NHCE (**Chapter III**) and the nearshore benthic ecosystem of Independence Bay (**Chapter VI**). A lack of data for the Sechura Bay Ecosystem during the El Niño period prevented a similar comparison; however, a single steady state model was constructed for the upwelling period of 1996, allowing for comparison to the model of the same period for Independence Bay.

Explorations of ecosystem dynamics in the three subsystems were conducted using Ecosim (**Chapters IV, VI, and VII**). Steady-state models of the pre-El Niño period (~1996) were subjected to different external "drivers" of dynamics until 2003. Drivers included: i) forced biomass changes of species/groups for which evidence supports predominantly environmentally-mediated dynamics (i.e. non-trophically-mediated), and ii) forced fishery changes (i.e. effort and/or fishing mortality). Historical time series data of captures and/or biomass changes were used as a measure of fit for the simulations. These time series served both as a reference for forcing biomass changes of drivers and for measuring the fit of the simulation for the remaining groups. While the ability to "force biomass" of specific groups has been an option in EwE for some time, to the best of our knowledge it has not been used in previously published works. This method was chosen in order to simplify our assumptions on how drivers' dynamics are mediated by the environment; however, additional process-oriented explorations were conducted separately for the important scallop populations of Independence (**Chapter VI**) and Sechura Bays (**Chapter VII**). Finally, predator-prey trophic control settings (e.g. bottom-up, top-down) were explored for the coastal upwelling (**Chapter IV**) and Independence Bay (**Chapter VI**) ecosystems.

Tables and Figures

Table I.1. Methods employed in each chapter

Chapter. Title	Time series analysis - (multiple regression)	Steady-state model comparison	Dynamic simulation
Chapter II. Trophic modeling of Eastern Boundary Current Systems: a review and prospectus for solving the “Peruvian Puzzle”			
Chapter III. Trophic modeling of the Northern Humboldt Current Ecosystem, Part I: Comparing trophic flows during 1995-96 and 1997-98		X	
Chapter IV. Trophic modeling of the Northern Humboldt Current Ecosystem, Part II: Elucidating ecosystem dynamics from 1995-2004 with a focus on the impact of ENSO			X
Chapter V. A catch forecast model for the Peruvian scallop (Argopecten purpuratus) based on estimators of spawning stock and settlement rate	X		
Chapter VI. Changes in trophic flow structure of Independence Bay (Peru) over an ENSO cycle		X	X
Chapter VII. Trophic and environmental drivers of the Sechura Bay Ecosystem (Peru) over an ENSO cycle	X		X

**Review only

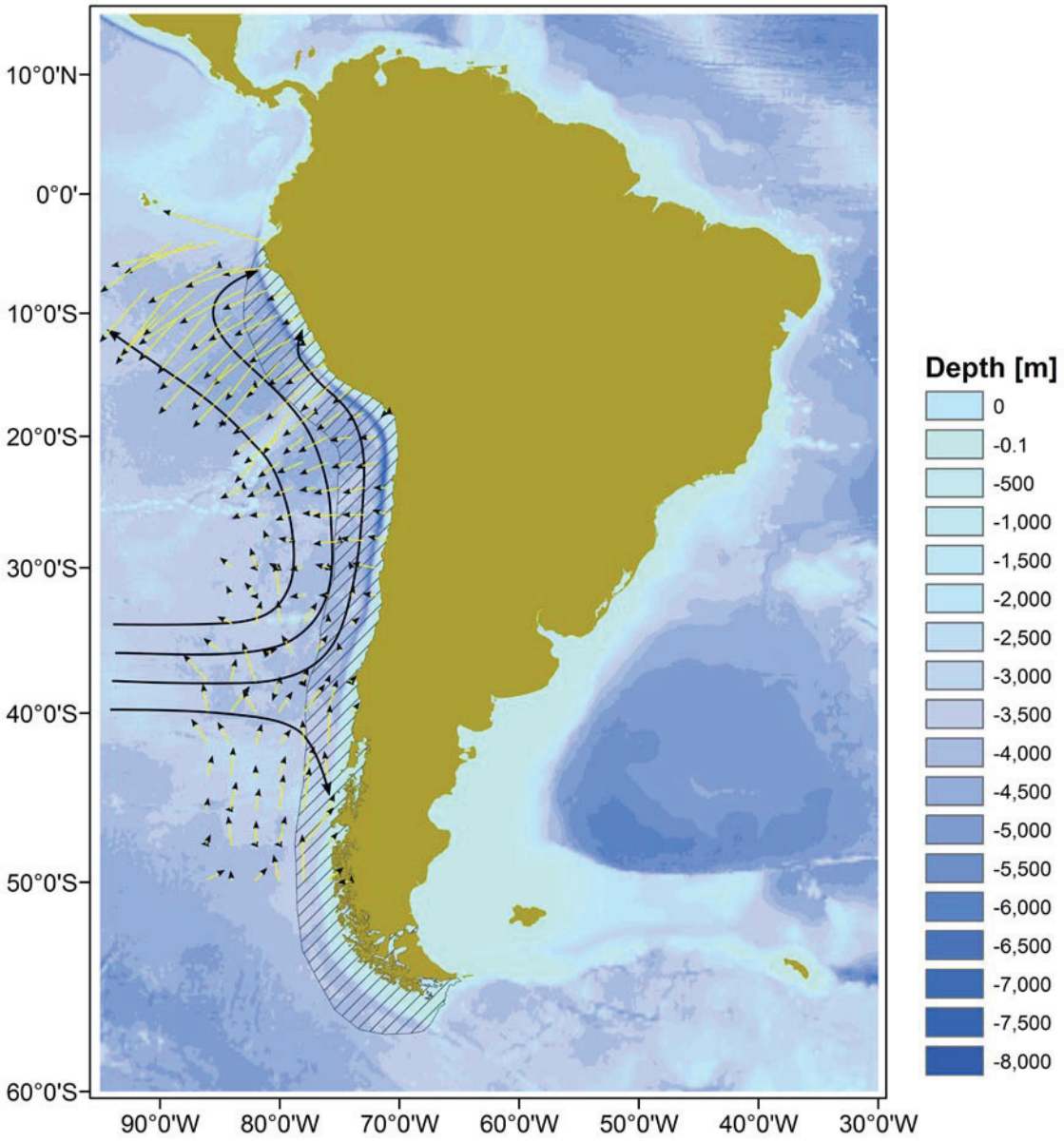

Figure I.1. The Humboldt Current Large Marine Ecosystem (hatched area). Black arrows denote dominant geostrophic flow directions. Yellow arrows denote vectors of winter surface Ekman transport ($t \cdot sec^{-1} \cdot m^{-1}$) (adapted from Parrish et al., 1983).

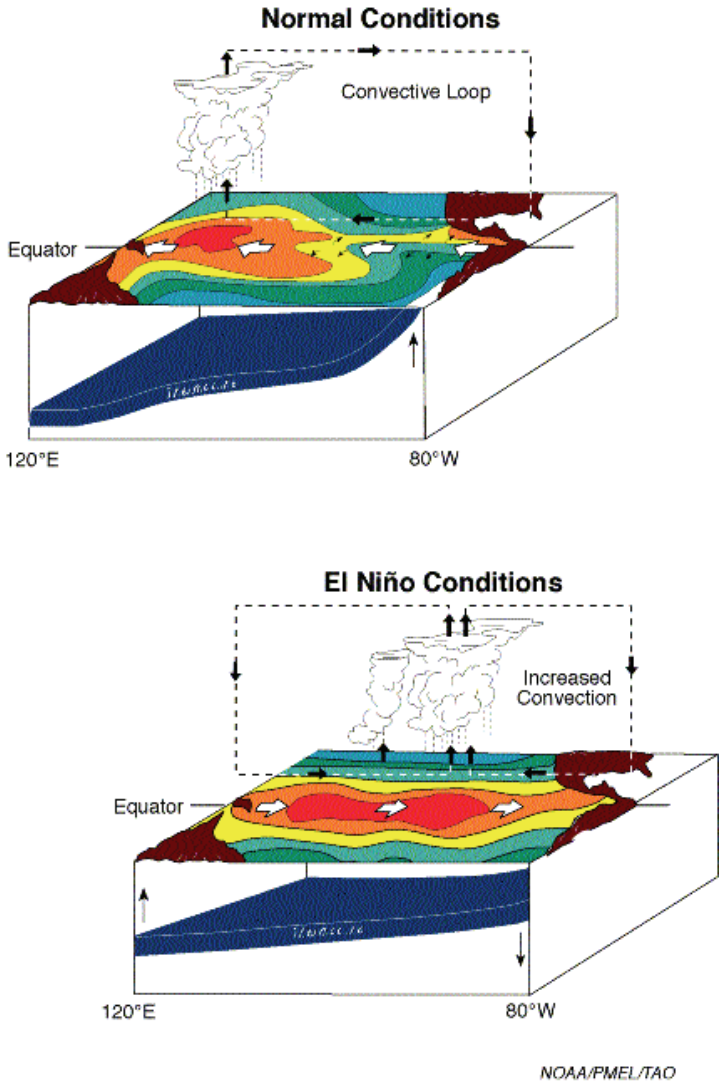

Figure I.2. Schematic diagram of normal (above) and El Niño (below) conditions in the Pacific Ocean. The underlying blue layer denotes the relative depth of the thermocline. Decreased trade winds during El Niño allow the basin-wide slope of the Pacific Ocean to relax. Surface waters flow back to the west and the thermocline is pushed downward (figure from NOAA, 2008).

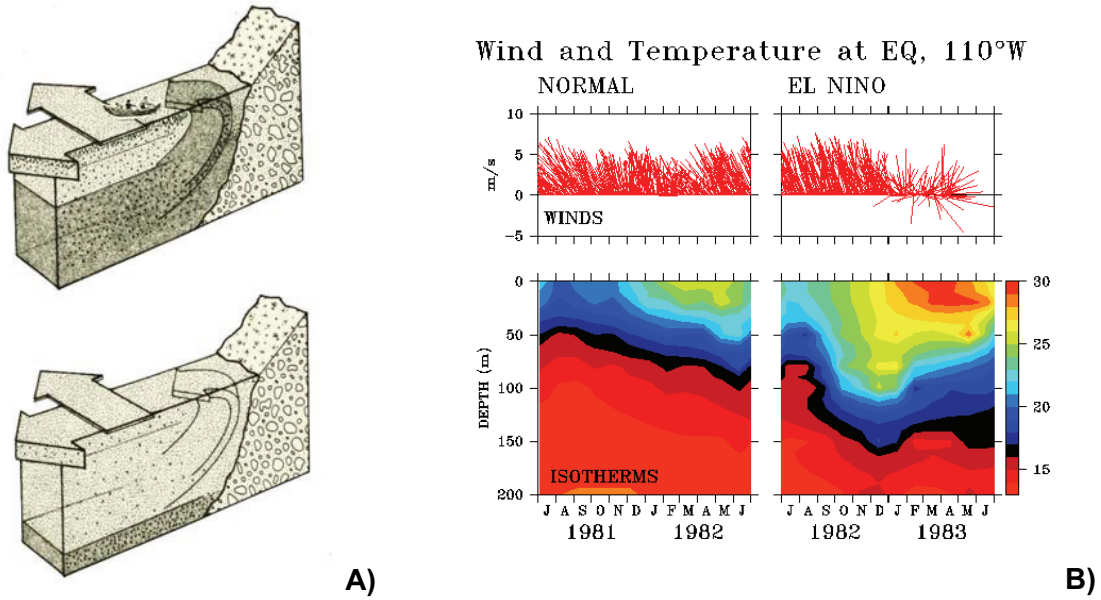

Figure I.3. Changes in upwelling characteristics associated with an El Niño event. A) Schematic diagram of wind-driven coastal upwelling in the southern hemisphere. Alongshore winds result in a net movement of water perpendicular and offshore and subsequent replacement by bottom waters. During El Niño, a lowering of the thermocline (bottom) results in the upwelling of nutrient poor water above the thermocline (Based on a diagram by R.T. Barber in Canby, 1984; reproduced in Arntz and Fahrbach, 1991). B) Changes in equatorial wind direction and strength (above), and thermocline depth during the strong El Niño event of 1982-83 (figure from NOAA, 2008).

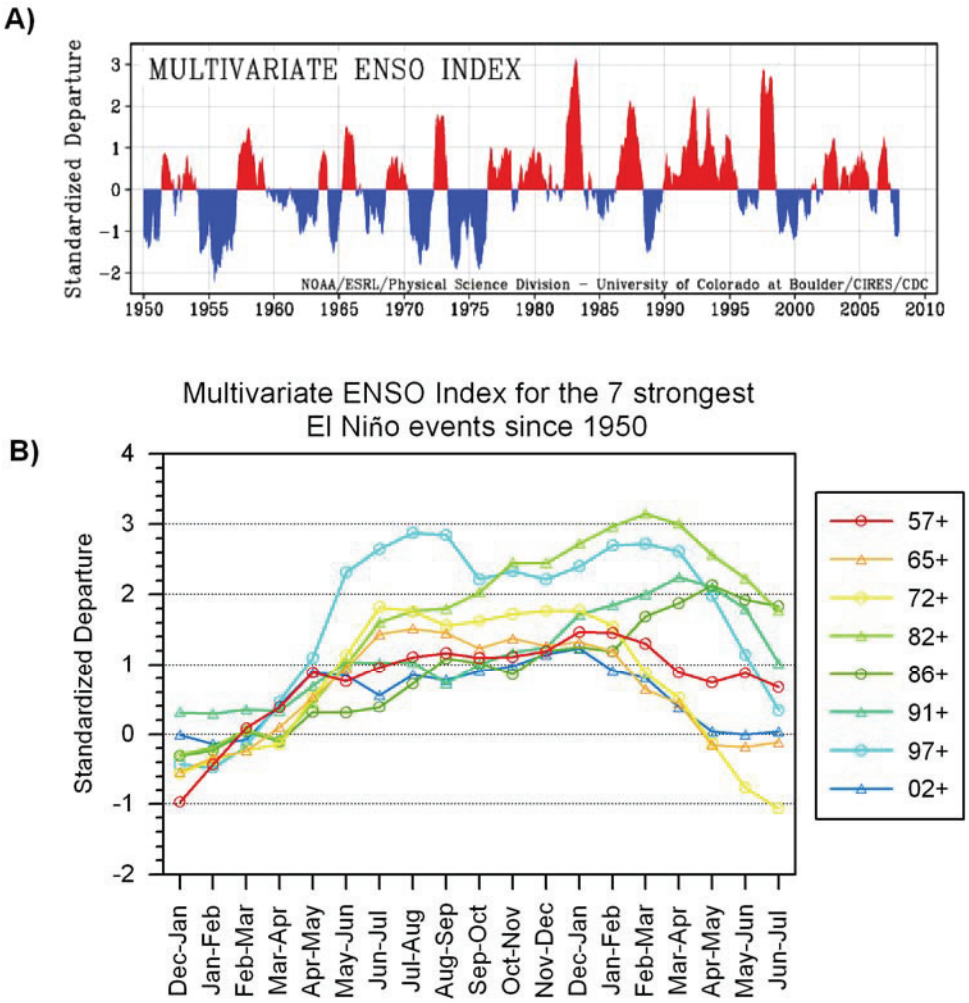

Figure I.4. Multivariate ENSO Index. A) From 1950-2007. B) 7 strongest El Niño events since 1950. All values are normalized for each bimonthly season so that the 44 values from 1950 to 1993 have an average of zero and a standard deviation of "1". (figures from NOAA, 2008)

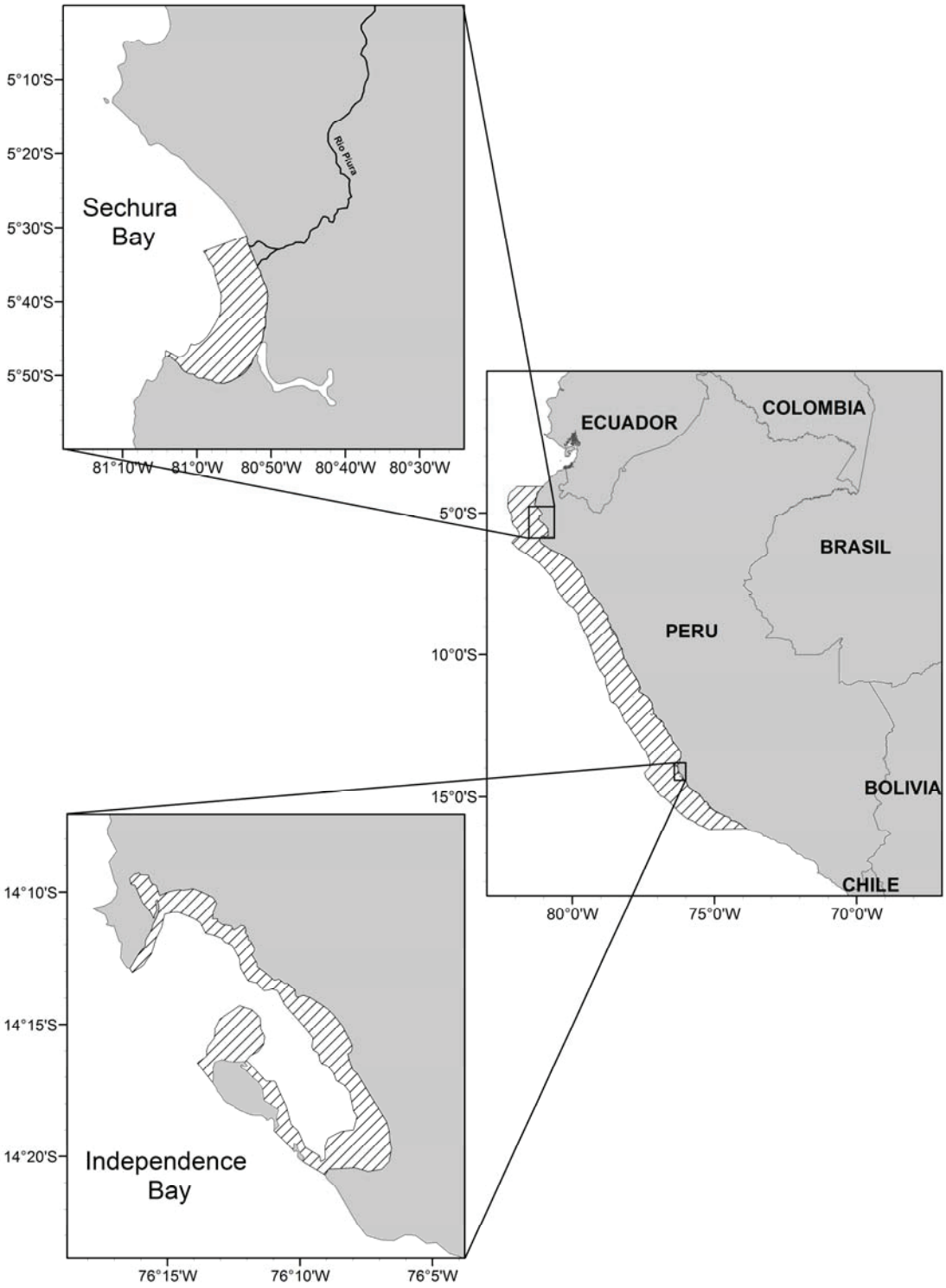

Figure I.5. Modeled subsystems of the Northern Humboldt Current Ecosystem. Sechura Bay (upper), coastal upwelling ecosystem (middle), Independence Bay (lower). The model area considered is hatched.

Chapter II. Trophic modeling of Eastern Boundary Current Systems: a review and prospectus for solving the "Peruvian Puzzle"

Marc H. Taylor[*] and Matthias Wolff

Author's posting. This is the author's version of the work. Please cite the final version published by Revista Peruana de Biologia. Article accepted December, 2006 and published August, 2007:
Taylor, M.H., Wolff, M., 2007. Trophic modeling of Eastern Boundary Current systems: a review and prospectus for solving the "Peruvian Puzzle". Revista Peruana de Biologia 14, 87-100.

Abstract

Eastern Boundary Current systems (EBCSs) are among the most productive fishing areas in the world. High primary and secondary productivity supports a large biomass of small planktivorous pelagic fish, "small pelagics", which are important drivers of production to the entire system whereby they can influence both higher and lower trophic levels. Environmental variability causes changes in plankton (food) quality and quantity, which can affect population sizes, distribution and dominance among small pelagics. This variability combined with impacts from the fishery complicate the development of management strategies. Consequently, much recent work has been in the development of multispecies trophic models to better understand interdependencies and system dynamics. Despite similarities in extent, structure and primary productivity between EBCSs, the Peruvian system greatly differs from the others in the magnitude of fish catches, due mainly to the incredible production of the anchovy *Engraulis ringens*.

[*] Corresponding author, Email: (marchtaylor@yahoo.com)

This paper reviews literature concerning EBCSs dynamics and the state-of-the-art in the trophic modeling of EBCSs. The objective is to critically analyze the potential of this approach for system understanding and management and to adapt existing steady-state models of the Peruvian system for use in (future) dynamic simulations. A guideline for the construction of trophodynamic models is presented taking into account the important trophic and environmental interactions. In consideration of the importance of small pelagics for the system dynamics, emphasis is placed on developing appropriate model compartmentalization and spatial delineation that facilitates dynamic simulations. Methods of model validation to historical changes are presented to support hypotheses concerning EBCS dynamics and as a critical step to the development of predictive models. Finally, the identification of direct model links to easily obtainable abiotic parameters is emphasized to add practicality to the model as a predictive tool.

1. Introduction

Eastern Boundary Current Systems (EBCSs) are among the most productive fishing areas in the world and the Humboldt Current Large Marine Ecosystem (HCLME) alone comprised between 6-13% of the world's annual catch between 1994-2003 (FAO, 2003). This productivity is due to the upwelling of cold, nutrient rich waters to the photic zone where it is taken up by primary producers – particularly, large diatoms. This high level of primary production forms the base of the food web, which is remarkably similar in all four of the main EBCSs (Humboldt Current, Canary Current, Benguela Current, and California Current). Species compositions are often different, but the general trophic organization is similar and includes numerous species of phytoplankton and zooplankton, relatively few species of small pelagic fish feeding directly on the plankton, higher carnivorous species of fish, and top predators such as tuna, birds, and marine mammals. The relatively small number of small pelagic fish species comprises the bulk of fisheries landings and has been proposed to be an important forcing group to both higher and lower trophic levels (i.e. "wasp-waist" control) (Cury et al., 2000). While these generalizations might be true to a certain extent for the aforementioned EBCSs, differences among systems complicate direct comparison (Moloney et al., 2005).

EBCSs differ remarkably in terms of fisheries production, likely due to physical differences in oceanography that affect biological production. Fisheries biologists have grappled to understand why the Peruvian fish catch (total and on a per area basis) is so much higher than that of all other EBCSs. This is mainly due to the huge production of the

Peruvian anchovy, *Engraulis ringens*, which has surpassed 10 million tons in production during several years. The "Peruvian puzzle" to fish production, as coined by Cury et al. (1998), seems to have more to do with prevailing oceanographic conditions than any particular physical attribute such as total area of continental shelf. Bakun (1996) eloquently demonstrated the physical differences between EBCSs in terms of their upwelling potential – Peru's advantage, due to its proximity to the equator and resulting large Rossby radius, lies in its capacity for strong upwelling under relatively low wind forcing conditions. This creates a "particularly rich, non-turbulent, benign environment" by which coastal plankton communities can develop and be maintained through longer residence times, thus favoring grazing fish populations (Bakun and Weeks, 2006). Production of anchovy, or more specifically their annual recruitment, has been shown to be at a maximum during conditions of intermediate strength of offshore transport (Parrish et al., 1983; Cury and Roy, 1989; Roy et al., 1992; Cury et al., 1998). In particular, a high level of recruitment and subsequent catch appears to occur within a narrow optimal "environmental window" of alongshore wind speeds coupled with a high degree of upwelling. This optimal wind speed falls between 5-6 m/s, a velocity which is at the upper limit of where wind begins to create hydrodynamically "rough" water conditions (Deacon and Webb, 1962). While strong upwelling provides increased nutrients to the photic zone, excess turbulence can be detrimental to primary producers by decreasing light penetration, and to grazers by increased dispersal of available food (Ware, 1992). Furthermore, trade winds set up a basin-wide slope in sea level in the Pacific, whereby Peru is able to maintain a shallow thermocline, leading to enhanced nutrient supply and productivity (Chavez et al., 2003). An interesting byproduct of these oceanographic conditions is that plankton probably become concentrated above the shallow thermocline, thus improving the grazing efficiency of small pelagic fish.

Environmental variability within EBCSs creates large changes in productivity, which is ultimately felt economically through decreased catches. In the case of the Peruvian upwelling system in the Humboldt EBCS, production of small pelagic fish is affected on annual scales (e.g. associated with El Niño-Southern Oscillation – ENSO, "El Niño") as well as larger decadal scales (Fig. II.1). Future management may benefit from a deeper understanding of how this environmental variability affects recruitment and trophodynamics of these economically important species as well as the overall productivity of the ecosystem.

Given the extent of declining fish catch worldwide, there has been significant support to reform the ways in which we manage and assess fishery resources for the purpose of sustained production. Traditional management has focused on the single species and has largely ignored inter-specific trophic interactions, the rationale being that

each species occupying a niche in the ecosystem is most affected by its own population dynamics and the basic parameters of growth and mortality. The fishery is perceived as an additional component to the population's mortality, a parameter that fisheries biologists can manage in order to maintain an optimal level of production over time (i.e. Maximum Sustainable Yield, "MSY"). These "traditional" single-species approaches have been criticized in recent years as being overly simplistic given the complexity of ecosystems. However, Mace (2004) states that to "scapegoat" all single-species models would be alarmist given that in many cases the suggested exploitation rates may not have been implemented successfully, and that a reduction in fishing mortality of a single species has actually proved successful in many stock recoveries. On the other hand, the management of small pelagic fish populations is complicated due to their specific characteristics: 1) highly stochastic populations linked to environmental variability, 2) some functional redundancy between species, and 3) a strong interdependence between the target species and the rest of the ecosystem. These factors call for a more holistic "Ecosystem Approach to Fisheries" (see Browman and Stergiou, 2004) and as a result, recent work in EBCSs has attempted to bridge the gap between theoretical and practical uses of multispecies models.

The objective of this paper is to suggest a methodological approach for developing models that will serve as a predictive tool for management in the Peruvian upwelling system. In order to arrive at a framework for such a tool, a literature review was conducted of trophic modeling of EBCSs with the objective of adapting existing steady-state models of the Peruvian system for use in dynamic simulations. Methods of model validation to historical changes are presented as a critical step to the development of predictive models for management. Finally, the identification of direct links of models to easily obtainable abiotic parameters is emphasized for adding practicality to the approach as a predictive tool.

2. Model considerations

One such tool that has gained popularity in recent years is the use of steady-state trophic models such as *Ecopath* (Christensen and Pauly, 1992), which allow the user to construct a simplified representation of the ecosystem based on the flows of energy among species or functional groups. With the further development of the accompanying dynamic simulation package, *Ecosim*, users are now able to explore past and future impacts of fishing and environmental disturbances and explore optimal fishing policies

(Walters et al., 2000). Data demands of the program package Ecopath with Ecosim (*EwE*) are also relatively smaller in comparison to other dynamic models (e.g. Multispecies virtual population models – MSVPAs, Individual-based models – IBMs), thus lending itself to wider use as a management tool.

As with any model, the focus and scope of the problem has to be addressed. First, one must simplify the infinitely complex ecosystem into a manageable representation through the identification of key functional species groups of similar life history, dynamics, and diet, and to focus on those relationships important to the problem at hand. Secondly, the definition of an appropriate temporal resolution (e.g. based on a yearly average, decadal average, seasonal, etc.) and spatial boundaries to the model are of utmost importance. In the following sections, considerations for modeling the dynamics of the Peruvian upwelling system are presented alongside a review of EBCS dynamics and previous models.

2.1 Functional groups and dynamics of EBCSs

Due to their ecological and economic importance, previous models have focused on small pelagic fish. Cury et al (2000) highlighted evidence suggesting both bottom-up and top-down control on production to predators and plankton, respectively. This “wasp-waist” forcing may be attributed to their grazing efficiency and large biomass that, in a sense, funnels energy through the relatively few species comprising the group. The importance of anchovy grazing on phytoplankton in coastal waters of Peru has even been compared to copepods, whereby carbon fixed by primary producers was estimated to be channeled through the trophic web equally between the two groups (Walsh, 1981). A further review of these and other findings by Alheit and Niquen (2004) led them to conclude that, “Understanding the trophic interactions between anchovy, sardines and zooplankton might be a key to understanding their dynamics in the [Humboldt Current].”

One of the most pressing questions that exist in EBCSs concerns the dynamics that govern small pelagics, and in particular, the factors responsible in a regime shift. Regime shifts typically involve a change in dominance between anchovy and sardine, yet may also include changes to the biomass of larger mackerels. The “classic” regime shift between sardine and anchovy appears to be a regular part of the dynamics in the Peruvian system as has been verified through the fossil record using fish scale deposits (DeVries and Pearcy, 1982). Recent evidence has linked these shifts with warm and cold temperature periods occurring on decadal scales over entire ocean basins (Alheit and Ñiquen, 2004).

In Peru, changes in small pelagic fish abundances can also be observed under the inter-annual scale disturbances associated with El Niño. Anchovy tend to occupy the nearshore areas within the first 30 nautical miles where there is colder water due to upwelling while sardines are often located further offshore. During El Niño, the intrusion of warm equatorial waters and the lowering of the thermocline result in elevated sea surface temperatures and upwelling is restricted to the upper warmer-water layer with a few limited cold-water cells. Anchovy populations retreat to these few remaining upwelling areas and sardines move inshore (Ñiquen and Bouchon, 2004). These dynamics in dominance and spatial distribution have previously been attributed to anchovy being better adapted to cold temperatures and sardines to warmer temperatures; however, Bakun and Broad (2003) point out that temperature may not necessarily be the cause given that in the western Pacific sardines do relatively well during cold periods, and that the two species tend to replace each other over longer (with respect to temperature fluctuations) time scales as the dominant grazer of plankton. These dynamics lend support for a secondary response to environmental forcing and further probing of the species' trophic interactions becomes necessary.

In most EBCSs it has been observed that some degree of functional redundancy or overlap exists among small pelagics feeding on plankton, yet marked differences in feeding preferences have also been observed. Sardines possess a particularly fine-meshed filtering apparatus in their gillrakers allowing for the filtering of smaller-sized particles. Anchovy, on the other hand, are more specialized and efficient at feeding on larger-sized particles (James and Findlay, 1989; Van der Lingen, 1994). The result of these adaptations, at least in the Benguelan populations, is that anchovy seem to have higher clearance rates (per weight) than sardine when particle size is greater than about 500-600µm (Van der Lingen, 1994). Particles of this size include large mesozooplankton such as calanoid copepods as well as chain-forming diatoms - known to comprise the major part of the Peruvian anchovy's diet.

In general, larger chain-forming diatoms are associated more with upwelling areas of higher nutrient concentrations while more oligotrophic environments tend to be dominated by smaller phytoplankton, and bacteria cycles become more important (Rodriguez et al., 2001). The warm phase during the 1970's and 80's in Peru resulted in a regime shift to sardine dominance with declining zooplankton concentrations in comparison to the 1960's and earlier, when anchovy was dominant (Alheit and Ñiquen, 2004; Ayón et al., 2004). Similarly, a reduction in the upwelling of cool, nutrient-rich waters during an El Niño event has also been linked to changes in the phytoplankton community in northern Chile, from the typical diatom-dominated phytoplankton to pico- (0.7–2.0µm) and nanoplankton (2.0–23.0µm) dominated (Iriarte and González, 2004). During the El

Niño in Peru in 1997-1998, anchovy presumably responded to these changes by retreating to the remaining centers of upwelling at about 16°S where diatom abundances were still relatively high (Ñiquen and Bouchon, 2004). However, in general diatom biomasses were greatly reduced and anchovy were forced to feed on larger relative quantities of zooplankton throughout the Peruvian coast (Fig. II.2).

Small pelagics will probably have very different diet matrices in Peru than in other EBCSs. Both sardine and anchovy are omnivores and likely opportunistic feeders that commonly switch to consume whatever the plankton composition happens to be. In the Benguelan system, anchovy are much more of a zooplankton feeder than in the Humboldt, feeding mainly on large calanoid copepods and euphausiids, ingested through particulate feeding (James, 1987; Van der Lingen, 2002). During normal upwelling periods, stomach contents of anchovy sampled off the Peruvian coast contained >95% diatoms (numbers) (Alamo et al., 1996b; Alamo et al., 1997a; Alamo et al., 1997b; Alamo and Espinoza, 1998; Espinoza et al., 1998a; Espinoza et al., 1998b; Blaskovic et al., 1999). Similar estimates have been used for trophic models in Peruvian and Chilean systems (Jarre et al., 1991; Neira et al., 2004). The more than ten-fold higher production of small pelagic fish in the Humboldt compared to other EBCSs has been attributed to anchovy feeding directly on phytoplankton (Walsh, 1981). This is logical given that feeding on one lower trophic level would provide about 10 times more food if we assume a mean transfer efficiency between trophic levels in aquatic systems of about 10% (Christensen and Pauly, 1993a; Pauly and Christensen, 1995).

2.2. Compartmentalization

As a result of these trophic interactions, recent models have paid much more attention to the compartmentalization of plankton and small pelagics; particularly, those models constructed for later use in dynamic simulations have focused on plankton divisions by cell size. The basic constructions of the four models reviewed (Jarre et al., 1991; Shannon and Jarre-Teichmann, 1999; Shannon et al., 2003; Neira et al., 2004) are shown in Table II.1. For the Benguelan models, zooplankton was split into three size groups: i. *Microzooplankton* (<200µm), ii. *Mesozooplankton* (200–2000µm), iii. *Macrozooplankton* (2-20mm). *Gelatinous zooplankton* (jellyfish and salps) was compartmentalized separately. The Chilean model separates the group into compartments of *Copepods* and *Euphasiids*. While this provides an important separation between the zooplankton consumed by anchovy and sardine (principally copepods) versus that of chub and horse mackerels (principally euphausiids), additional

compartmentalization is advised to account for the previously mentioned differences in particle size feeding preferences for anchovy and sardine. In particular, sardines are known to feed more heavily on cyclopoid copepods (usually <200μm) while anchovy feed more on larger calanoid copepods and euphausiids (James, 1987; Konchina, 1991; Van der Lingen, 2002). In the past model for Peru, zooplankton was not divided into size-specific groups, however, Jarre-Teichmann and Christensen (1998) recommended that a closer look at plankton compartments was needed to obtain a more detailed understanding of the system.

Small pelagic fish are compartmentalized fairly similarly for the main species of anchovy, sardine, chub mackerel (not in the Chilean model), and horse mackerel. As recommended for the modeling of life history dynamics (Christensen and Walters, 2004), separation of a single species into several functional groups, by size or life history classes, has been made in the S. Benguelan and Chilean models. In this way, differences in food intake, vulnerability to predation, and recruitment constraints related to juvenile size and fecundity can be accounted for. In the case of the S. Benguela model, horse mackerel is split into juvenile and adult groups due to differences in biomass, catch and diet (juveniles are strictly zooplanktivorous while adults eat zooplankton and fish). Other small pelagic fish are included in the Benguelan models such as *Mesopelagics*, *Redeye*, and *Other small pelagic fish*. The absence of mesopelagic fish in the other models may represent a significant shortcoming, as this group represents a large amount of biomass and is a potentially important food item to other species. The S. Benguela model estimates suggest that hake consumed 1.1 million tons of mesopelagic fish during the 1990's (Shannon et al., 2003). Mesopelagic fish have also been seen to venture further inshore during El Niño years in Peru, observable through acoustic surveys, catches, and in the stomach contents of coastal marine mammals (Arias Schreiber, 2003).

Demersal fish are given more attention in the Chilean model due to their importance to the region and possibly better data. These groups, especially hake, are often lacking sufficient data relating to life history, yet the two most recent models have incorporated separate stages for hake given the important predatory relationship described between adult hake on anchovy. In Peru, hake populations have suffered severely – to the point where the fishery was eventually closed in September 2002 and now operates at a much smaller scale. From diet studies, hake is observed to have undergone a severe change in diet; from adults feeding on other abundant demersals and sardine in a survey from 1985 to intense cannibalism among individuals of 4-5 years and older in 2001 (Ballón, 2005). Hake has important connections to the pelagic system as well, especially for small juveniles that feed more pelagically on euphausiids mainly (Shannon et al., 2004a; Ballón, 2005; Tam et al., 2006). The Peruvian hake population

was thought to have increased during the 1980's due in part to an increase in sardine abundance, which comprised a large portion of the adult hake's diet (Ballón, 2005). Besides hake (being the principle demersal species), *Other demersal fish* are either simply labeled as such (Jarre et al., 1991; Shannon and Jarre-Teichmann, 1999), further divided into *Pelagic*- and *Benthic-feeding* compartments (Shannon et al., 2003), or divided into individual species as is the case of Central Chilean model (Neira et al., 2004).

Cephalopods were considered to be an important functional group in the S. Benguela model (Shannon et al., 2003). Moloney et al. (2005) have standardized this group's production to consumption ratio, P/Q, at 0.3 in models of EBCSs. Production estimates vary, however, the group is notoriously productive and a voracious consumer, making it an important compartment to future models. The Humboldt squid, *Dosidicus gigas*, has gained importance in recent years in Peru as its biomass increased dramatically after the last El Niño in 1997-98. It has remained at high levels ever since despite the development of a large industrial fishery. Its distribution is more limited to the north of Peru, and is observed to feed opportunistically with a high degree of cannibalism – especially among larger size classes nearing the end of their lifecycle. Given its large consumption (estimated consumption to biomass ratio, Q/B, for summer 2005 in Peru was 8.91), the group has been thought to have an important impact on hake populations (specifically, the more pelagic-feeding juveniles) and was estimated to account for as much as 21% of the total mortality of hake. Furthermore, a 14% similarity in prey between the jumbo squid and hake may also indicate an important competitive relationship between the two species (Alegre et al., 2005).

2.3. Spatial boundaries

Steady-state trophic modeling requires that the user defines boundaries to the ecosystem under study. One can imagine the difficulties involved with an open marine system, such as a pelagic environment, where species are constantly on the move and in flux with prevailing oceanographic conditions. Connections to the coastal environment are also important, and for this reason there has been an attempt to delineate Large Marine Ecosystems (LMEs) that conceivably contain a high degree of interconnectedness, having important implications for management. The US National Oceanic and Atmospheric Administration (NOAA) have provided the following definition of a LME:

> *"Large Marine Ecosystems are regions of ocean space encompassing coastal areas from river basins and estuaries to the seaward boundaries of continental*

> *shelves and the outer margins of the major current systems. They are relatively large regions on the order of 200,000 km^2 or greater, characterized by distinct: (1) bathymetry, (2) hydrography, (3) productivity, and (4) trophically dependent populations"*. (www.lme.noaa.gov)

Presently, 64 LMEs have been described and represent about 95% of the world's annual marine fishery yields. The Humboldt Current, Canary Current, Benguela Current, and California Current EBCSs are also considered to be individual LMEs. Despite this delineation, trophic modeling efforts of EBCSs rarely focused on the entire LME. Is this significant or does it represent a shortcoming in our acceptance of defined LMEs as a useful concept for management?

In EBCSs, the width of the upwelling zone is a function of water depth, stratification, and latitude (ca. 10-30km wider near the equator due to Rossby radius). However, the productive band of high biomass and associated fisheries is often wider and can extend to over 100km (Ware, 1992). Nixon and Thomas (2001) provide a review of previous delineations of the Peruvian upwelling system and find that estimations of area range over ten-fold, from less than $40 \cdot 10^3 \cdot km^{-2}$ to over $500 \cdot 10^3 \cdot km^{-2}$. Most of the uncertainty arises from three main factors: 1) estimation based on the actual physical upwelling of water versus inclusion of a larger area of significant biological impact, 2) differing lengths of coastline used in the calculation, and 3) large seasonal and inter-annual variability in the extent of upwelling off Peru. The authors go on to provide their own estimates of size based on remote sensing estimates of surface water chlorophyll *a* concentrations; specifically the area of "productive habitat" where concentrations exceed 1.0 $mg \cdot m^{-3}$ was considered. Using this criteria, the size of the productive habitat was observed to vary 10-fold (including the ENSO event of 1997/98), presumably in relation to the degree of upwelling and, subsequently, nutrient concentrations in the photic zone. The use of remote sensing has undoubtedly shed a great deal of light on the variability in primary production for EBCSs, however the application of such a mobile boundary complicates the efforts of the modeler, especially if one is to attempt dynamic modeling over longer periods of time. In the case of modeling small pelagic fish populations, their distribution often occurs within a known range of the coast due to other limiting factors besides food, such as prevailing currents, which play important roles in their lifecycle. It is thus recommended that a defined spatial border be based on the life histories of the main functional groups influencing system dynamics.

In the cases of the Humboldt and Benguelan systems, trophic models have defined boundaries around particular stocks of small pelagic fish that often correspond with centers of upwelling. In the Humboldt, stocks of sardine and anchovy overlap in

latitudinal distribution in northern to central Peru, southern Peru to northern Chile, and off Talcuano in Chile (Serra, 1983), with an additional sardine stock off Coquimbo in Chile (Serra and Tsukayama, 1988) (Fig. II.3). These stocks are separated by areas of low Ekman transport at ~15°S and ~23°S, and by conditions of downwelling predominating south of 36°S (Fig. II.4). The Peruvian and Chilean regions differ in their upwelling characteristics as well, with stronger winds along the Peruvian coast upwelling subsurface countercurrent water, while off Chile subantarctic water of the equatorward flowing coastal current is upwelled (Wolff et al., 2003).

Jarre-Teichmann and others (Jarre et al., 1991; Jarre-Teichmann and Pauly, 1993; Jarre-Teichmann and Christensen, 1998; Jarre-Teichmann et al., 1998) have focused primarily on the northernmost stocks of Peru while Neira et al. (Neira and Arancibia, 2004; Neira et al., 2004) have modeled the zone of the southern stocks of central Chile (33°-39°S). The Benguelan EBCS has also been modeled separately for the different principle stocks of small pelagic fish in the northern (Shannon and Jarre-Teichmann, 1999) and southern regions (Shannon et al., 2000; Shannon et al., 2003; Shannon et al., 2004b) (Fig. II.3). While some connectivity may exist between stocks, they are essentially separately functioning populations and the size of the population, or absolute abundance, is related to the area in which there is closure of the life cycle (Sinclair, 1988; Sinclair and Iles, 1988, 1989). A nice example of this is given by Gutierrez and Herrera (Gutierrez Torero and Herrera Almirón, 2002) for the Peruvian anchovy showing that the species' biomass and distribution are correlated (Fig. II.5) and are influenced by the strength of upwelling. Thus, as upwelling increases (cold periods), the size of the closure of the lifecycle also increases.

In general, when the focus of a modeling exercise is on the description of a particular resource, it makes sense to define borders that will encompass the species' lifecycles under most conditions rather than to constantly reformulate borders based on a changing area of suitable habitat. While some connection between these small pelagic populations may exist, it is likely of less importance to within population dynamics. LME definitions may thus have practicality as a policy tool, yet modeling of the entire LME will likely benefit from the separation of these stocks and the corresponding lower trophic levels.

3. System characteristics

Carr (2002) compared potential productivity in the four main EBCSs using remote sensing between September 1997 and August 1999. Results indicated that in terms of primary productivity (extrapolated from chl *a* concentrations), the Humboldt system ranks third after the Benguelan and Canary systems. The Peruvian coastline, in particular, had by far the greatest productivity in the Humboldt Current, yet the entire Humboldt Current system's productivity was not considered to be exceptional. The robustness of the method of calculating primary productivity is difficult to assess without a crosscheck from field data, yet even a direct sample of chl *a* concentration would not give sufficient descriptive information concerning pico-, nano-, micro-, and chain-forming plankton proportions and their overall productivities. It seems likely that differences in plankton quality rather than quantity may be a key factor in explaining the exceptional anchovy production in Peru. Additionally, Peru seems to reflect an optimal situation for production with relatively constant upwelling year-round under wind speeds of intermediate strength, possibly providing an optimal situation for both adult feeding and recruitment.

The first comprehensive comparison between EBCS steady-state models was done by Jarre-Teichmann and Christensen (1998), wherein they compared subregions of the four main EBCSs: Peru 4-14°S, "Namibia" (*Benguela*) 15-35°S, Canary 12-25°N, and California 28-43°N. These models were compared under similar model constructions and scale (70 km from the coast), thus representing an ideal situation for comparison. The authors focused on the main fish species: anchovy, sardine, horse-mackerel, mackerel, and hake, and in describing and discerning local and global characteristics. The general structure of the trophic flow diagrams is similar for all four systems with functional groups located at similar trophic levels. "Size" (total biomass) and total system throughput (T) varied greatly between the systems primarily due to differences in entered values for primary production. The Peruvian system ranked highest in both categories; however, as previously mentioned, remote sensing estimates of primary production presented by Carr (2002) indicate that these values may be too high or at least not higher than the Benguelan system. Anchovy productivities were similar between systems and the fact that their natural mortality was always substantially higher than fishing mortality, even in the heavily-fished Peruvian system, points to their importance as a food source to the rest of the system (Jarre-Teichmann and Christensen, 1998). Sardine production was highest in the Namibian (Benguelan) system, where plankton composition may favor its feeding strategy.

Models presented by Jarre-Teichmann and Christensen (1998) are compared to the other previously mentioned large upwelling systems in Figure II.6. Differences in the

spatial delineation of the systems may affect many of the summary statistics provided by Ecopath, making comparisons difficult. Specifically, the inclusion of a larger proportion of oligotrophic oceanic waters further from the productive upwelling coast will dilute key descriptors such as biomass and total system throughput. The outer boundaries to the modeled areas were as follows: 70 km - North and Central Peru (Jarre-Teichmann and Christensen, 1998), 60 km - Central Chile (Neira et al., 2004), and 500m depth isocline - Northern and Southern Benguela (Shannon and Jarre-Teichmann, 1999; Shannon et al., 2003). These extensions from the coast are not largely different, but will have an affect on size-specific statistics (in Fig. II.6, all except *Mean trophic level of the fishery*).

One of the more revealing statistics is that of transfer efficiency (TE), which describes the proportion of energy entering a trophic level that is transferred to the next trophic level. It is calculated in Ecopath as the ratio between the summed exports and predation, and the energy throughput (total consumption). High gross food conversion efficiencies (GE) correspond to high production/consumption ratios, and lead to high transfer efficiencies (Christensen and Pauly, 1993a). TE is therefore restricted to describing consumer trophic efficiencies due to the fact that the present models do not quantify solar energy input to producer compartments. Previously, upwelling systems were thought to have a relatively low mean TE in comparison to the average of about 10% in other aquatic systems (Jarre-Teichmann, 1992; Christensen and Pauly, 1993a; Jarre-Teichmann and Pauly, 1993; Jarre-Teichmann and Christensen, 1998) due to the relatively short food chain length from primary producers or detritus to top predators in upwelling systems (Ryther, 1969). Jarre and Christensen (1998) observed TEs below 10% for their models, yet more recent models of the Southern Benguela system have much higher efficiency to trophic level V. The authors explain that this may be a result of the model's construction wherein the splitting of the zooplankton group caused a shift in their observed trophic level. In the models by Jarre and Christensen (1998), the trophic level of zooplankton is slightly above 2, while Shannon et al. (2003) have the following trophic level assignments: Microzooplankton 2.3; Mesozooplankton 2.6; Macrozooplankton 2.7, which shifts all subsequent consumer compartments to higher trophic levels. Christensen and Pauly (1993a) also showed a tendency of increasing trophic levels to "appear" as one describes diet compositions in greater detail. This seems to be supported by the newer models of the S. Benguela in which 31 compartments were used and subsequently have closer to 5 versus 4 trophic levels in the Jarre and Christensen (1998) models.

The higher TE of the N. Benguelan observed by Shannon et al. (2003) seems to be more of the exception than the norm among EBCSs. In particular, plankton available to small pelagic fish are of very different quality resulting in increased carnivory by anchovy,

more similar to the Peruvian situation under El Niño conditions. High TE values may indicate a "bottle-neck" of flows between zooplankton (TL II and III) and small pelagic fish (TL III and IV), pointing to their importance in the overall trophic structure of the ecosystem and possibly food limitation to small pelagics (Shannon et al., 2003). Not mentioned by the authors, but likely an important factor is that zooplankton biomass was not known, and thus was back-calculated assuming an ecotrophic efficiency (EE) of 0.95. In other words, the model assumes that 95% of the group's production will be consumed by higher predators, and it is possible that this assumption has elevated the TE values of TLs II and III.

High non-predatory losses (defined by low EE) are typical between producer and 1st consumer (herbivore) levels in EBCSs. This results in a large portion of primary production going directly to detritus where it is remineralized. In the case of the S. Benguela, it was estimated that between 55-60% of net primary production is consumed by herbivores with losses being attributed to a possible "match-mismatch" between zooplankton and phytoplankton blooms (Shannon et al., 2003). This parameter is however notoriously difficult to estimate and therefore is often left open for Ecopath to calculate. Nevertheless, in upwelling areas EE is assumed to be typically low for phytoplankton (~0.5) and in some cases for zooplankton compartments as well.

4. Validation of the model - linking cause and effect

The linking of cause and effect, or the creation of models that can at least reproduce observed historical responses to disturbances such as fishing, has been described as a critical step for applying trophic modeling to policy analysis (Shannon et al., 2004a). Within the Ecopath package, users can determine interactions within the steady-state model through the "mixed trophic impact" operation. This feature offers a test to the sensitivity of the model by changing the biomass of one particular functional group and viewing the impact of this change to all other compartments' biomasses. Direct (e.g. negative impact predator-prey) and indirect (e.g. competition, positive impact predator-prey) effects can be identified, helping one visualize new equilibriums under disturbances to individual groups. An example of this routine is shown in Figure II.7, generated from data presented in Jarre et al.'s (1991) model of the Peruvian system between 1960-69. We can immediately see that anchovy influences many other groups, in most cases these are easily interpretable; negative impacts to its competitors (sardine and other pelagics) and prey (zooplankton), and positive affects on its predators (mackerel, horse mackerel,

hake, and seabirds). Anchovy are also seen to have a net positive effect on the system, a feature that is primarily shared by groups at the base of the food chain - primary producers and detritus.

Recent models of the southern Benguela system have used routines in Ecosim for assessing the relative importance of human vs. environmental impacts on system dynamics. Within Ecosim, a user can view how a system is reacting along each time step (iterative), allowing for a more realistic impression of the intensity and duration of change before equilibrium is achieved. Using this tool, users can better describe the processes of cause and effect through time - an important dimension needed in validating a model's outcome to observed historic changes. Dynamic simulations compared these factors through the linking of steady-state models (Shannon et al., 2004b) and through fitting to time-series data (Shannon et al., 2004a). In both cases, a time period encompassing the observed shift in small pelagic dominance was used. These examples are presented as valuable proxies for future model validation in the Peruvian system in the following sections:

In the linking of two steady-states (Shannon et al., 2004b), models were constructed on decadal scales: the anchovy-dominant 1980's, and the 1990's when sardines increased in importance and anchovy populations declined. Dynamic simulations involved subjecting one of the models to conditions of the alternate period. These alternate state conditions forced either the rate of fishing mortality (*F*) to small pelagics (anchovy, sardine, adult horse mackerel, and juvenile horse mackerel) or "environmental forcing" by affecting the *vulnerability rates* (the instantaneous density of a prey vulnerable to a particular predator, Christensen et al., 2000) of zooplankton to sardines and anchovy. The resulting biomasses of key groups at equilibrium to the alternate state's values provided a measure of comparison for the different forcing.

Fitting to time-series (Shannon et al., 2004a) routines used annual estimates of catch and biomass for species or species groups for the period 1978-2002 as a baseline by which to gauge the fit of simulations through a comparison of sum of squares (SS). The effect of fishing on dynamics was forced with independent estimates of changing yearly fishing rates (fishing mortality or fishing effort). Again, environmental effects focused on vulnerability rates for the predator-prey interactions most sensitive to change (with emphasis on interactions of small pelagics) and for primary production (impacting phytoplankton P/B). A "fit to time-series" search routines for "best-fit" values were performed for vulnerabilities and turnover rates (P/B) for primary producers.

4.1. Fishing impacts

Changing fishing rate was shown to have a relatively smaller impact on system dynamics than environmental factors in the southern Benguela. In the case of the influence on a regime shift, as was tested with the linking of two steady-state models, the application of the alternate state's rate of fishing mortality did cause many biomasses to change in the correct direction but not of the same magnitude (Shannon et al., 2004b). Using a time series for changing fishing rates also only slightly improved the fit of the model's prediction of catch and biomass (2-3% reduction in *SS*) over a constant value of fishing mortality taken from the 1978 steady-state model. Moloney et al. (2005) points out that the South Benguelan fishery operates on a higher trophic level than in other EBCSs due to the differing diet of small pelagics, and composition of the catch. This resulted in a more than doubled estimate over the Peruvian fishery in *Flows required per unit of catch* ([t 1°prod] [t catch]$^{-1}$ km^{-2} y^{-1}). Despite this energetically more costly target species, the fishery in the southern Benguela was determined to require a smaller proportion of primary production to sustain it when compared to the Peruvian system (4% and 10%, respectively), reflecting the lower fishing rates in the Benguela. There may also be a larger impact from the fishery on the Peruvian system's dynamics due both to a larger total flow required to sustain the fishery as well as it being more focused on the dynamically important small pelagics. The mixed trophic impact analysis of the Peruvian system from 1960-69 also shows the fishery to be the highest-impacting group with a largely negative net effect overall (Fig. II.7).

4.2. Predator/prey impacts

The models of the Southern Benguela have focused on flows between zooplankton abundances as the primary driver to small pelagics and higher trophic levels. The strength of this forcing has been addressed through search routines within Ecosim for best-fit estimations of vulnerability. The estimated vulnerabilities that "best-fit" the stock dynamics in the southern Benguela resembled wasp-waist forcing, thus, supporting the findings of Cury et al. (2000). This resulted in zooplankton being top-down controlled by anchovy, sardine, round herring and juvenile horse mackerel (high vulnerability), and with anchovy, sardine, round herring, and small hake exerting bottom-up control over their predators (low vulnerability). The adjustments of these vulnerabilities produced the most significant improvements to the fit of the simulation (40% reduction in *SS* over fitting with fishing rates alone), thus stressing the importance of the parameter in modeling trophic dynamics and, in particular, the role of small pelagics in upwelling systems (Shannon et

al., 2004a). Further searches for a 'best fit' of primary production improved *SS* by 4-6% and 12%, when applied after and before vulnerability searches respectively.

Shannon et al. (2004b) adjusted vulnerabilities between sardine and anchovy and their prey in order to simulate changing plankton fraction abundances (and hence their vulnerabilities) during the observed regime change from the 1980's to 1990's steady state models. In the application of the alternate state's vulnerability values between these groups (phyto- and zooplankton), the "opposite" regime was obtained, and changes to biomasses of many groups were in the same direction and of a similar order of magnitude. Furthermore, changes to the vulnerability of mesozooplankton alone were found to have similar effects (although of a smaller magnitude) to those of changes to both meso- and macrozooplankton. This led the authors to conclude that, "Model shifts between an anchovy 'regime' (1980's) and the possible move towards a sardine 'regime' (1990's) in the southern Benguela ecosystem are likely to have been caused by changes in the availability of mesoplankton to anchovy and sardine" (Shannon et al., 2004b).

In both examples, environmental forcing was considered more important than the effects of fishing in driving small pelagic dynamics. Furthermore, these examples help to add support for two main hypotheses concerning EBCS dynamics: 1) Wasp-waist forcing, and 2) importance of plankton quality ("environmental forcing").

The authors were able to explain about half the variance in the time-series based on a combination of fishing, vulnerability settings and productivity patterns. Whether this reduction is "significant" is unclear and difficult to assess. Even though some time series are well reproduced by the simulation (e.g. sardine and anchovy), the authors point out that many other time series do not show much of a trend and thus their validity must be questioned. Overall, the authors stress that such simulations are meaningful as a first step towards ecosystem modeling as well as a tool in evaluating ambiguity in trends from the more traditional stock assessment and survey series.

5. Prospective for real-time prediction

The dynamic models presented suggest and illustrate the importance of the links between plankton and small pelagics in driving EBCS dynamics. Unfortunately, periodic sampling of the plankton over such large spatial scales is difficult and so creates problems when trying to apply forcing functions to trophic models for the purpose of real-time prediction. On the other hand, plankton changes (especially phytoplankton) may be linked

more easily to abiotic indices available through remote sensing (e.g. sea surface temperature - SST, upwelling indices, ENSO indices – ex. “NIÑO3”) in an attempt to create predictors of changing plankton biomass. The Peruvian system may represent an ideal situation for such an exercise given evidence of a strong direct trophic link between phytoplankton production and small pelagics. As mentioned before, plankton quality is possibly as important as, if not more important than quantity in small pelagic dynamics and so estimation of chl *a* pigment concentrations alone through remote sensing may prove insufficient in estimating changes among different phytoplankton size fractions. Fortunately, historical plankton sampling data exists for the Peruvian coastal waters from previous research cruises (IMARPE, performed seasonally), and may allow for the calculation of biomass for different size fractions of phytoplankton either by flow cytometry or through biovolume calculation from cell counts (see Edler, 1979; Hillebrand et al., 1999; Sun and Liu, 2003).

An initial exercise to convert abundance values derived from published IMARPE cruise data into biovolume reveals the importance of large celled diatoms in the coastal zone (ca. 85% of total phytoplankton volume), coinciding with the anchovy’s principle habitat. Other phytoplankton taxonomic groups appear to be less affected by their proximity to the nearshore upwelling zone (Fig. II.8). While the tendency of decreasing volume offshore is consistent with remote sensing data (SeaWifs), calculated biovolume values are much higher for the nearshore zone. Several factors could explain such a discrepancy: 1) Conversion factors for chl *a* to wet weight provide only a rough estimate; 2) Limited *in situ* sample size (n=39); 3) Cloud cover typical of the Peruvian coast during strong upwelling periods may result in underestimations of chl *a* concentrations of nearshore waters. The conversion of historical data into volume is a major objective of IMARPE and should shed light on the dynamics of the plankton community in the coming years.

Highly productive phytoplankton assemblages, dominated by chain-forming diatoms, have been shown to occur in the Humboldt Current during the upwelling of cold, nutrient-rich waters to the photic zone. Comparing the degree of upwelling of this water mass (e.g. area in km^2 where SST <20°C) to the biomass of different phytoplankton size fractions may provide a simple empirical relationship. The likelihood of a strong correlation existing between upwelling strength and increased food supply to anchovy is high given that both adult populations as well as fecundity (egg production) have been observed to increase during periods of increased upwelling (Figs. II.5 and II.9). Watters et al. (2003) made use of a similar empirical model to force primary production in their trophic model of the eastern tropical Pacific; SST anomalies were correlated to surface chlorophyll concentrations and a forcing function was applied only to the biomass of large

phytoplankton due to observations that the biomass of diatoms varies substantially during warm and cold events, whereas picoplankton (i.e. small phytoplankton) biomass is relatively stable (Bidigare and Ondrusek, 1996; Landry et al., 1996).

At present, we are unaware of any attempts to use trophodynamic models for real-time prediction. The reason is obvious enough - prediction requires: 1) reliable trophic models based on empirical evidence, 2) model tuning to historical changes, and 3) links between easily observable indices and change to key drivers of the system. Fortunately, the creation of predictive models for the Peruvian upwelling system has many previous examples of work in EBCSs from which to draw from. Within the Peruvian system itself, fish stock dynamics observed over different time scales (decadal and El Niño) also provide valuable information on the Peruvian system's response to perturbation, useful in model tuning. Recent years have seen a much more advanced and thorough collection of data (e.g. satellite imagery, oceanographic measurements, hydroacoustical fish stock assessments), especially during the last large El Niño of 1997/98, which provide an opportune data set for fisheries ecologists to address the "Peruvian puzzle".

6. Summary: The role of trophic modeling in solving the puzzle

Our understanding of the functioning of EBCSs has advanced greatly in the past 60 years since large-scale fisheries began to exploit their enormous capacity for fish production. Our knowledge of the Peruvian upwelling system has benefited from several disciplines – from underlying physical and geochemical processes to predator-prey dynamics and the impacts of man. This review has attempted to illustrate the continuing role that trophodynamic modeling can play in exploring past and future change as well as bridging the gap between theory and management. In summary, several considerations were highlighted for the future construction of trophodynamic models for the Peruvian system:

1. Compartmentalization
    a. Plankton – Size-fractionated compartments of zooplankton and phytoplankton to take into account the feeding differences between small pelagic fish species (e.g. diatoms, micro- meso- and macrozooplankton)
    b. Life-history – Intra-species separations by size or other life-history classification taking into account differences in food intake, vulnerability to predation, and recruitment (e.g. Peruvian hake).

c. Additional functional groups – Several new groups should be added given new insight into their trophic importance (e.g. mesopelagics, cephalopods, benthic vs. pelagic feeding demersals)

2. Spatial

a. Latitude – Definition of boundaries that allow for the closure of the life cycle for key functional groups. In the Humboldt LME, anchovy and sardine stock delineations appear to be correlated to upwelling centers (e.g. north and central stocks from about 4°-15°S).

b. Extension from the coast – Due to the highly variable upwelling changes in Peru, a stationary boundary is recommended that encompasses the spatial dynamics of the key populations and/or biologically productive zone (ca. 100km, Ware, 1992; Nixon and Thomas, 2001)

3. Temporal – Steady-state models based on yearly averages are the most feasible given the sampling frequency in Peru. Focusing on the data-rich years since 1996, an immediate exploration of the dynamics surrounding the last El Niño of 1997/98 seems possible. Adaptation of past trophic models of the 1960's would benefit from an exploration of the impressive longer time-series data presented in the book edited by Pauly and Tsukayama (1987b)

In conclusion, the complex dynamics of EBCSs and their connections to environmental variability present an ideal situation for the application of multispecies models for management. This is one of many examples of marine resources along the Chilean and Peruvian coastline affected by environmental variability, which are being addressed under the EU-project, CENSOR – "Climate variability and El Niño Southern Oscillation: Impacts for natural resources and management." The ability of models to predict some of these changes has thus been a focus of the project due to the connection of these resources to that of resource users' livelihoods.

Acknowledgements

This study was financed and conducted in the frame of the EU-project CENSOR (Climate variability and El Niño Southern Oscillation: Impacts for natural resources and management, contract No. 511071) and is CENSOR publication No. 049.

Table and Figures

Table II.1. Functional groups for four steady-state Ecopath models of EBCSs. Symbol (**) indicates that the group was split into two classes within the model (e.g. small and large, juvenile and adult).

	Shannon & Jarre (1999) NORTHERN BENGUELA	Shannon et al. (2003) SOUTHERN BENGUELA	Jarre et al. (1991) NORTH AND CENTRAL PERU	Neira et al. (2004) CENTRAL CHILE
PRIMARY PRODUCERS	Phytoplankton	Phytoplankton	Phytoplankton	Phytoplankton
	Benthic producers	Benthic producers	Benthic producers	
ZOOPLANKTON	Microzooplankton[1]	Microzooplankton[1]	Zooplankton	Copepods
	Mesozooplankton[2]	Mesozooplankton[2]		Euphausiids
	Macrozooplankton[3]	Macrozooplankton[3]		
	Gelatinous zooplankton[4]	Gelatinous zooplankton[4]		
SMALL PELAGIC FISH	Anchoveta[5]	Anchovy[5]	Anchoveta[37]	Anchovy**[37]
	Sardine[6]	Sardine[6]	Sardine[38]	Pilchard**[39]
	Goby[13]	Other sm. pelagic fish[8,12,13]	Mackerel[40]	Horse mackerel[41]
	Horse Mackerel[11]	Chub mackerel[10]	Horse Mackerel[41]	
	Mesopelagic fish[14,16]	Horse mackerel**[11]		
	Chub mackerel[10]	Mesopelagic fish[15,16]		
	Other sm. pelagic fish[8,12,9]	Redeye[9]		
OTHER PELAGICS	Cephalopods[17,18]	Cephalopods[17,18]	Other pelagics	
		Pelagic-feeding chondrichthyans		
DEMERSALS	Hake[19,20]	M.capensis**	Hake[42]	Chilean hake**[42]
	Other demersals[21,22,23,24,25,26]	M.paradoxus**	Other demersals	Black conger[51]
		Pelagic-feeding demersal fish		Rattail fish[52]
		Benthic-feeding demersal fish		Big-eye flounder[53]
				Cardinal fish[54]
				Pacific sand perch[55]
				Skates[56]
LARGE PELAGIC FISH	Large pelagic fish[27,28,29,30,31]	Snoek[30]	Bonito[43]	
	Chondrichthyans	Other large pelagic fish[27,28,29,31,35]		
		Apex predatory chondrithyans		
BENTHOS	Meiobenthos	Meiobenthos	Meiobenthos	Carrot prawn**[49]
	Macrobenthos	Macrobenthos	Macrobenthos	Yellow prawn[50]
SEABIRDS	Sea birds	Seabirds	Cormorant[47]	
			Booby[48]	
			Pelican[46]	
MARINE MAMMELS	Seals[32]	Seals[32]	Sea lion[44]	Sea lion[44]
	Cetaceans[(e.g. 33,34)]	Cetaceans[(e.g. 36)]	Fur seal[45]	
			Other mammals	

[1]2– 200 µm equivalent spherical diameter; nanoflagellates, ciliates, zooplankton larvae; [2]200– 2000 µm; copepods, in particular Calanoides carinatus and Calanus agulhensis; [3]2– 20 mm; mainly euphausiids (on which most of the macrozooplankton estimates are based), but also includes groups such as amphipods and fish larvae; [4]Cnidaria, Ctenphora, tunicates, chaetognaths; [5]Engraulis capensis; [6]Sardinops sagax; [8]Saury (Scomberesox saurus); [12]Flying fish (Exocoetidae); [13]Pelagic goby (Sufflogobius bibarbatus); [9]Round herring (Etrumeus whiteheadi); [10]Scomber japonicus; [11]Trachurus trachurus capensis; [14]Lanternfish (Myctophidae); [15]Lanternfish (Lampanyctodes hectoris); [16]Lightfish (Maurolicus muelleri); [17]Loligo vulgaris reynaudii; [18]Todarodes angolensis; [19]Merluccius paradoxus; [20]Merluccius capensis; [21]West Coast sole (Austroglossus microlepis); [22]Kingklip (Genypterus capensis); [23]Rattails (e.g. Malacocephalus laevis and Coelorinchus simorhynchus); [24]Gurnard (Chelidonichthys spp.); [25]Jacopever; ribbonfish (Lepidopus caudatus); and [26]Monkfish (Lophius spp.); [27]Albacore tuna (Thunnus alalunga); [28]Yellowfin tuna (Thunnus albacares); [29]Big-eye tuna (Thunnus obesus); [30]Snoek (Thyrsites atun); [31]Kob (Agyrosomus inodorus); [32]Cape fur seal (Arctocephalus pusillus pusillus); [33]Dusky dolphin (Lagenorhynchus obscurus); [34]Heaviside's dolphin (Cephalorhynchus heavisidii); [35]Geelbeck (Atractoscion aequidens); [36]Bryde's whale (Balaenoptera edeni); [37]Engraulis ringens; [38]Sardinops sagax ; [39]Strangomera bentincki; [40]Scomber japonicus; [41]Trachurus murphyi; [42]Merluccius gayi; [43]Sarda chilensis; [44]Otaria flavescens (byronia); [45]Arctocephalus australis; [46]Pelecanus thagus; [47]Phalacrocorax bougainvillii; [48]Sula variegate; [49]Pleuroncodes monodon; [50]Cervimunida johni; [51]Black conger (Genypterus maculates); [52]Rattail fish (Coelorhyncus Aconcagua); [53]Big-eye flounder (Hipoglossina macrops); [54]Cardinal fish (Epigonus crassicaudus); [55]Pacific sand perch (Prolatilus jugularis); [56]Skates (Raja spp.);

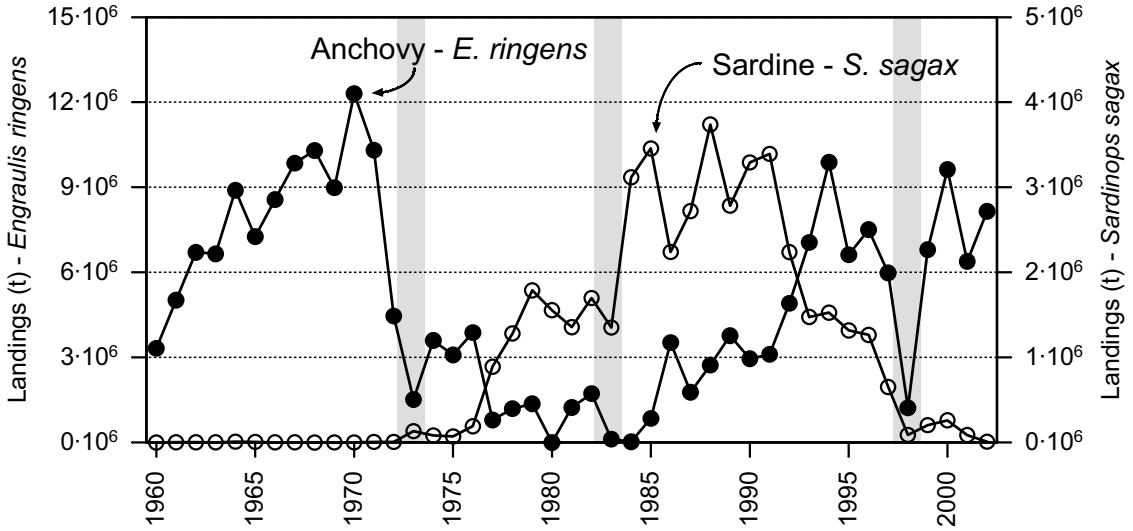

Figure II.1. Landings of anchovy, *Engraulis ringens*, and sardine, *Sardinops sagax*, in Peru (Sea Around Us, 2006). Grey shading denotes strong ENSO periods.

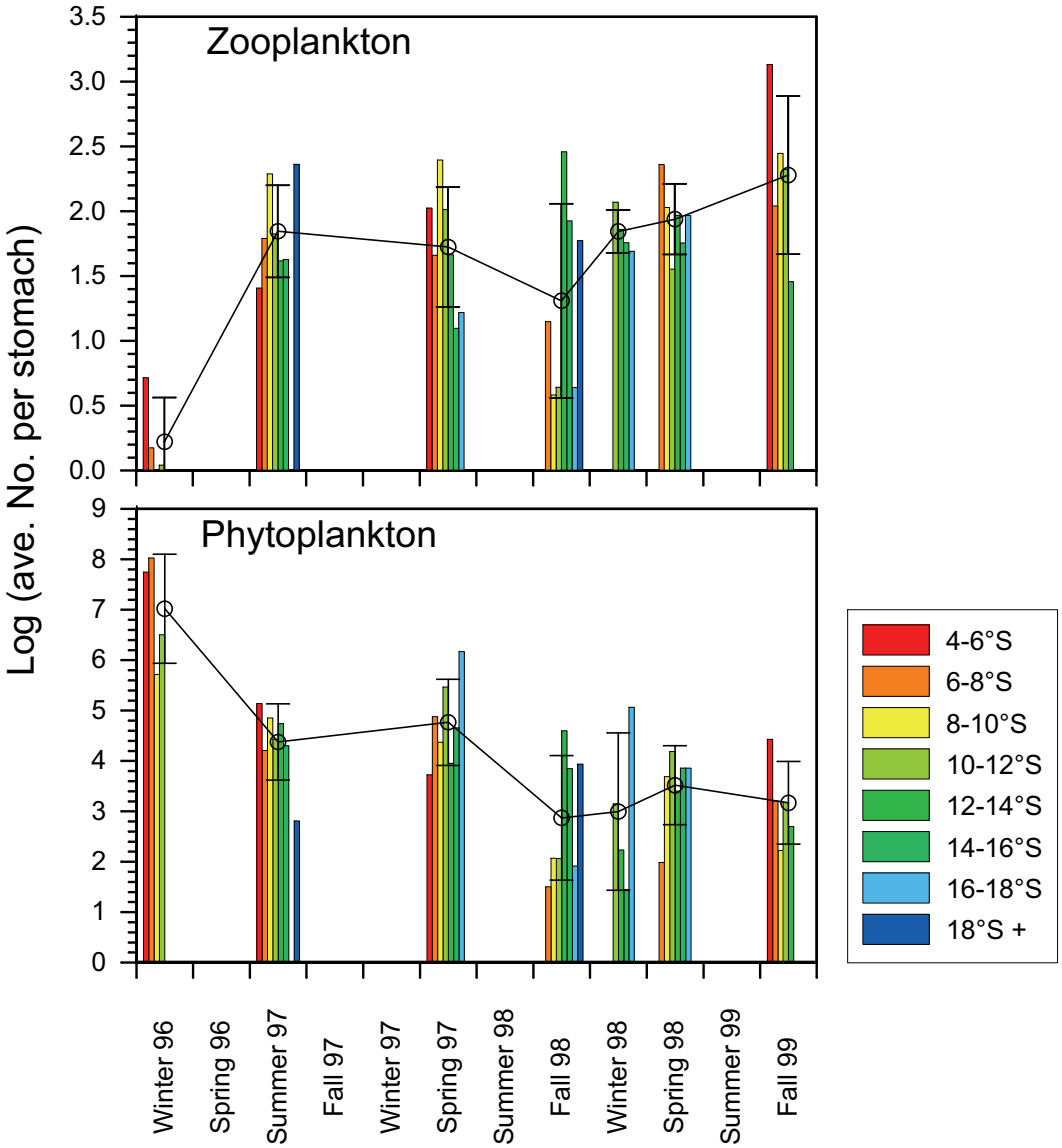

Figure II.2. Abundances of zooplankton and phytoplankton in anchovy Engraulis ringens stomach samples [Log(ave. No. per stomach)] by season between winter 1996 and fall 1999. Average values and standard deviation (open circles and bars) are calculated for available latitudes where samples were collected. Data is adapted from various publications of the Instituto del Mar del Peru-IMARPE, Callao (Alamo et al., 1996b; Alamo et al., 1997a; Alamo et al., 1997b; Alamo and Espinoza, 1998; Espinoza et al., 1998a; Espinoza et al., 1998b; Blaskovic et al., 1999).

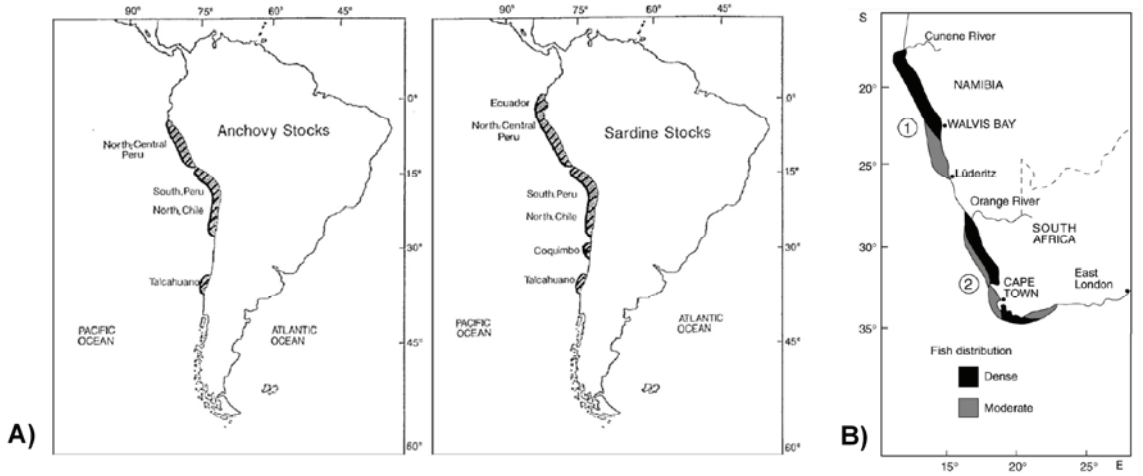

Figure II.3. Schematic presentation of areas of distribution of anchovy and sardine stocks in A) Humboldt Current LME (from Alheit and Ñiquen, 2004; reproduced with permission) and B) Benguela LME, (1) Northern Benguela upwelling system, (2) Southern Benguela upwelling system (from Shannon et al., 2003; reproduced with permission).

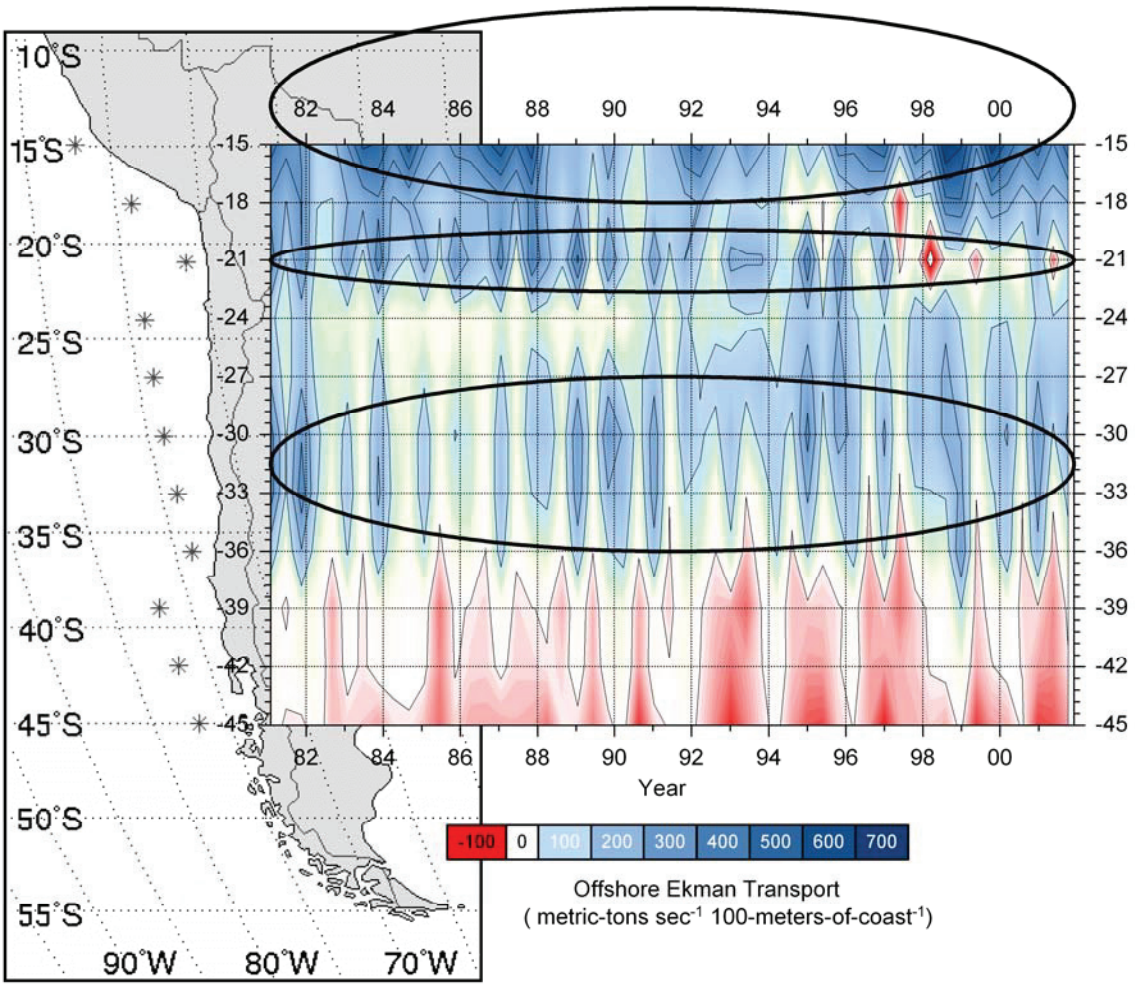

Figure II.4. Three main centers of upwelling in the Humboldt LME (circled) as inferred from estimations of offshore Ekman transport by latitude and time (average monthly values). Data and calculated values by the Pacific Fisheries Environmental Laboratory - NOAA (2006).

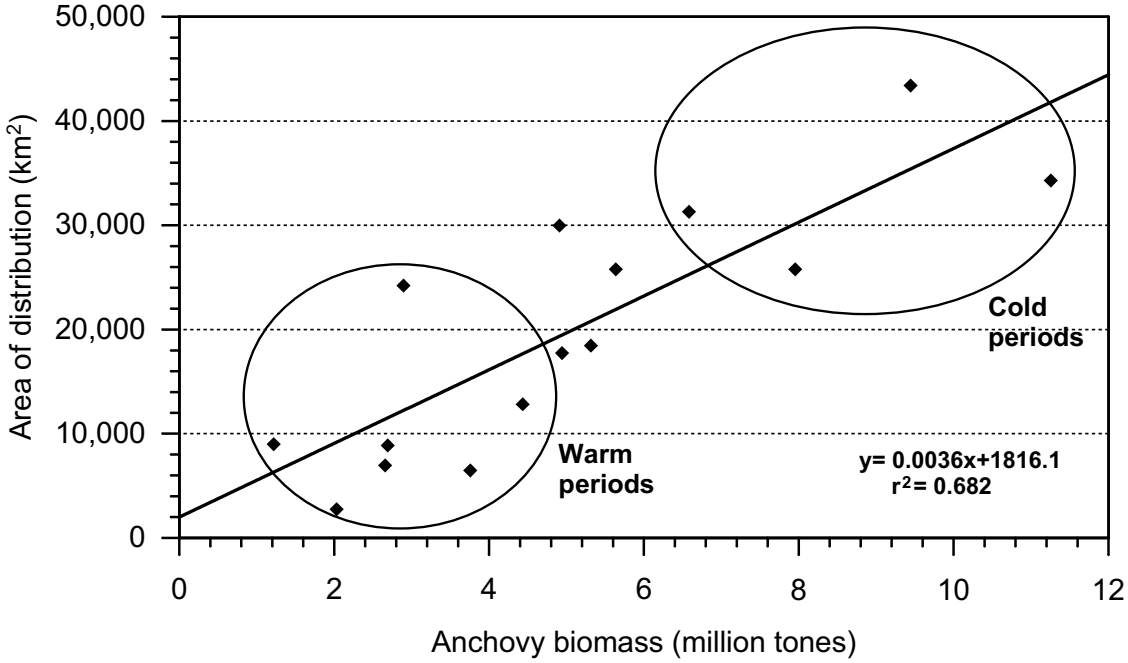

Figure II.5. Correlation between anchovy biomass and area of distribution in Peru (redrawn from Gutierrez Torero and Herrera Almirón, 2002). Biomass and area of distribution are seen to increase during cold periods of stronger upwelling.

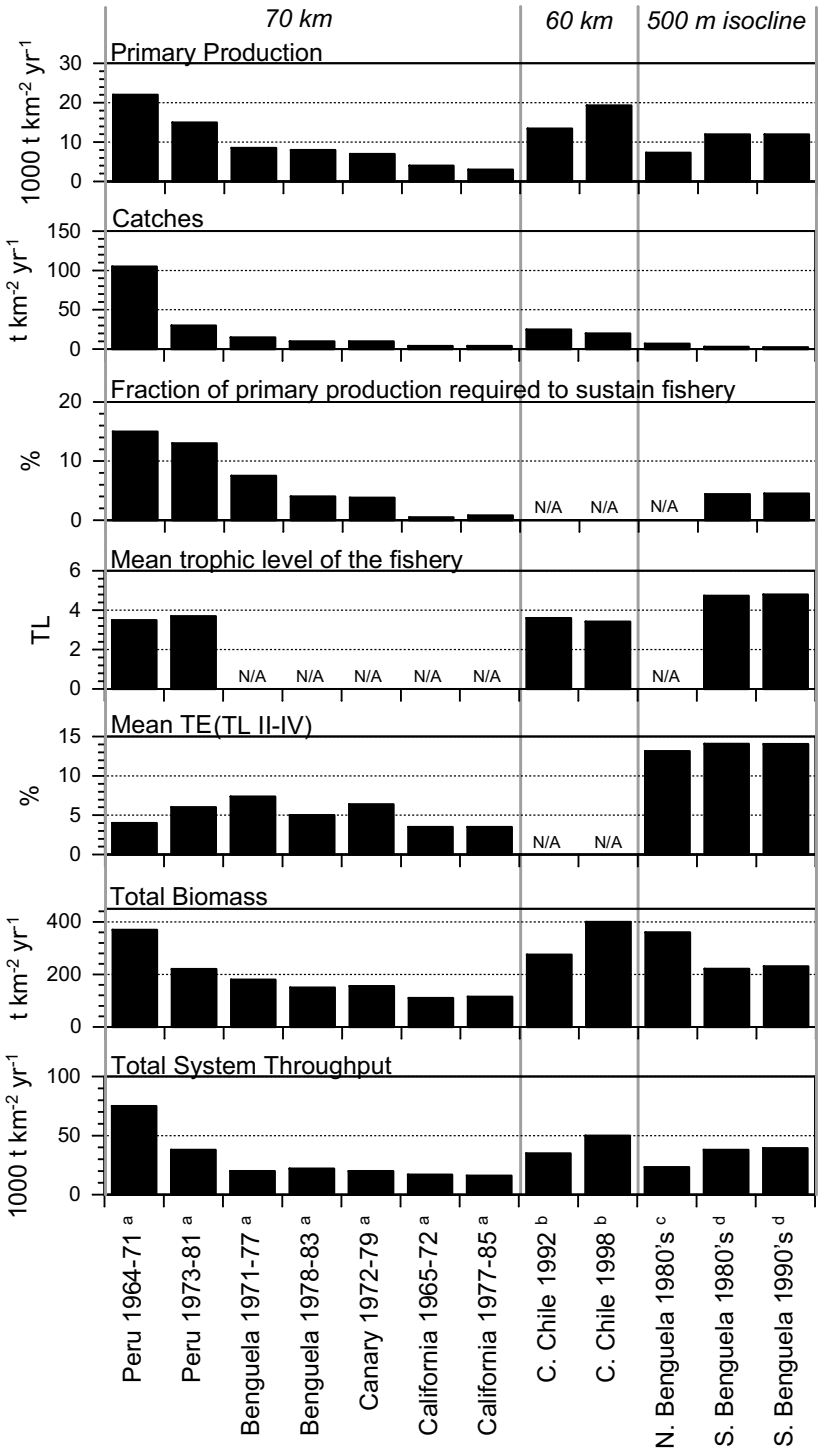

Figure II.6. Summary statistics of balanced Ecopath steady-state models for EBCSs. Grey vertical lines separate models using differing outer boundary definitions from the coast (value above). [a] (Jarre-Teichmann and Christensen, 1998); [b] (Neira et al., 2004); [c] (Shannon and Jarre-Teichmann, 1999); [d] (Shannon et al., 2003). *N/A* indicates values not provided by the authors.

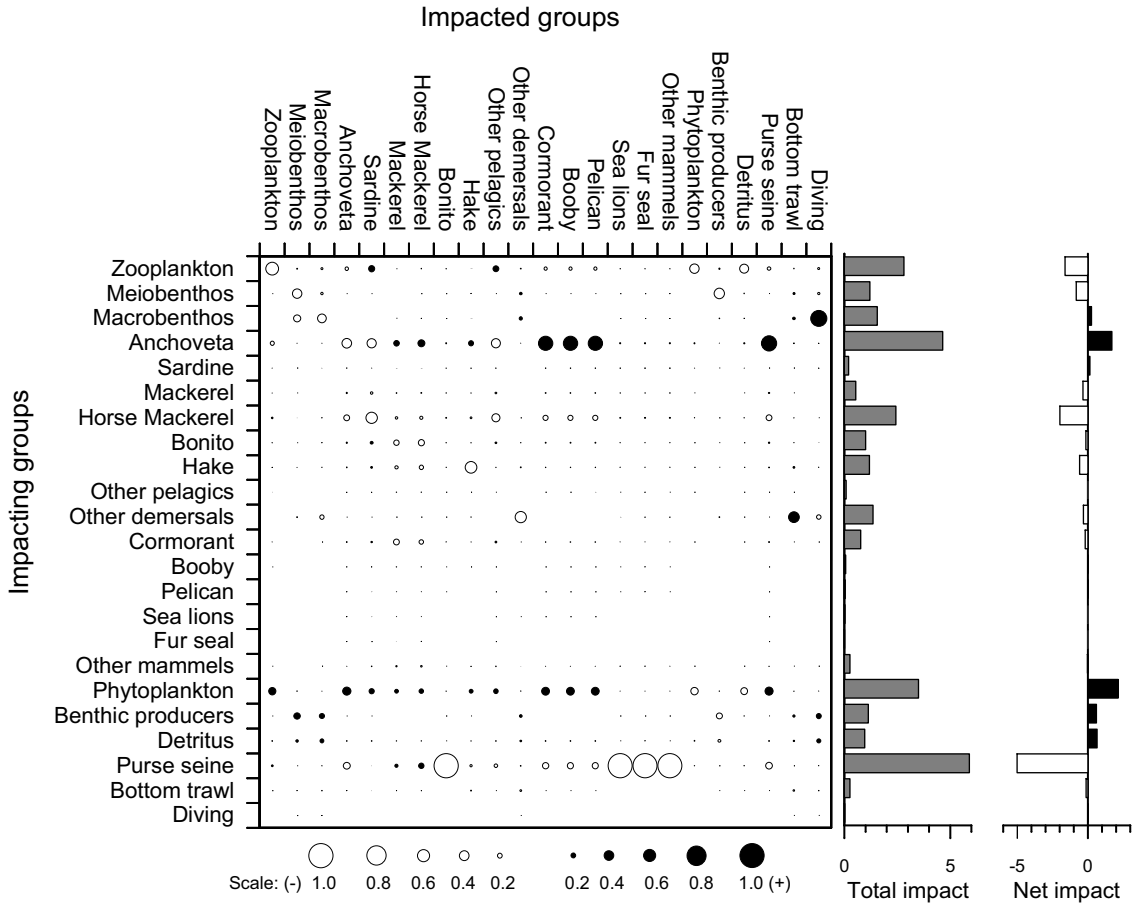

Figure II.7. Mixed trophic impact of the Peruvian upwelling system for the period 1960-69. Values are calculated by the program Ecopath through a input-output analysis as developed by Ulanowicz and Puccia (1990). Produced from data presented for the steady-state model by Jarre et al. (1991).

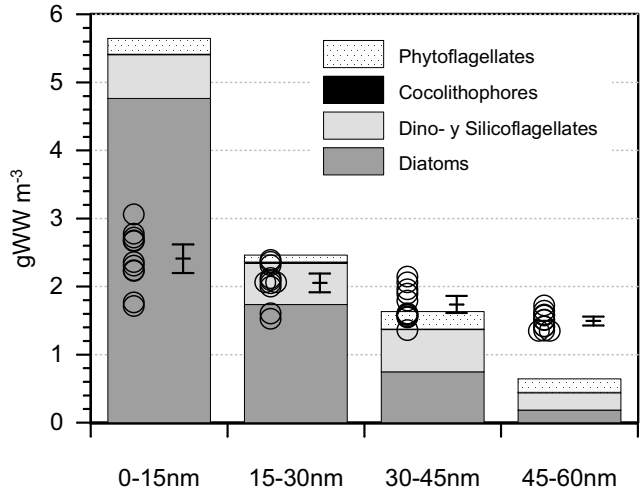

Figure II.8. Biovolume calculation (grams wet weight) of different phytoplankton fractions by distance from the coast (nautical miles) in Peru during summer 2000. Calculated from species abundance values from Delgado et al. (2001b). Remote sensing values from SeaWifs during the summer 2000 were converted from mg chl *a* m-3 to wet weight [chl*a*:Carbon (40:1) (Brush et al., 2002), Carbon:wet weight (14.25:1) (Brown et al., 1991)] and are presented for comparison (circles = eight-day averages; bar = seasonal average and SD).

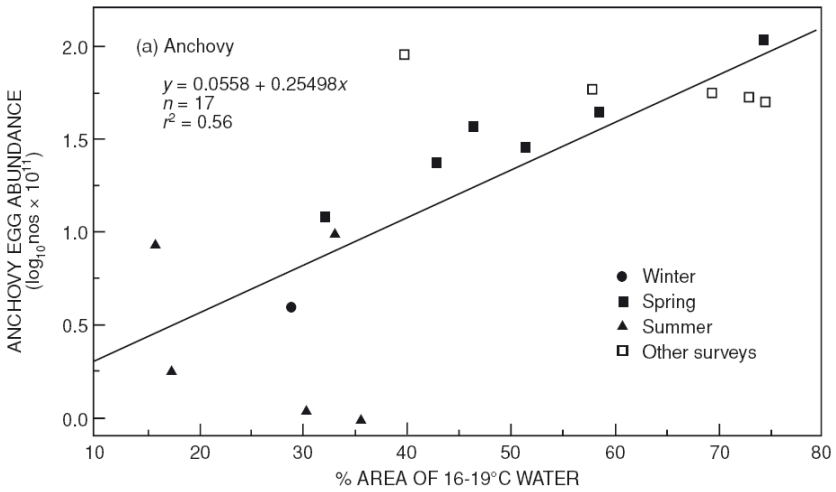

Figure II.9. Relationship between total anchovy egg numbers on the western Agulhas Bank (Benguela) and the area of 16-19°C water (arcsine transformed to improve normality) during SA SARP surveys (winter, spring and summer) and five pelagic spawner biomass surveys (November 1988-1992; from Richardson et al., 1998; reproduced with permission)

Chapter III. Trophic modeling of the Northern Humboldt Current Ecosystem, Part I: Comparing trophic flows during 1995-96 and 1997-98

Jorge Tam[*]*, Marc H. Taylor, Verónica Blaskovic, Pepe Espinoza, R. Michael Ballón, Erich Díaz, Claudia Wosnitza-Mendo, Juan Argüelles, Sara Purca, Patricia Ayón, Luis Quipuzcoa, Dimitri Gutiérrez, Elisa Goya, Noemi Ochoa, Matthias Wolff*

Author's posting. This is the author's version of the work. Please cite the final version to be published by Progress in Oceanography as part of the Proceedings of the Conference, *The Humboldt Current System: Climate, ocean dynamics, ecosystem processes, and fisheries*, Lima, Peru, November 27 - December 1, 2006. Article accepted November 8th, 2007

Abstract

El Niño 1997-98 was one of the strongest warming events of the past century, where phytoplankton species composition changed and biomass was greatly reduced along the Peruvian coast. While responses of the main fish resources to this natural perturbation are relatively well known, an understanding of the ecosystem response required a holistic analysis through an ecotrophic multispecies approach. In this work, we constructed trophic models of the Northern Humboldt Current Ecosystem (NHCE) were constructed for the periods 1995-96 and 1997-98 to explore the impact of El Niño. The model area includes the latitudes 4°-16°S and extends to 60 nm from the coast. The

[*] Corresponding author, Email: (jtam@imarpe.gob.pe)

model consists of 32 groups and differs from previous models of the Peruvian system through: (i) division of plankton into size groups to account for ENSO changes and feeding preferences of small pelagics, (ii) increased detail of demersal groups and separation of life history stages of hake, (iii) incorporation of mesopelagic fishes, and (iv) incorporation of the jumbo squid (*Dosidicus gigas*), which has gained in importance since the last El Nino 1997-98. Results show that the El Niño 1997-98 reduced the size and organization of flows of the NHCE, but the overall functioning of the ecosystem was maintained. The reduction of diatom biomass during El Niño forced omnivorous planktivorous fishes to switch to a more zooplankton-dominated diet, increasing their trophic level. Consequently, the trophic level increased for several predatory groups (mackerel, other large pelagics, sea birds, pinnipeds) and for fishery catch. A high biomass of macrozooplankton was needed to balance the consumption by planktivores, especially during El Niño period when diatoms diminish dramatically. Despite overall lower catches, the higher primary production required-to-catch ratio implied a stronger ecological footprint of the fishery and stresses the need for a precautionary management of fishery resources during and after El Niño. Energetic indicators such as the lower primary production/biomass ratio suggest a more energetically efficient state of the ecosystem, while network indicators such as the lower cycling index and lower relative ascendency are rather indicative of a less organized state of the ecosystem during El Niño. Compared to previous models of the NHCE, this study found: (i) shrinking of ecosystem size in term of flows, (ii) slight changes in overall functioning, and (iii) use of alternate pathways leading to a higher ecological footprint of the fishery.

1. Introduction

The northern part of the Humboldt Current Ecosystem off Peru has been modeled by several approaches: carbon and nitrogen budget models (Dugdale and MacIsaac, 1971; Walsh and Dugdale, 1971; Walsh, 1981), mass balance models (Jarre et al., 1989, 1991; Jarre-Teichmann and Pauly, 1993; Ballón, 2005), a size-based model (Carr, 2003) and an empirical model (Jahncke et al., 2004). The southern part of the HCE has also been modeled at several latitudes (Wolff, 1994; Ortiz and Wolff, 2002a; Arancibia et al., 2003; Neira and Arancibia, 2004; Neira et al., 2004). These models have allowed for the inclusion of the HCE in comparative analyses between ecosystems (Jarre-Teichmann, 1998; Jarre-Teichmann and Christensen, 1998; Jarre-Teichmann et al., 1998; Moloney et

al., 2005). However, none of these models have focused on the strong impact of the interannual variability associated with an El Niño event.

According to Alheit and Ñiquen (from Alheit and Ñiquen, 2004; reproduced with permission) a regime shift occurred in Peru during the change from a cold to a warm period between 1968-1970, characterized by a reduction of zooplankton volumes and a decrease of anchovy biomass, followed by an increase in sardine stocks. However, another regime shift back to a cold period occurred during 1984-1986, and was characterized by an increase of phytoplankton biomass, a recovery of zooplankton volumes (see Ayón et al., in press), excellent recruitments of anchovy, and a decrease in sardine biomass.

Arntz and Fahrbach (1991) summarized the effects of El Niño 1982-83 on the ecosystem. In the pelagic subsystem, the deepening of the thermocline and increase of temperature provoked a collapse of the traditional trophic web, causing emigration of anchovy, and immigration of tropical and oceanic species. Gutierrez (2001) and Bertrand et al. (2004) described the effects of El Niño 1997-98 on anchovy distribution and abundance, confirming its migration to deeper waters with a concentration in very coastal areas, and attributing its biomass reduction to a decreased effectiveness of acoustic sampling, unfavorable environmental conditions, increase of natural mortality (accompanied with lower daily ration and condition factor), and to a much lesser degree to predation and fishery. Bouchon et al. (2001) analyzed the ichthyofauna fluctuations over an El Niño Southern Oscillation (ENSO) cycle and concluded that in cold years the pelagic community is characterized by a high productivity and a low diversity, but in warm years this pattern is reversed, due to the immigration of offshore and tropical species and the reduction of a single main species (anchovy). While responses of the main fish resources to ENSO-related perturbations are relatively well known (Aguilar, 1999; Tarazona et al., 2001), an understanding of the ecosystem response requires a holistic ecotrophic multispecies approach.

Given the observed changes in biomass and species composition, it is expected that El Niño will impact the food web perturbing the main energy channel through anchovy, redistributing flows through alternate pathways.

Previous models of the NHCE (Jarre et al., 1991), which described the trophic flows along three decades (1953-1959, 1960-1969, 1973-1979), brought great insight into our understanding of the ecosystem functioning, yet biological changes in the last decade, the availability of new data sets, and the advancement of trophodynamic modeling allowed for the construction of a new, updated and more detailed (through the inclusion of additional functional groups) model. We divided the phytoplankton compartment into two groups (diatoms and dino- and silicoflagellates) and zooplankton into three groups (micro-

, meso- and macro-zooplankton) to account for the feeding preferences of different small pelagic fish. We incorporated the groups of mesopelagic fishes and jumbo squid, which have gained in importance since the last El Niño 1997-98. We also increased the detail of demersal groups and separated the hake into three different life history stages.

The objective of this study is to compare steady-state trophic models corresponding to a cold period (1995-96) and a warm El Niño period (1997-98). We hypothesized that El Niño represents a system perturbation producing a reduction in ecosystem organization. Furthermore, this study provides the basis for an accompanying paper (Chapter IV) where dynamic simulations of ecosystem changes during the ENSO cycle of 1997-98 and subsequent years are performed and discussed.

2. Methods

2.1. Input data

Our models of the Northern Humboldt Current Ecosystem (NHCE) extend from 4ºS to 16ºS, and 60 nm offshore, covering an area of approximately 165000 km^2 (Fig. III.1). Data from June 1995 to May 1996 and from May 1997 to April 1998 were used as inputs for the cold "upwelling" and warm "El Niño" steady-state models, respectively, covering a full "biological year" each (*i.e.* starting from about the middle of a calendar year).

The models included 33 functional groups, namely: 1) diatoms, 2) dino- and silicoflagellates, 3) microzooplankton (20-200 μm), 4) mesozooplankton (200-2000 μm), 5) macrozooplankton (2-20 mm), 6) gelatinous zooplankton, 7) macrobenthos, 8) sardine (*Sardinops sagax*), 9) anchovy (*Engraulis ringens*), 10) mesopelagics (*Vinciguerria lucetia*, *Lampanyctus* sp., *Leuroglossus* sp.), 11) jumbo squid (*Dosidicus gigas*), 12) other cephalopods (*Loligo gahi*, *Octopus vulgaris*, *Logigunculla* sp.), 13) other small pelagics, 14) horse mackerel (*Trachurus murphyi*), 15) mackerel (*Scomber japonicus*), 16) other large pelagics, 17) small hake (*Merluccius gayi peruanus*, < 29 cm), 18) medium hake (*M. gayi peruanus*, 30-49 cm), 19) large hake (*M. gayi peruanus*, > 50 cm), 20) flatfishes (*Paralichthys adspersus*., *Hippoglosina sp*.), 21) small demersals, 22) benthic elasmobranchs, 23) butter fishes (*Trachinotus paitensis*, *Stromateus stellatus*, *Peprilus medius*), 24) congers, 25) medium demersal fishes, 26) medium sciaenids, 27) sea robin (*Prionotus stephanophrys)*, 28) catfishes (*Galeichtys peruvianus*), 29) chondrichthyans, 30) seabirds (*Phalacrocorax bougainvillii*, *Sula variegata*, *Pelecanus thagus*), 31) pinnipeds (*Otaria flavescens*, *Arctocephalus australis*), 32) cetaceans, and 33) detritus.

Models were constructed using the Ecopath with Ecosim (EwE) 5.1 (2006 version) software (Christensen et al., 2000). Steady-state models are based on two equations for each functional group (Christensen and Pauly, 1992):

the energy balance equation

$$Q = P + R + UF \quad (1)$$

where: Q = consumption, P = production, R = respiration, UF = unassimilated food (including excretion and egestion).
and, the production components equation

$$P = B * M0 + EX + B * M2 + BA \quad (2)$$

where: M0 = non-predatory mortality (expressed as a function of ecotrophic efficiency, EE), M2 = predatory mortality (expressed as a function of diet composition, DC), EX = export (including catch C and net migration, NM), BA = biomass accumulation.

Thus, the models required as input data: wet weight biomass (B, $t \cdot km^{-2}$), production/biomass ratio (P/B, y^{-1}), consumption/biomass ratio (Q/B, y^{-1}), catch (C, $t \cdot km^{-2} \cdot y^{-1}$) and diet composition (DC) for each functional group. One unknown parameter (B, P/B, Q/B or EE) can be estimated when solving the system of linear equations.

Input data for the models were gathered from published and unpublished sources (Table III.1). Catch values were obtained from IMARPE (2006) landing statistics and the Sea Around Us (2006) database; some values of P/Q and UF were obtained from Moloney et al. (2005).

Sea surface phytoplankton biomass was calculated from relationships of upwelling area vs. chlorophyll *a* (Chl. *a*) threshold as calculated by Nixon and Thomas (2001). Conversion factors of carbon/ Chl. *a* = 40 (Brush et al., 2002) and wet weight/carbon = 14.25 (Brown et al., 1991) were used to arrive to wet weight units. Proportion of diatoms vs. silico- and dinoflagellates in both periods were obtained from a time series (1992-2000) of species cell counts carried out by Universidad Nacional Mayor de San Marcos UNMSM at Ancón Bay, Central Peru (77°11' W -11°46' S). Phytoplankton cell counts were converted to biovolume using geometric formulas and software of Sun and Liu (2003); cell dimensions were obtained from literature (e.g. Strickland et al., 1969; NODC, 2006; SERC, 2006) or measured under a microscope at the UNMSM. In order to convert biomass units from m^3 to m^2, a mixed layer depth of approximately 40 m was estimated averaging vertical profiles of chl. *a* from several latitudes along the Peruvian coast, using

data from Calienes et al. (1985). Zooplankton body masses were calculated from abundance and biomass data (Ayon Dejo and Giron Gutierrez, 1997) and biovolume was calculated from individual counts by taxonomic group using length:weight relationships from Rippe (1996) with body dimensions obtained from Santander et al. (1981). Biovolume conversions were also needed to convert stomach content data for sardine and anchovy (numbers of phytoplankton cells and zooplankton individuals per stomach by species) into fractions by weight.

Using qualitative pedigree categories, pedigree index values and confidence intervals were assigned to model parameters. Pedigree index values assigned to NHCE models parameters are shown in Table III.2. The Ecopath Pedigree Index (P), which scales between 0 and 1, was 0.638 ($t^* = 4.54$, $n = 32$, $p < 0.001$), indicating a good quality of the models with parameters mostly based on local data. For comparison, of 50 Ecopath models reviewed by Morissette (2007), only 4 models had higher pedigree indices than the present study (upper 7.5 %).

Conservative estimates of biomass of some groups were calculated by the software assuming an EE = 0.95 (microzooplankton, macrozooplankton, gelatinous zooplankton, small pelagics, small demersals and other cephalopods). Ecotrophic efficiency ($0<EE<1$) and gross efficiency ($0<GE<0.4$) served as constraints for balancing the models. Models were mostly balanced by adjusting the diets of some groups based on the confidence levels of their values. The balanced diet composition of predatory groups for both periods is presented in Table III.3.

Based on the input data, the EwE software allowed for the calculation of some ecosystem indicators based on the characteristics of the food web and the energy flow (Table III.4).

3. Results and Discussion

3.1. Biomass and catch changes

Outputs of the balanced models are presented in Table III.5. During the cold period (1995-96), diatoms, mesozooplankton, anchovy, horse mackerel, mackerel and jumbo squid were dominant in their respective trophic levels in the NHCE. During El Niño 1997-98, biomasses of most groups had decreased (anchovy, jumbo squid, horse mackerel, hake, demersal fishes, seabirds and pinnipeds), mainly due to biomass

reduction in the lower trophic levels (diatoms, micro- and mesozooplankton). During El Niño, bottom oxygen concentrations increased, improving conditions for the macrobenthos and increasing the feeding supply for demersal fishes. However, biomasses of demersal fish species decreased (e.g. hake, small demersals), because macrobenthos biomass improved mainly in the central zone off Peru (10-15°S), while in the northern zone (3-10°S), where most demersal fish resources inhabit, only macrobenthos diversity improved (Quipuzcoa and Marquina, 2001).

Biomasses of some groups increased (Fig. III.2), in some cases due to better adaptation to low nutrient conditions or higher temperatures (dinoflagellates, macrozooplankton) and/or immigration (mesopelagics, small pelagics, large pelagics and chondrichthyans). During El Nino 1997-98, Delgado (2001a) found dinoflagellates (*e.g. Ceratium breve, Ceratium praelongum*), and Ayón et al. (1997) found fish larvae (*e.g. Hoplunnis pacifica, Monolene maculipinna*) south of their characteristic distribution migrating with the intrusion of warm water masses.

Catch reductions accompanied biomass reductions (Fig. III.3), with the exception of high catch changes of mackerel and catfish, whose fishing mortalities were quite low in the cold period. However, despite a reduction of 19.2 % in the total catch/total biomass ratio in the warm period (Table III.6), a slope less than 1.0 in the relationship between biomass and catch changes can be interpreted as a delay in the fishery to both increases and decreases in resource biomass. Future management measures, should consider that the absolute reduction of catches of a species during El Niño is not enough to guarantee its sustainability. Rather, in addition to closed seasons and size limits, the relative reduction of catches should be at least proportional to the reduction of biomasses for a coherent catch reduction, thus, allowing the exploitation rate (F/Z) to be maintained at an acceptable level. The general biomass and catch reductions during El Niño can also be appreciated in the pyramids given in Fig. III.4.

Separation of phytoplankton in two functional groups (diatoms and silico-dinoflagellates) allowed for the following of alternate pathways and differential responses of consumers. The reduction of diatom biomass during El Niño, forced omnivore planktivorous fishes (anchovy and other small pelagics) to shift to a higher proportion of zooplankton in the diet, increasing their trophic level. Also, Espinoza and Bertrand (in press) found in anchovy stomach contents a higher fraction of zooplankton in 1997-98 than in 1996. Modeled TL of anchovy increased from 2.35 to 3.17 from the cold period (1995-96) to the warm period (1997-98) (Table III.5). Consequently, the TL of piscivorous groups (large pelagics, seabirds, pinnipeds) also increased. Sardine consumption of diatoms and dinoflagellates increased slightly, possibly in compensation for the increased

competition with anchovy for zooplankton, and because sardines are more efficient removers of small particles than anchovy (Van der Lingen et al., 2006).

Zooplankton sampling by IMARPE (300 μm mesh size nets towed from 50 m depth) captures mainly mesozooplankton, while macrozooplankton, specifically euphausiids, are usually undersampled due to their deeper distribution. For this reason, biomass of macrozooplankton is calculated by the model, resulting in 21.1 $t \cdot km^{-2}$ during 1995-96, and 34.8 $t \cdot km^{-2}$ during 1997-98. The high estimated biomasses are conservative estimates given that they were back-calculated using an ecotrophic efficiency (EE) of 0.95. Backcalculations of biomass are to be taken with caution and should ultimately be complemented with dynamic approaches using Ecosim, preferably with long time series, in order to represent more powerful constraints for models (Chapter IV; Guénette et al., in press). Nevertheless, the existence of such a high macrozooplankton biomass is supported by Antezana (Antezana, 2002a) who described adaptations of *Euphausia mucronata* indicating active use of the oxygen minimum layer, with high biomass values in the HCS of up to 500 g wet weight / 1000 m^3, between 100-200 m during the winter of 1974 (Antezana, 2002b). Neira et al. (2004) models also estimated high biomasses of euphausiids in order to meet the consumption requirements of predators and, furthermore, estimated an increase in biomass from 73.6 $t.km^{-2}$ in 1992 to 106.3 $t.km^{-2}$ in 1998 off Central Chile, in the Southern HCE.

Moreover, the temporal variation of the diet of anchovy reported by Espinoza and Bertrand (in press) emphasized the importance of zooplankton over phytoplankton. All this evidence points to a high biomass of macrozooplankton in the NHCE as a prey of several species, especially during El Niño periods when diatoms diminish dramatically.

3.2. Trophic flows

A comparison of ecosystem indicators of both models is presented in Table III.6. According to Ulanowicz (1997), the size of an ecosystem can be measured by its total activity in terms of flows, or the total system throughput. In addition to the total biomass reduction (-26.7 %), total system throughput had a dramatic reduction (-58.7 %), along with a reduction of absolute flows used for consumption, exports, respiration and detritus. This reduction in the size of the modeled ecosystem in terms of flows during El Niño is well reflected in the flow pyramids (Fig. III.4).

A large decrease in total primary production during El Niño 1997-98 (-59.5 %) was the main factor in the decreased ecosystem "size" or total system throughput. The relative changes in the percentage contributions of total throughput (Tab. 6) shows on one

hand an increase in consumption, and on the other hand a reduction in exports and flows into detritus. The relative reduction in exports and flows into detritus reflects an increase in grazing efficiency of meso- and macrozooplankton on phytoplankton. These relative flow changes were however small, indicating that although El Niño alters the system's size and some pathways, the overall ecosystem functioning is greatly maintained.

While a comparison between ecotrophic models should ideally be based on a common model structure (Moloney et al., 2005), it is noteworthy that the total system throughput (*ca.* 60000 $t.km^{-2}y^{-1}$) in the 1964-71 model before the anchovy collapse (Jarre-Teichmann et al., 1998) is similar to the value (55689 $t.km^{-2}y^{-1}$) obtained for the 1995-96 model. Despite this similarity, we should take into account that total system throughput is rather invariant to topological changes, but more affected by flow changes.

Main anchovy predators were horse mackerel, mackerel, hake and seabirds. Models results showed that predators consumed 28 % and 46 % of anchovy production in the cold period (1995-96) and warm period (1997-98), respectively. Medium hake mainly preyed upon anchovy, sea robin, small pelagics and small demersals, while jumbo squid preyed upon mesopelagics and macrozooplankton.

Transfer efficiencies (TE) during the cold period (1995-96) were similar as for other upwelling systems with most TEs under 10 % (Christensen and Pauly, 1995), except for a peak value at TL III (17 %) due to high utilization of anchovy production (Fig. III.5). The reduced TEs at high TLs during the El Niño period could reflect the bottom-up control of anchovy over pinnipeds and seabirds. Majluf (1989) mentioned that changes in the availability or abundance of anchoveta affect pinnipeds, when anchoveta is scarce, and fur seals have to take a wider range of prey. Tovar et al. (1987) concluded that a lack of food is the ultimate cause for the mass mortalities of seabirds, as for every El Niño there is a corresponding decline of guano bird numbers. In general, during El Niño there was an increased utilization of energy at lower levels, while higher TLs have similar TEs.

Analyzing the mixed trophic impacts, during the cold period (1995-96) there was a positive impact of macrozooplankton on several functional groups (*e.g.* sea robin, mesopelagic fishes, horse mackerel and mackerel), and during the warm period (1997-98) this positive impact intensified for mesopelagic fishes and other cephalopods.

Consumption of macrozooplankton increased by 65 % during El Niño, assuming it was the main prey group in both periods for mesopelagic fishes. During El Niño, several immigrants come from equatorial and oceanic waters, such as chondrichtyans, mesopelagics (lightfish and lanternfish), other small pelagics and other large pelagics, which could impact as preys or predators at different trophic levels. Mesopelagic *Vinciguerria* sp. is known to move towards the coast during El Niño, offering an abundant prey field for jumbo squid. The increasing trend of jumbo squid, after El Niño 1997/98, was

in parallel to an increase of mesopelagics, thus a possible bottom-up control of mesopelagics over jumbo squid was explored with dynamic simulations (Chapter IV).

3.3. Ecosystem indicators

Percentage changes of modeled ecosystem indicators from 1995-96 to 1997-98 (Table III.6) showed that the overall reduction in primary production during El Niño, produced coherent changes in trophic, fisheries, energetic and network indicators.

Fishery indicators showed a reduction in catches, accompanied by lower catch/biomass ratio and pelagic catch/demersal catch ratio, but higher TL of the catch and PPR/catch ratio. In the NHCE the mean TL of the catch increased temporarily (+19 %) during El Niño 1997/98 mainly due to the increase of anchovy TL and a higher proportion of other species in the catch (e.g. mackerel, horse mackerel and other large pelagics). When only demersal fishes are taken into account, TL of the catch decreases during El Niño (from 3.66 to 3.34). However, at a larger spatio-temporal scale, the mean TL of the catch showed a decreasing trend from 1980 to 1994 in the South Pacific (Pauly et al., 1998), suggesting a fishing down the food web process, probably influenced by the post-collapse recovery of anchovy, the main target species of the fishery. Despite lower catches (-41 %), the increase of TLs of target species resulted in a higher PPR/catch ratio (+39 %), which implies a stronger ecological footprint of the more ecologically-costly fishery and stresses the need for a precautionary management of fishery resources during and after El Niño. Most energetic indicators (net system production, net primary production and primary production/biomass ratio) decreased, except the higher system biomass/throughput ratio, indicating a more energetically efficient ecosystem (Odum, 1969) during El Niño. However, network indicators such as lower Finn's cycling index and relative ascendency indicated a less "organized" ecosystem (Ulanowicz, 1997) during El Niño. This result is similar to that of Jarre and Pauly (1993) who estimated a seasonal decrease of cycling in winter and spring, due to lower biomass and activity of zooplankton and benthos as the principal consumers of detritus.

El Niño 1997-98 produced changes in species diversity and increased energetic efficiency temporarily; however, during the cold period (1995-96) trophic flows were more articulated, showing better adaptation of cold water species to upwelling conditions. Using models before and after the anchovy collapse, Pauly (Pauly) also mentioned that the Peruvian upwelling ecosystem was better organized before the strong El Niño of 1972-73 than thereafter. On a smaller spatial scale, Taylor et al. (Chapter VI) also found

a similar increase in energetic efficiency and decrease in ecosystem organization at Independencia Bay during El Niño.

In general, biomass and trophodynamic changes indicated that during El Niño 1997-98, the ecosystem temporarily moved from its original optimum operating point (Kay, 1991), but returned to it, in agreement with the consideration that El Niño is a typical perturbation to the NHCE.

4. Conclusions

While past modeling efforts dealt with interdecadal changes (Jarre et al., 1991), this study focused on the interannual changes associated with El Niño and the Southern Oscillation (ENSO) cycle. The main finding of previous models was a decrease in relative ascendency from the 1950s to the 1970s, after the decline of the anchoveta, which led to an increase in parallel energy transfer. The new models, with increased details in the planktonic and demersal groups, and incorporation of mesopelagic fishes and jumbo squid, allowed to determine three main impacts of an El Niño natural perturbation on the food web: (i) shrinking of ecosystem size in terms of flows, (ii) slight changes in overall functioning, and (iii) use of alternate pathways leading to a higher ecological footprint of the fishery.

Our models showed that El Niño 1997-98 reduced temporarily the size and organization of the NHCE, but the overall functioning of the ecosystem was maintained, as seen through similar breakdown of flows (*i.e*. consumption, respiration, flow to detritus and export) and mean TE. The reduction of diatoms biomass during El Niño, forced omnivore planktivorous fishes to shift toward a zooplankton dominated diet, which increased their trophic level. Consequently, trophic levels of piscivorous groups were also increased. Sardine consumption of diatoms and dinoflagellates increased, in order to compensate for the increased competition with anchovy for zooplankton, and because sardines are more efficient removers of small particles than anchovy. A high biomass of macrozooplankton was needed to balance the consumption by planktivores, especially during El Niño periods when diatoms diminish dramatically.

El Niño increased temporarily the trophic level of the catch, and despite lower catches, the higher PPR/catch ratio implied a stronger ecological footprint of the fishery, which stresses the need for a precautionary management of fishery resources especially adapted for the conditions during and after El Niño. Energetic indicators showed lower system primary production/biomass ratio during El Niño indicating a more energetically

efficient ecosystem, however network indicators showed a lower cycling index, especially at higher trophic levels, and relative ascendency suggesting a less organized ecosystem during El Niño 1997-98. These results give support to our general hypothesis that El Niño is a typical perturbation in the NHCE.

Acknowledgements

We want to thank Renato Guevara, Miguel Ñiquen, Mariano Gutiérrez, Carmen Yamashiro and Sonia Sánchez from IMARPE, for the shared information. We also thank Arnaud Bertrand and Timothée Brochier from the Institute of Research for Development (IRD) for discussions on anchovy ecology, the staff of the Oceanographic and Fishery Biological Modelling Research Center (CIMOBP, IMARPE) and the staff of the CENSOR project for their helpful comments. We also thank Dr. Lynne Shannon and an anonymous referee for their critical suggestions on the manuscript. The INCOFISH (Integrating Multiple Demands on Coastal Zones with Emphasis on Fisheries and Aquatic Ecosystems) project (Work Package 2) financed Michael Ballón and Claudia Wosnitza-Mendo. This study was partly financed and conducted in the frame of the EU-project CENSOR (Climate variability and El Niño Southern Oscillation: Impacts for natural resources and management, contract No. 511071) and is CENSOR publication No. 0085.

Table III.1. Input data for the models of the NHCE and their sources. Biomass (B), production (P), consumption (Q) and catch (C).

Functional group	B		P/B		Q/B	C		Source
Period	1995-96	1997-98	1995-96	1997-98	1995-98	1995-96	1997-98	
1. Diatoms	53.416	14.761	265	210				B, P/B calculated from Nixon and Thomas (2001) curve, 85 % (1995-96) and 46% (1997-98) of diatoms calculated from Ancon, Central Peru (Ochoa pers. comm.) and Sanchez (1996) data converted to biovolume.
2. Silico- and dinoflagellates	9.426	17.328	265	210				B, P/B calculated from Nixon and Thomas (2001) curve, 15 % (1995-96) and 86% (1997-98) of silico- and dinoflagellates calculated from data converted to biovolume from Ancon, Central Peru (Ochoa pers. com.) and Sanchez (1996).
3. Microzooplankton (20-200 um)			256	256				P/B from Sorokin and Kogelschatz (1979), diet from Shannon et al. (2003).
4. Mesozooplankton (200-2000 um)	31.164	17	40	40				B calculated from IMARPE data (Ayon pers. comm.), P/B from Moloney et al. (2005), diet from Shannon et al. (2003).
5. Macrozooplankton (2-20 mm)					46.55			Q/B from Antezana (2002a), diet from Shannon et al. (2003).
6. Gelatinous zooplankton			0.584	0.584				P/B from Jarre et al. (1998), diet from Shannon et al. (2003).
7. Macrobenthos	20.729	25.605	1.2	1.2	10			B calculated from IMARPE data (Gutierrez and Quipuzcoa, pers. comm.), P/B and Q/B from Walsh (1981) in Jarre et al. (1989), diet from Shannon and Jarre (1999).
8. Sardine (Sardinops sagax)	7.567	7.909	1.4	1.4		7.97	3.33	B calculated from IMARPE acoustic data (Gutierrez pers. comm.), P/B from Patterson et al. (1992), diet calculated from Alamo et al. (1996b; 1996a; 1997b); Alamo and Espinoza (1997a; 1998); Blaskovic et al. (1998; 1999); Espinoza et al. (1998a; 1998b).
9. Anchovy (Engraulis ringens)	83.293	33.34	2	2		30.47	14.48	B from IMARPE VPA (Ñiquen pers. comm.), P/B from Csirke et al. (1996), diet calculated from Alamo et al. (1996b; 1996a; 1997b); Alamo and Espinoza (1997a; 1998); Blaskovic et al. (1998; 1999); Espinoza et al. (1998a; 1998b).
10. Mesopelagics	6.882	22.375	1.4	1.4				B calculated from relationship between Vinciguerria lucetia and Dosidicus gigas from IMARPE acoustic data 1999-2005 (Gutierrez pers. comm.), P/B calculated from maximum age, diet calculated from IMARPE data (Blaskovic pers. comm.).
11. Jumbo squid (Dosidicus gigas)	0.524	0.243	8.91	8.91		0.19	0.01	B calculated from relationship between CPUE and B of Dosidicus gigas from IMARPE acoustic data 1999-2005 (Gutierrez pers. comm.), P/B from Alegre et al. (2005), diet calculated from IMARPE industrial fleet data (Blaskovic pers. comm.), Schetinnikov (1989), Nigmatullin et al. (2001).
12. Other Cephalopods			4.3	4.3		0.05	0.01	P/B from IMARPE VPA (Arguelles, pers. comm.), diet from Cardoso et al. (1998) and Villegas (2001).
13. Other small pelagics			1	1		0.69	2.36	P/B from Shannon et al. (2003) for saury (Scomberesox saurus), flying fish (Exocoetidae), pelagic goby (Sufflogobius bibarbatus), diet based on Jarre et al. (1989).
14. Horse mackerel (Trachurus murphyi)	11.568	3.03	1.2	1.2		1.45	1.94	B from IMARPE acoustic data (Gutierrez, pers. comm.), P/B from Moloney (Moloney et al., 2005), diet calculated from IMARPE data (Blaskovic pers. comm.).

Functional group	B		P/B		Q/B	C		Source
Period	1995-96	1997-98	1995-96	1997-98	1995-98	1995-96	1997-98	
15. Mackerel (Scomber japonicus)	8.488	6.892	0.85	0.85		0.10	1.34	B from IMARPE acoustic data (Gutierrez pers. comm.), P/B from Jarre et al. (1989), diet calculated from IMARPE data (Blaskovic pers. comm.).
16. Other large pelagics	0.589	1.757	0.85	0.4		0.25	0.35	B calculated from catch equal to 50% production, P/B from Jarre et al. (1989), diet calculated from IMARPE data (Blaskovic pers. comm.).
17. Small hake (Merluccius gayi peruanus, < 29 cm)	2.771	1.245	0.928	1.317		0.97	0.56	B from IMARPE VPA (Wosnitza pers. comm.), P/B calculated as average of Z from VPA of the age groups involved (Ballon pers.comm.), diet calculated from IMARPE data (Blaskovic pers. comm.).
18. Medium hake (M. gayi peruanus, 30-49 cm)	0.414	0.163	1.627	1.946		0.22	0.11	B from IMARPE VPA (Wosnitza pers. comm.), P/B calculated as average of Z from VPA of the age groups involved (Ballon pers.comm.), diet calculated from IMARPE data (Blaskovic pers. comm.).
19. Large hake (M. gayi peruanus, > 50 cm)	0.055	0.028	1.044	1.516		0.02	0.01	B from IMARPE VPA (Wosnitza pers. comm.), P/B calculated as average of Z from VPA of the age groups involved (Ballon pers.comm.), diet calculated from IMARPE data (Blaskovic pers. comm.).
20. Flatfishes	0.04	0.01	0.304	0.304		0.01	0.00	B from swept area data corrected with hake VPA (Wosnitza pers. comm.), P/B from Neira et al. (2004), diet calculated from IMARPE data (Blaskovic pers. comm.).
21. Small demersals			2.3	2.3		0.02	0.02	B from swept area data corrected with hake VPA (Wosnitza, pers. comm.), P/B from Wolff et al. (1998), diet calculated from IMARPE data (Blaskovic pers. comm.).
22. Benthic elasmobranchs	0.078	0.045	1	1		0.03	0.04	B from swept area data corrected with hake VPA (Wosnitza, pers. comm.), P/B based on Shannon et al. (2003), diet calculated from IMARPE data (Blaskovic pers. comm.).
23. Butter fishes	0.032	0.006	0.8	0.8				B from swept area data corrected with hake VPA (Wosnitza pers.comm.), P/B from Wolff et al. (1998), diet calculated from IMARPE data (Blaskovic pers. comm.).
24. Conger	0.019	0.004	0.75	0.75				B from swept area data corrected with hake VPA (Wosnitza pers. comm.), P/B from Wolff et al. (1998), diet calculated from IMARPE data (Blaskovic pers. comm.).
25. Medium demersal fish	0.2	0.211	1.32	2.48		0.13	0.14	B from swept area data corrected with hake VPA (Wosnitza, pers. comm.), P/B calculated from catch curve for Paralabrax humeralis (Ballon pers. comm.), diet calculated from IMARPE data (Blaskovic pers. comm.).
26. Medium sciaenids	0.369	0.218	0.746	1.085		0.07	0.04	B from swept area data corrected with hake VPA (Wosnitza pers. comm.), P/B calculated from catch curve for Cynoscion analis (Ballon pers. comm.), diet calculated from IMARPE data (Blaskovic pers. comm.).

Functional group	B		P/B		Q/B	C		Source
Period	1995-96	1997-98	1995-96	1997-98	1995-98	1995-96	1997-98	
27. Sea robin (Prionotus stephanophrys)	0.789	0.319	3.4	3.22				B from swept area data corrected with hake VPA (Wosnitza pers. comm.), P/B calculated from catch curve (Ballon pers. comm.), diet calculated from IMARPE data (Blaskovic pers. comm.).
28. Catfish	0.577	0.65	0.9	0.9		0.07	0.54	B from swept area data corrected with hake VPA (Wosnitza pers. comm.), P/B from Wolff et al. (1998), diet calculated from IMARPE data (Blaskovic pers. comm.).
29. Chondrichthyans	0.027	0.078	0.486	0.486		0.01	0.02	B calculated from catch equal to 50% production, P/B calculated from Frisk et al. (2001) and Au and Smith (1997), diet calculated from IMARPE data (Blaskovic pers. comm.).
30. Seabirds	0.067	0.01	0.04	0.04	60			B from IMARPE abundance data converted to biomass (Goya pers. comm.), P/B and Q/B from Jarre et al. (1989), diet from Guillen (Guillén, 1990).
31. Pinnipeds	0.072	0.053	0.1	0.1	45.9			B from IMARPE abundance data converted to biomass (Goya pers. comm.), P/B from Jarre et al. (1989), Q/B from Muck and Fuentes (1987) in Jarre et al. (1989), diet from Arias (2003).
32. Cetaceans	0.062	0.067	0.1	0.1	20			B calculated from modelled biomass of mysticetes, small and large odontocetes (Kaschner, 2004), 1.1 sightings ratio 1997/1995 calculated from Bello et al. (1998). Q/B from Moloney et al. (Moloney et al., 2005), diet based on Jarre et al. (1998).

Table III.2. Pedigree index values assigned to model parameters. Biomass (B), production (P), consumption (Q), diet and catch (C). Lower pedigree index values correspond to guesstimates or other models, while higher pedigree index values correspond to high precision estimates locally based.

Group	B	P/B	Q/B	Diet	Catch
1. Diatoms	0.7	0.5			
2. Dino- and silicoflagellates	0.7	0.5			
3. Microzooplankton	0	0.6	0.6	0.2	
4. Mesozooplankton	0.7	0.6	0.6	0.2	
5. Macrozooplankton	0.7	0.6	0.6	0.2	
6. Gelatinous zooplankton	0	0.2	0.6	0.2	
7. Macrobenthos	0.7	0.2	0.6	0.2	
8. Sardine	0.4	1	0.6	1	1
9. Anchovy	0.4	1	0.6	1	1
10. Mesopelagics	0.4	0.1	0.6	0.2	
11. Jumbo squid	0.4	1	0.6	0.5	1
12. Other Cephalopods	0.4	0.7	0.6	0	1
13. Other small pelagics	0	0.7	0.6	0	1
14. Horse mackerel	1	0.7	0.6	0.5	1
15. Mackerel	1	0.7	1	0.5	1
16. Other large pelagics	1	0.7	0.6	0.5	1
17. Small hake	1	1	0.6	1	1
18. Medium hake	1	1	0.6	1	1
19. Large hake	1	1	0.6	1	1
20. Flatfishes	0.4	0.8	0.6	0.7	1
21. Small demersals	0.4	0.2	0.6	0	
22. Benthic elasmobranchs	0.4	0.2	0.6	0.7	1
23. Butter fishes	0.4	0.2	0.6	0.7	
24. Conger	0.4	0.6	0.6	0.7	
25. Medium demersal fish	0.4	0.8	0.6	0.7	1
26. Medium sciaenids	0.7	0.8	0.6	0.7	1
27. Sea robin	0.7	0.8	0.6	0.7	
28. Catfish	0.4	0.1	0.6	0.7	1
29. Chondrichthyans	0	0.5	0.6	0.7	1
30. Seabirds	1	1	0.6	1	
31. Pinnipeds	1	1	0.6	1	
32. Cetaceans	0.4	0.6	0.6	0	

Table III.3. Balanced diet composition of predatory groups during the cold period (1995-96) and warm period (1997-98).

Prey \ Predator	Years	3	4	5	6	7	8	9	10	11	12	13	14	15	16	17	18	19	20	21	22	23	24	25	26	27	28	29	30	31	32
1. Diatoms	1995-96	0.300	0.850	0.500			0.042	0.692				0.300		0.002						0.600		0.423									
	1997-98	0.200	0.300	0.500			0.123	0.017				0.300								0.600		0.447									
2. Dino- and Silicoflagellates	1995-96	0.100	0.050	0.100			0.003	0.004																							
	1997-98	0.200	0.500	0.400			0.051	0.000																							
3. Microzooplankton	1995-96	0.200	0.100	0.400			0.037	0.000						0.000																	
	1997-98	0.150	0.200	0.100				0.003																							
4. Mesozooplankton	1995-96				0.640		0.704	0.281	0.021	0.075		0.650		0.029						0.400		0.186					0.004				
	1997-98				0.640		0.566	0.603	0.021	0.056		0.650	0.002	0.003						0.400											
5. Macrozooplankton	1995-96				0.120		0.214	0.023	0.979	0.222	0.850		0.560	0.862		0.070	0.003	0.132			0.019	0.028		0.256	0.001	0.975	0.108				0.300
	1997-98				0.120		0.260	0.377	0.979	0.184	0.850		0.469	0.265	0.002	0.201	0.006	0.000			0.061			0.076	0.000	0.611		0.021			0.300
6. Gelatinous zooplankton	1995-96				0.040																				0.004						
	1997-98				0.040																	0.053									
7. Macrobenthos	1995-96					0.070							0.030			0.090	0.001	0.001	0.200		0.565	0.179	0.114	0.383	0.641	0.025	0.572				
	1997-98					0.070							0.020	0.020		0.190	0.069	0.004			0.552	0.500	0.114	0.861	0.473	0.171	0.950	0.083			
8. Sardine	1995-96															0.060					0.031				0.013						
	1997-98													0.017							0.017				0.004				0.447		
9. Anchovy	1995-96									0.043			0.200		0.699	0.358	0.645	0.005	0.500		0.078			0.100	0.184		0.198	0.213	0.877	0.539	0.100
	1997-98									0.040				0.401	0.623	0.069	0.082	0.023	0.455		0.082			0.018	0.190			0.208	0.377	0.377	0.100
10. Mesopelagics	1995-96									0.387				0.005				0.011							0.001					0.004	
	1997-98									0.337				0.001		0.151	0.173	0.002												0.058	
11. Jumbo squid	1995-96									0.120					0.071	0.112					0.022				0.005			0.667			0.200
	1997-98									0.242							0.012	0.111			0.005							0.042			0.200
12. Other Cephalopods	1995-96									0.077			0.120	0.102	0.088	0.070		0.002			0.114		0.037	0.043	0.008			0.009			
	1997-98									0.069						0.035	0.005	0.005			0.015		0.037	0.002	0.031			0.125			
13. Other small pelagics	1995-96									0.044			0.040		0.001	0.005	0.055				0.002			0.001	0.037		0.001		0.036	0.009	
	1997-98									0.040			0.029	0.199	0.210	0.163	0.205	0.020			0.005			0.011	0.051	0.218			0.126	0.008	
14. Horse mackerel	1995-96																				0.001								0.015	0.015	0.200
	1997-98																	0.005			0.005							0.021		0.011	0.200
15. Mackerel	1995-96																														0.200
	1997-98																	0.076													0.200
16. Other large pelagics	1995-96																								0.001						
	1997-98															0.003					0.005				0.002			0.374			
17. Small hake	1995-96									0.032								0.386										0.099		0.013	
	1997-98									0.032						0.016	0.147	0.406										0.058		0.050	
18. Medium hake	1995-96																				0.049		0.218					0.011			
	1997-98																						0.216					0.004			
19. Large hake	1995-96																											0.001			
	1997-98																											0.001			
20. Flatfishes	1995-96																				0.002		0.009	0.001							
	1997-98																				0.005		0.009								
21. Small demersals	1995-96										0.050		0.040	0.000	0.141	0.165	0.046	0.115			0.099		0.031	0.186	0.031				0.072	0.410	
	1997-98										0.050		0.001	0.093	0.165	0.150	0.289	0.069			0.117		0.031	0.030	0.200			0.021	0.050	0.471	
22. Benthic elasmobranchs	1995-96																														
	1997-98																														
23. Butter fish	1995-96																								0.001						
	1997-98																				0.003				0.002						
24. Conger	1995-96																	0.030			0.000										
	1997-98																														
25. Medium demersal fish	1995-96																		0.300		0.009		0.324	0.030	0.003					0.006	
	1997-98															0.020	0.001	0.014	0.545		0.040		0.326	0.002	0.017			0.021		0.015	

26. Medium sciaenids	1995-96												0.159		0.007				0.050					0.004
	1997-98										0.002	0.011	0.241		0.029				0.030					0.010
27. Sea robin	1995-96										0.070	0.250	0.159				0.233							
	1997-98								0.001				0.024				0.233					0.021		
28. Catfish	1995-96														0.002						0.114			
	1997-98														0.014									
29. Chondrichthyans	1995-96																							
	1997-98																							
30. Seabirds	1995-96																							
	1997-98																							
31. Pinnipeds	1995-96																							
	1997-98																							
32. Cetaceans	1995-96																							
	1997-98																							
33. Detritus	1995-96	0.400		0.200	0.800				0.010							0.184	0.034		0.021		0.003			
	1997-98	0.450		0.200	0.800				0.479						0.045		0.034				0.050			
Import	1995-96				0.130		0.100	0.050																
	1997-98				0.130		0.100	0.050																

Table III.4. Ecosystem indicators and their definitions.

Ecosystem indicator	Definition (Christensen, 1994)
Trophic indicators:	
Total system throughput	Sum of all flows in a system, represents the size of the system in terms of flows.
Total net primary production	Summed primary production from all producers.
Mean transfer efficiency	Geometric mean of transfer efficiencies for trophic levels II-IV.
Connectance index	Ratio of the number of actual links to the number of possible links. It can be expected to be correlated with maturity.
Mixed trophic impact	Combined direct and indirect trophic impacts that an infinitesimal increase of any of the groups is predicted to have on the other groups of the ecosystem.
Fishery indicators:	
Mean trophic level of the catch	Sum of trophic levels of species in the catch weighted by their contribution to the catch.
Gross efficiency of the fishery	The sum of all realized fisheries catches relative to the total net primary production.
Primary production required to sustain catches (PPR)	Flows in each path towards the catch of a group are converted to primary production equivalents using the product of catch, production/consumption and the proportion of each group in the path in the diets of the other groups.
Energetic indicators:	
System primary production/respiration	Ratio between total primary production and total respiration. In mature systems, the ratio should approach 1.
System primary production/biomass	Ratio between total primary production and total biomass. In mature systems, the ratio should decline.
System biomass/throughput	Ratio between total biomass and total system throughput. In mature systems, the ratio should increase.
Network indicators:	
Finn's cycling index	Fraction of an ecosystem's throughput that is recycled.
Relative ascendency	Ratio between ascendency and developmental capacity, a measure of ecosystem network efficiency (organization).

Table III.5. Model outputs of the NHCE during the cold period (1995-96) and warm period (1997-98). Trophic level (TL), biomass (B), production (P), consumption (Q), ecotrophic efficiency (EE), gross efficiency (GE), catch (C), fishing mortality (F), non-predatory mortality (M0) and predatory mortality (M2). Parameters in bold were estimated by the model.

1995-1996	TL	B	P/B	Q/B	EE	GE	C	F	M0	M2
Functional group / parameter		($t.km^{-2}$)	(y^{-1})	(y^{-1})			($t.km^{-2}.y^{-1}$)	(y^{-1})	(y^{-1})	(y^{-1})
1. Diatoms	1.00	53.416	265.000	-	**0.801**	-	0.000	**0.000**	**52.690**	**212.310**
2. Dino- and silicoflagellates	1.00	9.426	265.000	-	**0.960**	-	0.000	**0.000**	**10.643**	**254.357**
3. Microzooplankton	**2.25**	**20.484**	256.000	**1024.000**	0.950	0.250	0.000	**0.000**	**12.800**	**243.200**
4. Mesozooplankton	**2.13**	31.164	40.000	**125.000**	**0.515**	0.320	0.000	**0.000**	**19.397**	**20.603**
5. Macrozooplankton	**2.50**	**21.096**	**19.085**	46.550	0.950	0.410	0.000	**0.000**	**0.954**	**18.131**
6. Gelatinous zooplankton	**2.98**	**0.017**	0.584	**2.920**	0.950	0.200	0.000	**0.000**	**0.029**	**0.555**
7. Macrobenthos	**2.06**	20.729	1.200	10.000	**0.994**	**0.120**	0.000	**0.000**	**0.007**	**1.193**
8. Sardine	**3.16**	7.567	1.400	**14.000**	**0.853**	0.100	7.969	**1.053**	**0.206**	**0.141**
9. Anchovy	**2.35**	83.293	2.000	**20.000**	**0.469**	0.100	30.474	**0.366**	**1.063**	**0.572**
10. Mesopelagics	**3.49**	6.882	1.400	**14.000**	**0.575**	0.100	0.000	**0.000**	**0.595**	**0.805**
11. Jumbo squid	**4.18**	0.524	8.910	**25.457**	**0.940**	0.350	0.186	**0.354**	**0.534**	**8.021**
12. Other Cephalopods	**3.50**	**6.584**	4.300	**12.286**	0.950	0.350	0.055	**0.008**	**0.215**	**4.077**
13. Other small pelagics	**2.77**	**7.804**	1.000	**10.000**	0.950	0.100	0.688	**0.088**	**0.050**	**0.862**
14. Horse mackerel	**3.57**	11.568	1.200	**12.000**	**0.130**	0.100	1.451	**0.125**	**1.044**	**0.031**
15. Mackerel	**3.59**	8.488	0.850	**8.500**	**0.048**	0.100	0.096	**0.011**	**0.809**	**0.029**
16. Other large pelagics	**3.60**	0.589	0.850	**8.500**	**0.503**	0.100	0.250	**0.425**	**0.422**	**0.003**
17. Small hake	**3.77**	2.771	0.928	**6.187**	**0.623**	0.150	0.975	**0.352**	**0.350**	**0.226**
18. Medium hake	**3.66**	0.414	1.627	**10.847**	**0.394**	0.150	0.218	**0.526**	**0.987**	**0.114**
19. Large hake	**4.32**	0.055	1.044	**6.960**	**0.295**	0.150	0.017	**0.307**	**0.736**	**0.001**
20. Flatfishes	**3.60**	0.040	0.304	**2.027**	**0.821**	0.150	0.006	**0.158**	**0.055**	**0.091**
21. Small demersals	**2.45**	**7.089**	2.300	**15.333**	0.950	0.150	0.019	**0.003**	**0.115**	**2.182**
22. Benthic elasmobranchs	**3.48**	0.078	1.000	**6.667**	**0.401**	0.150	0.031	**0.401**	**0.599**	**0.000**
23. Butter fishes	**2.44**	0.032	0.800	**4.000**	**0.039**	0.200	0.000	**0.000**	**0.768**	**0.032**
24. Conger	**4.21**	0.019	0.750	**5.000**	**0.823**	0.150	0.000	**0.000**	**0.132**	**0.618**
25. Medium demersal fish	**3.38**	0.200	1.320	**8.800**	**0.997**	0.150	0.125	**0.626**	**0.005**	**0.690**
26. Medium sciaenids	**3.24**	0.369	0.746	**4.973**	**0.859**	0.150	0.067	**0.181**	**0.105**	**0.459**
27. Sea robin	**3.49**	0.789	3.400	**17.000**	**0.897**	0.200	0.000	**0.000**	**0.351**	**3.049**
28. Catfish	**3.31**	0.577	0.900	**6.000**	**0.893**	0.150	0.068	**0.118**	**0.096**	**0.686**
29. Chondrichthyans	**4.74**	0.027	0.486	**3.240**	**0.508**	0.150	0.007	**0.247**	**0.239**	**0.000**
30. Seabirds	**3.39**	0.067	0.040	60.000	**0.000**	**0.001**	0.000	**0.000**	**0.040**	**0.000**
31. Pinnipeds	**3.45**	0.072	0.100	45.900	**0.000**	**0.002**	0.000	**0.000**	**0.100**	**0.000**
32. Cetaceans	**4.25**	0.062	0.100	20.000	**0.000**	**0.005**	0.000	**0.000**	**0.100**	**0.000**
33. Detritus	1.00		-	-	**0.814**	-	0.000	**0.000**	**0.000**	**0.000**

Table III.5 (continued). Model outputs of the NHCE during the cold period (1995-96) and warm period (1997-98).

1997-1998	TL	B	P/B	Q/B	EE	GE	C	F	M0	M2
Functional group / parameter		($t.km^{-2}$)	(y^{-1})	(y^{-1})			($t.km^{-2}.y^{-1}$)	(y^{-1})	(y^{-1})	(y^{-1})
1. Diatoms	1.00	14.761	210.000	-	**0.945**	-	0.000	**0.000**	**11.652**	**198.348**
2. Dino- and silicoflagellates	1.00	17.328	210.000	-	**0.841**	-	0.000	**0.000**	**33.286**	**176.714**
3. Microzooplankton	**2.18**	**6.572**	256.000	**1024.000**	0.950	0.250	0.000	**0.000**	**12.800**	**243.200**
4. Mesozooplankton	**2.24**	17.000	40.000	**125.000**	**0.947**	0.320	0.000	**0.000**	**2.104**	**37.896**
5. Macrozooplankton	**2.12**	**34.773**	**19.085**	46.550	0.950	0.410	0.000	**0.000**	**0.954**	**18.131**
6. Gelatinous zooplankton	**3.00**	**0.003**	0.584	**2.920**	0.950	0.200	0.000	**0.000**	**0.029**	**0.555**
7. Macrobenthos	**2.06**	25.605	1.200	10.000	**0.995**	**0.120**	0.000	**0.000**	**0.006**	**1.194**
8. Sardine	**2.99**	8.318	1.400	**14.000**	**0.396**	0.100	3.334	**0.401**	**0.846**	**0.153**
9. Anchovy	**3.17**	33.340	2.000	**20.000**	**0.679**	0.100	14.477	**0.434**	**0.642**	**0.924**
10. Mesopelagics	**3.12**	22.375	1.400	**14.000**	**0.137**	0.100	0.000	**0.000**	**1.208**	**0.192**
11. Jumbo squid	**4.14**	0.243	8.910	**25.457**	**0.853**	0.350	0.014	**0.058**	**1.305**	**7.547**
12. Other Cephalopods	**3.14**	**0.227**	4.300	**12.286**	0.950	0.350	0.012	**0.053**	**0.215**	**4.032**
13. Other small pelagics	**2.85**	**21.419**	1.000	**10.000**	0.950	0.100	2.357	**0.110**	**0.050**	**0.840**
14. Horse mackerel	**2.60**	3.030	1.200	**12.000**	**0.616**	0.100	1.937	**0.639**	**0.461**	**0.100**
15. Mackerel	**3.74**	6.892	0.850	**8.500**	**0.279**	0.100	1.345	**0.195**	**0.613**	**0.042**
16. Other large pelagics	**3.99**	1.757	0.400	**4.000**	**0.687**	0.100	0.351	**0.200**	**0.125**	**0.075**
17. Small hake	**3.59**	1.245	1.317	**8.780**	**0.909**	0.150	0.556	**0.447**	**0.120**	**0.751**
18. Medium hake	**3.89**	0.163	1.946	**12.973**	**0.354**	0.150	0.107	**0.656**	**1.257**	**0.033**
19. Large hake	**4.51**	0.028	1.516	**10.107**	**0.286**	0.150	0.012	**0.429**	**1.082**	**0.005**
20. Flatfishes	**4.14**	0.010	0.304	**2.027**	**0.882**	0.150	0.001	**0.100**	**0.036**	**0.168**
21. Small demersals	**2.49**	**4.897**	2.300	**15.333**	0.950	0.150	0.016	**0.003**	**0.115**	**2.182**
22. Benthic elasmobranchs	**3.33**	0.045	1.000	**6.667**	**0.933**	0.150	0.042	**0.933**	**0.067**	**0.000**
23. Butter fishes	**2.64**	0.006	0.800	**4.000**	**0.845**	0.200	0.000	**0.000**	**0.124**	**0.676**
24. Conger	**4.12**	0.004	0.750	**5.000**	**0.000**	0.150	0.000	**0.000**	**0.750**	**0.000**
25. Medium demersal fish	**3.11**	0.211	2.480	**16.533**	**0.905**	0.150	0.144	**0.682**	**0.236**	**1.561**
26. Medium sciaenids	**3.50**	0.218	1.085	**7.233**	**0.977**	0.150	0.043	**0.197**	**0.024**	**0.863**
27. Sea robin	**3.27**	0.319	3.220	**16.100**	**0.052**	0.200	0.000	**0.000**	**3.054**	**0.166**
28. Catfish	**3.01**	0.650	0.900	**6.000**	**0.937**	0.150	0.544	**0.837**	**0.057**	**0.006**
29. Chondrichthyans	**4.40**	0.078	0.486	**3.240**	**0.501**	0.150	0.019	**0.244**	**0.242**	**0.000**
30. Seabirds	**4.01**	0.010	0.040	60.000	**0.000**	**0.001**	0.000	**0.000**	**0.040**	**0.000**
31. Pinnipeds	**3.86**	0.053	0.100	45.900	**0.000**	**0.002**	0.000	**0.000**	**0.100**	**0.000**
32. Cetaceans	**4.05**	0.067	0.100	20.000	**0.000**	**0.005**	0.000	**0.000**	**0.100**	**0.000**
33. Detritus	1.00	-	-	-	**0.824**	-	0.000	**0.000**	**0.000**	**0.000**

Table III.6. Comparison of ecosystem indicators from models of the NHCE for both periods, including % change from the cold period (1995-96) to the warm period (1997-98).

Ecosystem indicators	1995-96	1997-98	% Change
Trophic indicators:			
Total system throughput (t km^{-2} yr^{-1})	55689	22986	-58.7
Sum of all consumption (t km^{-2} yr^{-1})	28478 (51.1%)	12259 (53.3%)	-57.0
Sum of all exports (t km^{-2} yr^{-1})	2004 (3.6%)	718 (3.1%)	-64.1
Sum of all respiratory flows (t km^{-2} yr^{-1})	14688 (26.4%)	6065 (26.4%)	-58.7
Sum of all flows into detritus (t km^{-2} yr^{-1})	10519 (18.9%)	3944 (17.2%)	-62.5
Sum of all production (t km^{-2} yr^{-1})	23847	9957	-58.2
Total net primary production (t km^{-2} yr^{-1})	16653	6739	-59.5
Net system production (t km^{-2} yr^{-1})	1965	674	-65.7
Total biomass (excluding detritus) (t km^{-2})	302	222	-26.7
Mean transfer efficiency (II-IV)	10.17	11.72	15.2
Connectance index	0.168	0.174	3.6
System omnivory index	0.203	0.190	-6.4
Fishery indicators:			
Total catches (t km^{-2} yr^{-1})	42.70	25.31	-40.7
Mean trophic level of the catch	2.62	3.12	19.1
Gross efficiency (catch/total net primary production)	0.0026	0.0038	46.5
Total catch / total biomass	0.14	0.11	-19.2
Pelagic/demersal catches	26.98	16.28	-39.7
PPR (t km^{-2} yr^{-1})	2420.1	1995.6	-17.5
PPR / total primary production (%)	14.5	29.6	103.8
PPR / catch	56.675	78.844	39.1
Energetic indicators:			
System primary production / respiration	1.134	1.111	-2.0
System primary production / biomass	55.089	30.403	-44.8
System biomass / throughput	0.005	0.010	100.0
Network indicators:			
Finn's cycling index	12.61	7.49	-40.6
Ascendency/development capacity (%)	46.2	40.4	-12.6

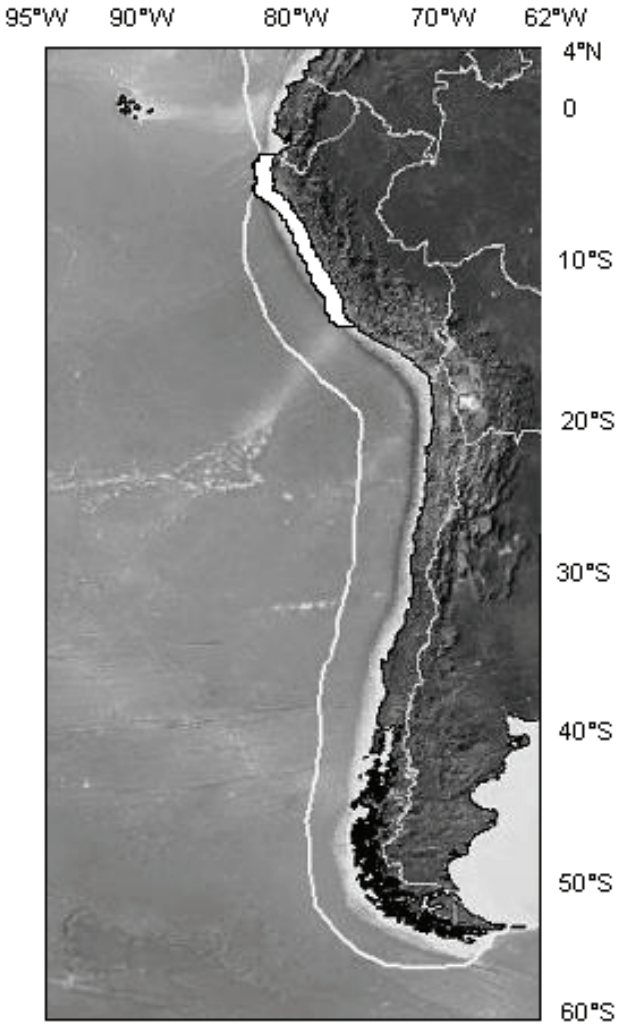

Figure III.1. Study area covers from 4ºS to 16ºS, and up to 60 nm (white shaded area), in the Northern Humboldt Current Ecosystem (delineated by the white line) (modified from EDC, 2006)

.

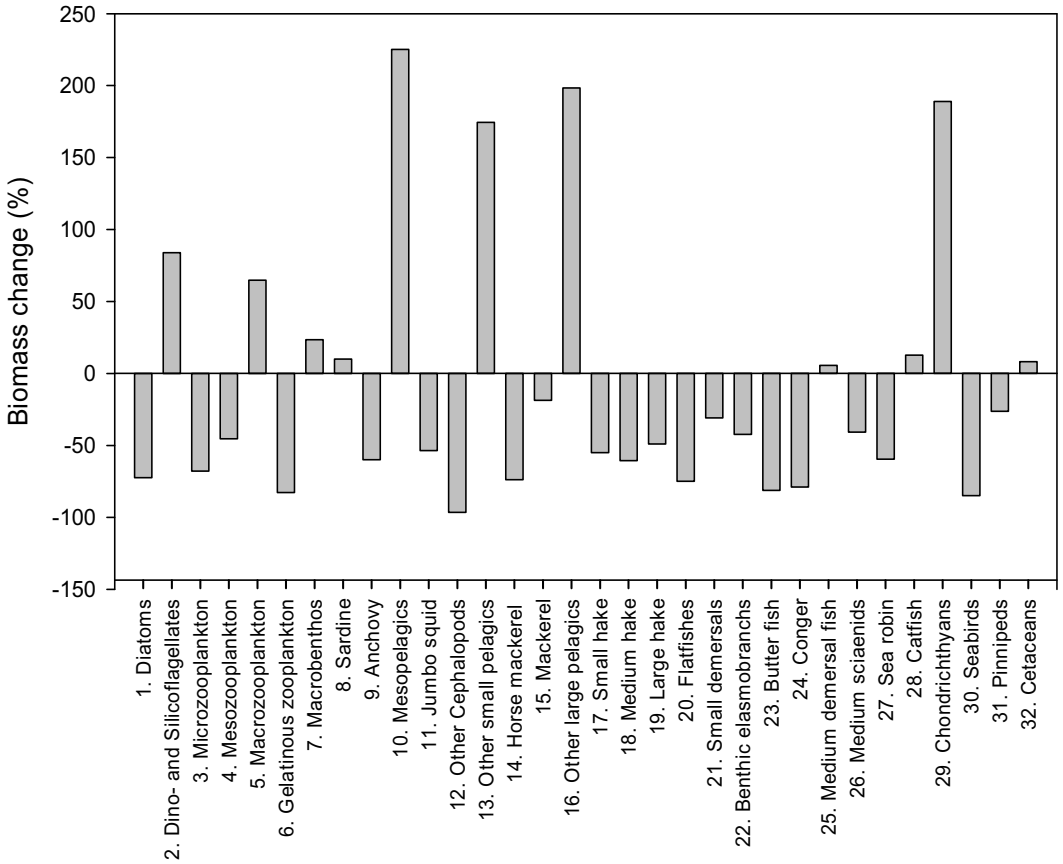

Figure III.2. Percentage biomass changes of functional groups from the cold period (1995-96) to the warm period (1997-98).

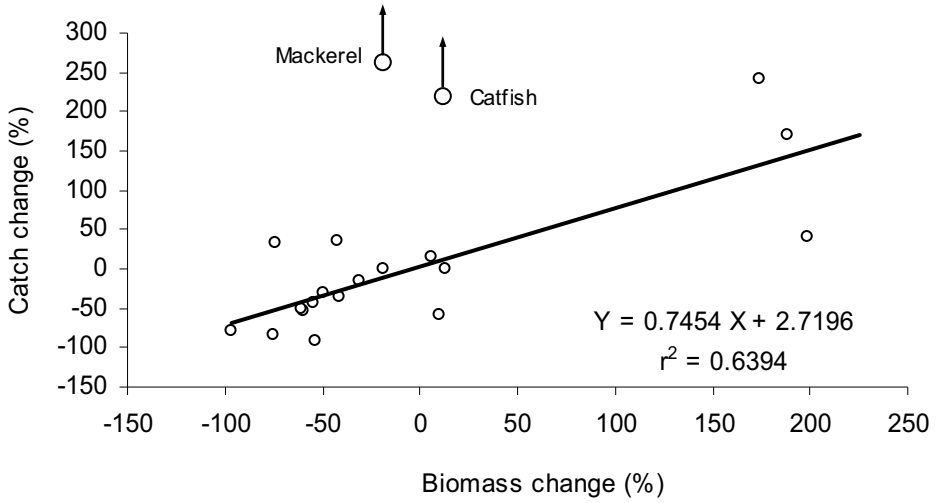

Figure III.3. Relationship between percentage biomass changes and percentage catch changes (excluding mackerel and catfish) from the cold period (1995-96) to the warm period (1997-98).

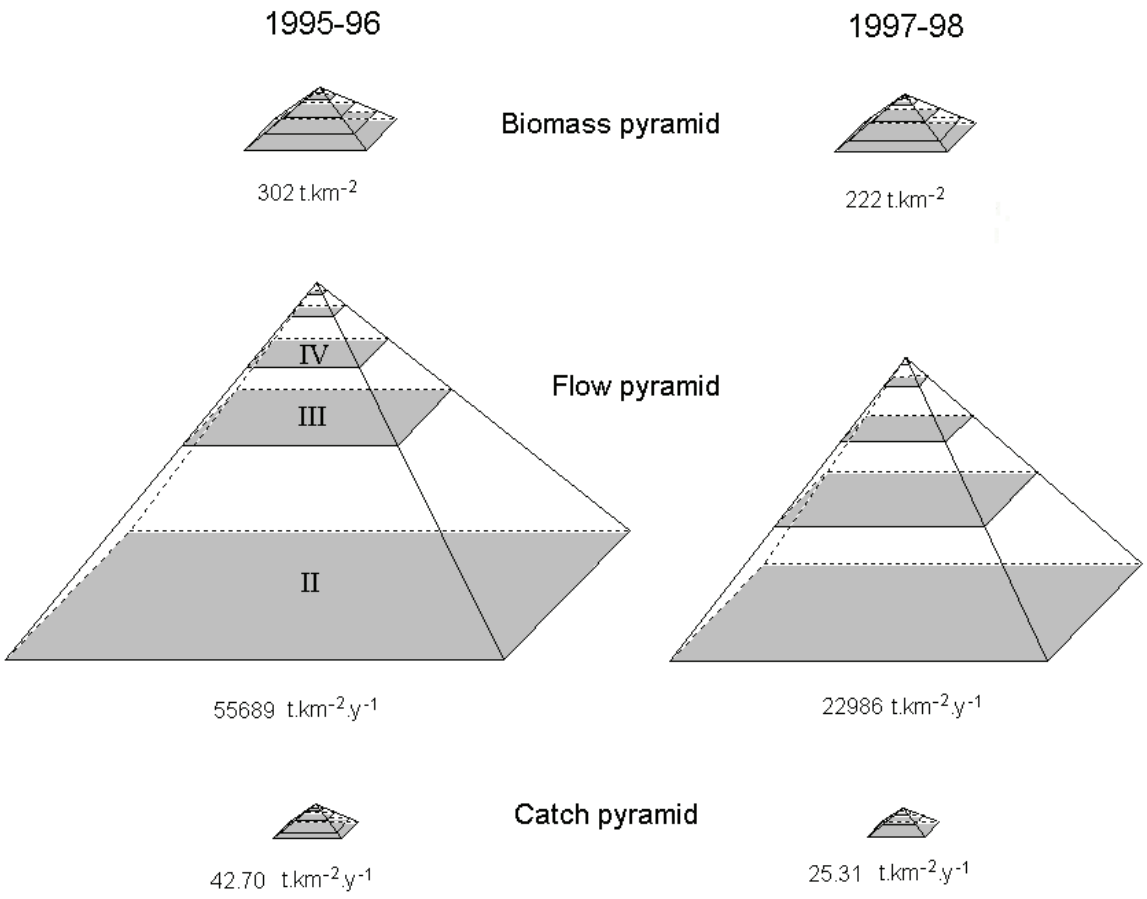

Figure III.4. Biomass (upper), flow (middle) and catch (lower) pyramids by discrete trophic levels in the cold period, 1995-96 (left) and the warm period, 1997-98 (right). The sizes of the pyramids are proportional to the values of biomass, flow or catch.

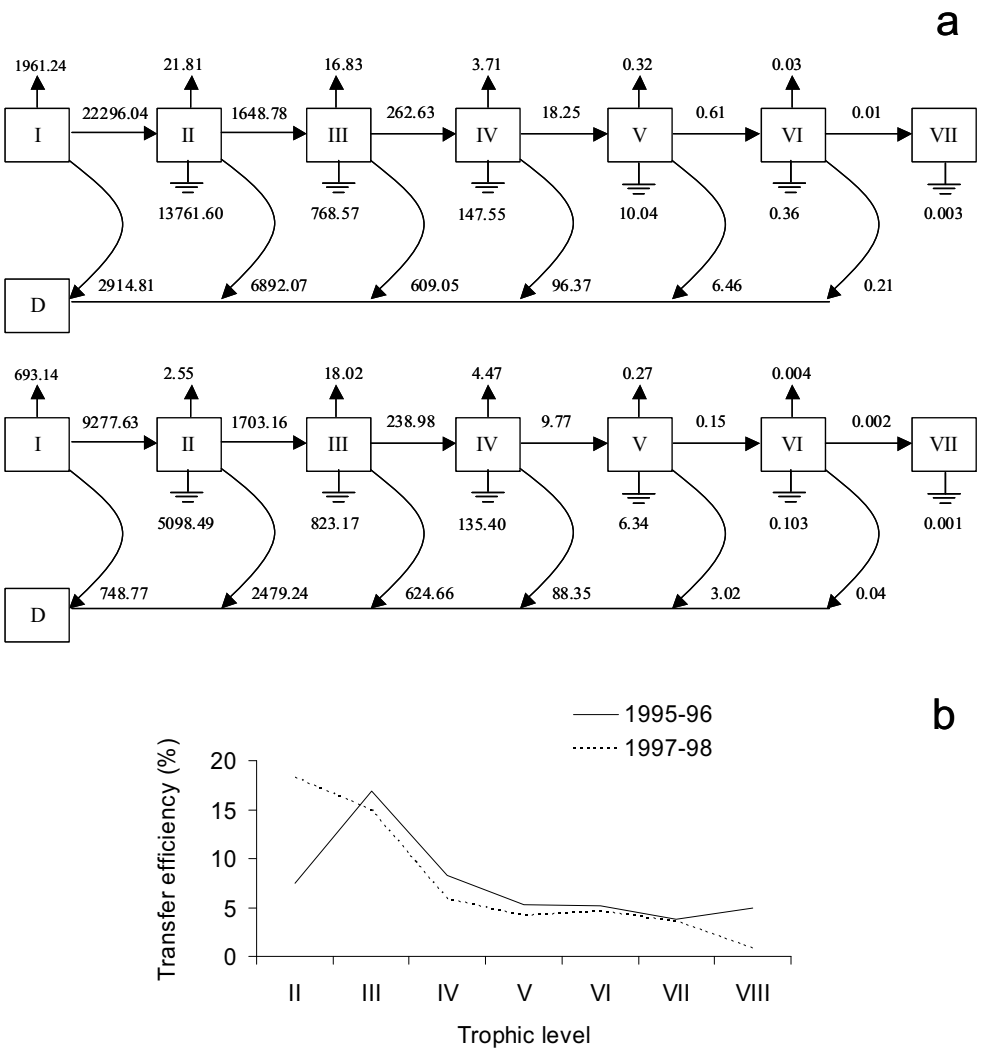

Figure III.5. NHCE canonical trophic food chains for the cold period (1995-96) and warm period (1997-98). Flow networks were aggregated into equivalent trophic chains with distinct trophic levels. Flows are in $t \cdot km^{-2} \cdot y^{-1}$, straight arrows indicate exports, ground symbols indicate respiration losses, and curved arrows indicate returns to detritus (a). Transfer efficiencies by trophic levels for the cold period (1995-96) and warm period (1997-98) (b).

Chapter IV. Trophic modeling of the Northern Humboldt Current Ecosystem, Part II: Elucidating ecosystem dynamics from 1995-2004 with a focus on the impact of ENSO

Marc H. Taylor[*]*, Jorge Tam, Verónica Blaskovic, Pepe Espinoza, R. Michael Ballón, Claudia Wosnitza-Mendo, Juan Argüelles, Erich Díaz, Sara Purca, Noemi Ochoa, Patricia Ayón, Elisa Goya, Dimitri Gutiérrez, Luis Quipuzcoa, Matthias Wolff*

Author's posting. This is the author's version of the work. Please cite the final version to be published by Progress in Oceanography as part of the Proceedings of the Conference, *The Humboldt Current System: Climate, ocean dynamics, ecosystem processes, and fisheries*, Lima, Peru, November 27 - December 1, 2006. Article accepted November 8th, 2007

Abstract

The Northern Humboldt Current Ecosystem is one of the most productive in the world in terms of fish production. Its location near to the equator makes it ideal for strong upwelling under relatively low wind forcing conditions. This creates optimal conditions for the development of plankton communities, which ultimately benefit populations of grazing fish such as the Peruvian anchoveta, *Engraulis ringens*. The ecosystem is also subject to extreme interannual environmental variability associated with the El Niño Southern

[*] Corresponding author, Email: (marchtaylor@yahoo.com)

Oscillation (ENSO) cycle, which has major effects on nutrient structure, primary production, and higher trophic levels. Here our objective is to elucidate the importance of several external drivers (i.e. reconstructed phytoplankton changes, immigration, and fishing rate) and internal control mechanisms (i.e. predator-prey controls) on ecosystem dynamics over an ENSO cycle. Steady-state models and time-series data from the Instituto del Mar del Perú (IMARPE) from 1995-2004 provide the base data for simulations conducted with the program Ecopath with Ecosim. Results show that all three external drivers were important to reproducing ecosystem dynamics. Changes in phytoplankton quantity and composition (i.e. contribution of diatoms and dino- and silicoflagellates), as affected by upwelling intensity, were important in ecosystem dynamics associated with the El Niño event of 1997-98 and the subsequent 3 year period. The expansion and immigration of mesopelagic fish following the El Niño event was important for dynamics in later years. Fishing rate changes were the most important of the three external drivers tested, helping to improve dynamics throughout the modeled period, and particularly during the post-El Niño period. Internal control settings show a mix of interactions; however a “wasp-waist” configuration around small pelagic fish is not supported. These results are discussed in light of the importance of ENSO on dynamics of the ecosystem with foci placed on important resources of Peru.

1. Introduction

Eastern Boundary Current Systems (EBCSs), including the Humboldt, Canary, Benguela, and California Currents, are among the most productive fishing areas in the world. High primary and secondary productivity supports a large biomass of small planktivorous pelagic fish, “small pelagics”, which are important drivers of production to the entire system whereby they can influence both higher and lower trophic levels (i.e. “wasp-waist” forcing Cury et al., 2000).

Despite similarities in structure, the Humboldt Current, and specifically, the Peruvian upwelling system, is exceptional in terms of fish landings (both total and on a per area basis), when compared to the other EBCSs. However, remote sensing estimates of primary production ranked the Peruvian upwelling system third behind the Benguela and Canary EBCSs (Carr, 2002). In a way, this supports previous hypotheses that emphasize the importance of both quality and quantity of upwelling potential. The northern Peruvian upwelling system’s proximity to the equator and resulting large Rossby radius makes it ideal for strong upwelling under relatively low wind forcing conditions (Cury and Roy,

1989; Bakun, 1996). These conditions create a “particularly rich, non-turbulent, benign environment” by which coastal plankton communities can develop and be maintained through longer residence times, thus favoring grazing fish populations (Bakun and Weeks, in press).

Peru’s proximity to the equator also results in the fact that it bears the brunt of the force of Kelvin waves that travel across the Pacific Ocean during an El Niño Southern Oscillation (ENSO) cycle. During the warm El Niño (EN) phase, the “basin-wide ecosystem” of the Pacific, which normally maintains a slope in sea level, thermal structure, and nutrient structure due to trade winds, is disrupted (Chavez et al., 2003). While upwelling may continue along the Peruvian coast, the lowered thermocline prevents the upwelling of deeper, nutrient-rich water to the photic zone. As a result, the “active zone” of higher primary productivity is reduced – nearly $1/10^{th}$ the size of a normal upwelling period during the last EN of 1997-98 (Nixon and Thomas, 2001).

Chavez et al. (1989) demonstrated that sea level and its effect on the thermocline depth are significantly related to nitrate concentration of upwelled water. Wind-forced offshore Ekman transport and the normal basin-scale slope increasing westward result in a lowered sea level in Peru, causing nutrient-rich water to be upwelled along the coast. Under these conditions diatoms dominate the nearshore phytoplankton community. They are particularly adapted to upwelling conditions through higher production rates and their ability to form resting spores, which sink and are subsequently returned to the surface via upwelling (Pitcher et al., 1992). In the Humboldt Current system, EN events prevent the upwelling of the deeper, nutrient-rich water, which results in a reduction of the larger size fraction of the phytoplankton community (e.g. diatoms) (Bidigare and Ondrusek, 1996; Landry et al., 1996; González et al., 1998; Iriarte and González, 2004). Subtropical phytoplankton species normally found further offshore are observed to replace the more typical cold-water species (Rojas de Mendiola, 1981; Ochoa et al., 1985; Avaria and Muñoz, 1987). These changes in the phytoplankton likely result in changes in the entire food web, with energy passing through alternative pathways before reaching a particle size suitable for the grazing by small pelagics (Chapter III; Sommer et al., 2002; González et al., 2004a; Iriarte and González, 2004).

This relatively straightforward, bottom-up perspective is complicated by other top-down processes such as predation and impacts from the fishery, which require a more holistic perspective. Fortunately, trophic modeling of EBCSs has a long history from which to draw upon; including steady-state models of the Peruvian (Walsh, 1981; Baird et al., 1991; Jarre et al., 1991; Jarre-Teichmann, 1992) and other upwelling systems (Shannon et al., 2003; Heymans et al., 2004; Neira and Arancibia, 2004; Neira et al., 2004; Moloney et al., 2005). The development of the program Ecopath with Ecosim (EwE) (Walters et al.,

1997) has allowed for further exploration through time, and has been applied specifically to dynamics in the southern Benguela system (Shannon et al., 2004a; Shannon et al., 2004b). A review of these advances (Taylor and Wolff, 2007) has assisted in the construction of steady-state models for the Peruvian system as presented by Tam et al. (Chapter III) and forms the basis for dynamic simulations conducted in this study.

Our objectives are to elucidate the mechanisms of dynamics in the Peruvian upwelling system over an ENSO cycle. We evaluate the importance of several external drivers on system change through time. These drivers include: (i) changes in phytoplankton biomass and composition, (ii) immigration / expansion of mesopelagic fish into the model area, and (iii) changes in fishing rates. Additionally, we explore internal control mechanisms of flows of energy between functional groups (e.g. bottom-up, top-down control). Generally, this study hopes to shed light on dynamics across several temporal scales, e.g. seasonal, inter-annual (ENSO), and multi-decadal scales; whereby the degree of upwelling and resulting primary productivity may similarly affect trophic dynamics.

We use the data-rich period of 1995-2004 as a starting point for model exploration and tuning, which will aid in future simulations regarding management.

2. Methods

Using the temporal dynamic routine, Ecosim, of the EwE package (Walters et al., 1997; Walters et al., 2000) we explored the relative importance of external and internal drivers of change in the northern Humboldt system from 1995-2004. External, non-trophically-mediated drivers considered were changes in phytoplankton biomass, fishing rate (effort and mortality), and oceanic immigrant biomass (mesopelagic fish). Internal, trophically-mediated, factors concerned an exploration of trophic flow controls (e.g. bottom-up, top-down) that govern predator-prey dynamics.

2.1. Description of the model

The steady-state model from Tam et al. (Chapter III) provided baseline values for the initial ecosystem state (1995-96 model), which encompass a full “biological year” (i.e. starting from about the middle of a calendar year). Spatial definitions were from 4°S-16°S and extend 60 nm (ca. 111 km) offshore from the coast of Peru (see Fig. III.1. in Tam et al., Chapter III). The models consisted of 33 functional groups including detritus, macrobenthos, 2 phytoplankton groups, 4 zooplankton groups, 8 pelagic fish groups, 2

cephalopod groups, 12 demersal fish groups (including 3 life-history stages for Peruvian hake, *Merluccius gayi peruanus*), sea birds, pinnipeds, and cetaceans.

The simulation runs conducted for this study with EwE calculates biomass changes through time by solving the set of differential equations:

$$dB_i/dt = g_i\left[\sum_k Q_{ki}(t)\right] - \sum_j Q_{ij}(t) - M0_i B_i - \sum F_{if}(t)B_i \qquad (1)$$

for species or functional groups i =1…n. The first sum represents the food-consumption rate, Q, summed over prey types k of species i, and g_i represents the growth efficiency (proportion of food intake converted into production). The second sum represents the predation loss rates over predators j of i. All Q's in these sums are calculated by equation 2. $M0_i$ represents the instantaneous natural mortality rate due to factors other than modeled predation. The final sum represents the instantaneous fishing mortality rate, F, as a sum of fishing components caused by fishing fleets f.

The Q_{ij} are calculated by assuming that the biomass of prey i, B_i, is divided into vulnerable and safe components, and it is the flux rates v_{ij} and v'_{ij} that move biomass into the vulnerable and safe pools, respectively. This assumption leads to the rate equation:

$$Q_{ij} = \frac{a_{ij}(t)v_{ij}(t)B_iB_j}{v_{ij}(t) + v'_{ij} + a_{ij}(t)B_j} \qquad (2)$$

where the total consumption rate Q_{ij} varies as a mass action product (avB_iB_j), and is modified downward by a "ratio dependent" effect ($v+v'+aB_j$) representing localized competition among predators. a_{ij} represents the rate of effective search by predator j for prey type i (for further information, see Walters and Martell, 2004). In *EwE*, the vulnerabilities for each predator-prey interaction can be explored by the user and settings will determine if control is top-down (i.e., Lotka-Volterra; >2.0), bottom-up (i.e., donor-driven; <2.0), or intermediate (≈2.0). The modeling software allows for adjusting the vulnerabilities by means of a fitting routine, where the sum of squares (SS) is minimized between observed and predicted log biomasses/catches:

$$SS = \sum\left[Log(B_{obs.}) - Log(B_{pred.})\right]^2 \qquad (3)$$

We applied this fitting routine with our time series data and the computed vulnerabilities were then discussed in the light of possible control mechanisms operating in the ecosystem.

Simulations measured the importance of three external drivers (see section 2.2) on dynamics of the Northern Humboldt Ecosystem from 1995-2004. In addition, we applied the "fit-to-time-series" search routine within EwE to determine a best possible combination of specific predator-prey controls (see section 2.3). The simulation's performance was measured by *SS* against available time-series data of yearly biomass and catch changes. Time-series were derived from estimates of biomass, catches, fisheries mortality, and fishing effort from IMARPE (Instituto del Mar del Perú) and other sources (Table IV.1). This data was adapted to the model area and biological year averages.

2.2. External drivers

External drivers were considered as non-trophic changes, not accounted for within the internal flows of the trophic model. These included: (i) "*PP*", phytoplankton biomass changes due to changes in upwelling and nutrients; (ii) "*F*", fishing rate changes; and (iii) "*I*", Immigrant biomass changes, specifically, the expansion and immigration of mesopelagic fish into the model area. Drivers were introduced successively in the model in all possible sequences and combinations in order to arrive to an average value of change in *SS* (n=15). External drivers where defined only by available or reconstructed long-term data series as described in the following sections.

Phytoplankton, *PP* – Long-term changes in phytoplankton biomass are available in the form of total surface chlorophyll *a* concentrations ($mg \cdot m^{-3}$) as derived from remote sensing data (SeaWifs), yet additional information was needed in order to split this biomass into its components for the two functional groups. We used a long-term data series of coastally-sampled phytoplankton carried out by the Universidad Nacional Mayor de San Marcos (Lima, Peru) in Bahía de Ancón (77°11' W -11°46' S), Central Peru from 1992-2000. The series consisted of periodically sampled surface phytoplankton species' cell counts which were then converted into biovolume using cell dimensions gathered from literature sources or measured by microscopy (Appendices 1 and 2). Cell dimensions were applied to geometric-shape assignments as described by Sun and Liu (2003) for the calculation of biovolume. Monthly average biovolume values by taxonomic grouping were plotted against temperature anomalies off Ancón as a possible indicator for upwelling strength. Biovolume was natural log transformed and yielded the following linear relationships:

$$LN(B) = 17.841 - 0.2184 * T_{anom.} \quad \text{(4) (Diatoms, } r\text{=-0.20, } p\text{=0.05)}$$

$$LN(B) = 16.603 + 0.1719 * T_{anom.} \quad \text{(5) (Dino- and silicoflagellates, } r\text{=0.14, } p\text{=0.18)}$$

where B = biovolume ($\mu m^3 \cdot 50ml^{-1}$), $T_{anom.}$ = temperature anomaly (°C). Typical of phytoplankton populations, a wide distribution of values was observed; however, diatom biovolume showed a negative trend and dino- and silicoflagellates a positive one, which is consistent with literature concerning the effects of ENSO on phytoplankton communities (Fig. IV.1a). The relationships were then applied to an index of integrated temperature anomalies for the entire Peruvian coast–the Peruvian Oscillation Index (POI) (Purca, 2005), which allowed for the reconstruction of coastal phytoplankton biovolume for the years 1995-2003. Despite a non-significant correlation for dino- and silicoflagellates, the relationships resulted in an acceptable range of surface phytoplankton biovolume. We nevertheless use only the proportions of the two phytoplankton fractions, which were then applied to absolute values as derived from remote sensing data (SeaWifs) of the model area. Conversion factors used for chlorophyll *a* (Chl *a*) to wet weight were as follows: Chl *a*:Carbon (40:1) (Brush et al., 2002), and Carbon:wet weight (14.25:1) (Brown et al., 1991). Finally, a uniform mixed layer depth of 40 m was assumed to arrive at units of biomass per m^2 as described by Tam et al. (Chapter III) (Fig. IV.1b).

Fishing rate, *F* – Time-series fishery changes were only available for anchovy, hake and jumbo squid; however, these species represent key target fisheries as well as important functional groups of the nearshore pelagic, nearshore demersal, and offshore pelagic ecosystem components, respectively. These include fishing mortality rates derived from single species Virtual Population Analyses for *Anchovy* and the three *Hake* subgroups, and changes in fishing effort for *Jumbo squid* (Table IV.2).

Immigration, I – While increases in biomass were calculated for several oceanic-associated functional groups during EN (Tam et al., Chapter III), long-term time series data was only available for *Mesopelagics – Lightfish and Lanternfish* as determined by acoustic surveys conducted by IMARPE. Distribution of *Mesopelagics* extends further offshore and thus we only considered the group's resident portion in the model area. The group's biomass increased and expanded into the model area following the EN of 1997-98. The changes in resident biomass due to non-trophic immigration / expansion were simulated by forcing the biomass of the *Mesopelagic*s.

2.3. Internal control mechanisms

Predator-prey forcing controls as determined by settings of prey vulnerability are important settings for the determination of top-down or bottom-up dynamics. “Mixed” or intermediate (*MX*; default v = 2.0) settings were used for the initial explorations of the influence of external drivers. Afterwards, a further fit-to-time-series search routine was run for the 30 most sensitive predator-prey interactions (as determined by a sensitivity routine of the program) in order to determine the best settings for reducing *SS*. The following interactions were also included to assess whether a “wasp-waist” configuration exists around sardine and anchovy: (i) meso- and macrozooplankton as prey to sardine and anchovy; and (ii) all interactions involving anchovy and sardine as prey. In total, 49 interactions were included in the search routine.

2.4. Focus on changes in main fishing targets

The dynamics of several main fishing targets or interactions of interest were also highlighted. Sources of mortality and diet changes throughout the simulation were observed for anchovy in order to interpret bottom-up and top-down factors on dynamics. Hake dynamics were of special interest due to the drastic decreases in population size since the last EN (Guevara-Carrasco, 2004; Ballón et al., in press). We specifically looked at the sources of mortality for the small size class to help shed light on the low recruitment levels of recent years.

3. Results

3.1. External drivers

The driver to phytoplankton biomass and composition improved the fit of the simulation overall, reducing *SS* by -2.7% (Fig. IV.2b) with greatest reductions in *SS* observed during the EN year 1997-98 and subsequent 3 year period (Fig. IV.2a). The driver to immigrant biomass (*Mesopelagics*) reduced *SS* overall by -9.2% (Fig. IV.2b) with greatest reductions in *SS* observed in later years when biomasses reached their highest levels (Fig. IV.2a). *SS* of the EN year 1997-98 alone was not improved with the addition of the immigrant driver (Fig. IV.2a). Fishing rate changes proved to be the most important of the three external drivers overall, reducing *SS* by -22.0% (Fig. IV.2b). Improvements were

observed throughout the simulated period except for the final year, and were generally more important during the post-EN years (Fig. IV.2a).

3.2. Search for vulnerabilities and best-fit configuration

The fit-to-time-series search for vulnerabilities routine revealed several important predator-prey interactions (Table IV.2), and further decreased *SS* by an additional -31.2% after the application of the three internal drivers *PP*, *F*, and *I* (total decrease in *SS* of -64.3%). The results did not support a wasp-waist configuration for small pelagics (agrees with Ayón et al., in press), as bottom-up configurations were estimated for sardines and anchovy on meso- and macrozooplankton; however, a bottom-up configuration was fit for interactions of sardine and anchovy, and their predators. Top-down configurations were estimated between mesopelagics and large hake on macrozooplankton. Of these, only mesopelagics contributed significantly to the predation mortality of macrozooplankton during the simulation. The configuration between mesopelagic fish and its main predator, jumbo squid, was 1.0 (bottom-up), helping to explain the expansion of the squid biomass following the EN of 1997-98. The final time-series trends of the simulation versus the base data is shown in Figure IV.3 for biomass and Figure IV.4 for catch data.

3.3. Focus on changes in main fishing targets

The changes to the anchovy biomass during EN were best explained through bottom-up processes dealing with prey availability. The reduction in diatom biomass during EN resulted in a higher contribution of zooplankton in the diet of anchovy. Increases in dino- and silicoflagellates in the diet of anchovy were minimal as this group contributes only a small proportion to their diet generally (Fig. IV.5). According to our model, during the EN year, 1997-98, predation mortality increased – mainly due to horse mackerel, but non-predatory losses were by far the largest source of mortality (Fig. IV.6) and coincide with increased time devoted to feeding as a result of decreased prey availability. After 1998-99, variability in mortality was mainly due to changing fishing mortality rates, which helped to explain the anchovy dynamics in the later years.

Decreases in the hake biomasses were well predicted by the simulation for all three size classes (Fig. IV.3). Looking in detail at the simulated mortalities for small juvenile hake indicated that cannibalism did not contribute greatly to the overall mortality even during the pre-crash years of 1995-96 and 1996-97. Predation mortality on small hake by jumbo squid remains fairly constant throughout the simulation despite the

increase in the squid's biomass. This predation mortality does, however, come to represent a higher portion of total mortality in the last year of the simulation following the reduction of the fishery. Fishing mortality is the most substantial source of mortality for all three hake groups, especially for the medium and large classes (Fig. IV.7).

The application of the immigrant driver simulated the expansion and immigration of mesopelagic fish into the model area. One obvious result of this is that the jumbo squid biomass also responded quickly as a main predator of mesopelagic fish and a shift in the jumbo squid's diet toward a larger proportion of mesopelagic fish was observed (Fig. IV.8). Small hake contributed minimally to the jumbo squid's diet throughout the simulation.

4. Discussion

We have chosen to use the model of 1995-96 as a starting point for several reasons, including: (i) starting point for reliable, periodic sampling conducted by IMARPE, (ii) fairly typical, "normal" upwelling period following anchovy recovery with several prior years of stable conditions, and (iii) precedes the strong EN event of 1997-98, offering insight into subsequent dynamics. We asked the question whether this EN event has been a principal perturbation and to what degree trophic interactions have played a role in the observed historical changes.

4.1. Role of external drivers

Phytoplankton – Given the major decrease in primary productivity that occurs during EN, it was assumed that the application of this driver would have a major bottom-up impact through the trophic web, and would partially explain the decreased biomass of the coastal ecosystem. In fact, we did find improvements in the fit of the simulation, especially during EN and the immediately following years. Later years show a reduced importance of the forced phytoplankton dynamics likely due to less yearly phytoplankton variability under the more "normal" upwelling conditions (Fig. IV.1b).

Copepods make up the majority of the mesozooplankton biomass in Peru and are known to be an important grazer of the larger microphytoplankton (DeMott, 1989; Sommer et al., 2002; Sommer et al., 2005). We see that the model correctly predicts a decrease in mesozooplankton biomass in response to the decreased diatom biomass of 1997-98. Contrary to the base data series of mesozooplankton, a rapid recovery is predicted

following the resumed higher diatom and total phytoplankton biomass (Fig. IV.3). Without speculating too much as to the reasons for this discrepancy, we believe that much additional work is required in the modeling of zooplankton groups. Despite this uncertainty, we are still able to simulate many higher trophic groups' dynamics in the correct direction, and in some cases of the same magnitude as the base data. This is especially true of the trophically-important anchovy dynamics for which data is more widely available.

Of particular importance to small pelagic dynamics are particle size feeding preferences observed for the different species. Sardines possess a particularly fine-meshed filtering apparatus in their gillrakers allowing for the filtering of smaller-sized particles. Anchovy, on the other hand, are more specialized and efficient at feeding on larger-sized particles (James and Findlay, 1989; Van der Lingen, 1994; Van der Lingen et al., 2006). The result of these adaptations, at least in the Benguelan populations, is that anchovy seem to have higher clearance rates (per weight) than sardine when particle size is greater than about 500-600 µm (Van der Lingen, 1994). These feeding differences have been dealt with in other trophic models by both separating zooplankton by size as well as through different vulnerabilities to grazing by small pelagics (Heymans and Baird, 2000; Shannon et al., 2003; Neira and Arancibia, 2004; Shannon et al., 2004a; Shannon et al., 2004b). We have further divided phytoplankton into two principal taxonomic groups for a similar reason. According to the biovolume conversions of diet data conducted for our base model (Tam et al., Chapter III) and other authors (Alamo, 1989; Espinoza and Blaskovic, 2000), anchovy were estimated to feed much more on diatoms than flagellates. Although diatoms are more associated with the nearshore cold habitat of the anchovy, they are usually smaller than the cited 500-600 µm optimal particle size. However, it is likely that aggregates of cell-chains allow anchovies to efficiently filter them as well. As a result of this detail in our model, anchovy dynamics are well simulated. According to the results of the simulation, the initial decrease in biomass during 1997-98 is mainly reproduced by forcing phytoplankton; specifically, a decrease in diatom biomass and, subsequently, a decrease in the second most important food item, mesozooplankton.

The predicted switch to a diet more dominated by zooplankton was not as complete as was observed from *in situ* samples (Chapter III)(Espinoza and Bertrand, in press) (Fig. III.5). There are several likely reasons: (i) Forced biomass changes of phytoplankton in the simulation may not have reduced the diatom biomass as dramatically as in reality; (ii) Anchovy were also observed to have moved closer to the coast and to deeper waters (up to 150 m) during the past EN (Bertrand et al., 2004), which may have been due to non-trophic reasons (e.g. physiological stress associated with the higher surface water temperatures), and possibly prevented feeding upon the remaining diatom

biomass; (iii) The starting diet may be to high (or not) on diatoms but it does not explain the lack of change in diet composition as this is calculated mainly from the changes in biomass and vulnerability. Espinoza and Bertrand (in press) have estimated the percent contribution in carbon units to anchovy diet from a longer series of sampled stomachs from 1996-2003. The author's results indicated a much higher proportion of mesozooplankton and macrozooplankton than have previously been estimated (98 % in carbon). While their diet data still needs to be weighted according to the distribution of the anchovy population, it may nevertheless point to an overestimation of the importance of phytoplankton in our originally calculated diet composition.

Fishing rates – The application of fishing rates improved the fit of the simulation throughout the simulated period and helps to explain the long-term dynamics of some of several main target species. Our findings of a 22.0% average decrease in long-term variance through the application of the fishing rates compares to a decrease of 2-3% in a similar study for the Southern Benguela (Shannon et al., 2004a). This large difference may point to higher fishery-related impacts in the Peruvian system. In a comparison of trophic models by Moloney et al. (2005), it was illustrated that the South Benguelan fishery operates on a higher trophic level than in other EBCSs due to the differing diet of small pelagics and composition of the catch; specifically, small pelagics are more zooplanktivorous than in the Humboldt, and the fishery catches contain a higher proportion of demersal fish. Due to this higher mean trophic level of the catch in the Southern Benguela, the statistic of *Flows required per unit of catch* ([t 1°prod] [t catch]$^{-1}$ km^{-2} y^{-1}) is more than double that of Peruvian catches, indicating more energetically-costly target species. Despite this cost, the authors determined that the Southern Benguelan fishery required a smaller proportion of total primary production to sustain it when compared to the Peruvian fishery (4% vs. 10%), reflecting the much higher fishing rates in the Peruvian system. The EwE simulation output calculates mortality rates through time, allowing for the determination of the importance of yearly fishing mortality changes for some key target groups' dynamics as discussed in the following sections.

For anchovy, we can observe that *F* values are much more variable than mortalities from predation (Fig. IV.7). In 1996-97, before the onset of EN, *F* values more than doubled. This is consistent with past EN events whereby the first phase of the EN drives stocks inshore, increasing their density and catchability (Csirke, 1989), whereas the second phase at the height of EN, possibly coinciding with the brunt of the arriving Kelvin wave, drives the anchovy stocks further inshore and/or to greater depths (Bertrand et al., 2004). As the yearly *F* values are based on a biological year (July-June), the 1996-97 value is partially influenced by the initial conditions of EN. In fact, positive temperature

anomalies for the Peruvian coast were noted as early as March 1997 and more than 2.8 million tonnes were landed during April and May alone. Shortly after these impressive catches, the anchovy fishery remained largely closed until the end of 1998, allowing the population to recover. *F* of anchovy was largely eliminated during EN due to the near closing of the fishery in response to the reduced biomass and the difficulty in fishing. Anchovy had moved closer to the coast and to deeper waters (up to 150m), which prevented large industrial purse seining (Arntz and Fahrbach, 1991; Bertrand et al., 2004). Dynamics of the anchovy population in the later years show a combination of elevated fishery and predation mortality as some predators began to recover, causing the less dramatic drop in biomass between the years of 2000-2003.

According to the VPA analysis conducted by IMARPE, hake reached biomass levels between 1993-96 that have not been seen since the late 1970's; however, this recovery was short-lived as dramatic declines have occurred since the last EN of 1997-98 and biomass has remained at alarmingly low levels for the past decade or so. As a result, the fishery closed in September 2002 and now operates at a much smaller scale. Several hypotheses have been offered to explain the crash, and include one or several of the following factors: (i) Low recruitment-success due to cannibalism of juveniles by adults 4-5 years and older (Ballón, 2005), (ii) Increased predation pressure on small hake due to the immigration / expansion of jumbo squid, (iii) Overfishing (Wosnitza-Mendo et al., 2005), and (iv) Demersal community changes affecting the prey of hake (Ballón, 2005). Looking in detail at the simulated mortalities for small juvenile hake indicates that cannibalism does not contribute significantly to the overall mortality even during the pre-crash years of 1995-96 and 1996-97 (Fig. IV.7). Fishing mortality, however, increased before EN and remained at high levels in all three hake groups until the closure in late 2002. These increases in *F* during the 1997-98 EN, in contrast to previous ENs where *F* generally decreases, were likely due to improved skills and technical development, and movement to the south of the trawler fleet in pursuit of hake (Wosnitza-Mendo et al., 2005). Further mortality is attributable to decreases in prey availability, especially for the medium and large hake groups. This scenario is supported by the findings of Ballón et al. (in press), who reviewed long-term trends in gonadosomatic indices for hake between the years 1972-2004 and found that positive temperature anomalies associated with EN resulted in lower stomach fullness and gonadosomatic indices, implying food-limited somatic production. The simulation predicts biomass gains for all three hake groups in the final year 2003-04 due to reduced *F* values upon the reduction of the fishery in 2002; however, this did not occur in reality, as observed by the base data (Fig. IV.3). Ballón et al. (in press) offer a non-trophic explanation—reproductive failure of hake. They observed that while large hake (>35 cm) show high values of condition and stomach fullness indices

during the 2000s, gonadosomatic indices have been decreasing since the mid 1980s. Additionally, sex ratios have shifted toward females (reaching almost 100% for fish larger than 35 cm), leading the authors to hypothesize that long-term pressure from the fishery may have disproportionately depleted males (males comprised 80% of the catches during the 1980s) to the point where females are now lacking a sufficient number of males to stimulate reproduction. Such a dependence on aggregates of males to induce spawning is typical of mating systems in cod-like species (Rowe and Hutchings, 2003). Nevertheless, our simulation supports the results of the VPA: that increases in *F* can explain the sharp declines observed from 1997-2002. When compared to the baseline natural mortality value (M=0.38) used in the VPA, total mortality values (Z) arrive to extremely high levels (above 2.0) for medium and large hake group, mainly through increases in *F*, and illustrate the pressure put on the group during the post-EN period as reflected by the subsequent declines in biomass.

Time-series data of changing fishing rates existed for only 3 species at the time of this study (anchovy, hake, and jumbo squid). Therefore, our results concerning the importance of the fishery on system dynamics may be somewhat conservative and future simulations may observe an even greater importance with the incorporation of fishing rate changes for additional functional groups.

Immigration – The outer border of the presented model extends to 60 nm (ca. 111 km), which is approximately the mean width of the shelf. Previous models of the Peruvian upwelling system by Jarre et al. (1991) were smaller in extension due to a focus on the main distribution of anchovy. A larger extension, has allowed us to incorporate most of the "active zone" or productive habitat in terms of primary production, which has been shown to vary about 10-fold depending on upwelling strength (Nixon and Thomas, 2001). A latitudinal extension between 4°-16°S has similarly attempted to encompass the entire main upwelling area bordered by the equatorial current in the north and a zone of decreased offshore Ekman transport further to the south beyond 16°S. This area is also observed to correspond to main stock delineations for northern Humboldt sardine and anchovy stocks (Alheit and Ñiquen, 2004). Despite this care to account for variability of principal functional groups, several more oceanic species are observed to immigrate or expand into the model area, especially during periods of upwelling and subsequent habitat reduction associated with EN. Sardine and mackerels, for example, are known to follow the offshore flow of oceanic water during the strong upwelling times of La Niña (Bertrand et al., 2004), and it has been hypothesized that underlying physiological restraints may also affect their distribution (Jarre et al., 1991). These non-trophic effects may help to

explain why some more oceanic groups' dynamics are not well predicted by the model, thus requiring their additional forcing.

Our results further show that the immigration of these groups during EN does not appear to have been a significant factor for the decreased biomass of more coastal species during the EN 1997-98. The longer-term expansion of mesopelagic fish, however, does appear to have had an impact on some groups, especially in later years when biomass in the model area reached its highest levels. While the cause of the mesopelagic fish outburst is not known, we speculate that either (i) the euphausiids biomass increased during EN in response to decreased grazing competition from mesozooplankton, and/or (ii) the lowering of the thermocline during EN may have caused a change in vulnerability of euphausiids—a principal prey for mesopelagic fish—allowing for an increase in predation by mesopelagic fish. Support for these scenarios comes from the findings of Tam et al. (Chapter III), where it was found that the overall consumption of macrozooplankton, increased during EN by 65%; mainly from mesopelagic fish and anchovy. This increase in total macrozooplankton consumption is partially derived from the *in situ* diet estimates of anchovy during EN 1997-98, which adds some confidence to our result; however, the increase in consumption from mesopelagic fish is related with their increased biomass only – due to the fact that a generalized diet, as derived from the study area samples from a different period, was used in both steady-state models. Therefore, these results must be taken with caution. Given euphausiids' strategy of predation avoidance through diel vertical migrations across the Oxygen Minimum Layer (OML, <1.0 $ml \cdot L^{-1}$) (Antezana, 2002a), it is possible that a deepening of the upper boundary of the OML may have caused increased vulnerability to predation. In any case, this increase in mesopelagic fish biomass during and after the EN of 1997-98 helps to explain the decreases in biomass of both mackerel groups through competition for macrozooplankton, a main prey for all three.

Another obvious result of the mesopelagic fish expansion is the bottom-up response of the key predator, jumbo squid. This has had some benefits in Peru through the sale of fishing permits to foreign offshore Japanese and Korean jigging vessels as well as becoming an important target species for the nearshore artisanal fisheries. Despite this, the fear of negative effects of the jumbo squid outburst on the more valuable hake population has caused alarm. The results of this study indicate that while some competitive effects do occur between jumbo squid and hake, the high fishing rates appear to have more responsibility in the hake's decline. While the direct predation mortality rates on small hake by jumbo squid appear relatively stable in the simulation, is should be noted that it is proportionally larger in the later years possibly due to groups' lower total mortality (Fig. IV.7).

4.2. Internal control mechanisms

The dramatic improvement in *SS* (31.2%) after the fit-to time-series routine highlights the importance of trophic control settings to internal dynamics of the model. Shannon et al. (2004a) also found that the routine improved the fit of the simulation in the Southern Benguela from 1978-2002 by 40% over the application of fishing rates alone. Our shorter time series makes for a less robust analysis; however, we will focus on the most important and interpretable interactions.

One of the more significant results of the vulnerability fitting exploration was that a purely wasp-waist configuration around small pelagics, typical for other EBCSs, is not supported. Cury et al. (2000) found a negative relationship between yearly zooplankton concentrations and small pelagic landings for several upwelling systems (California, Ghana and Ivory Coast, Oyashio (Japan), Black Sea, Southern Benguela) and hypothesized that zooplankton biomass is top-down controlled by pelagic fish. Shannon et al. (2004a; 2004b) further supported a wasp-waist configuration surrounding small pelagics in the Southern Benguela system through an exploration of data from 1972-2000 using EwE. On the other hand, Cury et al. (2000) mentioned that the Peruvian system was one of the few exceptions where zooplankton concentrations and small pelagic landings were positively correlated. Specifically, lower zooplankton concentrations (mainly mesozooplankton is sampled) were observed in Peru during the period of the mid 1970's to mid 1980's, coinciding with the period after the anchovy collapse. Zooplankton concentrations have since increased with the recovery of anchovy, but remain lower than the concentrations of the 1960's and early 1970's (Ayón et al., 2004). For the shorter time series modeled in this study we also found a bottom-up relationship between mesozooplankton and the predators – anchovy and sardine (agrees with Ayón et al., in press). Several possible factors that may help to explain the differences between the Peruvian upwelling system and other EBCSs are outlined in the following paragraphs.

It has been proposed that Peru's proximity to the equator allows for optimal conditions for upwelling and fish production (Cury and Roy, 1989; Bakun, 1996), possibly allowing plankton communities to become particularly rich above the stable and relatively shallow thermocline. Furthermore, the basin-wide slope of the thermocline in the Pacific may concentrate plankton, thus improving the grazing efficiency of small pelagic fish. We have demonstrated the importance of diatoms in the dynamics the Humboldt Current System, yet to the best of our knowledge a comparison of phytoplankton composition (*i.e.* based on cell size, taxa, unicellular vs. chain-forming, etc.) between EBCSs prevents us

to speculate if this is unique to Peru. However, it is possible that the optimal conditions in Peru may help maintain higher concentrations of chain-forming diatom communities near the coast, where anchovy populations dominate under normal upwelling conditions.

Highly concentrated plankton in Peru would not necessarily explain why zooplankton and small pelagics would both benefit simultaneously during periods of high upwelling. In fact, highly concentrated plankton might make top-down grazing pressure even more pronounced due to more efficient filter-feeding by anchovy, especially within its principal nearshore habitat (mainly <30 nm). This possibility is supported by Ayón et al. (in press) through evidence of top-down forcing on smaller scales in Peru; specifically, zooplankton biovolume was found to be significantly lower in areas of high anchovy and sardine biomass (acoustically determined, within a 5 km radius of the zooplankton sample). This finding is contrary to the negative correlation between large-scale trends of zooplankton volumes versus small pelagic fish biomass (Cury et al., 2000); however, Ayón et al. (in press) mention the importance of scale in explaining this discrepancy.

Cury et al. (2000) find significantly negative relationships for several upwelling systems (Ghana and Ivory Coast; Southern Benguela; Oyashio, Japan), yet the finding may be in part due to sampling bias, as zooplankton time series tend to be based on samples collected primarily on the shelf region. Time series of zooplankton over a larger extension from the coast and with evenly spaced sampling stations (California), find no significant correlation to small pelagic catches. Similarly, zooplankton sampling conducted by IMARPE is much more uniform and normally extends to ca. 185 km (100 nm) from the coast. This does not necessarily negate the possibility of wasp-waist forcing in Peru; however, it does imply that its occurrence may be on a smaller scale than is dealt with in our model.

Bottom-up configurations were found between sardine and anchovy to all their higher predator groups. In particular, the decreases in anchovy biomass associated with EN contributed to the decreases in several predatory groups, especially horse mackerel and small hake. Over longer time scales (i.e. decadal), both predators show flexibility in their diets, especially in relation to periods of low anchovy biomass as occurred during the mid 1970's to late 1980's—horse mackerel shift to zooplankton (Muck, 1989) and hake shift to sardine (Castillo et al., 1989). The shorter simulation period of this study appears to capture better the overall reduction in system size due to the reduced upwelling during EN. As a result, most functional groups of the coastal environment experience reductions in biomass, which may differ from dynamics on decadal time scales such as a regime change. Generally, our results support several previous studies presented in Pauly and Tsukayama (1987c), where teleosts, especially horse mackerel, are far more important consumers of anchovy than guano birds and pinnipeds; however acoustic surveys show

that teleost overlap with anchovy appears to have decreased significantly since 1997 (A. Bertrand, pers. com.).

A more probable bottom-up relationship is that between anchovy and seabirds and pinnipeds, whose distributions show a stronger overlap with anchovy habitat. Even with a fitted bottom-up configuration to anchovy, the model was unable to reproduce the large decreases in biomasses for seabirds and pinnipeds following EN. We believe that temporal changes (reduction) in anchovy vulnerability to predation may explain such a result. Muck and Pauly (1987) first proposed that sea birds are probably more affected by changes in vulnerability resulting from sea surface temperature-mediated distribution changes rather than by changes of anchovy biomass itself. As mentioned earlier, not only did anchovy retreat to remaining centers of upwelling during EN (from Alheit and Ñiquen, 2004; reproduced with permission), but were also observed to migrate to deeper waters (up to 150 m), allowed by a deepening of the thermocline (Bertrand et al., 2004). We believe that this movement made them less vulnerable to these predators. This is well illustrated in a diagram presented by Jarre et al. (1991) whereby changes in the vertical distribution of anchovy affect their vulnerability to predation or capture from seabirds, pinnipeds, and purse seiners. Diving sea birds are specialists on anchovy and have the shallowest effective hunting depth, and so would become the most susceptible to changes in the anchovy's vertical distribution. This non-trophic mediation process is supported by the dramatic decrease in sea bird biomass during the EN of 1997-98, and thus would need to be considered in future modeling exercises.

Other important internal controls are observed with the more oceanic-associated groups of the model. The expansion / immigration of mesopelagic fish into the model area impacted several groups directly, including possible top-down forcing of macrozooplankton and bottom-up forcing to jumbo squid. As mentioned before, this result must be taken with caution given that the diet of mesopelagic fish was not based on *in situ* measurements during the model period; however, the inclusion of several interactions involving macrozooplankton as prey in the vulnerability fitting routine suggests that their dynamics may be of more importance than previously thought. In particular, a top-down configuration between mesopelagics and macrozooplankton helped to explain decreases in macrozooplankton biomass, and subsequent decreases in several competitors for macrozooplankton (other cephalopods, mackerel, and horse mackerel). While these groups' distributions include a more oceanic offshore habitat, they nevertheless have important trophic connections to the coastal zone. Mackerels are known to be extremely dynamic in their distribution, coming closer to the coast both seasonally and during EN in response to decreased upwelling, whereby they may more heavily impact anchovy and other coastal species. Jumbo squid and other cephalopods also have important

connections across the shelf mainly due to life history stages and changes in diet. Specifically, cephalopods populations are subject to dramatic fluctuations and their impact on prey populations is equally variable. Their role as predators on fish and crustaceans clearly implicates them as a factor influencing natural mortality and recruitment success in stocks of commercial exploited species (Rodhouse and Nigmatullin, 1996). However, the impact of ommastrephid (jumbo squid) and loliginid squid on prey populations will be different; due to their differing distributions (loliginids are principally neritic).

4.3. Conclusions and future prospects

The introduction of several external drivers has allowed us to reproduce several key dynamics of the Northern Humboldt Current Ecosystem. Changes in phytoplankton associated with ENSO are shown to be important drivers on the short-term while fishing rates and immigrants add important dynamics in the long-term. This has helped to elucidate that the dynamics of the Humboldt Current Ecosystem associated with the impact of an El Niño event appear to be relatively restricted to the immediate years following the event, and that once normalization returns, the management of fishing rates will be increasingly important. The separation of principal phytoplankton taxa allows for the simulation of important changes of energy flow in the Humboldt Current Ecosystem over several temporal scales. Additionally, a link between the dynamics of the phytoplankton components and more easily observable environmental parameters, i.e. SST anomalies, takes a first step in the development of predictive models forced in real time.

A larger offshore extension allowed for the incorporation of important interactions between the coastal and more oceanic components of the ecosystem. Nevertheless, artificial forcing of mesopelagic fish was still necessary in reproducing the dynamics of the more oceanic-associated groups. Further investigation into the underlying drivers of the offshore ecosystem may become increasingly important in describing the dynamics of the more economically-important coastal upwelling system.

Internal control settings showed a mix of interactions; however a “wasp-waist” configuration around small pelagic fish is not supported. Specifically, top-down forcing of meso- and macrozooplankton by small pelagic fish is not observed.

Additional non-trophic interactions may also play important roles in dynamics (e.g. changes in vulnerability, recruitment, physiological constraints), and must be considered in future modeling efforts. We have highlighted possibilities of these in cases where the model fails to reproduce the historical trends. This has been an unexpected but extremely

positive outcome of the two parts of this work, and has helped to formulate further questions and investigation foci for the future.

Finally, future prospects for trophic modeling include the adaptation of longer reconstructed time series by Pauly and Tsukayama (1987a), Pauly et al. (1989) and Guenette et al. (in press) to the model in order to explore dynamics since the development of the industrial fishery around the 1950's. This would create a more robust analysis by which to further tune the internal forcing controls of the model, including the larger-scale dynamics of a regime shift. Ultimately, this will allow for further exploration of fishing scenarios for improved management of the ecosystem.

Acknowledgements

The authors acknowledge additional assistance and facilitation from the following people (in alphabetical order): Milena Arias-Schreiber, Arnaud Bertrand, David Correa, Michelle Graco, Renato Guevara, Mariano Gutierrez, Kristen Kaschner, Miguel Ñiquen, Ralf Schwamborn, Sonia Sánchez, and Carmen Yamashiro. We would like to also thank Carl Walters for the use of the Ecosim software. We also thank Dr. Lynne Shannon and an anonymous referee for their critical suggestions on the manuscript. The INCOFISH (Integrating Multiple Demands on Coastal Zones with Emphasis on Fisheries and Aquatic Ecosystems) project (Work Package 2) financed Michael Ballón and Claudia Wosnitza-Mendo. This study was partially financed and conducted in the frame of the EU-project CENSOR (Climate variability and El Niño Southern Oscillation: Impacts for natural resources and management, contract No. 511071) and is CENSOR publication No. 0086.

Tables and Figures

Table IV.1. Annual time-series data sets used in the Ecosim simulations.

Functional group	Data set	Comments	Used to force dynamics	Used to measure fit of simulation
1. Diatoms	Biomass (B)	SeaWifs; phytoplankton proportions reconstructed (see section 2.3)	+	+
2. Dino- and silicoflagellates	Biomass (B)	SeaWifs; phytoplankton proportions reconstructed (see section 2.3)	+	+
4. Mesozooplankton 200-2000 µm esd.	Biomass (B)	IMARPE survey (Ayón pers. comm.) – corrected using seasonal anomalies (1959-2001)		+
7. Macrobenthos	Biomass (B)	IMARPE benthic survey (1995-2003) (Gutierrez and Quipuzcoa, pers. comm.)		+
8. Sardine – Sardinops sagax	Biomass (B)	IMARPE acoustic survey (1995-1999) (Gutierrez, pers. comm.)		+
	Catches (C)	SeaAroundUs database (2006) (1995-2002)		+
9. Anchovy – Engraulis ringens	Biomass (B)	VPA estimates (1995-2003) (Niquen, pers. comm.)		+
	Fishing mortality (F)	VPA estimates (1995-2003)	+	
	Catches (C)	IMARPE catch statistics (1995-2003)		+
10. Mesopelagics – Lightfish and Lanternfish	Biomass (B)	IMARPE acoustic survey (1999-2003) (Gutierrez, pers. comm.)	+	+
11. Jumbo squid – Dosidicus gigas	Biomass (B)	IMARPE acoustic survey (1999-2003) (Arguelles, pers. comm.); 1995-1998 reconstructed from CPUE:acoustic ratio from 1999-2003		+
	Fishing effort (E)	Korean and Japanese industrial fleet data (1995-2003)	+	
	Catches (C)	Korean and Japanese industrial fleet data (1995-2003)		+
12. Other Cephalopods	Catches (C)	IMARPE catch statistics (1995-1999)		+
13. Other small pelagics – e.g. juvenile demersal fish	Catches (C)	SeaAroundUs database (2006) – Engraulidae, Ethmidium maculatum (1995-2002)		+
14. Horse mackerel – Trachurus murphyi	Biomass (B)	IMARPE acoustic survey (1995-2003) (Gutierrez, pers. comm.)		+
15. Characteristic large pelagic – Scomber japonicus	Biomass (B)	IMARPE acoustic survey (1995-2003) (Gutierrez, pers. comm.)		+
16. Other large pelagics	Catches (C)	IMARPE catch statistics (1995-1999)		+
17. Small hake – Merluccius gayi peruanus (<29cm)	Biomass (B)	VPA estimates (1995-2003) (Wosnitza-Mendo, pers. comm.)		+
	Fishing mortality (F)	VPA estimates (1995-2003)	+	
	Catches (C)	IMARPE catch statistics (1995-2003)		+
18. Med. hake – Merluccius gayi peruanus (30-49cm)	Biomass (B)	VPA estimates (1995-2003) (Wosnitza-Mendo, pers. comm.)		+
	Fishing mortality (F)	VPA estimates (1995-2003)	+	
	Catches (C)	IMARPE catch statistics (1995-2003)		+
19. Large hake – Merluccius gayi peruanus (>50cm)	Biomass (B)	VPA estimates (1995-2003) (Wosnitza-Mendo, pers. comm.)		+
	Fishing mortality (F)	VPA estimates (1995-2003)	+	
	Catches (C)	IMARPE catch statistics (1995-2003)		+
21. Small demersals	Catches (C)	IMARPE catch statistics (1995-1999)		+
22. Benthic elasmobranchs	Catches (C)	IMARPE catch statistics (1995-1999)		+
25. Medium demersal fish	Catches (C)	IMARPE catch statistics (1995-1999)		+
26. Medium sciaenids	Catches (C)	IMARPE catch statistics (1995-1999)		+
28. Catfish	Catches (C)	IMARPE catch statistics (1995-2002)		+
29. Chondrichthyans	Catches (C)	IMARPE catch statistics (1995-1999)		+
30. Seabirds	Biomass (B)	IMARPE survey (1995-2003) (Goya, pers. comm.)		+
31. Pinnipeds	Biomass (B)	IMARPE survey (1995-2003) (Goya, pers. comm.)		+

Table IV.2. Predator-prey vulnerabilities searched in the fit-to-time-series routine (in bold); *BU* = Bottom-up; *MX* = Mixed /Intermediate (default setting); *TD* = Top-down.

Predator / Prey	Diatoms	Silico- and Dinoflagellates	Microzooplankton	Mesozooplankton	Macrozooplankton	Sardine	Anchovy	Mesopelagics	Jumbo squid	Other small pelagics	Small hake	Small demersals	Conger	Med. sciaenids	P. stephanophrys
Mesozooplankton	**1 (BU)**	2 (MX)	2 (MX)												
Macrozooplankton	**1E+10 (TD)**	**1 (BU)**	**1E+10 (TD)**												
Sardine	2 (MX)	2 (MX)	2 (MX)	**1 (BU)**	**1 (BU)**										
Anchovy	**1E+10 (TD)**	2 (MX)	2 (MX)	**1 (BU)**	**1.16 (BU)**										
Mesopelagics				2 (MX)	**1E+10 (TD)**										
Jumbo squid				2 (MX)	2 (MX)		**1 (BU)**	**1 (BU)**	**1E+10 (TD)**	2 (MX)	**1E+10 (TD)**				
Other Cephalopods					**1 (BU)**							2 (MX)			
Horse mackerel					2 (MX)		**1 (BU)**			2 (MX)		2 (MX)			
Mackerel	2 (MX)		2 (MX)	2 (MX)	**1.55 (BU)**			2 (MX)				2 (MX)			
Other large pelagics							**1 (BU)**		2 (MX)	2 (MX)		2 (MX)			
Small hake					2 (MX)	**1 (BU)**	**1 (BU)**		**1 (BU)**	2 (MX)		2 (MX)			**1E+10 (TD)**
Med. Hake					2 (MX)		**1.16 (BU)**			**1E+10 (TD)**		**1E+10 (TD)**			**1.31 (BU)**
Large hake					**1E+10 (TD)**		**1 (BU)**	**1.02 (BU)**			**1E+10 (TD)**	**1.43 (BU)**	**1 (BU)**	**1E+10 (TD)**	**1E+10 (TD)**
Flatfish							**1 (BU)**								
Small demersals	**1E+10 (TD)**			**1E+10 (TD)**											
B. elasmobranchs					2 (MX)	**1 (BU)**	**1 (BU)**		2 (MX)	2 (MX)		2 (MX)	2 (MX)	2 (MX)	
Conger												2 (MX)			**1E+10 (TD)**
Med. demersal fish					2 (MX)		**1 (BU)**			2 (MX)		2 (MX)			
Med. sciaenids					2 (MX)	**1 (BU)**	**1 (BU)**	2 (MX)	2 (MX)	2 (MX)		2 (MX)		2 (MX)	
P. stephanophrys					**1 (BU)**										
Catfish				2 (MX)	2 (MX)		**1 (BU)**			2 (MX)					
Chondrichthyans							**1 (BU)**		2 (MX)		2 (MX)				
Seabirds							**1 (BU)**			2 (MX)		2 (MX)			
Pinnipeds							**1 (BU)**	2 (MX)		2 (MX)	2 (MX)	2 (MX)		2 (MX)	
Cetaceans					2 (MX)		**1 (BU)**		2 (MX)						

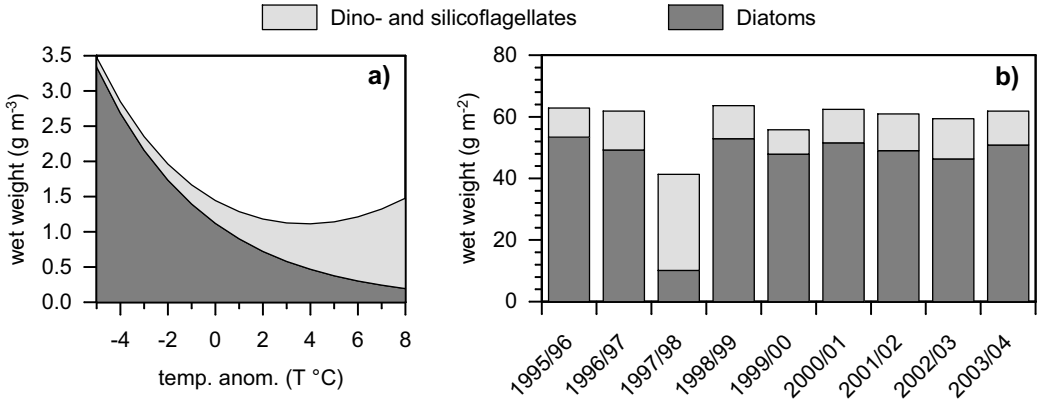

Figure IV.1. (a) Relationship between coastal surface phytoplankton biomass ($g \cdot m^{-3}$) as a function of sea surface temperature anomaly (°C); (b) reconstructed annual phytoplankton biomass values ($g \cdot m^{-2}$) used in the phytoplankton (*PP*) driver.

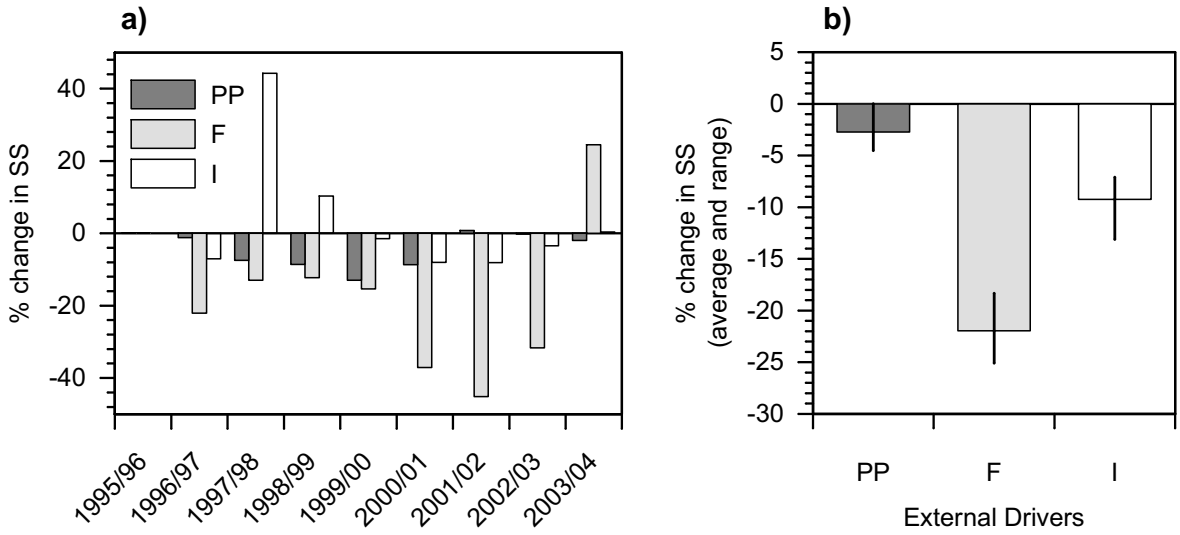

Figure IV.2. (a) Percent changes to sum of square differences, *SS*, after the application of different external 'drivers': phytoplankton biomass (*PP*); fishery rates (*F*); and immigrant biomass (*I*). *SS* changes by year after the individual application of each external driver. (b) Average and range of *SS* changes under the application of external drivers in all possible sequences and combinations. All simulations use intermediate, default control settings (i.e. all predator-prey vulnerabilities equal 2.0). Negative values (i.e. decrease in *SS*) indicate an improvement in fit.

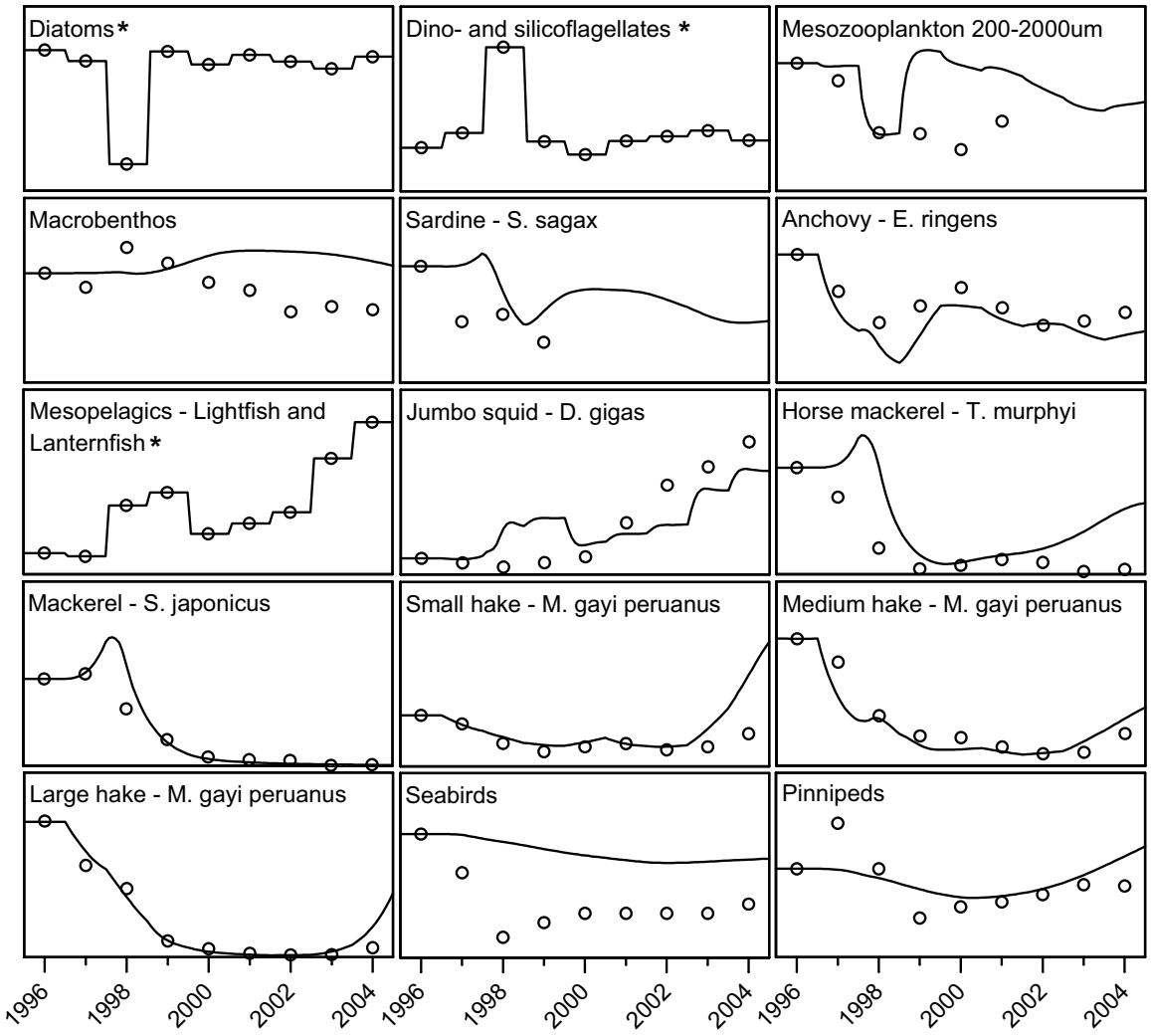

Figure IV.3. Time-series trends of biomass changes from the data sets (dots) and Ecosim simulations (lines). Presented is the best-fit simulation (i.e. lowest *SS*), using all drivers (*PP*, *F*, and *I*) followed by a "fit-to-time-series" routine for the 30 most sensitive predator-prey vulnerabilities. Yearly data points represent "biological years" (i.e. July-June of following year). Asterisks (*) indicate artificially-forced functional groups (*Diatoms*, *Dino - and silicoflagellates*, and *Mesopelagics*).

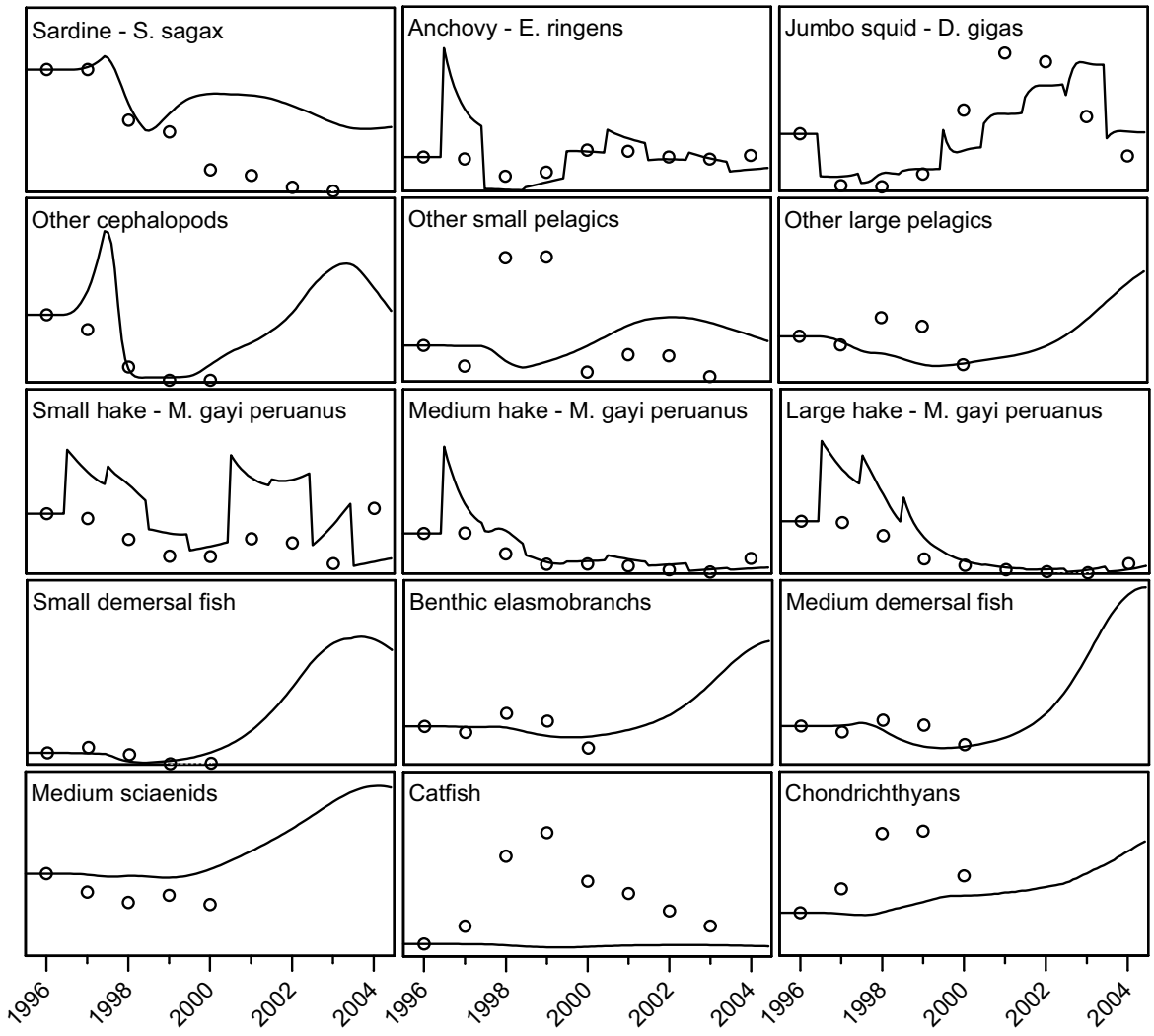

Figure IV.4. Time-series trends of fisheries catch changes from the data sets (dots) and Ecosim simulations (lines). Presented is the best-fit simulation (i.e. lowest *SS*), using all drivers (*PP*, *F*, and *I*) followed by a "fit-to-time-series" routine for the 30 most sensitive predator-prey vulnerabilities. Yearly data points represent "biological years" (i.e. July-June of following year).

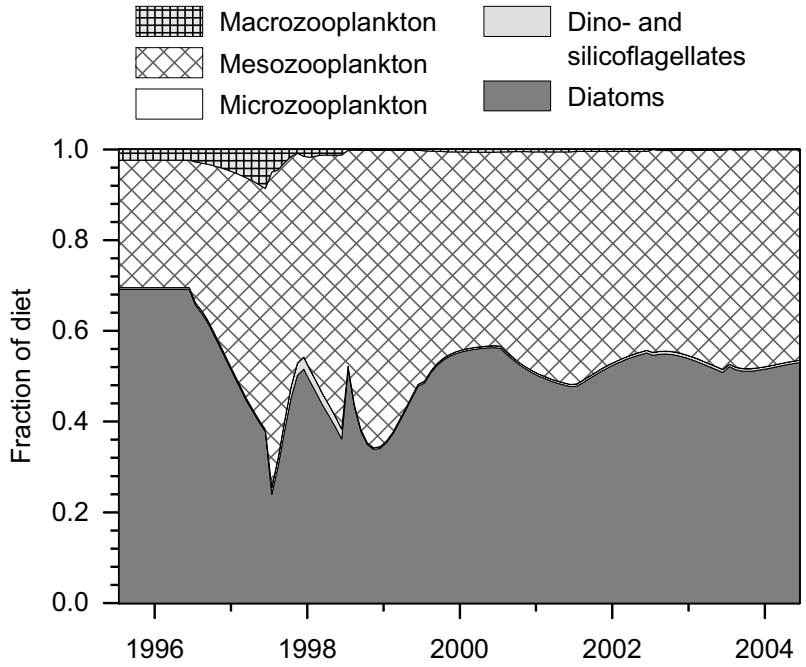

Figure IV.5. Contribution of prey items to the diet of anchovy through the Ecosim simulation.

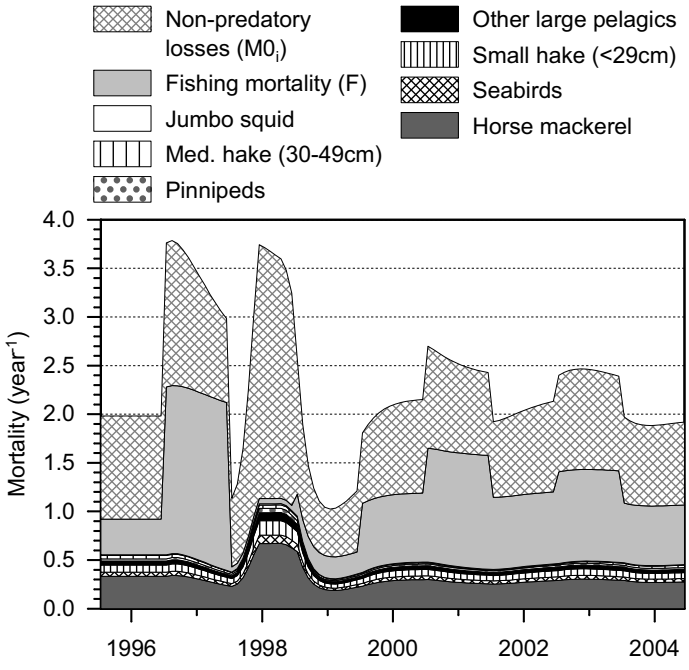

Figure IV.6. Sources of mortality of anchovy, *Engraulis ringens*, through the Ecosim simulation. Only the top 7 sources of predation mortality are shown (representing >95% of total predation mortality).

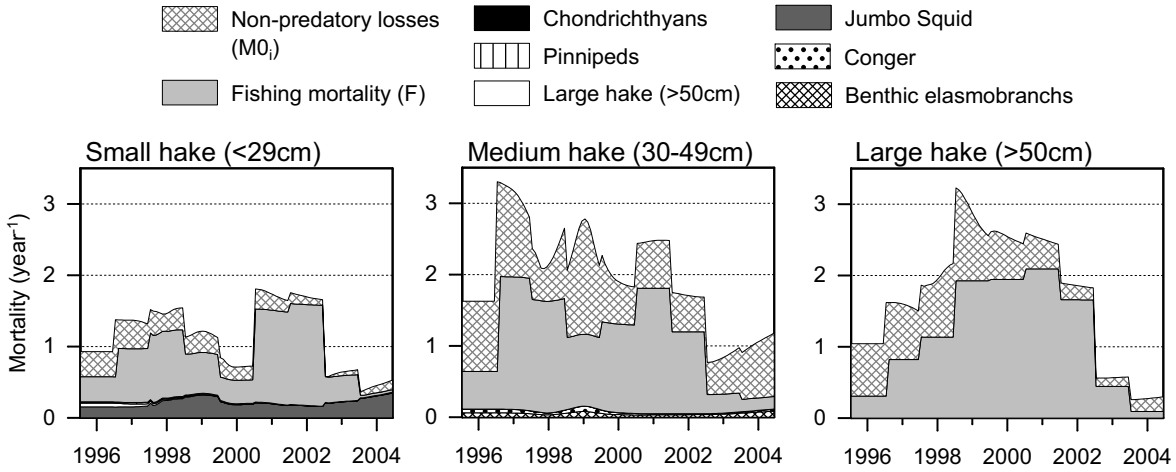

Figure IV.7. Sources of mortality for different size classes of hake, *Merluccius gayi peruanus*, through the Ecosim simulation.

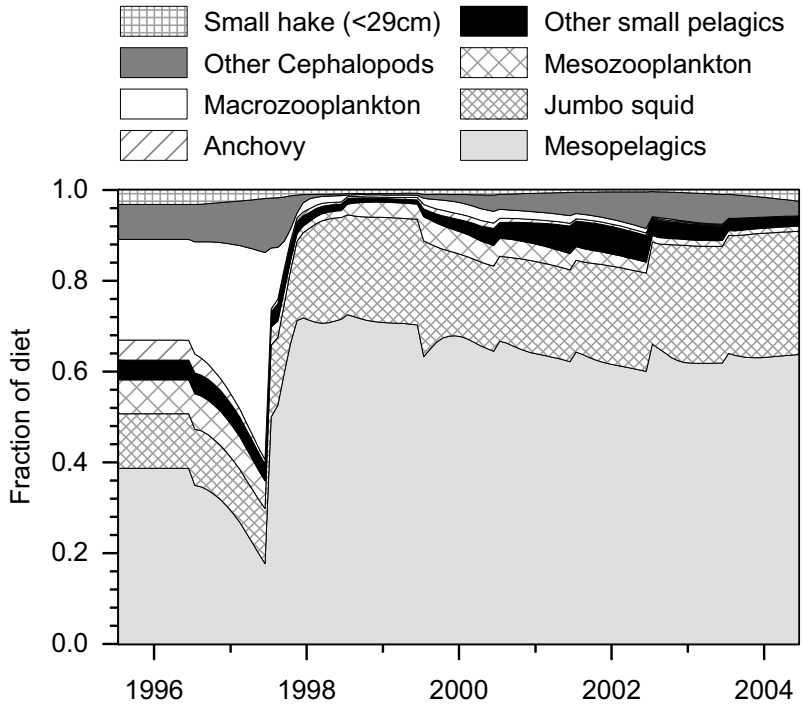

Figure IV.8. Contribution of prey items to the diet of jumbo squid, *Dosidicus gigas*, through the Ecosim simulation.

Chapter V. A catch forecast model for the Peruvian scallop (*Argopecten purpuratus*) based on estimators of spawning stock and settlement rate

Matthias Wolff[*]*, Marc Taylor, Jaime Mendo, Carmen Yamashiro*

Author's posting. This is the author's version of the work. Please cite the final version published by Ecological Modelling. Article accepted July 2nd, 2007 and published August 17th, 2007:
Wolff, M., Taylor, M., Mendo, J., Yamashiro, C., 2007. A catch forecast model for the Peruvian scallop (*Argopecten purpuratus*) based on estimators of spawning stock and settlement rate. Ecological Modelling 209, 333-341.
doi:10.1016/j.ecolmodel.2007.07.013

Abstract

The Peruvian Bay scallop *(Argopecten purpuratus*) fishery in Independencia bay (Southern Peru) is being subjected to great inter-annual variability in catch and effort, which is mainly due to the ENSO (El Niño- Southern oscillation) - caused changes in the population dynamics of the stock, which greatly proliferated during the El Niño events 1983 and 1998. As a consequence "gold rush" conditions arose and resource users profited from a multi-million dollar export business. After the El Niño booms, the system normalized and catches dropped to normal levels. This boom and bust situation has made a rational management of the resource difficult, and annual catches are considered unpredictable, just like the stochastic environment. This paper attempts to provide a catch forecast model to enable the scallop fishery to better prepare for and adapt to the ever-

[*] Corresponding author, Email: (matthias.wolff@zmt-bremen.de)

changing conditions of the scallop stock. The model proposes that annual catches are mainly the result of the recruitment success of the incoming new cohort, which is a function of adult spawning stock size and the number of settlers to the sea bottom. The latter is considered a function of the larval mortality rate and the temperature-dependent development time to the settlement stage, the former proportional to the catches taken over the spawning period (Nov.-April). Using monthly catch and temperature data for the period 1983-2005, we constructed a regression model to predict the catch for the year after the recruitment period (July-June) as a function of a) the catch during the spawning period (as a proxy for spawning stock biomass) and b) the settlement factor that was derived from the mean water temperature over the spawning period, an assumed instantaneous larval mortality rate, and the relationship between temperature and larval period to settlement. The resulting multiple regression (r^2 = =.930) proves that both factors can explain a large part of the inherent variability of the data. The model reveals that annual catches greatly depend on the spawning stock size when temperatures are low, while this factor decreases in importance with increasing temperatures, at which the settlement factor is much more influential instead. These findings are relevant for the stock management: at low temperatures, the maintenance of a large enough spawning stock over the spawning period (Nov.-Apr.) is decisive for the yield of the post-recruitment fishing period thereafter, while at increasing spawning temperatures, spawning stock size is of decreasing importance for determining the yield.

1. Introduction

The Peruvian Bay scallop (*Argopecten purpuratus*) is the main target of the multispecies diving fishery of Peru. It is being caught in shallow waters (5-30m) along the entire coastline, but substantial stocks and fisheries are concentrated around two areas only: Sechura bay in the north and Independencia bay in the south (Fig. V.1). In Independencia bay, the largest and most productive natural scallop banks are found.

During the El Niño warming event in 1983/84 the scallop population of Independencia bay exhibited an unprecedented proliferation, causing annual landings to rise from some hundred tons of normal (cold upwelling) years to about 25000t during the three years following the warming event (Wolff, 1985, 1987; Mendo et al., 1988; Arntz and Fahrbach, 1991) (Fig. V.1). A scallop export line was established and the scallop fishery became a multimillion dollar business, providing not only work for more than a thousand of divers, but also for a great number of middlemen, factory workers and exporters. This scallop

boom thus greatly improved the sustenance basis for thousands of associated families of the nearby town of Pisco.

This “gold rush” period for scallop fishery ended with a normalization of the ecosystem, an almost depletion of the natural scallop stock and the need for scallop divers to shift again to other resources besides the scallops (such as mussels, crabs, clams, octopods among others) and to become used again to low catches and income levels. Another El Niño event of about the same strength impacted the region again in 1997/1998 and the positive effect on the scallop population of the bay was very similar as during the preceding event 15 years ago. Unfortunately, total scallop harvest was much lower during these years due to a mismanagement (growth over fishing) of the resource (Wolff and Mendo, 2000).

Numerous studies have been conducted on the population dynamics of the scallop during normal years and during the El Niño impact (Wolff and Wolff, 1983; Wolff, 1985; Mendo et al., 1988; Mendo and Jurado, 1993; Wolff and Mendo, 2000) showing that population parameters greatly change over an El Niño- cycle, with recruitment and growth rates increasing with water temperature. These studies revealed that Argopecten purpuratus is a relatively short- lived species, whose population sizes greatly depend on the recruitment success of the same year.

Catches are as yet considered unpredictable due to the great environmental stochasticity of the ecosystem and the many abiotic and biotic factors that may affect stock size. As a consequence, the diving fishermen have become used to act like opportunistic predators, searching for and moving towards those areas where scallop abundance happens to be profitable. If this is not the case, other invertebrates are targeted. During the two Niño events mentioned, the diving fleet of Independencia bay increased from less than 100 boats in normal years to over 1000, operating in the zone.

The ability to predict annual scallop catches would greatly improve the situation of the fishery and the associated export business, since all stakeholders involved would have time to plan and to adjust to the ever changing conditions.

A first prediction of (at least) the order of magnitude of scallop catches in Independencia bay was attempted by Mendo & Wolff (2002), who found the mean temperature during the spawning period (November- April) to explain about 77% of the catch variation in the following “biological year” (from July-June).

This first model encouraged us to revisit the available data set of monthly scallop landings and temperatures of the bay from 1983-1998, to add more recent data (to 2005) and to try to improve the model.

We started with the above-mentioned simple linear regression, and asked for the possible mechanism behind the observed relationship between the temperature during

spawning and the catches in the following year. We reasoned that an increase in the annual recruitment rate of juvenile specimens to the fishery should mainly be the result of the number of settlers, which should be a function of the number of spawners (and thus the number of eggs released to the environment) as well as the natural larval mortality during the time period from egg release to settlement to the bottom substrate. While the former is influenced by the fishery, the latter should be greatly dependent on temperature, which accelerates larval development, shortens larval period and thus enhances survival.

Based on this reasoning we constructed a multiple regression model to predict the annual catches after the recruitment period (after July) from proxies for spawning stock biomass and settlement rate. The first was considered proportional to the catches during the spawning period; the latter was derived from a temperature dependent survival rate of the settlers (see below).

2. Material and Methods

2.1. Data used

The data used for the model were monthly scallop catches in Independencia bay and mean monthly water temperatures recorded at the La Vieja Island (see Fig. V.1) by the Instituto del Mar in Pisco during the period 1983-2005. Catch and temperature data by IMARPE are taken on a daily basis and are then averaged to monthly values. The first author has surveyed the catches in Independencia bay himself in the early 80ties and has compared his own estimates with those of IMARPE finding good agreement (Wolff and Wolff, 1983). The fourth author of this paper also confirms this. So the landings data are considered reliable.

2.2. Basic assumptions underlying the model

1) Scallop landings reflect the size of the scallop stock in the bay. If the stock increases or decreases, the fishery grows or shrinks accordingly, so that the relative fishing rate remains relatively constant and the catch is proportional to stock size.
2) Scallop landings during the post-recruitment period, which starts in winter (July/August) each year largely depend on the recruits spawned during the

preceding summer/autumn period (Nov-April) (Wolff, 1988; Wolff and Mendo, 2000), typical for annual "pulse fisheries".

3) Spawning stock is assumed proportional to scallop landings during spawning (Nov.-Apr.)
4) Larval survival in the natural environment (from egg release to settlement) is significantly lower than the observed 0.1% in the hatchery (Wolff et al., 1991).
5) Day degrees (dd) for larval development including successful settlement were considered to be approx. 400 for the temperature range relevant for the area (14-25°C), based on hatchery data by DiSalvo et al. (1984), Uriarte et al. (1996b) and Wolff et al. (1991). During typical cold water years (14°C) larvae would thus need over 28 days to settle, while only about 16 days are needed at the high El Niño temperatures of 25°C.

2.3. Model construction

The following steps were followed to construct the model:

An instantaneous daily larval mortality rate was estimated using the negative exponential mortality model below (equation 1) and a range of assumed survival rates: 0.01%. 0.001% and 0.0001%. The period to settlement (24.6 days) was estimated from the mean spawning temperatures of 16. 24 °C obtained from our time series (Table V.1) and the 400 dd.

$$M = \text{Ln } (Nt/No)/LP \quad (1),$$

where N_t is the number of settlers, N_0 is the number of eggs (arbitrary number), M is the instantaneous rate of natural mortality per day and LP (t) is larval period (in days)

Using the values for the larval period (LP) under the different spawning temperatures for the different years (Table V.1), the number of settlers, Nt ("now coined settlement factor, SF) was calculated rearranging the above equation 1 and replacing LP by the value of 400 for the day degrees(dd) divided by the spawning temperatures (T°C) (equation 1b):

$$SF = N_0 * e^{-M*400/T°C} \quad (1b)$$

We standardized SF as being 1 for the mean spawning temperature (T°C = 16.26) recorded in the study period (1983-2005) and calculated SF at other temperatures accordingly.

A stepwise multiple regression was calculated using the mean monthly catch and the temperature–dependent SF during the spawning period (Nov.-Apr.) as independent variables and the landings from July-June following the annual recruitment as dependent variable. Equation (1b) was repeatedly calculated with our different range values of M yielding envelop values for SF of different magnitude. These were then iteratively used for the regression analysis and the mortality rate that allowed for the best fit was finally chosen. Following the El Niño outburst 1998, scallop fishermen started to collect small seed scallop shortly after recruitment (May, June) and transferred this seed to grow out areas in the bay, where scallops were kept until market size (in November, December 1998) For this reason,.. the bulk of the scallop catch was not taken within the first months of the fishing season (which is usually the case), but later in the spawning season, increasing catches to unprecedented values during these months. The data of this period were therefore not comparable with the rest of the time series data and had to be excluded from the analysis (see Table V.1).

3. Results

3.1. Mortality rates, Settlement factor (SF), Model data input

Out of our seed values for the survival rate, 0.0001% survival to settlement corresponding to a mortality rate of 0,558 day^{-1} yielded estimates of the settlement factor (SF) that allowed for the best fit of the regression. The improvement of the fit from the other survival rate values tried (0.01% and 0,001%) was marginal, however (by + 0.81% and +0.04% respectively). When the survival rate was lowered beyond the 0.0001% value, the fit started to decrease. Table V.1 contains the input data to the multiple regression model.

3.2. Model output

Figure V.2 show the bivariate scatter plots of relative spawning stock (SS) versus catch (Fig. V.2a) and settlement factor (SF) versus catch (Fig. V.2b). Evidently, both

factors explain a great portion of the variation of the data, and the settlement factor alone is a relatively better predictor for the catch than the spawning stock.

Table V.2 gives a summary of the regression statistics of the multiple regression with catch as the dependent (y) and Settlement factor (SF) and spawning stock (SS) as the independent variables (x_1,x_2).

Figure V.3 shows the predicted versus the observed monthly catches for the period July-June based on the multiple regression (Fig. V.3a), as well as the confidents limits around the regression line (Fig. V.3b). The regression shows that the model is less able to predict low catch levels as many of the observed vs. predicted values lie near or outside the 95% confidence limits on the lower end. The following Table V.3 summarizes the analysis of the residuals.

Figure V.4 shows the predicted relative catch as a function of temperature and relative spawning stock size (here we used arbitrary values ranging from 10t-100t monthly catch during the spawning period. It is evident from predicted catch between low and high temperatures that stock size during spawning (SS) is important at low temperatures (14,15,16°C), while beyond 20°C the predicted catch is almost exclusively (>80%) a function of temperature (i.e. Settlement factor - SF).

4. Discussion

4.1 Predictive fisheries models and the mechanism proposed for the scallop model

Despite of occasional attempts of fisheries scientists to emphasize the importance of environmental variability (EV) for the dynamics of aquatic resources (see early contribution of Ricker (1958) in which he emphasizes the role of the environment in shaping the stock- recruitment relationship in marine fish or the classical book “Climate and Fisheries” of Cushing (1982). Wiff & Quiñones (2004), Chen & Hare (2006) and Nishida et al., (2007), modeling of the influences of environmental variability or environmental change on population dynamics is by many fisheries scientists still considered as not possible or even as not necessary. As Hilborn and Mangel (1997) stated: “Since fishing pressure can be managed but the environment cannot, the default assumption in fisheries models has been to assume that the changes are due to fishing pressure…thus, we leave the challenge of realistically considering environmental change for the next generation…”. It has been shown, moreover, that most environment-ecosystem interactions are non-linear and that a causal chain is often difficult to detect.

The non-linearity might also explain part of the often observed “breaking relations” described by Myers (1998), who showed that correlations between biological processes and environmental factors may be valid only for a small range of the environmental factor considered.

The model presented here is based on a time series of 22 years of monthly catches and environmental temperatures and a substantial knowledge of the population dynamics and early life history of the species modeled. This allowed us to propose a mechanism - a temperature-mediated change in the larval period, which directly relates to the relative number of survivors to settlement. In addition we postulate as a second factor influencing the recruitment success the absolute number of eggs spawned, which is assumed to be proportional to the catches during the spawning period.

We think that the temperature dependence of the larval period used in our model is valid, since it is based on laboratory experiences and since our model data remain within the in – situ temperature range (14-25°C) found for the scallop in Independencia bay. So the problem of “breaking relations” should not occur within this range of the environmental variable used. A key question that arises here is why just this one scallop species responds so favorably to the warming, while most other macro benthic species’ response is rather insignificant or even negative. Shouldn’t the proposed mechanism also hold for other species? Wolff (1987) based on a study on the population dynamics of this species during the El Niño period 1983/84 and on fossil studies by (Waller, 1969) offers an explanation by suggesting that Argopecten purpuratus is a relict of a tropical/subtropical fauna that once dominated the Peruvian shores during the Miocene. El Niño events may have occurred frequently enough, subsequent to the general cooling of the waters in the late Miocene to preserve the warm water characteristics of this species. Most recent macro benthic species of the bay are more typical upwelling – adapted, cold – water species, however, and rather stressed during the warm El Niño temperatures.

While the assumption of shortage of the larval period at El Niño temperatures is thus based on solid evidence, our estimate of the mortality rate is not. Larval mortality is known to be much higher in-situ than in hatcheries, but accurate estimates are not available, since in-situ measurements are very difficult. So we had to use an envelope of values of settler to released eggs ratio to search for the best fit of our regression. Surprisingly, all of our envelope values, when applied to calculate the settlement factor, yielded a high regression coefficient (r^2>0.92), with the ratio of 1:100000 providing the best fit (0.930). This suggests that the model results are quite robust over a wide range of M –values, and that the “real” in situ larval mortality rate may be in the order of magnitude estimated.

Possibly the most crucial assumption of our model is that of a constant and temperature-independent instantaneous daily mortality rate. By assuming this, we propose that larval mortality is mainly due to exposure to predation, considered independent of temperature. It could be argued, however, that predation rate may also increase with temperature. While we cannot exclude this to hold true for some species, most potential predators of the scallop larvae seem to be rather cold water adapted species, for which the high El Niño temperature may already represent adverse conditions beyond their physiological optimum (Mendo and Wolff, 2002).

Since the total number of days in the plankton is greatly reduced at higher temperatures, total exposure time to predation and to dispersal by currents, which may remove the larvae from the scallop banks, is also reduced and the number of settlers within the bay should greatly be increased. By standardizing the settlement factor for the average spawning temperature of 16.26°C recorded, we assumed that recruitment will be (on average) lower and higher at lower and higher temperatures respectively.

It may be asked if other factors, besides temperature (or co-varying with temperature), may also be influential for the varying recruitment success of the scallops during the study period. Here we should mention the increased oxygen saturation levels of bottom water of the bay during El Niño events (Wolff, 1987; Wolff and Mendo, 2000), which have been shown to also correlate with scallop biomass to a certain extent (Wolff, 1988). This factor may help to explain why high scallop biomass levels can be sustained in the bay during El Niño conditions, but hardly explains why just scallops were favored to such an extend. Changing food conditions could also be influential. It may be that a shift in the plankton composition as related to the warming during El Niño (from larger diatoms to smaller dinoflagellates) may have also positively impacted the scallop larvae and juveniles. One would expect, however, that other bivalves of the system should then have also been favored. The same argument holds for a possible release in predation pressure. If the scallop outburst was due to a release in predation pressure, why were other macro benthic species not favored?

Based on the above reasoning, we believe that the proposed mechanism, by which larval survival and recruitment success is increased with temperature, is valid.

The other main pillar of our model – the assumption that catches during the spawning season are suitable proxies for spawning stock size, which is also decisive for the annual recruitment success, may need some further clarification here. Contrary to many other countries of the region, Peru still allows for an open access fishery, so the diving fishing fleet of Independencia bay flexibly grows and shrinks with the natural scallop population, through migrating fishermen from the south and north of the country (Wolff and Mendo, 2000). This means that fleet size and catches have varied over the years and

the year's cycle in proportion to the available scallop harvest potential. Thus catches during the spawning period should be good proxies for the spawner biomass. While the latter can thus be assured, the number of released eggs/spawner may have also changed with temperature, as it has been shown that gonad recuperation was greatly accelerated during higher temperatures (Wolff, 1988). If so, the number of eggs spawned would not just be a function of spawning stock biomass but also of temperature, an effect not considered in our model. It is also possible that egg quality may have been influenced by the temperature regime and the onset of spawning, a factor shown to be important for fish such as Atlantic cod (Scott et al., 2006).

4.2 The model fit and catch predictability

If we examine the relative importance of our two factors -spawning stock and settlement factor- for predicting annual catches, we find that both factors alone may explain a substantial part of the inherent variability of the data. The contribution of the settlement factor was greater, however (Fig. V.2a) yielding a better fit in the bivariate correlation (r=0.724 compared to r=0.601 for the spawning stock). The overall fit of the multiple regression (r^2= 0.930) can be considered as remarkably good, also reflected in the narrow confidence belt around the regression line (Fig. V.3b) and the generally low residuals given in Table V.3. It is interesting to note, however, that the differences between recorded and predicted catches is greatest at the lowest recorded catch levels of 1 t and 7 t respectively (Table V.3). It is possible that these very low catch levels do not represent well enough the total catchable stock, since divers tend to target other invertebrates when scallop densities decrease beyond a threshold (ca.0.1 Ind. m^{-2}) (Wolff, pers. observation). However, Figure V.3 shows that the model does not only predict catches well for the two El Niño warming periods, but also for the last years (2001-2004), when low temperatures caused low spawning and low recruitment. Figure V.4 illustrates that the predicted annual catch greatly depends on the spawning stock size at low temperatures, while this factor decreases in importance at higher temperatures, at which the settlement factor becomes much more influential. These findings are of great relevance for the management of the stock: at low temperatures, the maintenance of a large enough spawning stock (equivalent to a minimum density of scallops in the environment) over the spawning period (Nov.-April) is decisive for the yield of the post-recruitment fishing period thereafter, while at increasing spawning temperatures, spawning stock size is of little importance for determining the yield. The parent stock-

recruitment relationship appears thus strong at low temperatures, and weak at the higher El Niño temperatures.

4.3. Concluding remarks

Compared to age-or size structured population models and Surplus production models, which in addition to catch data require substantial data on population size structure, growth, natural and fishing mortality and of fishing effort respectively, our model can do without these data. Instead, it just needs mean monthly temperatures and catches during the spawning period. This simplicity is a great advantage over many of those data intensive models, which may also suffer from incorrect assumptions regarding the constancy of growth and mortality rates over longer time periods. To the knowledge of the authors, a model based on the proposed mechanism has as yet not been applied to other fisheries, although attempts to empirically relate recruitment strength to spawning stock size and a series of environmental factors have been followed before. These attempts differ from the here presented one, in that they empirically establish stock-recruitment relationships, by using data on spawning stock size and number of recruits of a certain age of entry into the fishery, and then add additional environmental variables to the model. They mathematically extend beyond the traditional Ricker spawner-recruit model – by using generalised additive modeling approaches (Daskalov, 1999) or applying fuzzy logic (Nishida et al., 2007 for Bigeye Tuna in the Indian Ocean) or neural network analysis (Chen and Hare, 2006 for Pacific Halibut). These modernized versions have -no doubt- allowed to incorporate environmental variability and to greatly improve the fit to the data compared to the traditional empirical Ricker model. We choose another, however less empirical approach based on the assumption of a functional mechanism behind the recruitment success and derived a temperature dependent new variable, which we called “settlement factor”. This new variable explains a much larger part of the observed variability in annual catches then the spawning stock, pointing to the strong role of environmental variability in governing the population dynamics of the Peruvian bay scallop. Since the model is build on two factors only, the confidence belt around the predicted estimates is relatively narrow, when compared to recent models of a higher complexity.

The special success of this approach may lie in the biological characteristics of the scallop, which as a relict of formerly warm water fauna of the Peruvian coast, is greatly favored when tropical El Niño conditions appear in Independence bay. Thus, during these periods the “environmental window” (Cury and Roy, 1989) seems to open allowing the

stock to proliferate. Since the regression model explains large part of the variability of the data (r^2=0.930) it promises successful predictions of the Peruvian scallop catches of Independencia Bay. While the model's strength is its simplicity and the low data requirements, its applicability requires that the present fishing system (diving fishery, absence of closed seasons, no protected areas, minimum landing size of 65 mm shell height, open access) remains essentially unchanged.

Acknowledgements

This study was financed and conducted in the frame of the EU-project CENSOR (Climate variability and El Niño Southern Oscillation: Impacts for natural resources and management, contract No. 511071) and is CENSOR publication No. 0125.

Tables and Figures

Table V.1. Model input data

Spawning Period (Nov.-April)	Mean T (°C) during spawning	Monthly catches during spawning	Settlement factor (SF) at M=0.558(day-1)	Mean catch after recruitment (July-June)
1982/83	22.5	56.3	45.26	1384.0
1983/84	15.7	2247.0	0.61	2198.0
1984/85	14.7	1680.3	0.23	1720.0
1985/86	14.6	86.0	0.21	408.0
1986/87	16.9	12.7	1.68	1.0
1987/88	15.6	0.0	0.56	225.0
1988/89	15.6	486.8	0.56	7.0
1989/90	14.8	5.5	0.26	90.0
1990/91	15.4	74.3	0.46	128.0
1991/92	18.1	150.8	4.04	115.0
1992/93	15.7	48.5	0.61	77.0
1993/94	15.1	124.8	0.35	344.0
1994/95	16.2	703.3	0.95	355.0
1995/96	14.4	234.8	0.17	107.0
1996/97	18.8	65.2	6.40	479.0
1997/98	24.1	353.8	87.53	2938.0
(1998/99)*	(14.6)*	(2516.9)*	(0.209)*	(614.0)*
1999/00	14.5	739.3	0.19	110.9
2000/01	14.9	65.8	0.29	9.6
2001/02	15.2	7.8	0.38	6.7
2002/03	15.3	10.1	0.42	5.2
2003/04	15.4	5.6	0.46	10.2
2004/05	15.9	13.7	0.73	12.6

Table V.2. Regression statistics of derived multiple regression.

	Beta	Std. Err. B	B	Std. Err. B	t(19)	p-level
Intercept			-12.195	58.401	-0.209	0.836814
Spawning Factor	0.755	0.061	30.095	2.420	12.436	0.000000
Settlement Factor	0.638	0.061	0.894	0.085	10.514	0.000000

Regression Summary for Dependent Variable: Catch (July-June); R= .96445299; R^2= .93016957; Adjusted R^2= .92281900; F(2,19)=126.54; p<.00000; standard error of estimate: 225.71

Table V.3. Summary of analysis of residuals.

Year	Observed	Predicted	Residual	Standard P.v	Standard Residual	St. Err. Pred. value	Mahalanobis distance	Deleted Residuals	Cook's distance
1982/83	1384.0	1400.2	-16.2	1.16	-0.07	106.02	3.68	-20.73	0.001
1983/84	2198.0	2015.6	182.4	1.95	0.81	170.30	11.00	423.45	0.668
1984/85	1720.0	1497.4	222.6	1.29	0.99	125.16	5.50	321.38	0.208
1985/86	408.0	71.0	337.0	-0.53	1.49	55.04	0.29	358.29	0.050
1986/87	1.0	49.8	-48.8	-0.56	-0.22	56.74	0.37	-52.04	0.001
1987/88	225.0	4.6	220.4	-0.62	0.98	58.00	0.43	235.97	0.024
1988/89	7.0	440.0	-433.0	-0.06	-1.92	52.15	0.17	-457.38	0.073
1989/90	90.0	0.5	89.5	-0.62	0.40	57.98	0.43	95.86	0.004
1990/91	128.0	68.2	59.8	-0.54	0.27	55.24	0.30	63.58	0.002
1991/92	115.0	244.4	-129.4	-0.31	-0.57	50.96	0.12	-136.31	0.006
1992/93	77.0	49.6	27.4	-0.56	0.12	56.05	0.34	29.21	0.000
1993/94	344.0	109.9	234.1	-0.48	1.04	53.74	0.24	248.18	0.023
1994/95	355.0	645.3	-290.3	0.20	-1.29	59.24	0.49	-311.83	0.044
1995/96	107.0	202.9	-95.9	-0.36	-0.43	51.53	0.14	-101.17	0.003
1996/97	479.0	238.8	240.2	-0.32	1.06	53.03	0.21	254.23	0.023
1997/98	2938.0	2938.6	-0.6	3.13	0.00	201.05	15.71	-2.86	0.000
1999/00	110.9	654.6	-543.7	0.21	-2.41	61.33	0.60	-587.08	0.167
2000/01	9.6	55.2	-45.6	-0.55	-0.20	55.66	0.32	-48.51	0.001
2001/02	6.7	6.3	0.4	-0.61	0.00	57.80	0.42	0.44	0.000
2002/03	5.2	9.6	-4.3	-0.61	-0.02	57.67	0.42	-4.65	0.000
2003/04	10.2	6.7	3.4	-0.61	0.02	57.83	0.42	3.66	0.000
2004/05	12.6	22.1	-9.5	-0.59	-0.04	57.31	0.40	-10.11	0.000
Minimum	1.0	0.5	-543.7	-0.62	-2.41	50.96	0.12	-587.08	0.000
Maximum	2938.0	2938.6	337.0	3.13	1.49	201.05	15.71	423.45	0.668
Mean	487.8	487.8	0.0	0.00	0.00	73.17	1.91	13.71	0.059
Median	112.9	90.5	-0.1	-0.51	0.00	57.49	0.41	-1.21	0.004

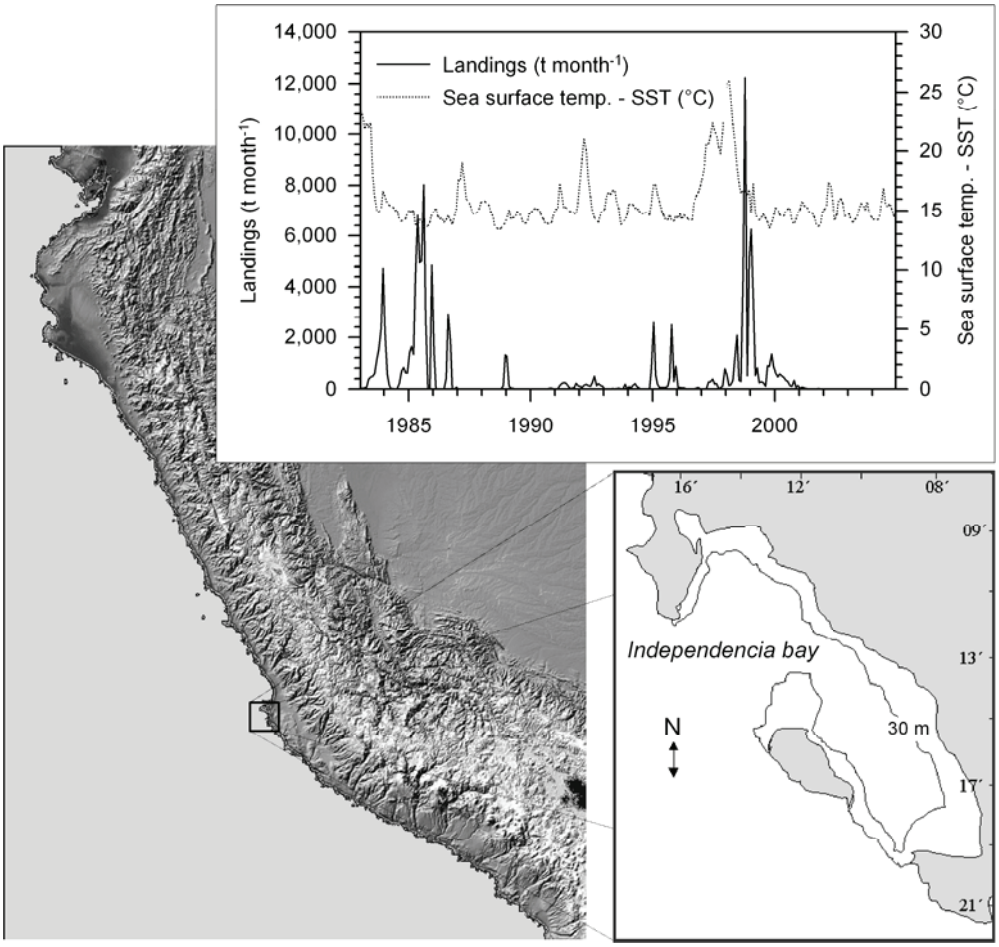

Figure V.1. Independence Bay (right); Scallop landings and SST (°C) (1983-2004) (left).

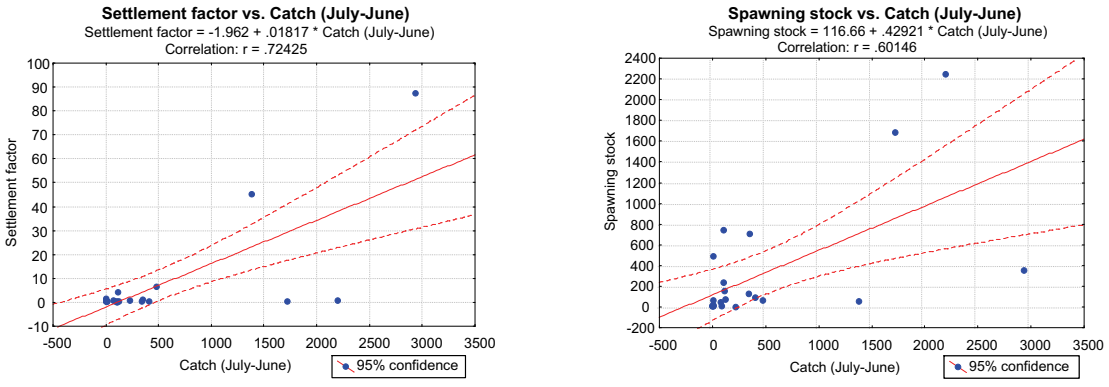

Figure V.2. a) Settlement factor (SF) and b) Spawning stock biomass (SS) as related to catches after the annual recruitment period (July-June).

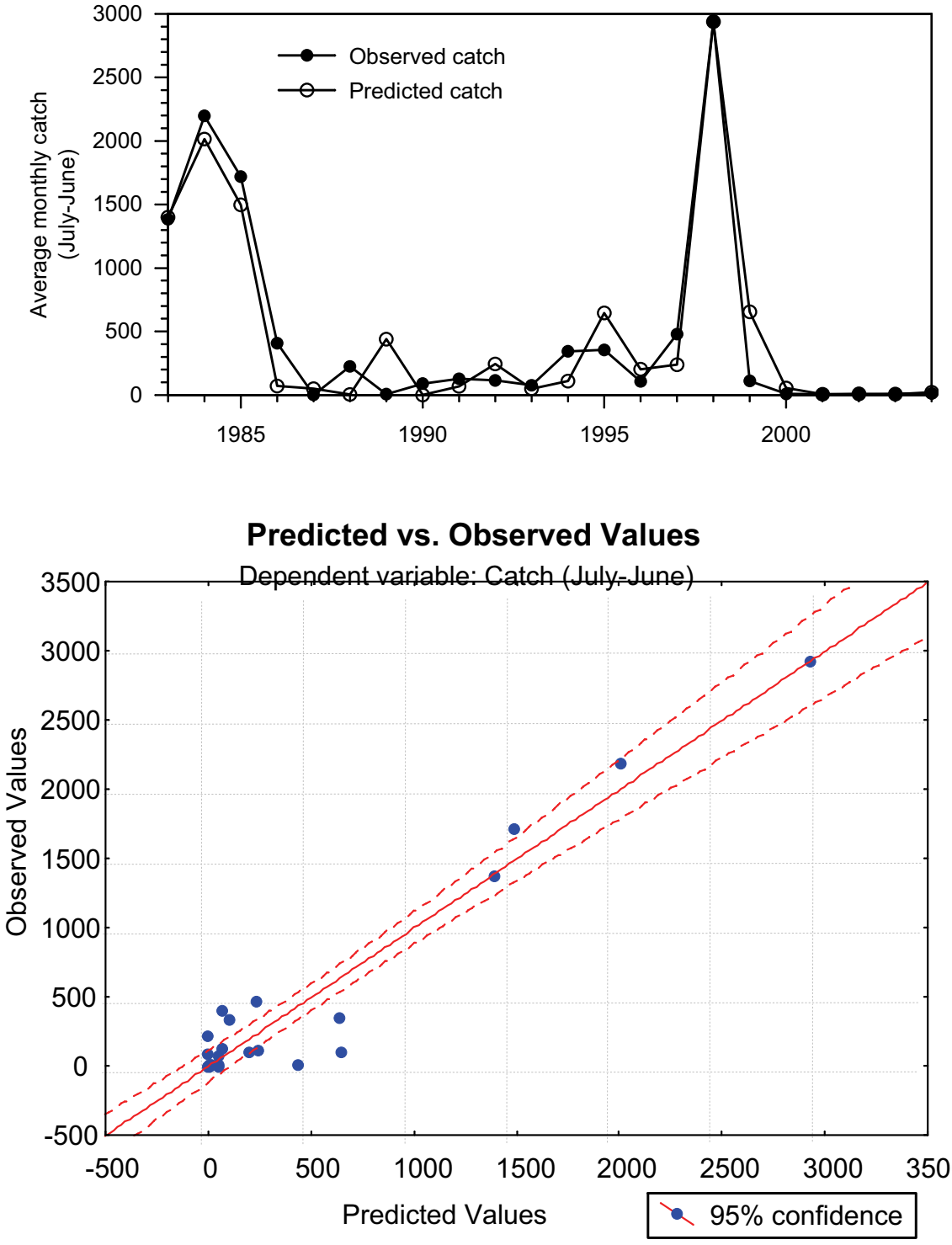

Figure V.3. Predicted versus recorded catches for the period 1983-2004 (graph below shows the confidence limits around the regression line).

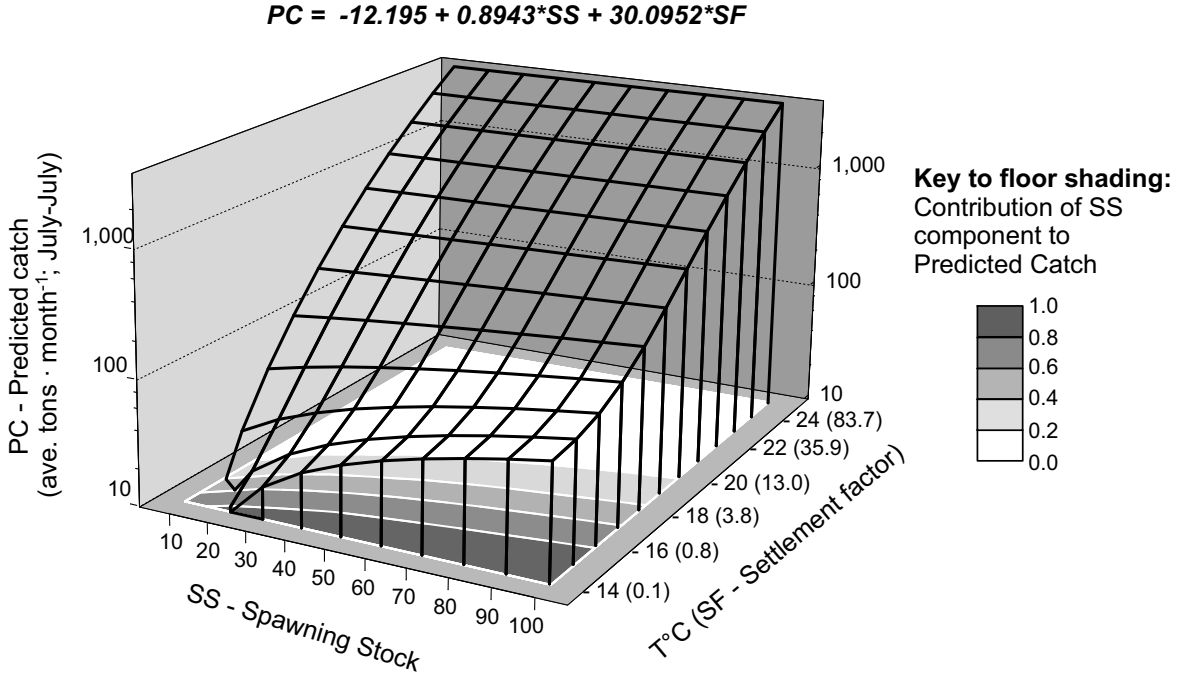

Figure V.4. Predicted monthly catches, PC (ave. catch in tons month-1; July-June), as a function of temperature (Settlement factor, SF, in parenthesis) and spawning stock, SS (ave. catch in tons month-1 over the previous spawning period, Nov.-Apr.). Floor shading shows the contribution of SS to the value of predicted catch (SS/PC).

Chapter VI. Changes in trophic flow structure of Independence Bay (Peru) over an ENSO cycle

Marc H. Taylor[*]*, Matthias Wolff, Jaime Mendo, Carmen Yamashiro*

Author's posting. This is the author's version of the work. Please cite the final version to be published by Progress in Oceanography as part of the Proceedings of the Conference, *The Humboldt Current System: Climate, ocean dynamics, ecosystem processes, and fisheries*, Lima, Peru, November 27 - December 1, 2006. Article accepted November 8th, 2007

Abstract

During the strong warm El Niño (EN) that occurred in 1997/98, Independence Bay (Peru) showed a ca. 10 °C increase in surface temperatures, higher oxygen concentrations and overall clearer water conditions due to decreased phytoplankton concentrations. Many benthic species suffered under these almost tropical conditions (e.g. macroalgae, portunid crabs, and polychaetes), while others benefited (e.g. scallop, sea stars, and sea urchins). The most obvious change was the strong recruitment success and subsequent proliferation of the scallop *Argopecten purpuratus,* whose biomass increased fifty-fold. To understand the changes in trophic flow structure that occur during EN, steady-state models of the bay ecosystem were constructed and compared for a normal upwelling year (1996) and during an EN event (1998), and longer-term dynamics (1996-2003) were explored based on time series of catch per unit effort (CPUE) and relative biomass for several groups using the Ecopath with Ecosim (EwE) software. Model inputs were based on survey and landings data of Instituto del Mar del Perú (IMARPE).

[*] Corresponding author, Email: (marchtaylor@yahoo.com)

Results indicated that while the total system size (throughput) is reduced by 18% during EN, mainly as a result of decreased total primary production, total biomass remains largely unchanged despite considerable shifts in dominance of functional groups (e.g. scallops replace polychaetes as the dominant consumer of plankton/detritus). Under normal upwelling conditions, strong predation by snails and crabs utilize the production of their prey species almost completely, resulting in higher energy transfer and organization of flows in higher trophic levels than during EN. However, during EN, the proliferation of the scallop *A. purpuratus* combined with decreased phytoplankton resulted in an increased overall energy cycling and utilization of primary production, while exports and flows to detritus are reduced. Our simulations suggest that the main cause for the scallop outburst and for the reduction in crab and macrophyte biomass was a non-trophic, temperature-dependent population response during the EN warming period, whereas other observed changes can be partially explained by trophic interactions: an EN caused decrease in the groups *Benthic detritivores*, *Miscellaneous filter-feeders*, *Herbivorous gastropods* and *Polychaetes*, and an increase in the groups *Predatory gastropods*, *Small carnivores*, *Sea stars* and *Octopus*. Predator-prey vulnerability settings, as calculated through the fitting routine of EwE, suggest an overall dominance of bottom-up control settings in the system.

1. Introduction

The Humboldt Current System (HCS), located in the south east Pacific along the coasts of Chile and Peru, is arguably one of the most productive marine systems in the world. This high productivity is the result of upwelling processes driven by southerly trade winds that bring cold, nutrient-rich water from depths of 40-80 m to the euphotic zone where it is utilized by phytoplankton photosynthesis (Barber et al., 1985; Arntz et al., 1991). As a result, the system supports a large biomass of small planktivorous pelagic fish - comprising the bulk of catches by the industrial fishing fleet. An important artisanal fishery also exists down to 15-30 m and in the intertidal areas (Arntz and Valdivia, 1985b; Arntz et al., 1988). Despite a relatively low annual harvest (ca. 200,000 $t \cdot yr^{-1}$) compared to the pelagic system, the exploited nearshore species are of high commercial value and this fishery supports thousands of fishers and their families (Wolff et al., 2003).

Under 'normal' upwelling periods, near-seafloor oxygen concentrations <0.5 $ml \cdot l^{-1}$ are typical (Zuta et al., 1983). This is due to the raised thermocline and the high input of settling organic matter out of the euphotic zone to the seafloor. Bacteria such as the

filamentous ('spaghetti') bacteria mainly belonging to the genus *Thioplaca*, are commonly found in association with the oxygen minimum zone (OMZ) (Arntz et al., 1991). At shallower depths, oxygen concentrations increase and are able to support a higher benthic biomass. This is also seen in Independence Bay where the deeper regions of the inner bay are of low biomass while the bay's perimeter of less than 30 m is the most productive and thus targeted by the artisanal fishery. These areas contain several molluscan and crustacean species but suspension feeders (mainly polychaetes) are dominant (Tarazona et al., 1991).

The HCS is highly dynamic, experiencing 'natural' perturbations on several different temporal scales (seasonal, interannual, decadal), which affect the system's productivity and ultimately the resource users as well. The most noteworthy and extreme is that of the warm "El Niño" (EN) phase of the El Niño Southern Oscillation (ENSO), which is a periodic event whereby an eastern flowing Kelvin wave travels across the Pacific Ocean and, upon reaching the South American coast, causes a deepening of the normally shallow thermocline and a rise in sea level. Although offshore transport may continue during an EN event, upwelled water originates from above the lowered thermocline and is nutrient poor (Barber and Chavez, 1983). As a result, the area of "productive habitat" (>1.0 mg chl*a* m^{-3}) is greatly reduced (Nixon and Thomas, 2001) as is overall primary production (Carr, 2002). This reduction in production at the base of the food web has been shown to negatively impact many pelagic coastal species (Chapters III and IV)

The effects of EN on benthic habitats can produce significant positive faunal changes mainly as a result of improved oxygen concentrations on the seafloor (Arntz et al., 1991). This is especially the case in shallow depths, where faunal density, biomass, species richness, and diversity have been observed to increase with EN (Tarazona et al., 1988a). Several species from the oceanic and equatorial, (sub) tropical areas are seen to immigrate to the Peruvian coast, such as swimming crabs and penaeid shrimps (Arntz et al., 1991). The most notable positive impact in Independence Bay is that of the resident scallop *Argopecten purpuratus*, which experiences much higher recruitment and subsequent proliferation. Past El Nino densities have reached up to 8 $kg \cdot m^{-2}$ and densities of 129 adult $scallops \cdot m^{-2}$ (Wolff, 1987; Arntz and Tarazona, 1990). Yearly surveys of the scallop population and associated macrobenthos of Independence Bay (Fig. VI.1) conducted by the Instituto del Mar del Perú (IMARPE) have observed biomass decreases in several functional groups during EN (e.g. macroalgae, benthic detritivores, herbivorous gastropods, predatory gastropods, portunid crabs, and polychaetes) and scallops come to nearly complete replace polychaetes as the main benthic feeder of plankton and detritus (Fig. VI.2).

During the last two very strong events of 1982/83 and 1997/98, populations of the scallops exploded in Independence Bay to levels exceeding normal upwelling years by about 50 times (Wolff, 1987; Wolff and Mendo, 2000). The scallop became the principal target of the artisanal fishery, which experienced “gold rush” conditions with unprecedented high catches and enormous revenues (Wolff, 1987, 1988, 1994; Wolff and Mendo, 2000; Mendo and Wolff, 2002). The diving fishery effort in Independence Bay increased mainly due to migration of fishers from other areas. As a result of this dynamic response of the fishery, catches largely reflect the actual changes in the scallop population. Other high priced species associated with the scallop habitat are octopus and crabs. While crab catches show a decrease during the 1997/98 EN, octopus landings increased nearly 5 times. The line and net fishing fleet remained roughly constant during the same period although catches increased by about 2.5 times mainly due to an increase in pelagic predatory species, which migrated towards the coast.

While a good base of knowledge exists concerning the main changes occurring in benthic coastal communities of the Peruvian coast, an ecotrophic approach to the effects of EN has yet to be employed. Here, our goal is to describe and understand the changes in the whole ecosystem from an energy flow perspective, following two approaches. First, we compare steady state models of the system for the upwelling and El Nino periods, and the second was to simulate ecosystem transition between these two states, using time series of catch per unit effort (CPUE) and compartment biomasses to understand the mechanisms leading to these changes. In particular, we address the following questions: i) Are the positive impacts observed in the shallow benthic community during an EN event (increase in species richness, and diversity) also reflected in the entire ecosystem through indicators of system maturity? ii) How is the system reorganized during an EN event? iii) What insight can be gained into the management of the fishery during an EN? iv) To what extent can observed changes in compartment biomass and productivities be explained by differential physiological response of (some of) the bay’s biota to the warming events and/or to trophic interactions? v) What is the trophic effect of the increased scallop biomass, the reduced primary production (through biomass decrease of *Phytoplankton* as well as *Macroalgae*) and the reduced crab predator biomass on the system?

2. Materials and Methods

2.1. Study area

Independence Bay (14.238° S, 76.194° W) is located approximately 250 km southeast of Lima (Fig. VI.1). The bay contains two main connections to the open ocean on either side of a bordering island, 'La Vieja', where cool nutrient-rich upwelled water is exchanged with the bay. Due to this hydrograpy, the conditions of the bay largely reflect the nearshore Peruvian upwelling system, characterized by low surface temperatures (14-18 °C) and bottom oxygen concentrations averaging 3.5 mg L^{-1} during normal upwelling periods. In the central part of the bay (>30 m depth), low oxygen conditions prevail (< 1.0 mg L^{-1}), benthic biomass is low and microbial processes dominate. During a strong EN event, temperatures increase as much as 10°C and oxygen conditions are improved at the lower depths. Artisanal fisheries include a diving fishery using hookah and compressor, which operates around the bay's rocky and soft-bottom habitats less than 30 m, and a gillnet and line fishery that targets larger littoral and pelagic fish species.

2.2. Model definition

The two steady-state models of Independence Bay are for the soft-bottom habitats of <30 m depth that fringe the bay, covering about 38% of the total bay area (65.8 km^2 out of a total of 172 km^2) (Fig. VI.1). This area was selected for the following reasons: i) importance in overall bay biomass, ii) availability of data, and iii) encompasses the main activities of the artisanal fishery. Model periods are for 1996 as a 'typical' upwelling year, and 1998, as representative of the end of the EN phenomenon of 1997/98 (Fig. VI.2). Models were constructed with 20 functional groups including *Detritus*, two producer groups (*Phytoplankton* and *Macroalgae*), *Zooplankton*, six benthic primary consumer groups (*Polychaetes*, *Scallops*, *Sea urchins*, *Herbivorous gastropods*, *Benthic detritivores*, and *Miscellaneous filter-feeders*), five benthic carnivore groups (*Predatory gastropods*, *Small carnivores*, *Predatory crabs*, *Sea stars*, and *Octopus*), three fish groups (*Littoral fish*, *Small pelagic fish*, and *Pelagic predatory fish*), and two top predatory groups (*Marine mammals* and *Sea birds*). Functional groups were designated according to similar diets, predators, productivities and individual body size (Table VI.1).

2.3. Basic modeling approach

A mass-balance modeling approach was applied using the software Ecopath with Ecosim 5.0 (EwE) (Christensen and Pauly, 1992; Walters et al., 1997), which allows quantifying and balancing trophic flows among components (functional groups) of an ecosystem and also permits the assessment of ecosystem dynamics under different scenarios of use or environmental change (www.ecopath.org). The Ecopath model links the production of each group with the consumption of all those groups trophically connected:

$$P_i = Y_i + B_i * M2_i + E_i + BA_i + P_i * (1 - EE_i) \qquad (1)$$

where P_i is the total production rate of (i), Y_i is the total fishery catch rate of (i), B_i the biomass of the group (wet weight), E_i the net migration rate (emigration – immigration), $M2_i$ is the total predation rate for group (i), BA_i is the biomass accumulation rate for (i). $P_i * (1\text{-}EE_i)$ is the 'other mortality' rate ($M0_i$), where *EE* is the "Ecotrophic efficiency" and is the proportion of the group's production that is consumed by higher trophic levels or is taken by the fishery (for further information, see Christensen et al., 2000). In order to ensure mass balance between the groups, a second master equation is used:

Consumption = Production + Respiration + Unassimilated food

A major input for the Ecopath model is the diet composition for all consumers, which gives the fraction of each functional group as food of the other groups of the system. This diet matrix is further used for the calculation of the trophic level of each model group:

$$TL_j = 1 + \sum TL_i * DC_{ij} \qquad (2)$$

where DC_{ij} is the fraction of prey (i), in the diet of the predator (j). The trophic level of the predator TL_j is calculated as the mean trophic levels of its prey ($\sum TL_i*DC_{ij}$) plus 1.0. Primary producer and detritus groups are assigned a trophic level of 1.0.

2.4. Input parameters

Input parameters are derived from various sources: local and regional estimates, empirical relationships, other models and guess estimates (Table VI.2). Input values for 1996 and 1998 steady-state models can be found in Table VI.3.

Biomass – Benthic macrofauna biomass was obtained from surveys conducted by IMARPE for the periods 19th-29th April, 1996 and 15th-24th July, 1998. A total of 223 and 252 quadrants of 1 m^2 each were sampled during the two periods, respectively. All epifauna and infauna of the upper sediment layer (approx. <5 cm depth) were collected by hand and placed in mesh bags of 500 mm mesh size. Abundance and weight were recorded for each species (for further information on sampling, see Samamé et al., 1985; Yamashiro et al., 1990). Groups of small epifauna (*Herbivorous gastropods*, *Benthic detritivores*, *Scallops*, *Small carnivores*) and *Polychaetes* were increased by 25% to correct for undersampling. *Miscellaneous filter-feeders* (consisting mainly of infaunal bivalves) were increased by 100% to also correct for undersampling; as much of this group's biomass is found deeper than 5 cm. Biomass corrections were based on complementary benthic evaluations conducted by the authors.

Estimates of *Phytoplankton* biomass for the 1996 model were taken from Peruvian coastal averages under 'typical' upwelling conditions (3.0 mL·m^{-3}) (Rojas de Mendiola et al., 1985) and EN conditions (Delgado and Villanueva, 1998; Villanueva et al., 1998). EN phytoplankton values were increased slightly over coastal averages (+15%) in order to balance the model. Values in mL·m^{-3} were converted to g·m^{-2} by assuming 1 mL = 1 g and then multiplying by an average depth for the model area of 15 m assuming a well-mixed water column.

Information on the *Zooplankton* in Independence Bay is limited and of qualitative nature only (Yamashiro et al., 1990), thus biomass was left open to be calculated by the steady-state model assuming an Ecotrophic efficiency (*EE*) of 0.95.

Biomass of highly mobile species such as octopus and fish were estimated from catch data by assuming that the fishery takes 50% of yearly produced biomass. *Small pelagic fish* are not a principal target of the artisanal fishery and so catch estimates are likely poor indicators of the available biomass. *Small pelagic fish* biomass was thus left open to be calculated by the steady-state model assuming an *EE* of 0.95 (Table VI.3).

Catches – Estimates of catch were derived from IMARPE catch statistics for the artisanal fishery from the 2 main landing sites for Independence Bay - San Andres and Laguna Grande. Unfortunately, landings data does not distinguish between the origin of

capture (i.e. habitat), and thus corrections were made based on the relative sizes of the habitats in the model (ca. 10% rocky, 90% soft-bottom) and the fact that most catches originating from rocky habitats come from outside the model area (ca. 10x greater than within the model). Taking into account the affinities of functional groups to particular habitats allowed for the following corrections: *Scallops* and *Predatory crab* catches come only from the soft-bottom habitats of the model and thus did not need correction; Fish groups, *Octopus*, and *Miscellaneous filter-feeders*, primarily found in soft-bottom habitats, were reduced by only 10% to correct catches associated with rocky habitats. To the contrary, catches of *Herbivorous gastropods*, *Predatory gastropods*, and *Sea urchins* were mainly associated with broken shell or rocky substrates, and were thus reduced by 80% (Table VI.3).

Production/Biomass (Total mortality) – Direct estimates of production to biomass ratios (*P/B*) or Total mortality (*Z*) existed for several benthic invertebrate groups in the model – Scallops, Predatory crabs, and Sea stars. Other groups were estimated using empirical relationships from Brey (2001) taking into account taxonomic group, mean body size, temperature of habitat, feeding modes, and habitat type. In most cases this provided realistic estimates; however, values for *Polychaetes* and *Misc. filter-feeders* were increased to 1.0 based on other estimates from the literature (Table VI.3).

P/B of *Phytoplankton* was estimated using a modified Eppley curve (Eppley, 1972) as described by Brush et al. (2002):

$$G = G_{\max} * f * LTLIM * NUTLIM \qquad (3)$$

where *G* = realized daily growth rate (d^{-1})(base e), *f* is the fraction of the day during which there is light, and *LTLIM* and *NUTLIM* are dimensionless ratios from 0 to 1 which describe light and nutrient limitation of growth, respectively (Kremer and Nixon, 1977). G_{max}, as given by Eppley (1972) describes an exponentially-shaped envelope for growth rates of phytoplankton under culture conditions without light or nutrient limitation (as recalculated by Brush et al., 2002):

$$G_{\max} = 0.97 * e^{0.0633*T} \qquad (4)$$

where *T* = water temperature. The 'normal' upwelling phytoplankton production 1996 assumed a mean temperature of 16°C with 50% light (from self-shading) and 0% nutrient limitation factors, while the EN condition of 1998 assumed a mean temperature of 26°C

with 80% light and 50% nutrient limitation factors. Calculated *P/B* ratios were high (245 and 365 for 1996 and 1998, respectively) yet the value of total production for the 1996 model in terms of carbon, i.e. ~ 800 g C $m^{-2}yr^{-1}$, using a wet weight:C conversion of 14.25:1 from Brown (1991), is conservative with respect to other estimates for the Peruvian coastal system under upwelling conditions, i.e. >1000 and >1500 g C $m^{-2}yr^{-1}$ from Walsh (1981) and Chavez and Barber (1985), respectively. *P/B* values for other groups are taken from the literature (Table VI.2)

Consumption (Q) and Conversion efficiency (GE) – Direct estimates of consumption rates (*Q/B*) were available for a few of the benthic invertebrate groups (*Octopus*, *Scallops, Predatory gastropods, and Predatory crabs*). For most other groups, ratios of Conversion efficiency (*GE*) or the ratio between Production and Consumption (*P/Q*) were applied (Tables VI.2 and VI.3).

Diet matrices – Direct diet studies for Independence Bay are limited and thus general knowledge from literature was used in the construction of diet matrices (Table VI.2). Initial attempts at balancing the 1996 model resulted in insufficient production of many smaller epifaunal herbivore and detritivore invertebrate groups (*Scallops, Sea urchins, Herbivorous gastropods, Benthic detritivores*, and *Misc. filter-feeders*) to meet the initial consumption values of the carnivorous benthic invertebrate groups (*Predatory gastropods, Small carnivores*, *Predatory crabs, Sea stars,* and *Octopus*). As macroinvertebrate groups are described to be rather unselective and opportunistic feeders, limited more by their modes of feeding (Wilson and Parkes, 1998), diet proportions were adjusted to reflect both predatory groups' consumption rates as well as the available production of prey groups. Base values of detritus feeding were assumed and calculated diets resulted in high proportions of *Polychaetes* in their diets – reflecting their high biomass and production in the benthic system in 1996. The 1998 situation was less problematic due to the reduction of carnivorous benthic invertebrate biomass as well as the increase in scallop biomass as prey. Assuming the readily available scallop biomass would be a favored prey, its proportion in diet was set high (60-75%) and the remaining diets were calculated as above (Table VI.4). Diets for fish species were obtained from FishBase (Froese and Pauly, 2006) and were adjusted to the fish groups based on relative species contribution from recorded catches.

2.5. Addressing parameter uncertainty

The balanced steady-state model for 1996 was subjected to the EwE resampling routine *Ecoranger* (Christensen and Walters, 2004) in order to assess the probability distributions of the input parameters. Using a Monte Carlo approach, the routine drew a set of random input variables from normal distributions for each basic parameter and all resulting combinations that satisfied mass-balanced constraints were recorded. Originally we allowed the routine to use confidence intervals as derived from a pedigree of the data sources, where highest confidence is placed in locally-derived data; however, the initial results often gave parameter values outside of reasonable biological constraints (e.g. high conversion efficiencies, high cannibalism) and thus we decided to fix all confidence intervals at 20% variation as was similarly done by Arias-González et al. (1997). We allowed resampling until 10,000 runs passed the selection criteria. The 'best' run was then chosen as that with the smallest sum of square residuals between the input parameters and the mean value of all successful runs (for more information, see Christensen et al., 2000).

2.6. Outputs / System statistics

Statistics for comparison of the two system states fall under the categories of community energetics, cycling indices, and system organization. Comparisons of the 'health' and maturity of the two system states drew on statistics from all three areas. Further general descriptive statistics from the calculated outputs of the models included: i) Total throughput (*T*) – measure of the total sum of flows within the system and indicates the 'size' or activity of the system; ii) Contributions to *T* from different types of flows - Consumption, Export, Respiration and Flows to detritus; iii) Breakdown of biomass and flows from different components of the system - Pelagic vs. benthic biomass and production; and iv) Changes in feeding modes – Herbivory : detritivory ratios.

Community energetics – Several indices of community energetics allowed for the comparison of ecological succession and relative maturity according to Odum (1969) and include: i) Total primary production (*PP*) to Total respiration (*R*) ratio (*PP/R*); ii) Biomass (*B*) supported by Total primary production (*PP/B*); iii) Biomass supported by Total throughput (*B/T*); and iv) Energy Transfer efficiency (*TE*) between discrete trophic levels.

Cycling indices – The Finn's cycling index (*FCI*) (Finn, 1976) is calculated as *Tc/T*, where *Tc* is the amount of system flows that are recycled compared to the total system

throughput, *T*. According to Odum (Odum, 1969) recycling increases in more mature and less stressed systems.

Growth and Development indices – Global measurements of system organization are calculated according to a network analysis based on flows among elements in the system as defined by Ulanowicz (1986). Indices include the aforementioned throughput (*T*), along with a measure of ascendancy (*A*), and development capacity (*C*). Ascendancy incorporates both size and organization of flows into a single measure and is calculated as throughput (*T*) multiplied by mutual information (*I*) – concerns the diversity and evenness of flows between compartments (Baird et al., 1998). Development capacity is the theoretical upper limit to ascendancy and thus the dimensionless *A/C* ratio allows for a comparable measure of ecosystem development and is predicted to be higher in more mature ecosystems (Ulanowicz, 1986). The difference between development capacity and ascendancy (*C*-*A*) is the system overhead (*Φ*) and gives a measure of the system's 'strength in reserve' from which it can draw to meet perturbations (Ulanowicz, 1986).

Fishery – *Other statistics allow for the assessment of the fishery activity such as its* Gross efficiency (catch / net *PP*), mean trophic level of the catch, and primary production needed to sustain the fishery.

2.7. Simulating transition from upwelling to El Niño stage

The simulation runs conducted for this study with EwE calculates biomass changes through time by solving the set of differential equations:

$$dB_i/dt = g_i\left[\sum_k Q_{ki}(t)\right] - \sum_j Q_{ij}(t) - M0_i B_i - \sum F_{if}(t)B_i \qquad (5)$$

For species or functional groups i =1…n. The first sum represents the food-consumption rate, Q, summed over prey types k of species i, and g_i represents the growth efficiency (proportion of food intake converted into production). The second sum represents the predation loss rates over predators j of i. $M0_i$ represents the instantaneous natural mortality rate due to factors other than modeled predation. The final sum represents the instantaneous fishing mortality rate, F, as a sum of fishing components caused by fishing fleets f.

The Q_{ij} are calculated by assuming that the B_i are divided into vulnerable and invulnerable components (Walters et al., 1997), and it is the flux rates v_{ij} and v'_{ij} that move biomass into the vulnerable and safe pool, respectively. This assumption leads to the rate equation:

$$Q_{ij} = \frac{a_{ij}(t) v_{ij}(t) B_i B_j}{v_{ij}(t) + v'_{ij} + a_{ij}(t) B_j} \qquad (6)$$

where the v_{ij} and v'_{ij} parameters represent rates of behavioral exchange between invulnerable and vulnerable states and a_{ij} represents rate of effective search by predator j for prey type i. The exact setting of the v_{ij}, remains uncertain, but the modeling software allows for adjusting the vulnerabilities by means of a fitting procedure, through which the sum of squares between observed and simulated (log) biomasses are minimized (see Walters et al., 1997). In EwE, the vulnerabilities for each predator-prey interaction can be explored by the user and settings will determine if control is top-down (i.e., Lotka-Volterra; >2.0), bottom-up (i.e., donor-driven; <2.0), or intermediate (≈2.0). We applied this fitting routine with our time series data. The computed vulnerabilities were then discussed in the light of possible control mechanisms operating in the ecosystem.

As input for simulations of the ecosystem response to ENSO we used catch per unit of effort (CPUE) data of the fishery resources of the system for the period 1996-2003 (including the EN year 1998) as proxies for stock biomass, together with biomass data obtained from the benthic surveys done by IMARPE for the years 1996, 1997, 1998 and 1999 (Table VI.5).

To distinguish between trophic and non-trophic effects on functional group biomass changes, we forced the biomass changes of several functional group 'drivers' to the model, in order to measure their impact on the fit of the model. Drivers included the relative biomass changes of 4 highly-dynamic functional groups whose dynamics were known to be at least partially affected by non-trophic environmental changes associated with ENSO variability: *Phytoplankton* (*PP*), *Macroalgae* (*MA*), *Predatory crabs* (*C*) and *Scallops* (*S*). We successively forced the biomass changes of these groups for the simulated time period of 8 years (1996-2003) and recorded the changes in fit as calculated by the sum of squares between the predicted and observed estimates.

An initial exploration of the dynamics using the default predator-prey vulnerability settings for all interactions either decreased the fit of the simulation or made only small improvements. Thus, we decided to first introduce all four drivers in combination and allowed EwE to search for the best predator-prey vulnerability settings. Using these

optimized vulnerability settings we again addressed the importance of each driver through single or combined introduction to force the model through time.

3. Results

3.1. General descriptive

Initial parameters of the balanced model can be found on the Pangaea website (Taylor et al., 2007a, 2007b). The Ecoranger resampling routine resulted in balanced models in 0.75 % and 2.20 % of the runs for the 1996 and 1998 models, respectively. The 'best' fitting model parameters are shown in Table VI.3. Summary statistics are presented in Table VI.6. The 'size' as measured by the total system throughput (*T*) indicates that the 1996 was larger (34208 vs. 24827 t km^{-2} yr^{-1}) mainly as a function of higher primary production. Contributions to *T* from different types of flows indicate that the EN state is characterized by higher absolute and relative flows due to consumption (11918 t km^{-2} yr^{-1} and 48.0% of *T*) and respiration (7097 t km^{-2} yr^{-1} and 28.6 % of *T*) and lower absolute and relative flows into detritus (14.8 % of *T*) and as exports (8.6 % of *T*). These results indicate better utilization of primary production through increased consumption and decreased losses to detritus as is reflected by the increased *EE* values for phytoplankton and detritus compartments. The overall ratio of herbivory to detritivory feeding decreased slightly during 1998 (6.54 and 5.22 for 1996 and 1998, respectively). Ratios between pelagic and benthic biomass and production were similar for both 1996 and 1998 states with the benthic system dominating in terms of biomass (pelagic / benthic biomass ratios equal 0.13 and 0.14 for 1996 and 1998, respectively) while the pelagic components accounted for most of the production (pelagic / benthic production ratios equal 8.46 and 7.79 for 1996 and 1998, respectively). Besides major changes in primary production between the two periods which greatly impacted *T*, the overall biomass of trophic levels II and above is virtually unchanged despite significant changes to several individual functional groups.

3.2. Community energetics

Several statistics on community energetics point to the 1998 EN state as being of a higher maturity than in 1996. The primary production to total respiration ratio (*PP/R*) came closer to the proposed value of 1.0 for mature systems (Odum, 1969) (2.979 and 1.302 for 1996 and 1998, respectively). Total primary production to biomass (*PP/B*) and

biomass to total throughput (*B/T*) ratios indicated that the 1998 state could support a higher relative biomass per unit of primary production and total throughput. On the contrary, mean transfer efficiency (*TE*) was higher for the 1996 state (Fig. VI.3) due in part to a high utilization of herbivore and detritivore production by predatory invertebrates, as well as higher cannibalism, and can be observed in the high *EE* values for these groups (groups 5-14, Table VI.3). This 'bottleneck' of flows did not occur in 1998 due both to a decrease in predator biomass and an increase in primary consumer biomass due to the proliferation of *Scallops*. As *TE* can only be calculated for consumer groups, and Ecopath does not quantify solar energy input to producer compartments, mean *TE* reflects the geometric mean of trophic levels II-IV only. Thus, the decrease in *TE* occurred despite an overall improvement in other holistic community energetic indices in 1998; specifically, a higher utilization of primary production and detritus.

3.3. Cycling indices

A higher degree of cycling, as indicated by the Finn's cycling index, was calculated for the 1998 EN period (5.11 % and 8.88 % for 1996 and 1998, respectively). Again, the higher utilization of primary production and detritus was mainly responsible for this result. Removing this influence is possible with the related Predator cycling index, which showed that the 1996 state had more cycling at the higher trophic levels (9.07 % and 5.14 % for 1996 and 1998, respectively).

3.4. Development / Maturity indices

The Ascendancy to Development Capacity ratio (*A/C*) was slightly higher during normal upwelling conditions in 1996 (33.0 % and 27.5% for 1996 and 1998, respectively) and indicates that this state shows more maturity (i.e. higher total flows and predictability of flows). On the other hand, the higher proportion of System Overhead (*Φ/C*) for 1998 indicates that the EN state was less developed and more able to handle perturbations.

3.5. Fishery

The boom of the *Argopecten purpuratus* during EN was mostly responsible for the more than 18-fold increase in total catches for the model area to 248.9 $t \cdot km^{-2} \cdot yr^{-1}$. *Pelagic predatory fish* catches increased about 7-fold and as a result the model back-calculated a higher *Small pelagic fish* biomass for 1998. The gross efficiency (catch / net *PP*) of the

fishery increased 25-fold and the primary production required per unit of catch decreased, due mainly to the lower trophic level of the scallop (Mean *TL* of catch – 2.74 and 2.05 for 1996 and 1998, respectively). The highly dynamic nature of the diving fishery in response to changing resource abundances also plays an important role. As the catch of scallops was mainly driving the changes in effort, they show fairly similar fishing mortality (*F*) values for the two periods, while other groups that were reduced in biomass show higher *F* values (*Misc. filter-feeders* and *Predatory gastropods*) (Table VI.3). Overall, the expansion of the fishery, combined with the decreased primary productivity, resulted in a value of 18 % of total primary production needed to sustain the fishery – an 11-fold increase from 1996.

3.6. Model groups responses to forcing scenarios

In the simulations that follow, possible mechanism behind the observed system changes are analyzed.

Scenario 1 (S1): EN caused observed decrease in primary production (due to lack of nutrient upwelling) triggers bottom-up controlled changes in other system compartments.

As shown by Fig. VI.4, significant bottom-up effects due to the decrease in *Phytoplankton* and *Macroalgae* biomass during the El Nino period (1997/98) resulted in decreases in the groups *Polychaetes*, *Misc. filter-feeders* and *Herbivorous gastropods.* A slightly lagged response is also seen by *Predatory gastropods*, which decreased in biomass. While the single addition of the *Macroalgae* driver decreased SS more than that of *Phytoplankton* (-8.1 % and -2.7 %, respectively), the average improvement in combination with other drivers was greater from the *Phytoplankton* driver at -2.8 % (Fig. VI.5).

Scenario 2 (S2): EN caused observed decrease in *Predatory crab* biomass (due to temperature stress causing mortality and migration to deeper waters), which relieves some top-down pressure in the system.

The model predicted a small increase in biomass of the groups *Sea stars* and *Small carnivores* as a result of the reduced crab biomass (Fig. VI.4). The application of the *Predatory crab* driver resulted in an average decrease of -4.8 % in SS (Fig. VI.5).

Scenario 3 (S3): EN caused increase in scallop biomass triggers changes in other system compartments.

Fig. VI.4 shows the model response to the changes of *Scallop* biomass during the EN warming with several observed changes reflected in the model response: 1) increase in the groups *Predatory gastropods*, *Small carnivores*, *Octopus, Sea stars*, and 2) decrease in the groups *Polychaetes, Herb. gastropods, Benthic detritivores,* and *Misc. filter-feeders*. The model also predicts an increase in *Predatory crab* biomass, which is contrary to the observed changes and further supports that the decreased biomass during the EN warming was likely a non-trophically mediated effect; specifically mass mortality and emigration to deeper, cooler waters (Arntz and Fahrbach, 1991). Despite some improvements, the average change from the application of the *Scallop* driver was an increase of 1.8 % in SS, indicating a decrease in fit.

Scenario 4 (S4): Externally forced *Scallop* outburst and biomass decrease of *Primary producers* and *Predatory crabs* (resulting from physiological responses of these groups to the EN warming/nutrient depletion) force other functional groups to respond trophically.

The previously mentioned improvements from each driver sum up explain the dynamics in the majority of groups (Fig. VI.4).

3.7. Vulnerability estimates

Table VI.7 summarizes the vulnerabilities computed for Scenario 4. v-values <1.2 were considered bottom-up control (BU), between 1.2 and 2 (mixed control, MX) and above 2 top-down control (TD).

Accordingly, top-down control is suggested for: i) *Predatory gastropods* on *Polychaetes*, *Benthic detritivores* and *Misc. filter-feeders*; ii) *Predatory crabs* on *Scallops*; and iii) *Sea stars* on *Predatory gastropods*.

Bottom-up control configurations are more dominant and are suggested for: i) *Polychaetes* to *Predatory crabs*; ii) *Scallops* to *Predatory gastropods* and *Octopus*; iii) primary producers and *Zooplankton* prey to fish groups; and iv) *Littoral fish* and *Small pelagic fish* to *Marine mammals* and *Sea birds*.

4. Discussion

4.1. Summary statistics, flow structure and maturity

The 'size' or total throughput *T* of Independence Bay under normal upwelling conditions (1996 model; *T*=34208) is higher than has been observed for other coastal zones along the Pacific coast, specifically, Gulfo Dulce, Costa Rica (*T*=1404) and Tongoy Bay, Chile (*T*=20835) (Wolff, 1994; Wolff et al., 1996), due mainly to its high primary production associated with recently upwelled, nutrient-rich water entering the bay. When our results are compared to models of specific habitats in Tongoy Bay constructed by Ortiz and Wolff (2002b), the sand-gravel habitat is most similar in terms of *total throughput* (*T*=33579). This type of substrate is typical of Independence Bay and is associated with strong currents where oxygen concentrations are increased through mixing and circulation and allow for a higher macrofaunal biomass. Similar values of production, flows to detritus, respiration, and exports are also observed between this habitat in Tongoy Bay and the model of Independence Bay under upwelling conditions.

While our estimate of Total throughput is not directly comparable to models that use differing units to describe flows (e.g. dry weight or carbon units), we are able to compare the proportions of types of flows. The proportion of flows to detritus in Independence Bay during upwelling (33.9 %) is similar to that of Tongoy (29 %) as well as several US bay systems; e.g. Narragansett Bay (33%), Delaware Bay (30%), and Chesapeake Bay (27%) (Monaco and Ulanowicz, 1997). However, only the models of the South American bays calculated high proportions of exports as well (29-34 % vs. 7-10 % for US bays). Part of the difference may be attributable to higher exchange rates / low residency time of water in relatively open bays like Independencia and Tongoy, resulting in more export of production (Rybarczyk et al., 2003); however, the high degree of primary production going unutilized and remaining in the sediments may be more typical of upwelling systems.

The dynamic nature of the artisanal fishery in response to changes in resources helps maintain the system's efficiency in the face of reduced predation pressure. In response to the scallop boom during EN, fishers migrated to Independence Bay from other areas along the Peruvian coast. A main proportion of these migrant fishers were from Sechura Bay in the north of Peru, where the largest fishery for scallops during normal years is found. These fishers were mainly involved in the diving fishery, which increased in effort by 170% in 1998 compared to the previous year. Peak fishing effort reached as high as 4932 boat trips per month (October 1998) compared to typical levels of around 750. Fishers also shifted their efforts to an almost exclusive targeting of

scallops, yet other species associated to the soft-bottom habitats were also taken. Octopus is a particularly favored resource due to a high market price, and it also is known to increase in biomass during EN (Arntz et al., 1988). Their increase is likely a result of increased production for *Octopus mimus* under the warmer conditions, which may buffer the increased fishing pressure. *O. mimus* growth and reproduction have been shown to be temperature-mediated (Cortez et al., 1999) and embryonic development time is also greatly accelerated under EN-like conditions in the laboratory (Warnke, 1999). Another increase occurred in the catches of *Pelagic predatory fish*. This is explainable through the overall shrinkage of the upwelling zone during EN and the subsequent intrusion of oceanic waters, which several predatory fish species are associated with (e.g. *Scomber japanicus*, *Sarda chilensis*, and *Scomberomerus sierra*). This movement may be further related to the pursuit of prey, as anchovy stocks were observed to both concentrate near the coast and then retreat southward to the latitudes near Independence Bay as recorded by acoustic surveys (Ñiquen and Bouchon, 2004).

The expansion of the fishery is also observed through much higher indices of gross efficiency (catch/net PP) and 18 % of total primary production required to sustain the fishery. This value is high given that the low mean trophic level of the fishery of 2.05, yet is lower than the value (25.1 %) calculated by Pauly and Christensen (1995) for upwelling systems. Nevertheless, for an artisanal fishery, it shows a remarkable efficiency of harvest. On the contrary, the value for normal upwelling conditions (1996) is extremely low at 1.4 %, and illustrates the near subsistence levels where the fishery typically operates. As a result, fishers are moving towards a combination of fishing and culture of scallops in Independence Bay in order to maintain income levels between EN “boom times”.

Nixon (1982) showed that there is a highly positive correlation between primary production and fishery yield in coastal lagoons, yet Independence Bay catches are highest during the period of lowest primary production. While the fish catches also increased during EN mainly due to immigrations of fishes towards the coast, it is the catches of benthic resources that are the most positively affected. Improved oxygen concentration has been suggested as more important in the proliferation of less abundant benthic species (Arntz and Fahrbach, 1991). Under the warmer, more oxygenated conditions of EN, overall consumption rates of several primary consumers (i.e. *Scallops*, *Herbivorous gastropods*, and *Benthic detritivores*) increased in order to sustain the increased production rates – as calculated from *in situ* or empirically-based estimates. As a result, we estimate that primary production during an EN event is almost completely consumed in Independence Bay. We needed to make several assumptions concerning the levels of primary production in the bay due to a lack of *in situ* samples and remote sensing

estimates – due to problems of resolution and cloud cover for such a small coastal area. However, the result of near complete consumption of primary production during EN is plausible given the clear, tropical-like water conditions and decreases in benthic detrital material observed during past EN events. Based on the model's calculations, we see that the incredible recruitment and production increases of scallops are contributing most to this result, as they consume an estimated 58 % of the phytoplankton production during EN. Wolff et al. (2007) found that the increase in scallops was likely a non-trophic effect of reduced larval development time in warmer temperatures, as observed for *A. purpuratus* under culture conditions, which may reduce predation mortality through faster settlement to the sea floor. Therefore, the incredible recruitment of a single species, in combination with the optimal growth conditions provided by the increased oxygen concentrations, are more likely the cause for increase in fisheries yield.

Indicators of system maturity show some contradictions – some point to higher maturity and development for 1996 while others for the EN state (1998). From a community energetics point of view, the EN state is able to support a similar biomass compared to 1996 despite lower primary production (*PP/B* ratio) and total throughput (*B/T* ratio), and thus the system's primary production to respiration ratio is closer to the value of 1.0 predicted for mature systems (Odum, 1969). Similarly, an increased Finn's cycling index is observed during EN due to a better utilization of primary production and detritus by the first consumers (mainly scallops). The substantially larger flows at the lower trophic levels help mask the more negative impacts of the higher trophic levels. The *TEs* of higher trophic levels are decreased and contribute to an overall lower *TE* for 1998. This is due to the negative impact of EN to the main benthic predatory groups, *Predatory gastropods*, *Small carnivores*, and especially *Predatory crabs*. These impacts are also observed through a decreased *Predatory cycling index* and *Finn's mean path length* during EN, indicating poorer cycling and transfer of energy in the higher trophic levels of the food web.

Relative Ascendancy (*A/C*) indicates a slightly higher development and maturity for the normal upwelling 1996 state (33.0 %) compared to 1998 (27.5 %). Related is the percent Overhead (*Φ/C*), which indicates that the less mature EN state is perhaps the better at withstanding perturbations. This is contrary to much of what we see in terms of community energetics and thus further interpretation is necessary. Baird et al. (Baird et al., 1991) found a similar discrepancy when comparing *A/C* to *FCI* in several marine ecosystems, where a negative correlation between the two indices was observed despite the hypothesis that both indices increase with system maturity. They hypothesized that the discrepancy may lie in the fact that higher stressed systems frequently impact higher-level species to a greater extent than the lower trophic components. As a result, the

release of standing biomass of higher trophic levels can be taken up through increased recycling via short intense loops.

It does appear that the higher trophic levels were more severely impacted by EN in Independence Bay. The most significant "short intense loop" would be the cycle through *Detritus*, which increases during EN and results in the higher *FCI* for the 1998 model. As phytoplankton and macroalgae production were reduced significantly in the 1998 model (14214 vs. 9247 t m^{-2} y^{-1} for 1996 and 1998, respectively), and consumption actually increased due primarily to filter-feeding scallops, the proportion of recycled detritus is significantly higher in 1998.

This result is highly dependent on the decreased primary production. As an illustration of this influence, we can increase the primary production in the 1998 model to the levels of 1996 in order to observe a less-biased comparison (Fig. VI.6). We see that the *FCI* would decrease to a slightly lower value than 1996. However, the relative Ascendancy (*A/C*) and Overhead (*Φ/C*) increase and decrease, respectively, but not to the levels of 1996. Ascendancy is both a function of total throughput (*T*) and system development (i.e. average mutual information, *I*), and while the simulated increase in primary production *would* bring *T* to a similar level as 1996, the EN state still shows lower *I*. Using these values the EN state would appear as of lower maturity despite improved overall community energetics.

Our models do not include information on the microbial loop, which is likely highly enhanced during the warm, oxygen-rich conditions of EN, and would likely add considerable flows and recycling to the EN model. While bacterial cycles are often removed in other models due to their high flows overshadowing other activities in the system (Christensen, 1995), they may be of particular importance in our understanding of benthic processes of renewal in the Peruvian upwelling system. Thus, future research plans to investigate these important energy pathways for use in future models.

A community analysis for Independence Bay conducted by Wolff and Mendo (2002) indicated that benthic diversity and evenness increased during EN. An initial attempt to model the trophic changes also showed a high maintenance of overall flow structure. The authors proposed that this rapid adjustment to abiotic changes suggests that EN could be regarded as a system condition to which the benthic community has well adapted during the course of evolution. This hypothesis is supported by the present study's results, yet may best apply to lower trophic levels that respond quicker to the perturbation. Trophically higher benthic predatory groups have been observed to recover quite quickly (e.g. predatory crabs) after EN, which is likely due to temporary emigrations to deeper waters rather than environmentally-induced mortality. In this respect, the post-EN situation, with higher primary production, higher primary consumer biomass from

scallops, and a return of predatory groups, may show an enhanced ecosystem over the pre-EN state. This may be seen as a long-term positive impact and would foster the idea that EN is an integral part of the dynamics of the HCS (Arntz and Valdivia, 1985a).

4.2. Simulation of bottom-up and top-down effects

When our model was forced with the observed decrease in primary producer biomass (*Phytoplankton* and *Macrophytes*) during the EN warming, the model response confirms some of the observed changes in compartment biomasses: *Misc. filter-feeders* and *Herbivorous gastropods,* are negatively affected and (to a lesser extent) *Polychaetes* as well as *Benthic detritivores,* which also decrease in biomass. Other direct or indirect effects seem rather negligible. Interestingly, *Macrophytes*, when used as a single model driver, better explain the observed ecosystem changes (lowering SS) than *Phytoplankton*.

The system impact of a reduction in the *Predatory crab* biomass (release of top-down control), seems to be mainly on *Sea stars* and *Small carnivores* that are favored (as competing predators), but the model response is rather insignificant for the other groups of the system.

Neither EN triggered changes in the bottom-up (*Phytoplankton* and *Macrophytes*), nor the top-down (*Predatory crabs*) forcing show any significant effect on the scallop biomass, suggesting that trophic linkages of scallops with their food and predators are not relevant causes for the observed proliferation of the scallop stock. This is an important finding, since predatory crabs are well known scallop predators and their biomass reduction during the EN warming has been related to the scallop proliferation (Wolff and Alarcon, 1993; Wolff and Mendo, 2000).

While the scallop outburst during EN is important from a holistic/energetic point of view, its application as a driver did not improve the fit of the simulation considerably. This may in part be due to lags in the dynamics of several function groups as compared to the reference data; however, the simulation correctly predicts the several positively affected groups (*Predatory gastropods*, *Small carnivores*, *Octopus, Sea stars*) and negatively affected groups (*Polychaetes, Herb. gastropods,* and *Misc. filter-feeders)*, supporting the central role of the scallop as prey for several consumer groups and as a competitor for other filter-feeders. It is likely that earlier observed decreases in several competing primary consumer groups may be due to the non-trophic negative effects of competition for space, as the scallop banks became so thick in parts as to obscure the sea floor with several layers of scallops.

It is evident from the foregoing that the scallop outburst is caused by other than trophic effects but, through the scallop proliferation, the system is greatly changed in its

flow structure. The combined trophic effect of the scallop proliferation, and the reduction in the biomass of primary producers and *Pred. crabs* on other groups of the model is evident from our simulations (scenario 4) (Fig. VI.4), clearly confirming the above-mentioned trophic linkages within the system.

When forcing by the relative fishing rate of the diving and finfish fishery is removed in our simulations, the simulated biomass trajectories of the model groups were almost identical to those of scenario 4, suggesting a very limited role of the fishery in shaping the trophic flow structure of the system. This may be explained by the fact that the diving fishery targeted mainly scallops and its increase in catch rate was about proportional to the scallop biomass increase; and the changes in finfish fishing rate were small over the whole period.

4.3. Vulnerabilities

It is important to emphasize that the forcing of the 'drivers' did not improve the fit of the simulation without first allowing the EwE fitting of vulnerabilities. This is contrary to the findings of a similar exploration of the larger Peruvian Upwelling system (Chapters III and IV) whereby even default vulnerability values reproduced many important dynamics. This may in part be due to a slightly higher level of data quality in the steady-state model as reflected in the Ecopath Pedigree Index (0.638 vs. 0.597 for Independence Bay, scales between 0 and 1 with highest values for direct measurements of the same system) although the differences in environmental impact between the benthic and pelagic habitats likely plays a role. Furthermore, the less-mobile nature of the benthic organisms may prevent avoidance of deleterious conditions, thus making the effects of perturbations more pronounced. Nevertheless, the computed vulnerabilities seem plausible, but should be considered with caution, since the time series available for the present study was quite short. In our upcoming research we will be able to extend the data set over longer periods and may be able to confirm some of the vulnerability estimates of this study.

Generally, bottom-up configurations were fit for the more pelagic components of the system such as the important flow starting with plankton to *Small pelagic fish* to the higher predators *Marine mammals* and *Sea birds*. *Littoral fish* also provide an important link between benthic primary production and invertebrate production to *Marine mammals* as well. Top-down configurations occurred more in the benthic components of the system. This may be expected given the high EE rates calculated for many benthic primary consumers during the normal upwelling year of 1996 due to high utilization by higher trophic levels. In addition, the fact that only 0.75 % of the Ecoranger runs resulted

in a balanced model (as compared to 2.20 % in the 1998 model) illustrates the tightly coupled flows to the benthic predatory groups, which restricted the parameter possibilities for the starting 1996 steady-state model.

A top-down configuration was fit for the *Scallop* to *Predatory crab* interaction. This is possible during normal upwelling periods as the crabs *Cancer setosus* and *Cancer porteri* are the dominant consumers of benthic production; however, the crab decrease during EN is not evidently responsible for the scallop outburst. Furthermore, this setting must be taken with caution as both groups were forced through time and thus the result is likely an artifact. Top-down configurations between *Predatory snails* and several of its prey (*Polychaetes*, *Benthic detritivores* and *Misc. filter-feeders)* help to explain their decreases after the EN period. Again this must be taken with caution as it can not be ruled out that some competitive interactions with scallops for space may have also attributed to their declines rather than from top-down predation.

The finding that the scallop and other filter-feeders may bottom-up control their predators appears plausible, since their central role as prey of the macrobenthic community has been shown before (Wolff and Alarcon, 1993). Despite the immediate negative effects of EN on several higher benthic predators, the increased biomass of the scallop afterwards helps in the recovery of *Predatory gastropods*, Small carnivores, *Predatory crabs*, and *Sea stars*, which all show higher post-EN biomasses when compared to 1996. Furthermore, the (possibly normal) bottom-up control of filter-feeders by phytoplankton under upwelling conditions may indeed be inverted during EN, when *Scallops* are estimated to have consumed 58 % of phytoplankton production alone. A similar role has been identified for the introduced Manila clam *Tapes philippinarum* in the Venice Lagoon system, whereby there is a high-energy throughput passing though the species from lower to higher trophic levels when compared to other groups at a similar trophic level (Pranovi et al., 2003). Furthermore, it was suggested that this strong top-down control of phytoplankton by *T. philippinarum* may be responsible for the system not returning to a phytoplankton-based trophic web (Libralato et al., 2004). While the expansion of *A. purpuratus* in Independence Bay is much more short-lived (approx. 3 years to return to pre-EN levels), it is likely that recovery times of other benthic primary consumers would be partially hindered through competition for food and space.

4.4. Conclusions

Overall, it appears that the energy flow structure in Independence Bay is more or less maintained during an El Niño event despite negative impacts to several higher

benthic trophic levels. In particular, the proliferation of the scallop *A. purpuratus* allows for a certain degree of compensation in maintaining the energy flow structure of the bay despite the reduction in primary production. While some alleviation of top-down predation pressure may be felt by benthic primary consumers through the non-trophically-mediated decreases of crabs, the overall bottom-up affects of reduced primary production (macroalgae and phytoplankton) appear responsible for the reduced biomass in several functional groups. As seen for many areas along the Peruvian coast during El Niño, Independence Bay comes to resemble a more tropical ecosystem with warm clear waters and lower nutrient concentrations. Combined with higher consumption values during El Niño, the system utilizes most of the phytoplankton production, and exports of primary production to detritus are greatly reduced. While the El Niño state appears to show some higher efficiency in overall energetics, the structure and development appears impacted.

The rapid response and adaptedness of the artisanal fishery also increases the system's efficiency in the face of decreased predation mortality; however, this increased pressure may have added some stress to negatively impacted functional groups through higher fishing mortality. A management plan that allows for the newly recruited *A. purpuratus* population to fully grow and develop may not only reap higher monetary gains as suggested by Wolff and Mendo (2000), but may also enhanced post-El Niño system through facilitation of the recovery of benthic predatory groups.

Acknowledgements

The authors are grateful for the support and assistance from the following: Dr. Villy Christensen of the Fisheries Centre, University of British Columbia, for his helpful advice regarding the use of Ecoranger routine within Ecopath with Ecosim; Dr. Tom Brey of the Alfred Wegener Institute for Polar and Marine Research (AWI) for helpful discussions regarding benthic invertebrate energetics and for the use of his somatic production models; Dr. Carl Walters for the use of the Ecosim software. This study was financed and conducted in the frame of the EU-project CENSOR (Climate variability and El Niño Southern Oscillation: Impacts for natural resources and management, contract 511071) and is CENSOR publication 0050.

Tables and Figures

Table VI.1. Functional groups and representative species. Species listed are not exhaustive (small benthos groups show the most important species, representing > 95% of biomass and/or species averaging >1 g m^2).

Functional group	Species
2. Macroalgae	*Rhodymenia* sp.**, *Macrocystis* sp.**, *Gigartina* sp.**, *Codium* sp., *Ulva* sp.**, ***Caulerpa* sp., *Lessonia nigrescens***
4. Polychaetes	*Diopatra* sp., ***Chaetopteridae***
5. Scallops	*Argopecten purpuratus*
6. Sea urchins	*Tetrapigus níger, Arbacia spatuligera, Arbacia* sp., *Loxechinus albus,* ***Strongylocentrotus* sp.**
7. Herbivorous gastropods	*Crepipatella dilatata, Crepipatella* sp., *Tegula euryomphalus, Tegula atra, Tegula* sp., *Crucibulum* sp., *Aplysia* sp., *Mitrella* sp.
8. Benthic detritivores	*Ophiuroidea***, *Pagurus* sp., *Eurypanopeus sp.***, *Taliepus marginatus*
9. Misc. filter-feeders	Ascidians, *Aulacomya ater, Glycimeris ovata, Actinia* sp., *Prothothaca thaca, Sponges, Semele solida, Chama* sp.
10. Predatory gastropods	*Bursa ventricosa,* ***Bursa nana,*** *Bursa* sp.***,*** *Thais chocolata,* ***Thaididae*** sp.***,*** *Priene rude,* *Cymatium weigmani, Cymathidae* sp.***,*** *Argobuccinum* sp.***,*** *Sinum cymba*
11. Small carnivores	*Oliva peruviana, Oliva* sp., *Nassarius dentifer, Nassarius gayi, Nassarius* sp., *Trophon* sp., *Crassilabrum crassilabrum, Natica* sp., *Xantochorus* sp., ***Solenosteria gatesi, Solenosteria* sp., *Polinices uber***
12. Predatory crabs	*Cancer setosus, Cancer porteri, Cancer coronatus, Cancer sp., Hepatus chilensis,, Platyxanthus cockeri,* ***Callinectes arcuatus, Callinectes sp.***
13. Sea stars	*Luidia bellonae, Luidia magallanica, Luidia* sp., *Asterina chilensis, Patiria chilensis,* ***Heliaster helianthus***
14. Octopus	*Octopus mimus*
15. Littoral fish	*Isacia conceptionis, Seriolella violacea, Paralabrax humeralis, Cheilodactylus variegatus, Labrisomus philippii, Hemilutjanus macrophthalmos, Acanthistius pictus, Paralichthys adspersus, Cynoscion analis, Sciaena deliciosa, Calamus brachysomus, Mugiloides chilensis, Diplectrum conceptione, Chloroscombrus orqueta, Sphyraena ensis, S. idiastes, Myliobatis peruvianus, Orthopristis chalceus, Mugil cephalus,* ***Diplectrum conceptione, Chloroscombrus orqueta, Sphyraena ensis, Sphyraena idiastes, Myliobatis peruvianus***
16. Small pelagic fish	*Sardinops sagax sagax, Ethmidium maculatum,* ***Trachinotus paitensis***
17. Pelagic predatory fish	*Trachurus picturatus murphyi, Cilus gilberti, Scomber japonicus,* ***Sarda chiliensis chiliensis, Auxis rochei, Scomberomorus sierra***
18. Marine mammals	*Otaria byronia, Arctocephalus australis*
19. Sea birds	*Leucocarbo bougainvillii, Sula variegata, Pelecanus thagus*

Key: underlined = not found / recorded in captures in 1998, ** = found in 1998 but low in biomass, **bold** = not found / recorded in captures in 1996

Table VI.2. Sources of input data for the Independence Bay steady-state models

Functional group / parameter	Biomass - B_i (t km^{-2})	Production rate - P_i/B_i (y^{-1})	Consumption rate - Q_i/B_i(y^{-1})	Conversion efficiency – GE_i	Ecotrophic efficiency – EE_i	Catches - Y_i (t km^{-2} y^{-1})	Diet composition – DC
1. Phytoplankton	GU based on Rojas de Mendiola et al. (1985), Delgado and Villanueva (1998)	GU based on modified Eppley curve (Eppley, 1972; Brush et al., 2002)	-	-	EO	-	-
2. Macroalgae	IE	GU based on Macchiavello et al. (1987)	-	-	EO	-	-
3. Zooplankton	EO	GU based on Mendoza (1993), Hutchings et al. (1995)	GU adapted from Polovina and Ow (1985)	EO	GU	-	GU
4. Polychaetes	IE	GU based on Martin and Grémare (1997)	EO	GU	EO	-	GU
5. Scallops	IE	Mendo et al. (1987), Stotz and Gonzalez (1997)	GU based on Wolff (1994)	EO	EO	IS	GU based on Rouillon (2002)
6. Sea urchins	IE	EM	EO	GU	EO	IS	GU
7. Herbivorous gastropods	IE	EM	EO	GU 0.3 based on Mann (1982)	EO	IS	GU
8. Benthic detritivores	IE	EM	EO	GU	EO	-	GU
9. Misc. filter-feeders	IE	GU based on Wolff (1994)	EO	GU	EO	IS	GU
10. Predatory gastropods	IE	EO	GE based on Huebner and Edwards (1981)	GU 0,3 based on Huebner and Edwards (1981)	EO	IS	GU, IC
11. Small carnivores	IE	EM	EO	GU	EO	-	GU partially based on Keen (1972) for gastropod spp., IC
12. Predatory crabs	IE	Wolff and Soto (1992)	Lang (2000), Wolff and Soto (1992)	EO	EO	IS	GU based on Leon and Stotz (2004), IC
13. Sea stars	IE	Ortiz and Wolff (2002)	EO	GU	EO	-	GU, IC
14. Octopus	GU based on catch data	EO	Wolf and Perez (1992), Vega and Mendo (2002)	Wolf and Perez (1992), Vega and Mendo (2002)	EO	IS	GU, IC
15. Littoral fish	GU based on catch data	GU 1,2 based on Wolff (1994)	EO	GU	EO	IS	GU based on FISHBASE (2006)
16. Small pelagic fish	EO	GU	EO	GU 0,1 based on Moloney (2005)	GU	IS	GU based on FISHBASE (2006)
17. Pelagic predatory fish	GU based on catch data	GU 0,85 based on Jarre et al. (1991)	EO	GU 0,1 based on Moloney (2005)	EO	IS	GU based on FISHBASE (2006)
18. Marine mammals	GU	GU based on Jarre, et al. (1991)	EO	GU	EO	-	GU
19. Sea birds	GU	GU based on Moloney (2005)	EO	GU based on Moloney (2005)	EO	-	GU
20. Detritus	EO	-	-	-	-	-	-

Abbreviations: IE = IMARPE benthic macrofauna evaluation, EM = empirical model (Brey, 2001), EO = Ecopath output, GU = guess estimate, IC = iterative consumption routine (for opportunistic feeding; described herein), IS = IMARPE landings statistics

Table VI.3. Input-output parameters for steady-state models of Independence Bay in 1996 and 1998 after application of the Ecoranger resampling routine. Ecopath calculated parameters in **bold**.

Functional group / parameter	Trophic Level		B_i ($t\ km^{-2}$)		P_i / B_i (y^{-1})		Q_i / B_i (y^{-1})		EE_i		GE_i		Catch ($t \cdot y^{-1}$)		F_i		$M0_i$		$M2_i$	
	1996	1998	1996	1998	1996	1998	1996	1998	1996	1998	1996	1998	1996	1998	1996	1998	1996	1998	1996	1998
1. Phytoplankton	**1.00**	**1.00**	51.398	24.816	255.228	366.172	-	-	**0.340**	**0.958**	-	-	0.000	0.000	**0.000**	**0.000**	**168.495**	**15.261**	**86.734**	**350.911**
2. Macroalgae	**1.00**	**1.00**	69.204	8.656	15.840	17.954	-	-	**0.136**	**0.375**	-	-	0.000	0.000	**0.000**	**0.000**	**13.685**	**11.217**	**2.155**	**6.737**
3. Zooplankton	**2.23**	**2.26**	**28.270**	**29.425**	45.827	38.767	175.677	145.755	0.890	0.916	**0.261**	**0.266**	0.000	0.000	**0.000**	**0.000**	**5.027**	**3.240**	**40.800**	**35.527**
4. Polychaetes	**2.06**	**2.06**	324.892	45.927	0.899	1.042	**5.611**	**4.844**	**0.603**	**0.299**	0.160	0.215	0.000	0.000	**0.000**	**0.000**	**0.357**	**0.731**	**0.542**	**0.311**
5. Scallops	**2.00**	**2.00**	7.049	434.504	1.576	2.305	10.037	**14.789**	**0.806**	**0.458**	**0.157**	0.156	2.230	235.421	**0.316**	**0.542**	**0.306**	**1.248**	**0.954**	**0.515**
6. Sea urchins	**2.10**	**2.10**	7.925	11.040	0.551	0.650	**2.589**	**2.891**	**0.949**	**0.563**	0.213	0.225	1.458	0.002	**0.184**	**0.000**	**0.028**	**0.284**	**0.339**	**0.366**
7. Herbivorous gastropods	**2.00**	**2.00**	25.244	5.952	0.925	1.101	**2.778**	**3.793**	**0.788**	**0.943**	0.333	0.290	0.177	0.012	**0.007**	**0.002**	**0.196**	**0.063**	**0.722**	**1.036**
8. Benthic detritivores	**2.00**	**2.00**	70.679	11.314	0.989	1.337	**5.425**	**5.287**	**0.845**	**0.801**	0.182	0.253	0.000	0.146	**0.000**	**0.013**	**0.153**	**0.267**	**0.836**	**1.057**
9. Misc. filter-feeders	**2.24**	**2.22**	82.134	12.111	1.018	0.987	**4.859**	**4.762**	**0.949**	**0.994**	0.210	0.207	1.389	1.935	**0.017**	**0.160**	**0.052**	**0.006**	**0.949**	**0.821**
10. Predatory gastropods	**2.93**	**2.98**	28.104	10.955	**1.653**	**1.407**	4.731	4.549	**0.805**	**0.640**	0.349	0.309	1.326	1.838	**0.047**	**0.168**	**0.322**	**0.506**	**1.284**	**0.733**
11. Small carnivores	**2.96**	**2.99**	9.974	7.595	0.897	0.790	**4.952**	**3.705**	**0.918**	**0.865**	0.181	0.213	0.000	0.000	**0.000**	**0.000**	**0.073**	**0.106**	**0.824**	**0.684**
12. Predatory crabs	**3.35**	**3.09**	27.781	14.870	2.165	2.191	9.889	9.092	**0.930**	**0.191**	**0.219**	**0.241**	3.417	1.673	**0.123**	**0.113**	**0.151**	**1.772**	**1.891**	**0.306**
13. Sea stars	**3.11**	**3.03**	11.567	20.286	0.692	0.734	**3.254**	**3.446**	**0.860**	**0.304**	0.213	0.213	0.000	0.000	**0.000**	**0.000**	**0.097**	**0.511**	**0.595**	**0.223**
14. Octopus	**3.57**	**3.15**	0.315	1.425	4.878	4.809	**11.441**	**12.361**	**0.846**	**0.614**	0.426	0.389	0.749	3.153	**2.377**	**2.212**	**0.750**	**1.854**	**1.750**	**0.742**
15. Littoral fish	**2.86**	**2.99**	1.774	0.353	1.307	1.139	**10.426**	**10.281**	**0.846**	**0.951**	0.125	0.111	0.977	0.206	**0.551**	**0.584**	**0.201**	**0.056**	**0.555**	**0.500**
16. Small pelagic fish	**2.24**	**2.26**	**5.869**	**23.144**	1.939	2.168	**20.868**	**17.957**	0.967	0.867	0.093	0.121	0.298	0.195	**0.051**	**0.008**	**0.063**	**0.288**	**1.825**	**1.871**
17. Pelagic predatory fish	**3.24**	**3.26**	1.360	11.516	0.771	0.845	**7.928**	**7.710**	**0.679**	**0.449**	0.097	0.110	0.584	4.349	**0.430**	**0.378**	**0.248**	**0.466**	**0.093**	**0.002**
18. Marine mammals	**3.45**	**3.39**	0.052	0.010	0.101	0.100	**49.087**	**38.278**	**0.000**	**0.000**	0.002	0.003	0.000	0.000	**0.000**	**0.000**	**0.101**	**0.100**	**0.000**	**0.000**
19. Sea birds	**3.30**	**3.33**	0.056	0.009	0.034	0.036	**62.560**	**52.151**	**0.000**	**0.000**	0.001	0.001	0.000	0.000	**0.000**	**0.000**	**0.034**	**0.036**	**0.000**	**0.000**
20. Detritus	**1.00**	**1.00**	-	-	-	-	-	-	**0.187**	**0.483**	-	-	0.000	0.000	**0.000**	**0.000**	**0.000**	**0.000**	**0.000**	**0.000**

B_i = Biomass, P_i/B_i = Production rate, Q_i/B_i = Consumption rate, EE_i = Ecotrophic efficiency, GE_i = Gross efficiency or conversion efficiency (P_i/Q_i), F_i = Fishing mortality, $M0_i$ = Non-predation mortality, $M2_i$ = Predation mortality

Table VI.4. Diet matrices for steady-state trophic models of Independence Bay for 1996 and 1998 after application of the Ecoranger resampling routine.

Prey / predator	Model	3	4	5	6	7	8	9	10	11	12	13	14	15	16	17	18	19
1. Phytoplankton	1996	0.702	0.293	0.787				0.709							0.802			
	1998	0.698	0.301	0.821				0.721							0.795			
2. Macroalgae	1996				0.811	0.783	0.191							0.235				
	1998				0.808	0.801	0.226							0.255				
3. Zooplankton	1996	0.190	0.051					0.195		0.002				0.513	0.198	0.470		
	1998	0.208	0.047					0.175		0.002				0.340	0.205	0.521		
4. Polychaetes	1996				0.090				0.398	0.462	0.292	0.384		0.207				
	1998				0.091				0.052	0.074	0.027	0.039		0.094				
5. Scallops	1996								0.018	0.011	0.011	0.014	0.065					
	1998								0.746	0.613	0.765	0.758	0.743					
6. Sea urchins	1996									0.030		0.032						
	1998									0.059		0.034						
7. Herbivorous gastropods	1996								0.046	0.037	0.032	0.033	0.069					
	1998								0.026	0.031	0.016	0.017	0.033	0.019				
8. Benthic detritivores	1996								0.159	0.149	0.094	0.106	0.194	0.003				
	1998								0.055	0.072	0.028	0.034	0.056	0.015				
9. Misc. filter feeders	1996								0.196	0.164	0.134	0.164	0.220					
	1998								0.049	0.056	0.025	0.029	0.030					
10. Predatory gastropods	1996										0.108	0.145	0.255	0.001				
	1998										0.033	0.037	0.050	0.031				
11. Small carnivores	1996								0.020	0.015	0.015	0.014	0.045	0.000				
	1998								0.021	0.030	0.012	0.016	0.027	0.024				
12. Predatory crabs	1996										0.191			0.001				
	1998										0.033			0.028				
13. Sea stars	1996										0.025			0.000				
	1998										0.031			0.093				
14. Octopods	1996												0.153					
	1998												0.060					
15. Littoral fish	1996													0.001			0.251	0.093
	1998													0.026			0.098	0.100
16. Small pelagic fish	1996													0.001		0.530	0.699	0.907
	1998													0.015		0.479	0.847	0.900
17. Pelagic predatory fish	1996																0.050	
	1998																0.055	
18. Marine mammals	1996																	
	1998																	
19. Sea birds	1996																	
	1998																	
20. Detritus	1996	0.108	0.655	0.213	0.099	0.217	0.809	0.096	0.164	0.129	0.097	0.109		0.038				
	1998	0.094	0.653	0.179	0.101	0.199	0.774	0.104	0.051	0.063	0.032	0.036		0.059				

Values of 0.000 indicates a proportion of <0.0005

Table VI.5. Biomass data for model groups derived from IMARPE benthic surveys in Independence Bay (1996, 1997, 1998, and 1999). Longer time series (1996-2003) were calculated from estimates of catch per unit effort (CPUE). Relative CPUE changes were used to reconstruct the longer time series relative to the 1996 starting values from the steady-state model.

Year / Groups	Pp-1	Ma-2	Po-4.	Sc-5	Su-6	Hg-7	Bd-8	Mf-9	Pg-10	Sc-11	Pc-12	Ss-13	Oc-14	Lf-15	Ppf-17
1996	51.4	69.2	324.9	7.0	7.9	25.2	70.7	82.1	28.1	10.0	27.8	11.6	0.3	1.8	1.4
1997	28.6	56.6	224.2	28.5	7.4	16.5	24.2	37.7	14.5	10.6	31.4	19.6	0.7	1.5	1.8
1998	28.6	7.6	43.5	564.2	10.9	6.7	13.8	8.2	9.8	6.8	4.5	20.1	0.2	0.2	2.7
1999	51.4	31.1	0.2	233.3	11.7	17.1	27.8	26.7	49.2	25.2	13.9	32.3	0.1	1.7	1.3
2000	51.4			120.6							29.8		0.1	2.4	0.3
2001	51.4			16.1							73.8		0.1	2.4	9.3
2002	51.4			2.7							41.6		0.1	3.5	3.5
2003	51.4			3.7							39.2		0.1	3.8	3.9

Table VI.6. System statistics, cycling indices, and informational indices for the two modeled periods of Independence Bay. Changes in values from the 1996 state to the 1998 state are given as a percent.

Summary Statistics	**1996**	**1998**	**% Change**
Sum of all consumption (t km^{-2} yr^{-1})	8389 (24.5%)	11919 (48.0%)	42.1
Sum of all exports (t km^{-2} yr^{-1})	9444 (27.6%)	2145 (8.6%)	-77.3
Sum of all respiratory flows (t km^{-2} yr^{-1})	4772 (14.0%)	7097 (28.6%)	48.7
Sum of all flows into detritus (t km^{-2} yr^{-1})	11603 (33.9%)	3666 (14.8%)	-68.4
Total system throughput (t km^{-2} yr^{-1})	34208	24827	-27.4
Sum of all production (t km^{-2} yr^{-1})	16133	11610	-28.0
Calculated total net primary production (t km^{-2} yr^{-1})	14214	9242	-35.0
Net system production (t km^{-2} yr^{-1})	9442	2146	-77.3
Total biomass (excluding detritus) (t km^{-2})	754	674	-10.6
Pelagic / benthic biomass	0.13	0.14	15.6
Pelagic / benthic production	8.46	7.79	-8.0
Connectance Index	0.222	0.224	0.9
System Omnivory Index	0.169	0.122	-27.8
Herbivory / detritivory	6.54	5.22	-20.2
Fishing			
Total catches (t km^{-2} yr^{-1})	12.605	248.930	1874.9
Mean trophic level of the catch	2.73	2.05	-24.9
Gross efficiency (catch/net PP)	0.001	0.027	2936.5
PP required / catch.	29.39	9.26	-68.5
PP required / Total PP (%)	1.43	17.85	1148.3
Community energetics			
Total primary production / total respiration	2.979	1.302	-56.3
Total primary production / total biomass	18.861	13.715	-27.3
Total biomass / total throughput	0.022	0.027	22.7
Cycling indices			
Finn's cycling index (% of total throughput)	5.11	8.88	73.8
Predatory cycling index (% of throughput w/o detritus)	9.07	5.14	-43.3
System development			
System Overhead / Capacity (%)	67.0	72.5	-1.2
Ascendancy / Capacity (%)	33.0	27.5	-16.7

Values in brackets are in percent of Total system throughput

Table VI.7. Vulnerabilities calculated by EwE with the application of all four drivers (*Phytoplankton*, *Macroalgae*, *Scallops*, *Predatory crabs*).

	Prey \ predator	3	4	5	6	7	8	9	10	11	12	13	14	15	16	17	18	19
1	Phytoplankton	**BU**	MX	MX				MX							**BU**			
2	Macroalgae				MX	MX	MX							**BU**				
3	Zooplankton	**TD**	MX					MX		MX				**BU**	**BU**	**BU**		
4	Polychaetes				MX				**TD**	MX	**BU**	MX		**BU**				
5	Scallops								**BU**	MX	**TD**	MX	**BU**					
6	Sea urchins									MX		MX						
7	Herbivorous gastropods								MX	MX	MX	MX	MX					
8	Benthic detritivores								**TD**	MX	MX	MX	**BU**	MX				
9	Misc. filter-feeders								**TD**	MX	**BU**	MX	**BU**					
10	Predatory gastropods										**BU**	**TD**	**BU**	MX				
11	Small carnivores								MX	MX	MX	MX	MX	MX				
12	Predatory crabs										MX			MX				
13	Sea stars										MX			MX				
14	Octopus												**TD**					
15	Littoral fish													MX			**BU**	**BU**
16	Small pelagic fish													MX		**BU**	**BU**	**BU**
17	Pelagic predatory fish																MX	
18	Marine mammals																	
19	Sea birds																	
20	Detritus	MX	**BU**	MX	MX	MX	MX	MX	**BU**	MX	MX	MX		**BU**				

BU = Bottom-up control (vulnerability <<2.0), *TD* = Top-down control (vulnerability >>2.0), *MX* = Mixed/intermediate control (vulnerability values between 1.2-2.0)

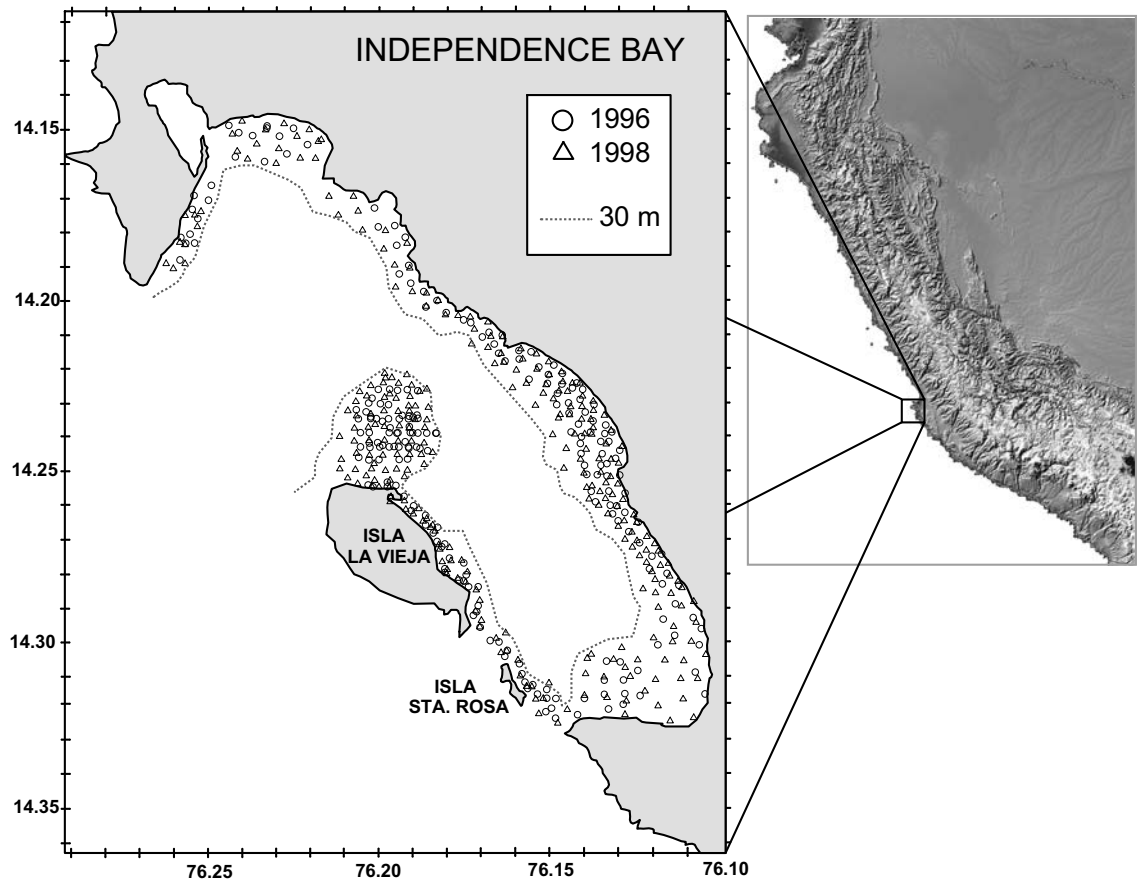

Figure VI.1. Map of the Peruvian coast and the study site, Independence Bay. Macrobenthic fauna sampling stations are indicated by circles for 1996 (n = 223) and triangles for 1998 (n = 252). The 30 m depth isocline is indicated by a dashed line.

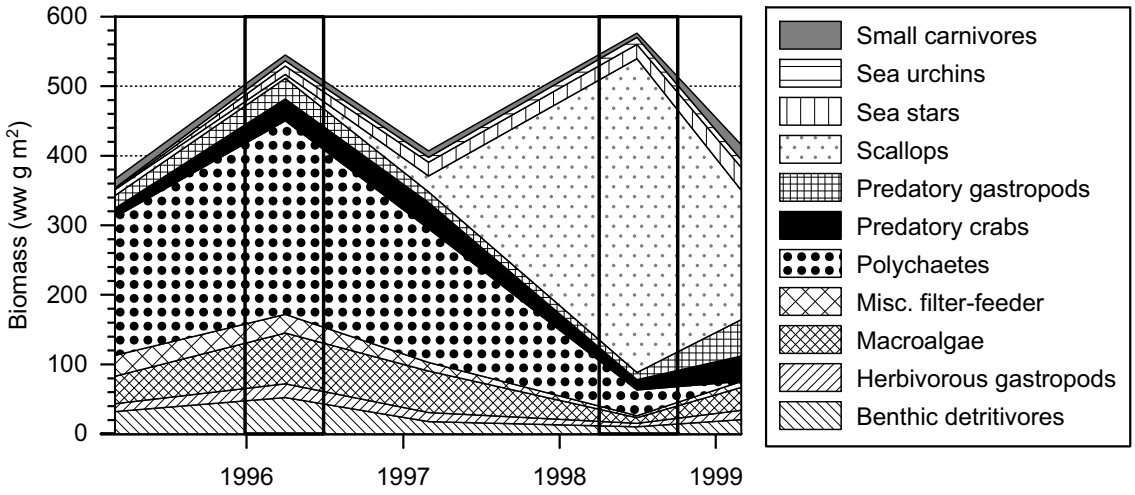

Figure VI.2. Biomass changes of benthic macrofauna observed from 1995-1999 (IMARPE). Boxes indicate model periods.

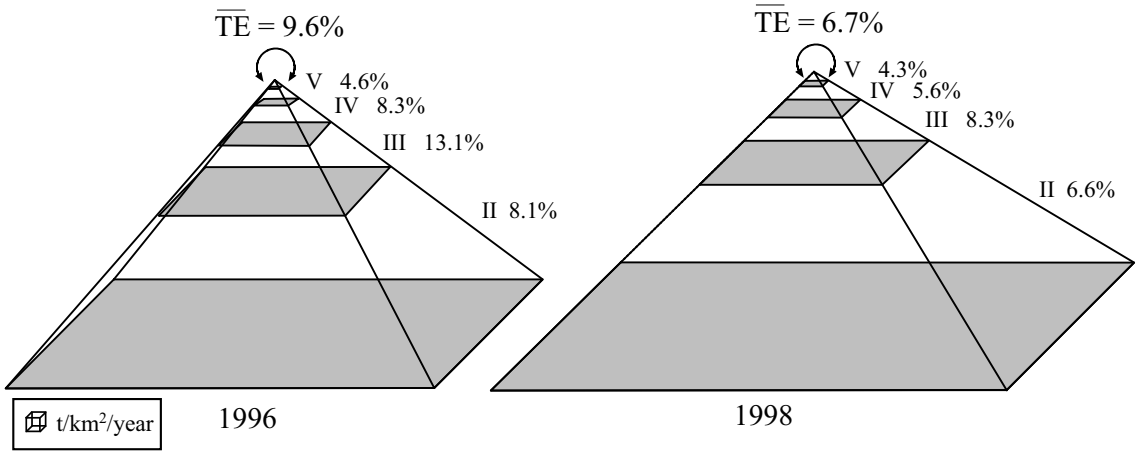

Figure VI.3. Modified Lindeman pyramids of flows for steady-state models of Independence Bay. Transfer efficiencies are given for discrete trophic levels. Mean transfer efficiency is the geometric mean of trophic levels II-IV.

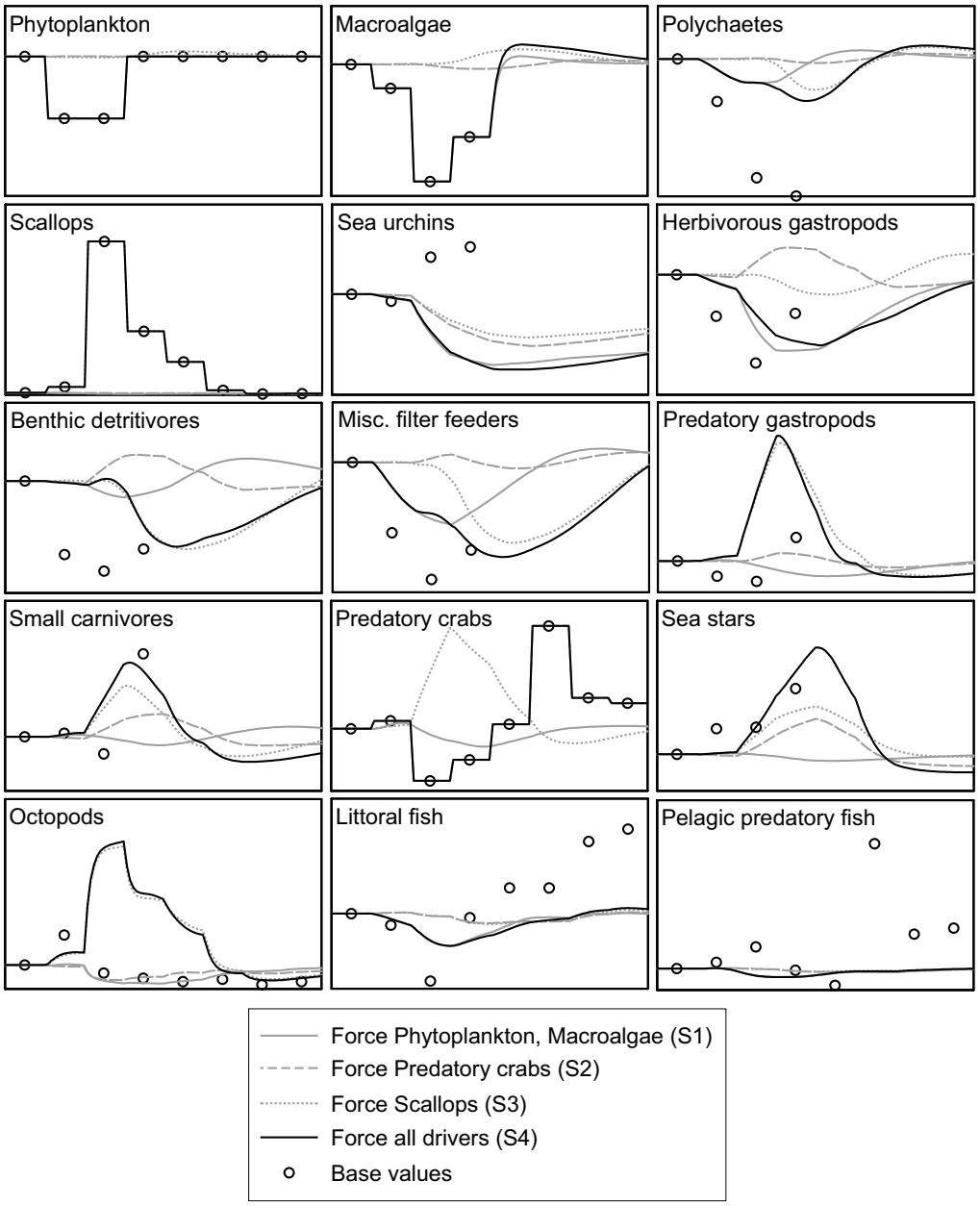

Figure VI.4. Simulated versus observed biomass changes. All simulations consider changes in fishing effort (fishing and diving). Simulation trajectories are shown for each of the 3 scenarios (S1, bottom-up effect of reduced primary production – “Force Phytoplankton, Macroalgae”; S2, top-down effect of reduced benthic predation – “Force Predatory crabs”; and S3, effect of scallop proliferation – “Force scallops”) plus a combination of all four drivers applied together (S4, “Force all drivers”).

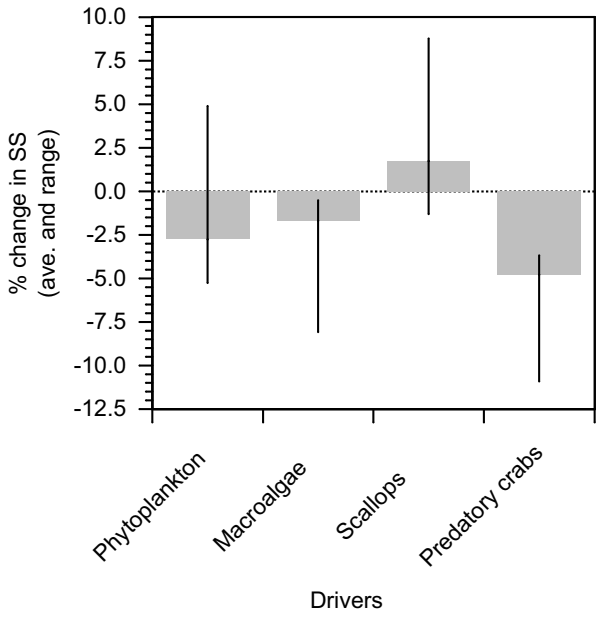

Figure VI.5. Percent changes to sum of squares, SS, of the 1996-2003 simulation after the forcing of biomass changes of several functional groups 'drivers'. Drivers were applied in all possible sequences and combinations and *SS* was corrected for artificial improvements caused by the fitting of the driver's dynamics. Average change (bar) and range (line) are displayed. Negative values (i.e. decrease in *SS*) indicate an improvement in fit.

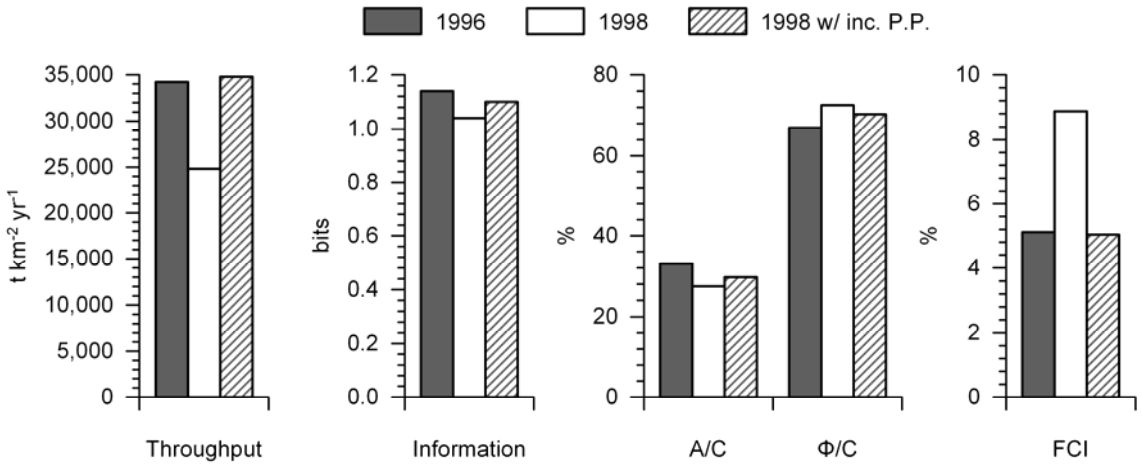

Figure VI.6. Simulation of increasing primary production in the 1998 model to normal upwelling levels (1996 model values for *Macroalgae* and *Phytoplankton*) on indices of Relative Ascendancy (*A/C*), Relative Overhead (*Φ/C*), Mutual Information (*I*), and Finn's cycling (*FCI*). Reference values for the 1996 model's indices are given for comparison

Chapter VII. Trophic and environmental drivers of the Sechura Bay Ecosystem (Peru) over an ENSO cycle

Marc H. Taylor[*]*, Matthias Wolff, Flora Vadas, Carmen Yamashiro*

Author's posting. This is the author's version of the work. Please cite the final version published by Helgoland Marine Research. Article accepted October 10th, 2007 and published March, 2008:
Taylor, M.H., Wolff, M., Vadas, F., Yamashiro, C., 2008. Trophic and environmental drivers of the Sechura Bay Ecosystem (Peru) over an ENSO cycle. Helgoland Marine Research 62 (suppl. 1), 15-32. DOI: 10.1007/s10152-007-0093-4.

Abstract

Interannual environmental variability in Peru is dominated by the El Niño Southern Oscillation (ENSO). The most dramatic changes are associated with the warm El Niño (EN) phase (opposite the cold La Niña phase), which disrupts the normal coastal upwelling and effects the dynamics of many coastal marine and terrestrial resources. This study presents a trophic model for Sechura Bay, located at the northern extension of the Peruvian upwelling system, where ENSO-induced environmental variability is most extreme. Using an initial steady-state model for the year 1996, we explore the dynamics of the ecosystem through the year 2003 (including the strong EN of 1997/98 and the weaker EN of 2002/03). Based on support from literature, we force biomass of several non-trophically-mediated 'drivers' (e.g. *Scallops*, *Benthic detritivores*, *Octopus*, and *Littoral fish*) to observe whether the fit between historical and simulated changes (by the trophic model) is improved. The results indicate that the Sechura Bay Ecosystem is a relatively

[*] Corresponding author, Email: (marchtaylor@yahoo.com)

inefficient system from a community energetics point of view likely due to the periodic perturbations of ENSO. A combination of high system productivity and low trophic level target species of invertebrates (*i.e.* scallops) and fish (*i.e.* anchoveta) result in high catches and an efficient fishery. The importance of environmental drivers is suggested given the relatively small improvements in the fit of the simulation with the addition of trophic drivers on remaining functional groups' dynamics. An additional multivariate regression model is presented for the scallop *Argopecten purpuratus*, which demonstrates a significant correlation between both spawning stock size and riverine discharge-mediated mortality on catch levels. These results are discussed in the context of the appropriateness of trophodynamic modeling in relatively open systems and how management strategies may be focused given the highly environmentally-influenced marine resources of the region.

1. Introduction

Sechura Bay (5.6° S, 80.9° W) (Fig. VII.1) is located in northern Peru and is considered within the zone of transition between cold water transported from the south by the Humboldt Current and warm water of the tropical equatorial region. Under normal upwelling conditions, this transition is found north of the bay; however, during the warm phase of the El Niño Southern Oscillation (ENSO), "El Niño" (EN), this transition zone is shifted southward by reflected Kelvin waves upon arrival to the coast. The bay is relatively shallow with depths of less than 30 m extending to 10 km from the shore.

Under upwelling conditions, the bay shows high primary productivity due to high nutrient availability and relatively warm water conditions when compared to higher latitudes (average temperature ca. 20°C). This productivity supports a large artisanal fishery in the bay of ca. 4,300 registered fishers and 970 boats (DIREPRO, 2006). Additionally, migrant fisher communities may also come to the bay during non-EN periods to take advantage of the abundant fish and invertebrate resources. One example is that of the scallop *Argopecten purpuratus*, which maintains large populations in the bay and is a main target species due to a profitable export market. As a result, the state of Piura accounts for about 30% of total Peruvian landings of *A. purpuratus* (Ministry of Fisheries, 2004).

Due to the bay's position near the transition zone of the Humboldt Current Large Marine Ecosystem, even EN events of smaller magnitude such as in 1991/92 and 2002/03, which may not be felt at higher latitudes, can be observed in Sechura Bay

through higher sea surface temperature (SST). Extreme EN events, such as occurred in 1997/98, resulted in much higher SST as well as increased rainfall and subsequent river discharge into the bay (Fig. VII.2). This environmental variability associated with ENSO is likely to play an important role in the dynamics of the ecosystem.

The objective of this study is to explore the importance of trophic and environmental drivers of dynamics to historical changes in Sechura Bay (1996-2003) through the use of a trophic flow model and dynamic simulations. Specifically, we force both fishing effort and the production of several functional group 'drivers', whose dynamics are well cited in the literature as being non-trophically mediated, in order to measure their relative importance in the dynamics of the remaining functional groups of the model. An additional exploration of the influence of environmental factors on the economically-important populations of *A. purpuratus* is also presented.

2. Materials and Methods

2.1. Trophic model description

A mass-balance modeling approach was applied using the software Ecopath with Ecosim 5.0 (EwE) (Christensen and Pauly, 1992; Walters et al., 1997), which allows quantifying and balancing trophic flows among components (functional groups) of an ecosystem and also permits exploration of ecosystem dynamics under different scenarios of use or environmental change (www.ecopath.org). The Ecopath model links the production of each group with the consumption of all those groups trophically connected:

$$P_i = Y_i + B_i * M2_i + E_i + BA_i + P_i * (1 - EE_i)$$

where P_i is the total production rate of (i), Y_i is the total fishery catch rate of (i), $M2_i$ is the total predation rate for group (i), B_i the biomass of the group, E_i the net migration rate (emigration – immigration), BA_i is the biomass accumulation rate for (i), while $M0_i = P_i \cdot (1-EE_i)$ is the 'other mortality' rate for (i) (Christensen et al., 2000). In order to ensure mass balance between the groups, a second master equation is used:

$$Consumption = Production + Respiration + Unassimilated\ food$$

A steady-state model of Sechura Bay was constructed based on the year 1996 and includes the area south of the Piura River of <30 m depth (total area of ca. 400 km^2) (Fig. VII.1), which incorporates the main area of the artisanal fishery (Gonzales and Yépez 2007). The model contained 21 functional groups including *Detritus*, two producer groups (*Phytoplankton* and *Macroalgae*), *Zooplankton*, six benthic primary consumer groups (*Polychaetes*, *Scallops*, *Sea urchins*, *Herbivorous gastropods*, *Benthic detritivores*, and *Miscellaneous filter feeders*), five benthic carnivore groups (*Predatory gastropods*, *Small carnivores*, *Predatory crabs*, *Sea stars*, and *Octopods*), three fish groups (*Littoral fish*, *Small pelagic fish*, and *Pelagic predatory fish*), *Cephalopods*, and two top-predator groups (*Marine mammals* and *Sea birds*). Functional groups were designated according to similar diets, predators, productivities and individual body size (Table VII.1).

2.1.1. Data sources

Input parameters are derived from various sources: local and regional estimates, empirical relationships, other models and assumed estimates (Table VII.2). Final values are shown in Tables VII.3 and VII.4.

Biomass – Benthic macrofauna biomass was obtained from a survey conducted by IMARPE in September 1996. Epifauna and infauna of the upper sediment layer (approx. <5 cm depth) were collected from 71 quadrants of 1 m^2 each, and abundance and weight were recorded for each species (for further information on sampling, see Samamé et al., 1985; Yamashiro et al., 1990) (Fig. VII.1). Groups of small epifauna (*Herbivorous gastropods*, *Benthic detritivores*, *Scallops*, *Small carnivores*) and *Polychaetes* were increased by 25% to correct for undersampling. *Miscellaneous filter feeders* (consisting mainly of infaunal bivalves) were increased by 100% to also correct for undersampling, as much of this group's biomass is found deeper than 5 cm.

Estimates of *Phytoplankton* biomass were based on SeaWifs (Feldman and McClain, 2007) remote sensing estimates of sea surface chlorophyll *a* (chl *a*) concentrations ($mg \cdot m^{-3}$) for the immediate region (4.9-6.6°S, 80.2-81.7°W) from December 1997 – April 2007, excluding EN values. Conversion factors used for chl *a* to wet weight were as follows: chl *a*:Carbon (40:1) (Brush et al., 2002), and Carbon:wet weight (14.25:1) (Brown et al., 1991). Finally, sea surface biomass was multiplied by a mean depth of 15 m, assuming a well-mixed water column, to arrive at units on a per m^{-2} basis.

Information on the *Zooplankton* in Sechura Bay is limited and thus we used average values from IMARPE cruise samplings from 1995-1999, excluding EN values, for the immediate region (5°-6°S, <82°W; n=60).

Biomass of highly mobile species such as octopus, cephalopods, and fish species were estimated from catch data by assuming that the fishery takes 50% of yearly produced biomass (Table VII.3).

Catches – Estimates of catch were derived from IMARPE catch statistics for the artisanal fishery from the 2 main landing sites for Sechura Bay - Parachique and Puerto Rico. Catches were summed according to species' functional groups (Fig. VII.3) for use in the steady-state model and for the measuring of performance of the simulations (see *Simulations of temporal dynamics*)

Production/Biomass (Total mortality) – Direct estimates of production to biomass ratios (*P/B*) or Total mortality (*Z*) existed for several benthic invertebrate groups in the model – *Scallops*, *Predatory crabs*, and *Sea stars*. Other groups were estimated using empirical relationships from Brey (2001) taking into account taxonomic group, mean body size, temperature of habitat, feeding modes, and habitat type. In most cases this provided realistic estimates; however, values for *Polychaetes* and *Misc. filter-feeders* were increased to 1.0 based on other estimates from the literature (Table VII.3).

P/B of *Phytoplankton* was estimated using a modified Eppley curve (Eppley, 1972) as described by Brush et al. (2002):

$$G = G_{\max} * f * LTLIM * NUTLIM$$

where G = realized daily growth rate (d^{-1})(base e), f is the fraction of the day during which there is light, and $LTLIM$ and $NUTLIM$ are dimensionless ratios from 0 to 1 which describe light and nutrient limitation of growth, respectively (Kremer and Nixon, 1977). G_{max}, as described by Eppley (1972) describes an exponentially-shaped envelope for growth rates of phytoplankton under culture conditions without light or nutrient limitation (as recalculated by Brush et al., 2002):

$$G_{\max} = 0.97 * e^{0.0633*T}$$

where T = water temperature (°C). The 'normal' upwelling phytoplankton production of 1996 assumed a mean temperature of 20°C with 50% light (from self-shading) and 0%

nutrient limitation factors. *P/B* values for other groups are taken from the literature (Table VII.2)

Consumption (Q) / Conversion efficiency (GE) – Direct estimates of consumption rates (*Q/B*) were available for a few of the benthic invertebrate groups, (*Octopods*, *Scallops, Predatory gastropods, and Predatory crabs*). For most other groups, ratios of Conversion efficiency (*GE*) or the ratio between Production and Consumption (*P/Q*) were applied (Tables VII.2 and VII.3).

Diet matrices – Direct diet studies for Sechura Bay are limited and thus general knowledge from literature was used in the construction of diet matrices (Table VII.2). Macroinvertebrate predator groups are described to be rather unselective and opportunistic feeders limited more by their modes of feeding (Wilson and Parkes, 1998). Therefore, diet proportions were adjusted to reflect both predatory groups' consumption rates as well as the available production of prey groups. Specifically, the diets of carnivorous benthic invertebrate groups (*Predatory gastropods, Small carnivores*, *Predatory crabs, Sea stars,* and *Octopods*) assumed a base percentage of detritus feeding (10-20%) and then production of their prey was iteratively distributed based on the consumption rates of the aforementioned benthic predators. Diets for fish species were obtained from FishBase (Froese and Pauly, 2006) and were adjusted to the fish groups based on relative species contribution from recorded catches (Table VII.4).

2.1.2. Addressing parameter uncertainty

The balanced steady-state model for 1996 was subjected to the resampling routine *Ecoranger* in order to assess the probability distributions of the input parameters. Using a Monte Carlo approach, the routine drew a set of random input variables from normal distributions for each basic parameter and all resulting combinations that satisfied mass-balanced constraints were recorded. Originally we allowed the routine to use confidence intervals as derived from a pedigree of the data sources, where highest confidence is placed in locally-derived data (Table VII.5); however, the initial results often gave parameter values outside of reasonable biological constraints (e.g. high conversion efficiencies, high cannibalism) and thus we decided to fix all confidence intervals at 20% variation as was similarly done by Arias-González et al. (1997). We allowed resampling until 10,000 runs passed the selection criteria. The 'best' run was then chosen as that with the smallest sum of square residuals between the input parameters and the mean value of all successful runs (for more information, see Christensen et al., 2000).

2.1.3. System statistics and indices

The Ecopath with Ecosim package allowed for the calculation of several statistics of the steady-state model concerning flow structure and community energetics. These allowed for the comparison of Sechura Bay to published models of other coastal systems.

General descriptive statistics include: i) Total throughput (*T*) – measure of the total sum of flows within the system and indicates the 'size' or activity of the system; and ii) Contributions to *T* from different types of flows - Consumption, Export, Respiration and Flows to detritus.

Several indices of community energetics are presented that allow for the interpretation of system's 'maturity' according to Odum (1969). Mature systems are hypothesized to be highly efficient in terms of energy transfer to higher trophic levels and, thus, able to sustain a higher biomass in proportion to primary production. The following indices of community energetics are calculated: i) Total primary production (*PP*) to Total respiration (*R*) ratio (PP/R); ii) Biomass (*B*) supported by Total primary production (*PP/B*); iii) Biomass supported by Total throughput (*B/T*); and iv) Energy Transfer efficiency (*TE*) between discrete trophic levels. Calculated ratios of production to respiration (P/R) and respiration to assimilation (R/A) were compared with independent estimates of similar taxa from the literature in order to gauge biological consistency.

Statistics concerning the fishery and its efficiency were also presented, including: i) Gross efficiency (catch / net *PP*); ii) Mean trophic level of the catch; and iii) Primary production needed to sustain the fishery.

2.2. Simulations of temporal dynamics

Using the 'best' steady-state model for 1996 as a starting point (as defined by the Ecoranger routine described above), we explored the temporal dynamics of the ecosystem from 1996-2003 using the Ecosim routine of the EwE package. Following the forcing of the yearly fishing effort for the two fishing fleets, *Fishing* and *Diving*, we applied several functional group 'drivers' to the model in order to measure their impact on the fit of the model. Drivers included the relative biomass changes of 4 trophically-important and highly-dynamic functional groups (*Scallops*, *Benthic detritivores*, *Octopods*, and *Littoral fish*) as calculated from catch per unit effort (CPUE). These drivers are well cited in the literature as having significant environmental influences on their dynamics. Populations of the scallop *A. purpuratus* in Independence Bay have been shown to fluctuate more in

response to temperature-mediated larval development time and subsequent mortality changes rather than from purely trophic changes (Wolff et al., 2007; Taylor et al., in press). Penaeid shrimp dynamics in the region have been correlated to shifts in carrying capacity as a result of variable SST and river discharge (Mendo and Tam, 1993). As the catches of the *Benthic detritivore* group are dominated by shrimp, we have included this group as a non-trophic mediated driver. *Octopus* was included due to the observed temperature-mediated growth and reproduction for *Octopus mimus* (Cortez et al., 1999), helping explain the large booms of octopus during EN periods (Arntz et al., 1988). Additionally, *O. mimus* embryonic development time has also been shown to be greatly accelerated under EN-like conditions in the laboratory (Warnke, 1999), which may also contribute to increased production rates. Finally, the immigration of subtropical fish species southward is linked to the intrusion of subtropical equatorial waters during EN (Arntz and Tarazona, 1990) contributing to the *Littoral fish* dynamics.

Drivers' biomasses were then fixed through time in all possible sequences and combinations (n=64). The performance of each simulation was measured against the time-series of observed relative biomass changes (CPUE) for the remaining unforced groups through the calculation of the sum of squares (*SS*):

$$SS = \sum \left[Log(B_{obs.}) - Log(B_{pred.}) \right]^2$$

where $B_{obs.}$ = observed biomass (g·m^{-2}), and $B_{pred.}$ = predicted biomass (g·m^{-2}).
The simulation runs conducted for this study with EwE calculates biomass changes through time by solving the set of differential equations:

$$dB_i / dt = g_i \left[\sum_k Q_{ki}(t) \right] - \sum_j Q_{ij}(t) - M0_i B_i - \sum F_{if}(t) B_i$$

for species or functional groups i =1…n. The first sum represents the food-consumption rate, Q, summed over prey types k of species i, and g_i represents the growth efficiency (proportion of food intake converted into production). The second sum represents the predation loss rates over predators j of i. $M0_i$ represents the instantaneous natural mortality rate due to factors other than modeled predation. The final sum represents the instantaneous fishing mortality rate, F, as a sum of fishing components caused by fishing fleets f (for further information, see Walters and Martell, 2004).

2.3. Exploration of environmental drivers to scallop production

A multiple regression analysis was conducted to explore the influence of environmental factors on the dynamics of the economically-important scallop (*Argopecten purpuratus*) population in Sechura Bay. Using the methods employed by Wolff et al. (2007) for the scallop stocks in Independence Bay, Peru (16°S), the model attempts to forecast scallop catch as a function of the environmental conditions during the previous spawning period. Specifically, the dependent variable was defined as the scallop 'catch' (kg), versus the independent variables 'spawning stock' (kg) and the temperature-dependent 'settlement factor' (arbitrary units) for scallop recruitment. *Settlement factor* is based on a day-degree larval development time, whereby higher temperatures shorten the development time and consequently the pre-settlement mortality. In addition, we added the independent factor of 'river discharge' ($m^3 \cdot s^{-1}$) as Sechura Bay experiences highly variable input of freshwater from the Piura River depending on rainfall associated with ENSO, which affects the salinity of the bay.

The variables were defined as follows: *Catch* is calculated as the average monthly catch from September-August. *Spawning stock* is calculated as the average catch during the six-month main spawning season (January-June) preceding the catch. *River discharge* is the average river discharge recorded during the catch period (September-August). *Settlement factor* is calculated from the average temperature six-month main spawning season (January-June).

Data-series and their sources: Monthly catches (IMARPE); Sea surface temperature (SST) collected in Sechura Bay (IMARPE); and Piura River discharge (Sanchez Cerro Bridge, Piura – Sistema de Alerta Temprana 'SIAT').

Assumptions of the model:

1. Scallop landings reflect the size of the scallop stock in the bay. If the stock increases or decreases, the fishery grows or shrinks accordingly, so that the relative fishing rate remains relatively constant and the catch is proportional to stock size.
2. Scallop landings during the post-recruitment period, which starts in late winter (Aug./Sept.) each year largely depend on the recruits spawned during the preceding summer/autumn period [January-June, note: this period is slightly later than that of Independence Bay as determined by histological analysis of gametogenesis (IMARPE, Huayurá, pers. comm.)], typical for annual "pulse fisheries".

3. Spawning stock is assumed proportional to scallop landings during spawning (January-June).

4. Larval survival in the natural environment (from egg release to settlement) is significantly lower than the observed 0.1% in the hatchery (Wolff et al., 1991).

5. Day degrees (dd) for larval development including successful settlement were considered to be approx. 400 for the temperature range 14-25°C, based on hatchery data by DiSalvo et al. (1984), Uriarte et al. (1996a) and Wolff et al. (1991). During cold water conditions (14°C) larvae would need over 28 days to settle, while only about 16 days are needed at the high EN temperatures of 25°C.

6. Piura River discharge is a good proxy for hydrological changes in Sechura Bay (e.g. change in salinity or sedimentation rate), which may impact the adult stock production.

3. Results

3.1. Trophic model

Initial parameters of the balanced model can be found on the Pangaea website (Taylor et al., 2007c, 2007d). Ecoranger resampling resulted in balanced models in 2.62% of the runs with the 'best' fitting model parameters shown in Table VII.3. The analysis of trophic flows in Sechura Bay for 1996 indicates an intermediate level of consumption of phytoplankton production by higher trophic levels (EE=0.69) and low recycling of detritus (EE=0.10). This inefficiency explains the high proportions of Total throughput (*T*) (27820 $t \cdot km^{-2} \cdot yr^{-1}$) allocated to Exports (28%) and Flows to detritus (31%). Inefficient transfer of energy to higher trophic levels is reflected by the mean transfer efficiency value of 6.6% (geometric mean of trophic levels II-IV). Furthermore, the relatively high PP/R ratio (2.97) indicates that the system may be considered developing and immature (Table VII.6).

Respiration rates and conversion efficiencies can vary widely, especially depending on the population structure – whereby younger individuals will generally invest more energy in production while older individuals will respire most of their assimilated consumption. Nevertheless, the model estimates of respiration fell within acceptable ranges as described in the literature for taxonomic groups. P/R ratios of fish groups ranged between 0.117 and 0.181, which is slightly higher than the mean value of 0.11 presented by Humphreys (1979). Benthic invertebrate P/R ratios had a wide range (0.193 – 0.948), but the average value of 0.475 is also very close to mean values of 0.482 and

0.439 for aquatic invertebrates as described by Humphreys (1979) and Schwinghamer et al. (1986), respectively. All but one (Scallops – 0.838) of our R/A estimates for benthic invertebrates fall within the expected range of 0.5 – 0.75 given by Mann (1982). The average R/A ratio was 0.693, which is similar to the average value of 0.7 given by Davis and Wilson (1985) for macroinvertebrates.

The total fishery catches are high (87 $t \cdot km^{-2} \cdot yr^{-1}$). Due to the targeting of low trophic level primary consumer species (e.g. *Engraulis ringens*, *Anchoa nasus*, and *Argopecten subnodosus*) the mean trophic level of the catch is close to 2.0 (2.15). As a result, the fishery has a high Gross efficiency (catch/net PP; 0.01) and low PP required per unit of catch (15.66). Overall, the fishery requires 6.6% of the total PP to sustain it (Table VII.6).

3.2. Simulations

The initial application of fishing effort changes for the two fleets slightly improved the fit between the observed and simulated catches (ca. -6.4% in *SS*), indicating some affect to overall dynamics. The application of the functional group drivers had little positive improvement on the fit of the simulation (-1.7% to 11.1% average change in *SS* for all drivers, Fig. VII.4). *Scallop CPUE* was the only drivers that improved fit on average (-1.7% in *SS*, respectively), although the improvement was minimal. The impact of each individually-applied driver on simulated dynamics can be seen in Fig. VII.5.

3.3. Multiple regression

None of the independent variables were significant predictors of catch when applied alone [Spawning stock (SS) p = 0.347; Settlement factor (SF) p = 0.215; River discharge (RD) p = 0.236]. When SS and SF were applied together, as done by Wolff et al. (2007) for Independence Bay, the regression was not significant (R^2 = 0.362; p = 0.509). The addition of the independent variable RD increased the fit dramatically (R^2 = 0.959; p = 0.060); however, a significant regression was achieved only from the combination of the independent variables SS and RD (without SF) (R^2 = 0.916; p = 0.024*). Predicted vs. observed values of scallop catch can be seen in Fig. VII.6 along with the statistics of the multiple regression. The relationship reveals that spawning stock size and river discharge influence catch levels positively and negatively, respectively.

4. Discussion

4.1. General system configuration

Sechura Bay is located near the northernmost extension of the Peruvian coastal upwelling where, due to its proximity to the equator and resulting large Rossby radius, strong upwelling occurs even under relatively low wind-forcing conditions. Estimates of chl *a*, as derived from remote sensing during non-EN years, showed relatively typical values of the coastal Peruvian upwelling system (3.00 mg chl a·m^{-3}) and production rates under upwelling conditions are assumed to be at the higher end due to a higher mean sea surface temperature. For example, when compared to the southern extension of the main upwelling zone near Independence Bay (16°S), mean temperatures in Sechura Bay are approximately 4°C higher (20° vs. 16°C), resulting in a 29% increase in phytoplankton production rates according to the modified Eppley curve presented by Brush et al. (2002). In part due to this high primary production, the Total throughput in Sechura Bay was estimated at 27820 t·km^{-2}·yr^{-1}, which is of a similar magnitude to other coastal bays along the coast of South America (Tongoy Bay, Chile (20594), Ortiz and Wolff, 2002a; Independence Bay, Peru (34208), Taylor et al., in press).

Despite the advantages of a combined upwelling and higher mean SST for high primary production, the lower subtropical latitudes of the western coast of South America are subject to the highest interannual SST variability associated with ENSO (Lluch-Cota et al., 2001; Montecinos et al., 2003). This variability is caused by oscillations in the zone of transition between the cold waters of the Humboldt Current and the warm waters of the tropical equatorial region, and may act as a periodic perturbation to “reset” the system and prevent the development of a high trophic efficiency. Under the negative SST anomalies of 1996, the system is functioning as a typical upwelling region with exports and flows to detritus equaling 28% and 31%, respectively, due to inefficient consumption of primary production. While our estimate of Total throughput is not directly comparable to models that use differing units to describe flows (e.g. dry weight or carbon units), we are able to compare the proportions of types of flows. The proportion of flows to detritus in Sechura Bay is similar to those estimated for several US bay systems (Narragansett Bay (33%), Delaware Bay (30%), and Chesapeake Bay (27%) by Monaco and Ulanowicz, 1997) and other bay systems along the coast of South America (Tongoy Bay (29%) by Ortiz and Wolff, 2002a; Independence Bay (34%) by Taylor et al. Chapter VI). However, only the models of the South American bays calculated high proportions of exports as well (29-34% vs. 7-10% for US bays). Rybarcyzk et al. (2003) found a similarly high proportion of export flows (26%) for Somme Bay, France, which they in part attribute to high exchange

rates / low residency time of water in the system. Sechura Bay is in fact a very open bay and losses of primary production may occur; however, the benthic evaluations conducted in 1996 observed standing detrital material at about one third of the sample locations, which may be evidence of primary production going unutilized and remaining in the sediments under strong upwelling conditions.

Indices of community energetics show a similar degree of development when compared to the bays of Independence (16°S) and Tongoy (30°S) (PP/R, PP/B, and T/B ratios); however, the mean transfer efficiency of trophic levels II-IV is lowest in Sechura Bay (6.6%) as compared to the other South American bay systems (9.6% and 11.4% for Independence and Tongoy, respectively) probably due to the fact that perturbations frequently impact higher-level species to a greater extent than the lower trophic components (Baird et al., 1991). This is likely due to the fact that higher trophic levels have lower production ratios and thus slower biomass recovery times. As transfer efficiency indicates the development of higher trophic connections, the latitudinal trend of increasing transfer efficiencies at higher latitudes may be related to decreasing ENSO-related variability and impact to the coast of the Humboldt Current ecosystem.

4.2. Role of fishing

The fishery is highly productive with catches equaling 87 $t \cdot km^{-2} \cdot yr^{-1}$ for 1996. The catch is dominated by small pelagic fish; specifically, Peruvian anchoveta, *Engraulis ringens* (84.6% of total catch), and Longnose anchovy, *Anchoa nasus* (10.9% of total catch). Due to the low trophic level of these groups, the efficiency of the fishery is high, which is sustained by a smaller fraction of the total primary production (6.6%) when compared to average estimates of upwelling systems (25.1%) (Pauly and Christensen, 1995).

Sechura is one of the largest bays of the western South American coast, measuring 89 km from north to south with oxygenated bottom depths <30 m extending about 10 km offshore. Below 30m benthic biomass drops off significantly due to decreased oxygen concentrations. For this reason, the diving fishery operates almost exclusively in shallow depths (<30 m). Despite such an expansive area for exploitation, the diving fishery in Sechura is a relatively recent development, spurred on in the early 1990's by a boom in the scallop fishery and the introduction of diving techniques to the area of fishers from the south (i.e. hookah and air compressor systems). As a result, between 1994 and 1997 the diving fleet increased to include nearly 500 boats (Tafur et al., 2000). Nevertheless, the fishing mortality rates of the benthic target species are very

low, even for the targeted scallops. For example, an exploitation ratio (F/Z) of 7% for scallops in Sechura Bay compares to 23-25% for Independence Bay (Taylor et al., in press). It is likely that both the young state of development of the diving fishery, as well as the higher associated costs of travel to the farther fishing grounds in the larger Sechura Bay, may limit to some extent the overall impact and help to explain the low fishing mortalities of the benthic resources (Table VII.3).

The addition of fishing effort dynamics did make some improvement to the fit of the simulations (-6.4% in *SS*), implying that changing fishing intensity may have some impact on the overall changes of catch through time. Given the low fishing mortality rates associated with the targets of the *Diving* fleet (i.e. benthic invertebrate groups), this improvement is mainly attributable to slightly better fits in the targets of the *Fishing* fleet. In particular, the increases in relative biomass for *Littoral fish*, *Pelagic predatory fish*, and *Cephalopods* (Fig. VII.5) are slightly improved through the introduction of decreasing fishing effort in the *Fishing* fleet (Fig. VII.3).

Despite this improvement, the impact of the artisanal fishery in Sechura appears small and in stark contrast to what has been observed for the Peruvian upwelling system overall with respect to the industrial fishery. Taylor et al. (Chapter IV) showed that the changes in industrial fishing rates in the upwelling region (4°-16°S, 110 km extension from the coast) helped to explain 27.1% of the biomass and catch dynamics during the same time period of 1996-2003. In contrast, the artisanal fishery seems to operate more in response to the fluctuating availability of resources and does not have the same problems of overcapacitation as has been shown for the industrial fishery (Fréon, 2006).

4.3. Applicability of trophic modeling to the Sechura Bay Ecosystem

Through the modeling of trophic flows for Sechura Bay we have gained insight into the general system configuration during periods of normal upwelling (1996) and provide some of the first estimates of fishing mortality of the benthic resources, which appear to be very low. The application of Ecoranger has helped to add some weight to our input parameters due to the fact that locally-derived estimates of production, consumption, and diet were scarce. Our assumptions regarding these values allowed for the initial balancing of the model, and confidence intervals of 20% give favorable results from the Ecoranger resampling routine whereby resulting energy budgets of functional groups are within acceptable ranges. Generally, highest respiration rates were found for the warm-blooded sea birds and marine mammals, and lower values for poikilotherms (fish and invertebrates), with less mobile benthic invertebrates having the lowest respiration ratios

(R/A). Furthermore, within the invertebrate groups, lowest respiration rates are calculated for strongly carnivorous groups (predatory gastropods, octopods, and cephalopods). Higher assimilation efficiencies have been proposed for carnivorous organisms possibly due to the high nutrient value of their food (Welch, 1968); however, this tendency is not supported for aquatic mollusks (Huebner and Edwards, 1981) and thus our decision to leave unassimilation ratios for all benthic invertebrates at the Ecopath default of 20% may be reasonable. The lower R/A ratios calculated in the model are rather a result of higher conversion efficiencies ("gross efficiency", GE) (0.3-0.35) as is supported by Huebner and Edwards (1981) for carnivorous invertebrates as well as from local estimates of *Octopus mimus* (Wolff and Perez, 1992; Vega and Mendo, 2002) and the jumbo squid, *Dosidicus gigas* (Alegre et al., 2005).

We hypothesized that the fit of the simulations would be improved through the forcing of functional group 'drivers' whose changes in biomass and production were known to be a result of non-trophic environmentally-mediated interactions (*i.e. Scallops*, *Benthic detritivores* (shrimp), *Octopus*, and *Littoral fish*). Overall these drivers help little in explaining the remaining functional groups dynamics. We propose three hypotheses for the poor performance of the dynamic simulation.

First, the Sechura Bay ecosystem is highly open to outside influences and thus the scale of the model does not reproduce well the dynamics of functional groups whose life cycles are enclosed in a larger geographic area or whose distribution is linked to particular water masses. We have taken into account the southward migration of more tropical equatorial-associated fish species to Sechura Bay due to their possible impact to benthic resources; however, other groups also show important dynamics on a larger scale. *Small pelagic fish* catch dynamics in Sechura are mainly due to latitudinal migrations of the stocks in response to changing centers of upwelling and associated plankton variability. One example is the southward retreat of the Peruvian anchoveta during the strong EN of 1997/98 (Alheit and Ñiquen, 2004), which helps explain the decreased catches in Sechura. *Cephalopod* catches have increased following the EN of 1997/98 to become an important target of the artisanal fishery. This is due almost exclusively to large-scale increases in population growth and range expansion of the Jumbo squid, *Dosidicus gigas*. Evidence suggest that its large scale expansion is a bottom-up response to increases in its principle prey – mesopelagic fish (*e.g. Vinciguerria lucetia*) Taylor et al. (Chapter IV). Mesopelagic fish themselves are not found much within the shelf region of Peru, but adult Jumbo squid in their reproduction phase or nearing senescence can be found in coastal waters (Argüelles et al., in press) where they are targeted by the artisanal fishery. It is also worthwhile to note that the model presented in Taylor et al. (Chapter IV) for the Northern Humboldt Current system took care to define both offshore (~110 km) and latitudinal (4°-

16°) boundaries that enclosed the life cycles and spatial movements of main functional groups in response to ENSO variability. As a result, the model could explain more of the time series variability after the introduction of drivers (-33% in *SS*); however, even with this large scale, the forcing of the mesopelagic fish expansion into the model area proved to be an important factor in the dynamics of more coastally-associated groups (-9% in *SS*). Thus, we believe that the applicability of trophodynamic models depends on a certain degree of "closure" of trophic flows in order to be able to reproduce dynamics.

Secondly, other groups' dynamics, besides the forced drivers, may also be highly influenced by environmental variability. It is possible that given the dramatic changes in temperature and salinity in Sechura Bay, other less mobile benthic invertebrate species may also be affected by ENSO-related variability. Respiration rates of poikilotherms are sensitive to changes in temperature and thus, depending on the organism's tolerances, conversion efficiencies may also be affected. Several ongoing studies regarding these influences are being conducted within the CENSOR project, which will aid future modeling efforts.

Finally, the data availability and quality may have affected the accuracy of some parameters and time series data sets. We have constructed our model for the base year of 1996 for several reasons: 1) availability of benthic biomass estimates; 2) it marks beginning of constant monitoring of catch and effort data by IMARPE; and 3) it precedes the strong EN event of 1997/98, which offers insight into system dynamics resulting from extreme environmental variability. Our catch and effort data comes from the two main ports in the bay (Puerto Rico and Parachique). Biomass estimates were available for benthic groups based on evaluations conducted by IMARPE in 1996, but fish and cephalopod biomasses were approximated by assuming that the fishery takes about 50% of these groups' production. Such fishing rates are likely given the operating capacity of the fishers, especially regarding the fleets geared toward anchovy and other pelagic fish. Furthermore, the artisanal fleet has traditionally focused on fishing and thus we have more confidence in relative biomass changes as calculated by CPUE. On the other hand, the diving activities are both less intensive as well as relatively young in development. Although these activities have continued to grow since the mid-1990s, relative changes as calculated by CPUE for our time series may be less indicative of the actual resource dynamics. Future simulations will be able to take advantage of improved time series as derived from more regularly conducted benthic evaluations by IMARPE since 2000.

4.4. Importance of environmental variability and implications for management

Although Sechura Bay is a system relatively open to outside influences, the dynamics of some principle resources may still be largely influenced by local variability. We have explored one such example with the scallop *Argopecten purpuratus* for which a simple two-factor multiple regression model is able to predict catches.

Scallop biomass has been shown to be enhanced in southern Peru and northern Chile during EN events (Wolff, 1987; Stotz, 2000). These events improve benthic oxygen concentrations through a lowering of the thermocline and also increased metabolic activity (respiration, somatic growth) in response to the increased temperature. New findings suggest that reduced mortality in the larval stage, due to faster development to settlement times, may be mainly responsible for population booms during EN periods (Wolff et al., 2007). Our exploration of the environmental influences on the scallop stock in Sechura Bay suggests a greater importance of riverine inputs to the bay. The importance of both spawning stock (positive) and river discharge (negative) suggest some degree of self-recruitment with the additional negative effect (*i.e.* mortality) of riverine discharge on the adult population.

Contrary to Independence Bay and many of the main scallop habitats in northern Chile that border the Atacama Desert (known as the most arid region on Earth), Sechura experiences seasonal rainfall and, additionally, flooding is common during EN events. For example, the last EN of 1997/98 increased the discharge volume of the Piura River more than 4 times the normal levels, causing massive flooding damage to the region. In addition, mean temperatures are consistently higher in Sechura as compared to the south, and thus scallop recruitment appears to be less limited by extreme cold conditions and in fact scallops may spawn multiple times in the year (IMARPE, pers. comm.). The importance of riverine input to the bay on scallop mortality has long been suggested by fishers, either through increased sediment load affecting their filtering capacity or through salinity changes. We believe that while sediment loads may increase in the bay, these changes are likely to be temporary and, furthermore, *A. purpuratus* appears to be well-adapted to periodic sedimentation events in other areas (*e.g.* wind-blown terrigenous material to Paracas Bay, Peru). On the other hand, physiological studies of *A. purpuratus* have shown that the scope for growth is greatly diminished by reduced salinity with negative values calculated for salinities below 27‰ (Navarro and Gonzalez, 1998). Unfortunately, longer time series of salinity changes in the bay are not available; however, Aronés et al. (in press) have measured salinities of ca. 23‰ off Paita Bay during the EN of 1997/98 (immediately north of Sechura; average of a 4 station transect extending >25 km

offshore). With the implementation of regular environmental sampling series within the CENSOR project, future EN events will provide a test to this hypothesis for Sechura Bay.

It is likely that similar explorations for other resources may also show an importance of environmental variability on resource dynamics in Sechura Bay. This information will have importance in the designation of management strategies in response to ENSO. Previously, artisanal fishers have operated in a highly mobile manner in response to changing resources (*e.g.* migration of fishers towards population increases of *A. purpuratus* in Independence Bay during EN periods), however increasing regionalization may make this more difficult in the future.

Even if the responses of resources are successfully linked to environmental variability, the predictions of strong EN phenomena are presently only accurate for a few months to half a year, thus preventing longer-term strategies for fishers. Nevertheless, forecasts of even a few months could mean substantial benefits; in fact some Peruvian fishers and farmers have based their seeding or harvesting schedules (albeit erroneously at times) on the ENSO predictions of the NOAA website. As these predictions improve, as well as the known responses of resource availabilities, we may see an increased importance of ENSO forecasting to management strategies. For example, forecasting would allow culturists time for harvest or relocation of scallops to other areas, and fishers could make gear changes or other adjustments in preparation for switching to alternative resources.

Significant emphasis has been placed in recent years on developing an ecosystem-based approach to fisheries (for a review, see Browman and Stergiou, 2004). Trophic modeling tools such as EwE have no doubt shed new light on our understanding of ecosystem dynamics and continue to increase in importance for management. Additionally, the incorporation of environmental drivers on ecosystem dynamics is often needed to reproduce historical changes. This study confirms this, and furthermore indicates that systems which are both open to outside influences or bordering variable water masses may be less predictable from a trophic modeling perspective than more closed systems.

Acknowledgements

The authors are grateful for the support and assistance from the following: Dr. Villy Christensen of the Fisheries Centre, University of British Columbia, for his helpful advice regarding the use of Ecoranger routine within Ecopath with Ecosim; Dr. Thomas Brey of

the Alfred Wegener Institute for Polar and Marine Research (AWI) for helpful discussions regarding benthic invertebrate energetics and for the use of his somatic production models; Dr. Jorge Tam and David Correa of the Instituto del Mar del Péru (IMARPE) for fruitful discussions and their help in retrieval of SeaWifs data; and three anonymous reviewers whose comments and suggestions greatly improved the earlier manuscript. This study was financed and conducted in the frame of the EU-project CENSOR (Climate variability and El Niño Southern Oscillation: Impacts for natural coastal resources and management, contract No. 511071) and is CENSOR publication 269.

Tables and Figures

Table VII.1. Functional groups and representative species for the steady-state model of Sechura Bay in 1996. Species listed are not exhaustive (small benthos groups show the most important species, representing > 95% of biomass and/or species averaging >1 g m^2).

Functional group	Species
2. Macroalgae	*Caulerpa sp.* (99.4%), *Rhodymenia sp.* (0.6%)
4. Polychaetes	*Lumbrineris sp.*, *Magelona phyllisae*
5. Scallops	*Argopecten purpuratus*
6. Sea urchins	*Arbacia sp.* (98.3%), *Tetrapigus niger* (1.7%)
7. Herbivorous gastropods	*Aplysia sp.* (51.2%), *Littorina sp.* (21.3%), *Scurria sp.* (10.7%), *Astraea buschii* (8.4%), *Tegula atra* (5.0%), *Tegula verrucosa* (1.1%), *Chiton sp.* (0.6%), *Tegula sp.* (0.6%), *Anachis sp.* (0.5%), *Mitrella sp.* (0.3%), *Columbella sp.* (0.2%)
8. Benthic detrivores	Clypeasteroida (35.8%), *Pagurus sp.* (21.5%), *Cycloxanthops sp.* (18.9%), *Brandtothuria sp.* (7.7%), *Turritella broderipiana* (4.7%), *Ophiuroidea* (3.5%), *Majidae* (3.3%), *Eurypanopeus sp.* (1.7%), *Dissodactylus sp.* (1.2%), *Litopenaeus sp.*, *Farfantepenaeus californiensis*, *Penaeus sp.*
9. Misc. filter feeders	*Actinia sp.* (61.6%), *Tagelus sp.* (26.7%), *Chione sp.* (5.8%), *Halodakra subtrigona* (3.4%), *Glycimeris sp.* (2.2%), *Terebra purdyae* (0.3%)
10. Predatory gastropods	*Sinum cymba* (45.8%), *Thais chocolata* (26.2%), *Bursa sp.* (9.6%), Priene (7.8%), *Thais kiosquiformis* (3.7%), *Hexaplex brassica* (3.5%), *Thais haemastoma* (1.6%), *Bursa ventricosa* (1.3%), *Bursa nana* (0.5%)
11. Small carnivores	*Crassilabrum sp.* (54.4%), *Polinices uber* (26.4%), Solenosteria fusiformes (8.9%), *Triumphis distorta* (5.5%), *Natica unifasciata* (1.4%), *Nassarius sp.* (1.2%), *Prunum sp.* (1.1%), *Oliva sp.* (1.0%)
12. Predatory crabs	*Cancer porteri* (94.2%), *Callinectes arcuatus* (4.2%), *Callinectes toxotes* (1.6%)
13. Sea stars	*Luidia magallanica*
14. Octopods	*Octopus mimus*
15. Littoral fish	*Cynoscion analis* (58.3%), *Sciaena deliciosa* (10.4%), *Peprilus medius* (6.4%), *Stellifer minor* (6.4%), *Paralabrax humeralis* (5.3%), *Paralonchurus peruanus* (4.2%), *Anisotremus scapularis* (2.9%), *Isacia conceptionis* (2.8%), *Labrisomus philippii* (1.0%), *Gerres cinereus* (0.8%), *Cheilodactylus variegatus* (0.6%), *Larimus sp.* (0.5%), *Calamus brachysomus* (0.4%)
16. Small pelagic fish	*Engraulis ringens* (87.8%), *Anchoa nasus* (11.3%), *Mugil cephalus* (0.6%), *Sardinops sagax sagax* (0.3%), *Odontesthes regia regia* (0.1%)
17. Pelagic predatory fish	*Mustelus sp.*,*Triakis sp.* (92.4%), *Scomber japonicus* (5.9%), *Mustelus whitneyi* (1.7%)
18. Marine mammals	*Otaria byronia*, *Arctocephalus australis*
19. Sea birds	*Leucocarbo bougainvillii*, *Sula variegata*, *Pelecanus thagus*
20. Cephalopods	*Loligo gahi*, *Dosidicus gigas*

Table VII.2. Sources of input data for the steady-state model of Sechura Bay in 1996

Functional group / parameter	B_i (t km^{-2})	P_i/B_i (y^{-1})	Q_i/B_i (y^{-1})	GE_i	EE_i	Y_i (t km^{-2} y^{-1})	DC
1. Phytoplankton	Converted chl a estimates from SeaWifs (Feldman and McClain, 2007)	GU based on modified Eppley curve (Eppley, 1972; Brush et al., 2002)	-	-	EO	-	-
2. Macroalgae	IE	GU based on Macchiavello et al. (1987)	-	-	EO	-	-
3. Zooplankton	IMARPE cruise averages 1995-1999 for the area 5°-6°S and within 82°W	GU based on Mendoza (1993), Hutchings et al. (1995)	GU adapted from Polovina and Ow (1985)	EO	GE	-	GU
4. Polychaetes	IE	GU based on Martin and Grémare (1997)	EO	GU	EO	-	GU
5. Scallops	IE	Mendo et al. (1987), Stotz and Gonzalez (1997)	Wolff (1994)	EO	EO	IS	GU based on Rouillon (2002)
6. Sea urchins	IE	EM	EO	GU	EO	-	GU
7. Herbivorous gastropods	IE	EM	EO	GU 0.3 based on Mann (1982)	EO	-	GU
8. Benthic detrivores	IE	EM	EO	GU	EO	IS	GU
9. Misc. filter feeders	IE	GU based on Wolff (1994)	EO	GU	EO	IS	GU
10. Predatory gastropods	IE	EO	GE based on Huebner and Edwards (1981)	GU 0,3 based on Huebner and Edwards (1981)	EO	IS	GU, IC
11. Small carnivores	IE	EM	EO	GU	EO	IS	GU partially based on Keen (1972) for gastropod spp., IC
12. Predatory crabs	IE	Wolff and Soto (1992)	Lang (2000), Wolff and Soto (1992)	EO	EO	-	GU based on Leon and Stotz (2004), IC
13. Sea stars	IE	Ortiz and Wolff (2002a)	EO	GU	EO	-	GU, IC
14. Octopods	GU based on catch data	EO	Wolf and Perez (1992), Vega and Mendo (2002)	Wolf and Perez (1992), Vega and Mendo (2002)	EO	IS	Cortez et al. (1999), IC
15. Littoral fish	GU based on catch data	GU 1,2 based on Wolff (1994)	EO	GU	EO	IS	GU based on FISHBASE (2006)
16. Small pelagic fish	GU based on catch data	GU	EO	GU 0,1 based on Moloney (2005)	GU	IS	GU based on FISHBASE (2006)
17. Pelagic predatory fish	GU based on catch data	GU 0,85 based on Jarre et al. (1991)	EO	GU 0,1 based on Moloney (2005)	EO	IS	GU based on FISHBASE (2006)
18. Marine mammals	GU	GU based on Jarre et al. (1991)	EO	GU	EO	-	GU
19. Sea birds	GU	GU based on Moloney (2005)	EO	GU based on Moloney (2005)	EO	-	GU
20. Cephalopods	GU based on catch data	Z derived from VPA (IMARPE) (Argüelles, pers. comm.) for *Loligo gahi*	EO	(Neira and Arancibia, 2004)	EO	**IS**	**(Cardoso et al., 1998; Villegas, 2001)**
21. Detritus	EO	-	-	-	-	**-**	**-**

Abbreviations: GC = gut content, IE = IMARPE benthic macrofauna evaluation, EM = empirical model (Brey, 2001), EO = Ecopath output, GU = guess estimate, IC = iterative consumption routine (described herein), IS = IMARPE landings statistics

Table VII.3. Input-output parameters for the steady-state model of Sechura Bay in 1996 after application of the Ecoranger resampling routine. Ecopath calculated parameters in **bold**.

Functional group / parameter	Trophic Level	B_i (t km^{-2})	P_i / B_i (y^{-1})	Q_i / B_i (y^{-1})	EE_i	GE_i	UA_i/Q_i	P/R	R/A	Catch (y^{-1})	F_i	$M0_i$	$M2_i$
1. Phytoplankton	**1.00**	21.335	343.886	-	**0.685**	-	-	-	-	-	-	**108.454**	**235.432**
2. Macroalgae	**1.00**	284.607	16.092	-	**0.042**	-	-	-	-	-	-	**15.412**	**0.680**
3. Zooplankton	**2.18**	27.874	40.059	157.883	**0.780**	**0.254**	0.20	**0.464**	**0.683**	-	-	**8.813**	**31.246**
4. Polychates	**2.06**	45.897	1.091	**4.474**	**0.825**	0.244	0.20	**0.438**	**0.695**	-	-	**0.191**	**0.900**
5. Scallops	**2.00**	23.689	1.364	10.556	**0.884**	**0.129**	0.20	**0.193**	**0.838**	2.340	**0.099**	**0.158**	**1.108**
6. Sea urchins	**2.11**	22.798	0.597	**2.786**	**0.666**	0.214	0.20	**0.366**	**0.732**	-	-	**0.199**	**0.398**
7. Herbivorous gastropods	**2.00**	25.258	1.235	**4.116**	**0.665**	0.300	0.20	**0.600**	**0.625**	-	-	**0.414**	**0.821**
8. Benthic detritivores	**2.00**	36.795	1.302	**6.806**	**0.910**	0.191	0.20	**0.314**	**0.761**	0.144	**0.004**	**0.117**	**1.181**
9. Misc. filter feeders	**2.24**	22.064	1.094	**5.044**	**0.736**	0.217	0.20	**0.372**	**0.729**	0.001	-	**0.289**	**0.805**
10. Predatory gastropods	**3.07**	37.297	**1.511**	3.881	**0.747**	0.389	0.20	**0.948**	**0.513**	0.379	**0.010**	**0.383**	**1.118**
11. Small carnivores	**2.87**	14.669	0.537	**2.677**	**0.673**	0.201	0.20	**0.335**	**0.749**	0.001	-	**0.176**	**0.361**
12. Predatory crabs	**3.20**	7.379	2.002	8.703	**0.684**	**0.230**	0.20	**0.404**	**0.712**	-	-	**0.633**	**1.369**
13. Sea stars	**3.15**	1.033	0.731	**3.670**	**0.741**	0.199	0.20	**0.332**	**0.751**	-	-	**0.189**	**0.542**
14. Octopods	**3.74**	0.015	4.911	**12.799**	**0.899**	0.384	0.20	**0.922**	**0.520**	0.033	**2.247**	**0.496**	**2.168**
15. Littoral fish	**2.81**	2.613	1.195	**14.300**	**0.694**	0.084	0.20	**0.117**	**0.896**	1.795	**0.687**	**0.366**	**0.142**
16. Small pelagic fish	**2.12**	82.134	1.727	**18.706**	**0.639**	0.092	0.35	**0.166**	**0.858**	81.409	**0.991**	**0.623**	**0.113**
17. Pelagic predatory fish	**3.15**	1.161	0.869	**8.123**	**0.464**	0.107	0.30	**0.181**	**0.847**	0.425	**0.367**	**0.466**	**0.037**
18. Marine mammals	**3.34**	0.019	0.103	46.179	**0.000**	**0.002**	0.20	**0.003**	**0.997**	-	-	**0.103**	**0.000**
19. Sea birds	**3.19**	0.020	0.037	60.156	**0.000**	**0.001**	0.26	**0.001**	**0.999**	-	-	**0.037**	**0.000**
20. Cephalopods	**3.14**	0.371	4.249	**11.125**	**0.522**	0.382	0.20	**0.477**	**1.001**	0.822	**2.218**	**2.031**	**0.000**
21. Detritus	**1.00**	-	-	-	**0.105**	-	-	-	-	-	-	**0.000**	**0.000**

B = biomass, P_i / B_i = production rate, Q_i / B_i = consumption rate, EE_i = ecotrophic efficiency, GE_i = conversion efficiency, UA_i/Q_i = unassimilated portion of consumption, P/R = production/respiration ratio, R/A = respiration/assimilation ratio, F_i = fishing mortality, $M0_i$ = non-predatory natural mortality, $M2_i$ = predation mortality

Table VII.4. Diet matrix for the steady-state model of Sechura Bay in 1996 after application of the Ecoranger resampling routine.

Prey \ Predator	3	4	5	6	7	8	9	10	11	12	13	14	15	16	17	18	19	20
1. Phytoplankton	0.764	0.327	0.788				0.701							0.901				
2. Macroalgae				0.800	0.808	0.198							0.259					
3. Zooplankton	0.149	0.052					0.197		0.000				0.502	0.099	0.483			0.300
4. Polychates				0.102				0.108	0.125	0.097	0.103		0.189					
5. Scallops								0.098	0.105	0.085	0.106	0.109						
6. Sea urchins									0.206		0.173							
7. Herbivorous gastropods								0.083	0.073	0.079	0.090	0.092						
8. Benthic detritivores								0.171	0.178	0.157	0.174	0.171	0.003					
9. Misc. filter feeders								0.070	0.084	0.061	0.078	0.084						
10. Predatory gastropods								0.235		0.140	0.153	0.168	0.001					
11. Small carnivores								0.021	0.023	0.018	0.022	0.025	0.000					
12. Predatory crabs										0.159		0.176	0.001					
13. Sea stars										0.008			0.000					
14. Octopods												0.175						
15. Littoral fish													0.001			0.252	0.105	
16. Small pelagic fish													0.001		0.517	0.699	0.895	0.700
17. Pelagic predatory fish																0.048		
18. Marine mammals																		
19. Sea birds																		
20. Cephalopods																		
21. Detritus	0.087	0.622	0.212	0.097	0.192	0.802	0.101	0.215	0.206	0.196	0.099		0.043					

Table VII.5. Pedigree index values assigned to model parameters for the steady-state model of Sechura Bay in 1996. Biomass (B), production (P), consumption (Q), diet and catch (C). Lower pedigree index values correspond to guesstimates or other models, while higher pedigree index values correspond to high precision estimates locally based. Pedigree = 0.462 (t*=2.21).

Functional group	B	P/B	Q/B	Diet	C
Phytoplankton	0	0.2			
Macroalgae	1	0.6			
Zooplankton	0	0.6	0.1	0	
Polychates	1	0.5	0	0	
Scallops	1	1	1	0.7	1
Sea urchins	1	0.5	0	0	
Herbivorous gastropods	1	0.5	0	0	
Benthic detrivores	1	0.5	0	0	1
Misc. filter feeders	1	0.5	0	0	1
Predatory gastropods	1	0.5	0	0	1
Small carnivores	1	0.5	0	0	
Predatory crabs	1	1	1	1	
Sea stars	1	0.5	0	0	
Octopods	1	1	1	0.2	1
Littoral fish	0.4	0.1	0	0.2	1
Small pelagic fish	0	0.1	0	0.2	1
Pelagic predatory fish	0.4	0.1	0	0.2	1
Marine mammels	0	0.2	0.2	0.2	
Sea birds	0	0.2	0.2	0.2	
Cephalopods	0.4	1	0.6	0.5	

Table VII.6. System statistics and flow indices for the steady-state model of Sechura Bay in 1996.

Summary Statistics	**Sechura Bay - 1996**
Sum of all consumption (t km^{-2} yr^{-1})	7227 (26%)
Sum of all exports (t km^{-2} yr^{-1})	7908 (28%)
Sum of all respiratory flows (t km^{-2} yr^{-1})	4008 (14%)
Sum of all flows into detritus (t km^{-2} yr^{-1})	8676 (31%)
Total system throughput (t km^{-2} yr^{-1})	27820
Fishing	
Total catches (t km^{-2} yr^{-1})	87.349
Mean trophic level of the catch	2.15
Gross efficiency (catch/net PP)	0.007
PP required / catch.	15.66
PP required / Total PP (%)	6.64
Community energetics	
Total primary production / total respiration	2.973
Total primary production / total biomass	18.137
Total biomass / total throughput	0.024

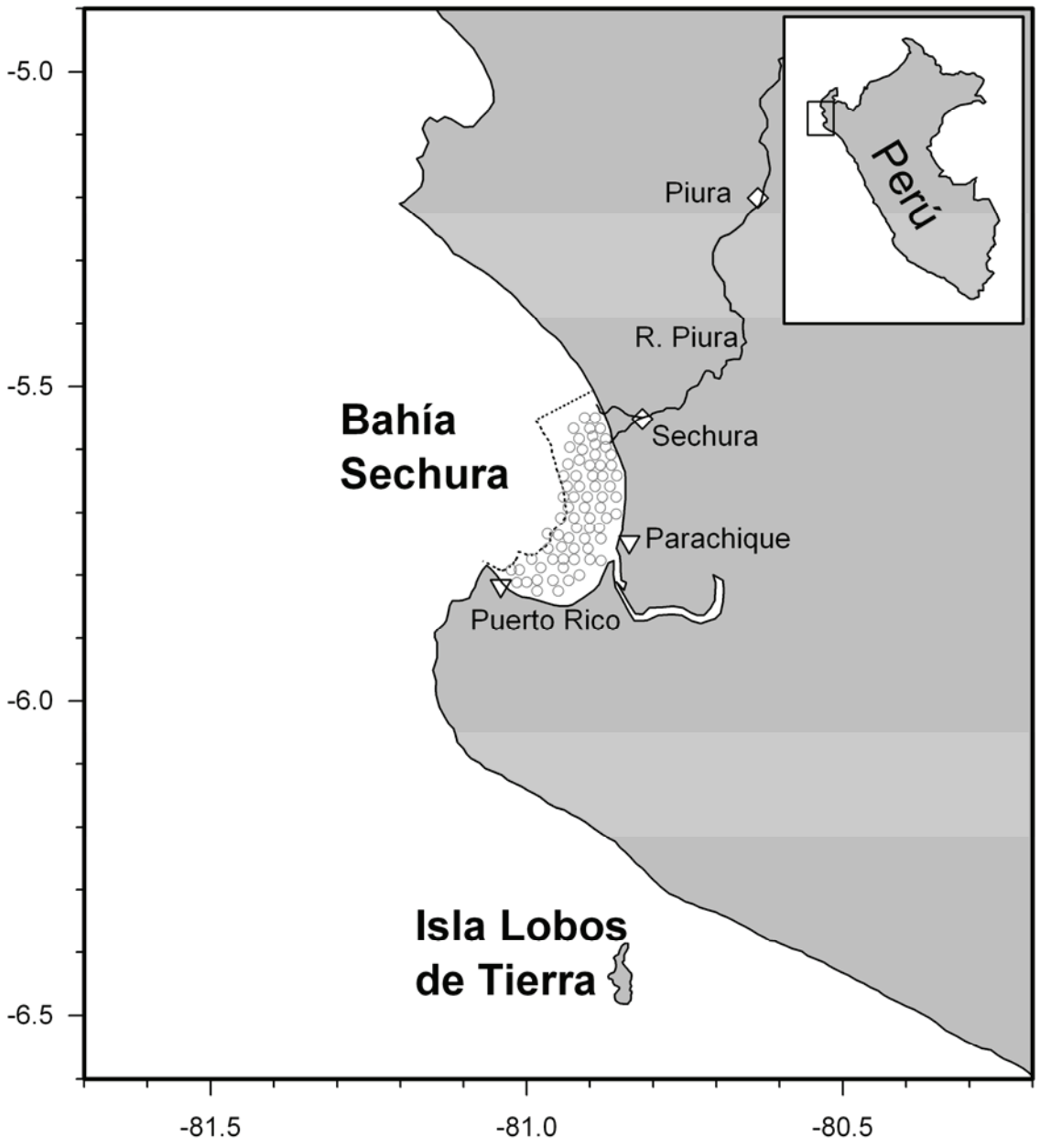

Figure VII.1. Map of Sechura Bay. Macrobenthic fauna sampling stations from September 1996 are indicated by gray circles (n = 71). The area considered in the trophic model is from the mouth of the River Piura southward and extending offshore to the 30 m depth isocline (indicated by the dashed line). Main cities (diamonds) and ports (triangles) are shown.

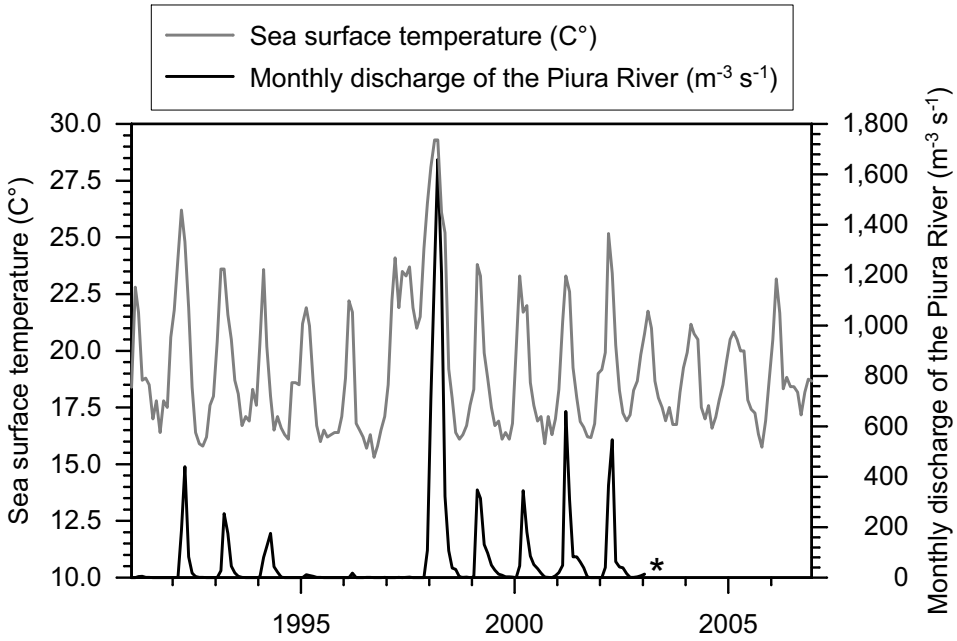

Figure VII.2. Monthly averages of sea surface temperature (C°) of Sechura Bay and discharge of the Piura river (as measured at the Piura bridge; * series ends in 2003).

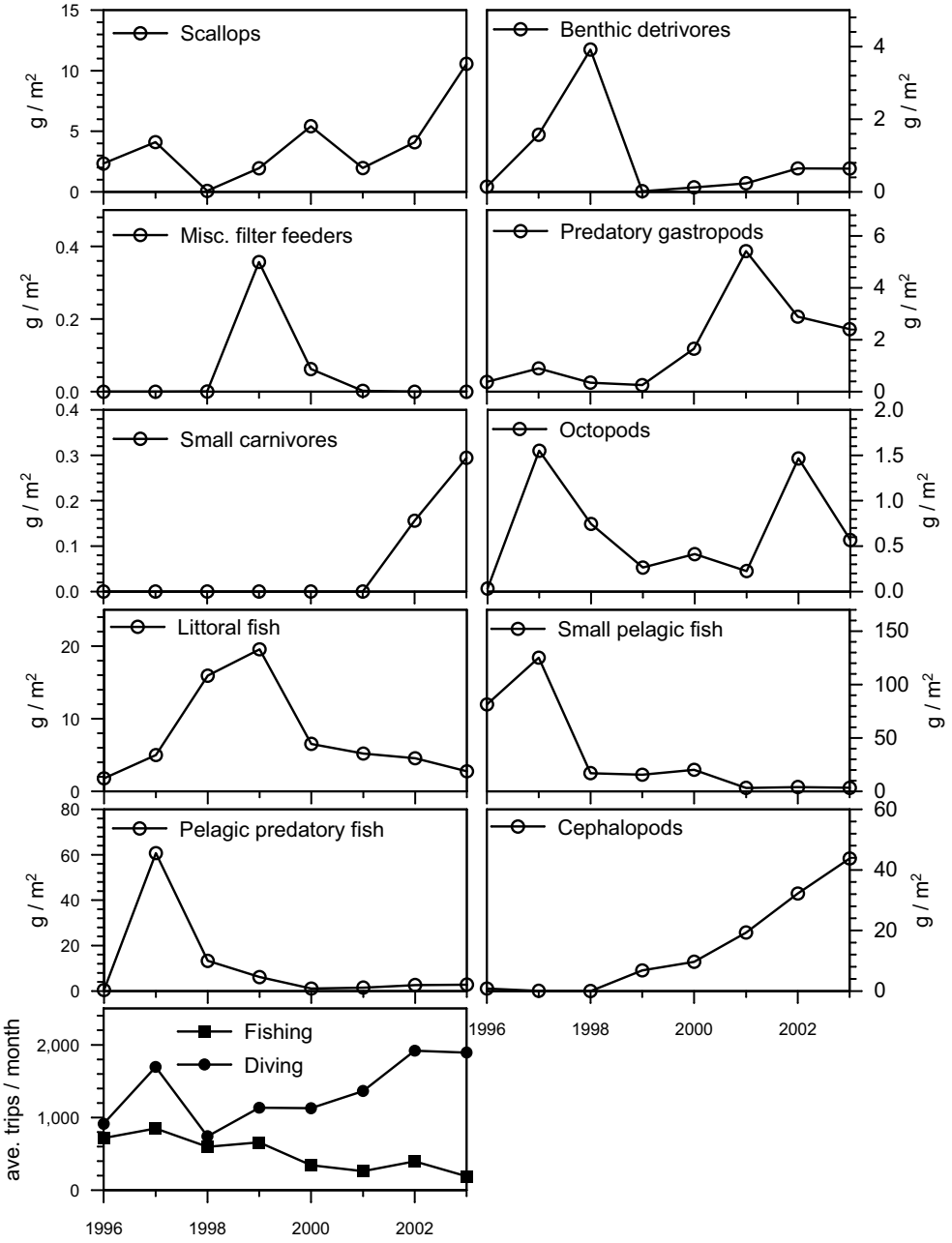

Figure VII.3. Yearly captures from Sechura Bay by functional group as used for fitting the simulations from 1996-2003. Landings data provided by IMARPE were converted to the same unit values as the model ($g \cdot m^{-2} \cdot y^{-1}$) through division by the model area (400 km^2). Bottom graph shows yearly average fishing effort for the two fleets, *Fishing* and *Diving* (effort units = average $trips \cdot month^{-1}$).

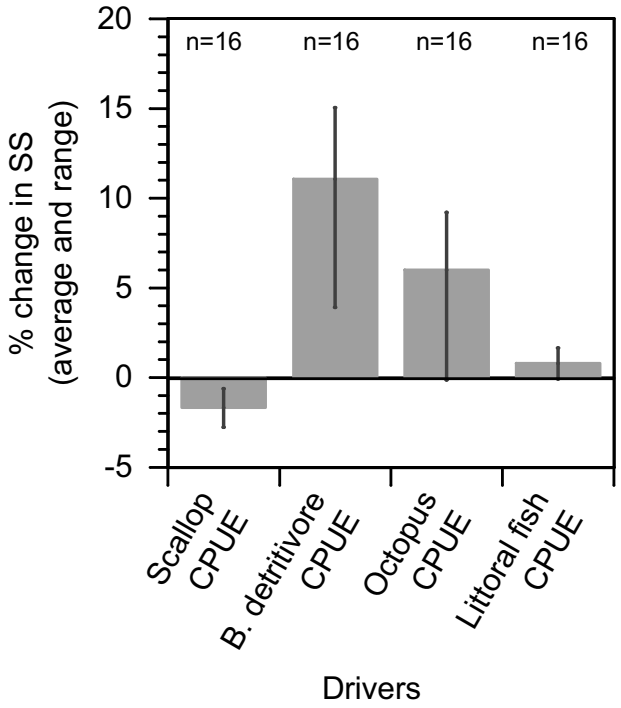

Figure VII.4. Percent changes to sum of squares, SS, of the 1996-2003 simulation after the forcing of relative biomass (CPUE) changes of several functional groups 'drivers'. Average change (bar) and range (line) are displayed. Drivers were applied in all possible sequences and combinations and *SS* was corrected for artificial improvements caused by the fitting of the driver's dynamics. Negative values (i.e. decrease in *SS*) indicate an improvement in fit.

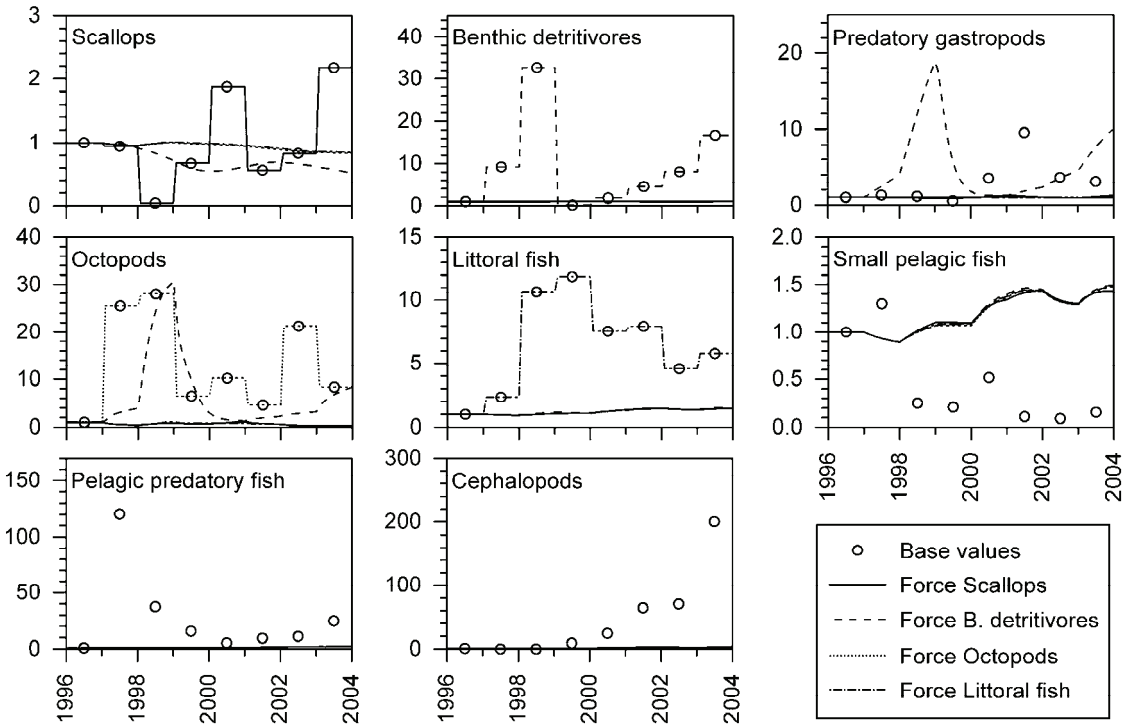

Figure VII.5. Simulated versus observed (catch per unit effort) relative biomass changes. All simulations consider changes in fishing effort (fishing and diving). Simulation trajectories are shown for each of the four 'drivers' (*Scallops*, *Benthic detritivores*, *Octopods*, *Littoral fish*) as applied individually.

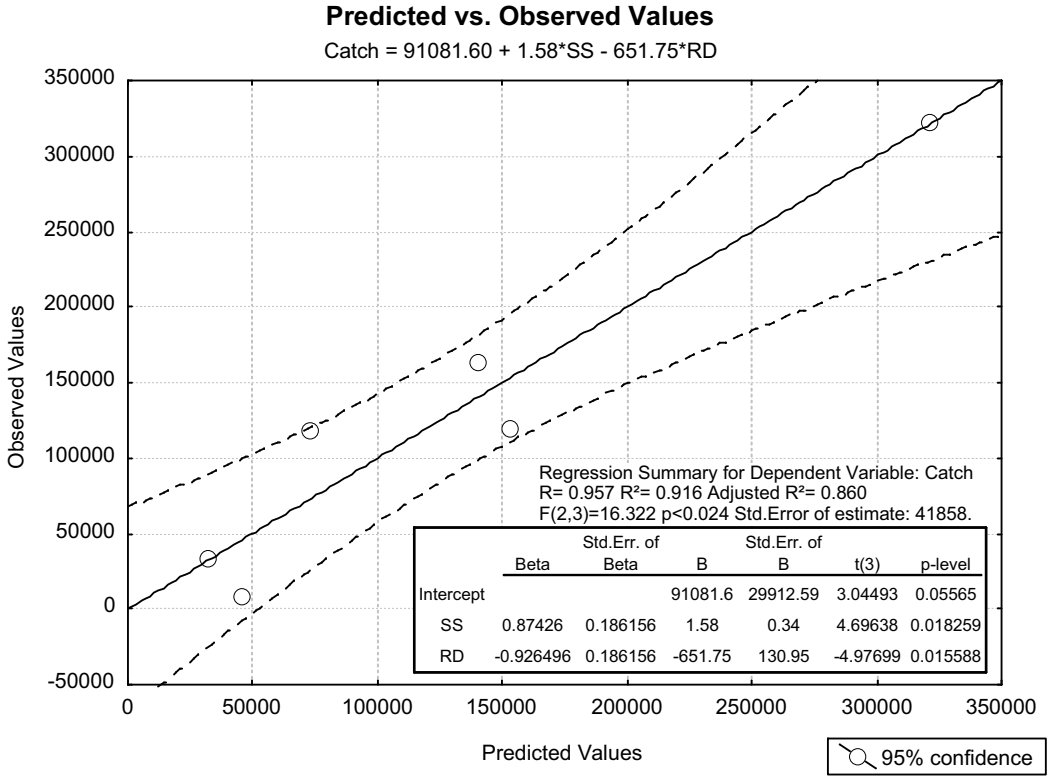

Figure VII.6. Predicted vs. observed values of annual catches (kg; ave mo. catch Sep-Aug) for the scallop Argopecten purpuratus as calculated by the multiple regression analysis. Independent variables include: *Spawning stock* (SS) (kg; average monthly catch of previous Jan-Jun) and *River discharge* (RD) ($m^3 \cdot s^{-1}$; Sep-Aug).

Chapter VIII. General Discussion

Resource dynamics of the NHCE are, without a doubt, strongly influenced by environmental variability. The most visible changes are associated with the occurrence of strong El Niño events – e.g. mass mortalities of seabirds and sealions, the occurrence of immigrant tropical fish species in catches, huge scallop population increases, etc. Additionally, trophic connections and human impacts from fishing create a complex mix of responses, making prediction difficult. The present thesis has applied a broader, quantified approach to viewing these dynamics on an ecosystem level. We find that, under normal upwelling, the high primary production of the nearshore coastal subsystem is inefficiently used due to the associated low oxygen conditions of the benthic environment. Environmental factors dominate over trophic interactions in the dynamics of its benthic resources. On the other hand, the more mobile resources of the larger coastal upwelling subsystem show stronger trophic interactions and the impacts of the associated fishery are also more important to its dynamics. The NHCE largely maintains its energy flow structure during strong El Niño events and even increases its efficiency through improved used of the (reduced) primary production. Nevertheless, slower-responding higher trophic levels, which include most relevant fishery resources, are most impacted.

The following discussion further elaborates on these findings. It is broken into sections comparing NHCE functioning across subsystems, including their respective responces to ENSO-related variability. Following, is a discussion on the capabilities and limitations of the Ecopath with Ecosim approach, through use of examples presented in the thesis. Finally, I discuss the future prospectives for this approach towards the realization of predictive models for use in management scenarios.

The subsystems of the NHCE

The nearshore benthic and coastal upwelling subsystems of the NHCE differ significantly in their flow characteristics during normal upwelling periods. Both systems have a high total throughput due to the elevated primary production, but the nearshore system appears limited in its ability to make efficient use of this production, likely due to the metabolic constraints of low oxygen concentration for consumers. As a result, both Independence and Sechura Bays have PP/R rates close to 3.0 indicating high autotrophy

while the larger coastal upwelling system is closer to 1.0, indicating closer to full utilization of produced energy with a smaller proportion of exports.

The larger coastal upwelling subsystem model includes a mix of the main upwelling center and offshore oceanic waters. With an outer boundary of 110 km, we include a significant proportion of heterotrophic (i.e. "destructive") waters where primary production is low and heterotrophic consumption is dominant (see Shushkina et al., 1978) (Fig. VIII.1). Previous Ecopath models of the coastal upwelling system were defined by about half the offshore extension as our model (Jarre et al., 1991; Jarre-Teichmann, 1992) and thus focused on the more productive nearshore habitat where higher PP/R ratios exist. Our models estimate that over 80% of detritus is recycled and only 3.1-3.6 % of flows are exported. This value compares to values of particulate organic carbon (POC) fluxes in offshore waters in the Southern Humboldt (Coquimbo, Chile; 30°S), where an estimated 3.5% of carbon produced in the photic zone reaches a depth of 300m (González et al., 1998; González et al., 2004b). This high level of efficiency may be attributable to a stable thermocline allowing for the development of rich plankton communities. Nutrients are also recycled in a conveyor belt fashion with upwelling at the coast bringing nutrient rich waters to the surface where phytoplankton communities can develop. These waters are moved offshore through Ekman transport and lagging zooplankton blooms are typically found further offshore (Ayón, pers. comm.). Shushkina et al. (1978) observed that phytoplankton biomass maintains high levels near the edge of the Peruvian shelf (sampling done ~7°30'S; ~90 km offshore); however, productivities are much lower, possibly due to diminished nutrient availability. In this frontal zone, huge numbers of meso- and macroplankton were found (predominantly euphausiid – *Euphausia macronata*, whose biomass reached 750 $g \cdot m^{-2}$, and in the layers of maximum accumulations up to 27 $g \cdot m^{-3}$), which acted as a "living filter" of the passing phytoplankton. Intense grazing activity by meso- and macrozooplankton has been shown as an important mechanism for vertical fluxes of POC through fecal pellet sedimentation, although a significant amount of this material is further utilized by cyclopoid copepods before reaching deeper layers (Gonzalez et al., 2000). The accumulation of zooplankton at the front also becomes a major feeding ground for whales, squid, and fishes (Shushkina et al., 1978), forming another important cross-shelf connection for higher trophic levels in our model. For example, the simulations of **Chapter IV** showed that the migration or expansion of jumbo squid after the strong EN of 1997/98 may have affected both offshore competitors, such as the mackerel species, and coastal species, such as juvenile hake, through increased predation. Eventually, the unutilized POC will settle to the lower layers whereby bacterial processes can continue to break down the organic material and enrich

the lower water layers. The end result is a high utilization of production within the shelf region encompassed by our larger coastal pelagic model.

The nearshore benthic subsystem is highly productive yet is unable to make full use of all primary production. As a result, large accumulations of detrital material are observed in the benthic environment, resulting in oxygen depletion below the mixed layer (~30m). Above this depth, benthic faunal biomass is much higher (10-30 fold). Nevertheless, even in shallower waters the benthic faunal biomass is likely limited by low oxygen concentrations rather than food levels. Being located in the heart of the upwelling cell may also limit the development of later succession stages of the zooplankton community which are principal consumers of primary production further offshore. Therefore, the status of upwelling systems as being inefficient appears to be dependant on the scale addressed. Finally, it must be reiterated that our models do not include bacterial activity. If included in the future, we expect actual PP/R ratios to be even lower (Christensen and Pauly, 1993a), however the general tendencies in efficiency are likely to be the same among subsystems.

The effect of ENSO on energy flow structure

Differences in spatial scale also affect the response of ENSO related variability on energy flow structure. Intra-system comparisons of steady-state models revealed responses for the nearshore benthic (Independencia Bay, **Chapter VI**) and the coastal upwelling (**Chapter III**) subsystems of the NHCE independently, which are compared in the following section.

During EN, both subsystems decrease substantially in "size", or total flows, due primarily to bottom-up decreases in primary production. They both show lower system organization of flows (relative ascendancy, A/C) with cycling and connectedness most affected in upper trophic levels (predatory cycling index, PCI). This is also logical in that higher trophic levels generally have lower turnover rates and thus will respond more slowly to changes in the environment. Lower trophic levels are also represented by higher species richness, and may contain a higher degree of functional redundancy, allowing for faster adjustment to changing conditions and helping to maintain flow structure.

Both subsystems show improvements in overall efficiency during EN through decreased flows to detritus and exports, although this improvement was most dramatic in the nearshore benthic system (i.e. Independence bay). This improved efficiency is largely attributable to the increased biomass of *A. purpuratus* as an efficient consumer of detritus

and phytoplankton, allowing for a high degree of cycling between trophic levels 1 and 2. Whether or not the same improved efficiency would occur in areas with little or no *A. purpuratus* recruitment is difficult to say definitively; however, it seems likely for areas where improved oxygen concentrations allow for enhanced utilization of accumulated detritus.

Both subsystems handle the overall perturbation of even strong EN events quite well. The effect of decreased primary production during strong EN events appears to be rather short-term (3-4 years). Interestingly, this is the same average periodicity of EN events, and may signal some adaptedness of the species. The frequency and strength of variability also appears important for trophic flow structure; specifically, mean transfer efficiency (TE) during upwelling periods is positively correlated with latitude in three bay models along the western coast of South America – Sechura (6°S, TE=6.6%), Independence (16°S, TE=9.6%), and Tongoy (30°S, TE=11.4%; model by Ortiz and Wolff, 2002a). Since the lower latitudes experience higher interannual SST, they may be more frequently "reset" by ENSO variability, thus preventing higher efficiency and development.

Exploration of trophic controls revealed a dominance of bottom-up or intermediate configurations. The spatial scale of the coastal upwelling model may have played a role in some interactions – for example, small pelagic fish may top-down control zooplankton on smaller scales. The smaller scale of the nearshore benthic system was also dominated by bottom-up or intermediate controls with a few top-down configurations between primary consumers and their benthic predators. In both subsystems, EN appears to have impacted higher predatory groups disproportionately as observed through decreased cycling at higher trophic levels and, possibly, their ability to induce top-down effects. This is consistent with previous findings for systems characterized by high environmental forcing (bottom-up control), whereby predation effects may not increase spatial and temporal variability of the prey species over that which is already controlled by the residual variability of the environment (Benedetti-Cecchi, 2000).

Finally, benefits to the fishery from EN are mixed among the three areas modeled. The nearshore benthic resources of Independence Bay and Sechura Bay were highly impacted by direct environmental changes associated with EN. In Independence Bay, EN causes elevated temperature and oxygen, and immigrations of valuable offshore and equatorial fish species occur. Large increases in valuable benthic resources, e.g. scallops and octopus, improved the economic conditions of the fishers. In contrast, Sechura Bay is highly affected by increased riverine input during EN, which appears to increase mortality in scallop population. The larger coastal upwelling subsystem experienced record catches of anchovy during the initial stage of the strong EN of 1997/98 due to the concentration of the stocks; however as the EN developed, bottom-up reductions in primary production

affected most trophic levels, including valuable anchovy and hake populations. Overall, the more industrialized fisheries that target anchovy and hake appear to influence long-tern dynamics, whereas changes in artisanal fishery effort tend to be more driven by resource dynamics than the other way around.

Assessment of the EwE approach

An "ecosystem approach to fisheries" (EAF; Garcia et al., 2003) is becoming increasingly supported as a necessary shift in fisheries management. Ecopath with Ecosim (EwE) represents one of many models in a growing list, yet it is undisputedly the most widely used multispecies model in the world. This is due to its ease of operation and use of parameters that are more readily available to fishery scientists and has permitted its use by a wide range of users within academia to marine resource managers as a way to understand the functioning of ecosystems through comparison and exploration. Nevertheless, it is by no means an easy task to construct a model with meaningful outputs and users will likely need to have a sound understanding of the modeled ecosystem and ecosystem functioning in general to gain from such an exercise. Arriving to a model that is useful for predictive scenarios management is usually a long-term and ongoing process. The three main routines of the program are suggested to be used in sequence; beginning with the steady-state modeling of Ecopath, followed by the testing and tuning – through vulnerability settings and mediation functions – of the model to historical time series in Ecosim and, finally, spatial explorations in Ecospace.

Applicability and keys to successful use

The use of EwE appears to be more in line with practical management now than it has in the past. Initial explorations in Ecopath – before the development of the dynamic components of Ecosim and Ecospace – were largely focusing on comparisons of ecosystems and understanding the differences between systems. One of the first syntheses of a wide range of models came in the form of a book edited by Christensen and Pauly (1993b) in which several models were compared using the, at the time, newly-created and greatly improved Ecopath II software. Specifically, their final chapter summarized trends of several statistics of growth and development across different types of ecosystems (Christensen and Pauly, 1993a). With the development of dynamic simulations like Ecosim, such comparisons are less often conducted. In the words of one of our anonymous reviewers, "…comparison of [steady-state models], in absence of

dynamics and comparison with time series, can lead to spurious results and a false sense of security. This is why this way of doing things has been abandoned and that the use of Ecosim and time series is considered more adequate". While we acknowledge this point, and have thus done the additional Ecosim explorations needed for understanding dynamics, the comparison of two steady-state models of similar structure (**Chapters III and VI**) has allowed an initial understanding of the impact of ENSO from a holistic perspective and appears to have served the objectives of this thesis well. The ability of EwE to conduct both whole ecosystem analysis as well as dynamic simulations in fact sets the EwE apart from "Minimum Realistic Models" that restrict construction to include only those species most likely to have important interactions with the species of interest (Plagányi, 2007).

In 2002, the International Whaling Commission (IWC) conducted a workshop whose objective was to outline modeling approaches for exploring cetacean-fishery competition. One of the outcomes was a defined set of system characteristics that made for "easier" multispecies modeling. These included (IWC, 2004):

i) reasonable data availability
ii) relatively simple foodwebs
iii) strong species interactions
iv) relatively closed system boundaries
v) low (or obvious) environmental forcing

The larger coastal upwelling system appears to satisfy the first three points. It is a long-studied system with well documented data sets on the pelagic resources. Upwelling systems are generally considered to contain both relatively simple foodwebs and strong species interactions; however, the single factor of strong environmental variability from ENSO likely disqualifies the NHCE as an easier system for modeling, and may also prevent the fulfillment of the fourth point concerning spatial boundaries. For example, reduced upwelling will not only decrease total primary production, but will also affect the spatial extension of different habitats and their associated biota. In the following sections we will discuss how these less than optimal aspects were dealt with, including insight into how future explorations may be improved.

Incorporating environmental factors

Plagány's (2007) review of multispecies models revealed a relatively wide range of models that are able to incorporate some degree of environmental effects. A majority of applications appear to be focusing on low-level dynamics, e.g. primary production dynamics mediated by temperature, currents, wind, and nutrient forcing; however, higher level physical/biological processes are also possible with several models, e.g. temperature mediated growth, changes in carrying capacity, and oceanic transport.

In EwE, environmental factors are primarily incorporated through the use of forcing functions, which can be applied over annual or long-term scales. A rather straightforward example is to have a forcing function affecting either seasonal or long-term primary production rates; however, the forcing functions in EwE are quite flexible, and permit the user to apply them to specific interactions at higher trophic levels (e.g. by manipulation of foraging arena parameters).

Applications of forcing functions directly linked to environmental time series are rare in published EwE works to date, even for the more straightforward example of changing primary production. This is likely due to the fact that often no single environmental factor acts alone. Higher trophic level dynamics may be additionally affected by a mix of environmental and trophic (bottom-up and top-down) factors that complicate our ability to filter out the environmental component. Past works using EwE have dealt with this by either applying actual environmental time series as mediations to particular trophic groups (e.g. Field et al., 2006), or by using a "fit-to-time-series" routine to derive annually adjusted forcing functions, which must then be interpreted (i.e. to actual time series) (Shannon et al., submitted).

In the works of this thesis we have chosen to artificially force dynamics of those groups for which there was support for environmental mediation. While the form of the underlying mediation relationships between environmental and species group dynamics have been explored in some cases (e.g. exponential increase in larval survival to settlement with increasing temperature; Fig. V.4), we used this information only to support the artificial forcing of their dynamics. We built on previous work by Watters et al. (2003) in reconstructing phytoplankton changes using a combination of sea surface temperature anomalies and remote sensing estimates of chl *a*. Additionally, we forced the dynamics of several upper level groups to assess their importance as trophic drivers to other groups. Thus, the underlying processes of the environmental mediation have either been dealt with separately (e.g. for *Argopecten purpuratus* in **Chapters V and VII**), or not at all. Ultimately, mediation functions should be resolved based on the underlying mechanisms for organisms along the Pacific South American coast. At present, their dynamics are not

fully understood, and studies have been based on rather descriptive approaches (Thatje, 2008). As a first step, this novel approach has allowed us to use this descriptive data as a basis for exploration of trophic drivers.

Spatial considerations

One of the main findings of the thesis concerns the importance of system closure (of flows) for successful dynamic modeling. Our findings indicate that this may have partially contributed to the observed differences in reproducing dynamics between the three models. This aspect was considered in defining the coastal upwelling model and likely improved its performance in reproducing historical trends. We defined the boundaries of the coastal upwelling ecosystem with dynamics in mind and tried to encompass the system's offshore extension as defined by the productive zone of primary production, while the latitudinal extensions were chosen as limits in extension for the north-central Peruvian anchovy stock. Despite these careful considerations, the external forcing of mesopelagic fish immigration/expansion into the model area was important in overall dynamics. In the bay systems modeled, some degree of closure was assumed for many of the benthic resources. This assumption is even supported for broadcast spawner species such as the scallop *Argopecten purpuratus*, whereby the size of the spawning stock is a significant predictor of next year's catch (i.e. through recruitment) in both bay systems (**Chapters V and VII**). Nevertheless, the small size of the model does not encompass the dynamics of more mobile species, like fish. Specifically, the dynamics of transient or non-resident species groups (e.g. pelagic predatory fish, tropical fish immigrants) and species with closures of life history extending over larger areas (e.g. anchovy) are not well reproduced in the smaller bay models.

Data requirements

It is quite obvious that modeling success is directly related to reasonable data availability. The qualifier "reasonable" is the key, as it would be unrealistic to hope for detailed, locally-derived information for all input parameters. EwE is less data intensive than biogeochemical models but requires data that are difficult to obtain such as diet compositions and species abundance estimates (Plagányi, 2007). For our models, we have good data from standardized monitoring of biomass and fisheries-related data since 1996. Direct sampling of biomass was needed for estimating the starting biomass values of the steady state models. Dynamics appear to have been best reproduced for those

groups where data was more available through routine monitoring, or where the fishery is directly targeting the resource and thus gave confident estimates of relative biomass changes as calculated from CPUE. Additionally, the use of long and continuous time series is recommended for a more robust analysis. It is difficult to extend the time series backwards in time for our bay models due to a lack of information before the modeled period. The analysis of the dynamics in the coastal upwelling model, however, can benefit from much longer time series for some main target species of the industrial fishery. A major obstacle will be the reconstruction of biomass changes for groups previously assessed (e.g. squid, mesopelagics) for which interactions may be more important than previously realized.

A final note on the use of time series concerns the use of Virtual Population Analysis (VPA) derived estimates of fisheries mortality (F). Considering that the method assumes a constant level of natural mortality, the calculated changes in F may absorb some changes in natural mortality. This may become particularly problematic when assessing predator prey interactions through the tuning of vulnerability settings. For example, an increase in predation mortality would be attributed to the fishery and, as a consequence, the interaction may be fitted with a lower vulnerability than it should. This can be remedied by using only Multi-Species Virtual Population Analysis (MSVPA) estimated F values (Christensen, pers. comm.). However, these types of analysis are seldom used. In the NHCE, variable predation mortality for anchovy has been incorporated in a previous VPA using consumption estimates of several predators (guano birds, bonito, seals) (Pauly et al., 1987), and future simulations may benefit from actualizing these time series. Such considerations should be emphasized to users of EwE to better interpret possible shortcomings of the analysis.

Future prospects

The presented works should be viewed as initial explorations into the dynamics of the NHCS. They go beyond traditional single-species explorations by attempting to distinguish between fishery, trophic, and environmental factors as drivers of dynamics in the system. Due to data limitations, the meso-temporal scale proved to be the most practical for an initial exploration, yet it is important to continue with present monitoring efforts and (when possible) reconstruct past historical time series for a more robust analysis.

For the coastal benthic subsystem, annually conducted evaluations in the bays of Independence and Sechura will continue to improve the time series in these important areas of the artisanal fishery. Further monitoring of expanding aquaculture activities of *A. purpuratus* should be incorporated in future explorations as they have become important additional impacts to the ecosystem in the past years. One of the main assumptions of our bay models concerns the diet matrices used. The restriction of mass balance and the application of the Ecoranger routine allowed for acceptable values; however, these can be improved through local diet studies in the future. Finally, our results suggest that environmental factors may dominate the dynamics of many benthic organisms. More local studies concerning these influences are recommended and, in fact, several participants of the CENSOR project have either recently published or will soon publish data to shed light on these topics (Carre et al., 2005; Peña et al., 2005; Lazareth et al., 2006; Lazareth et al., 2007; Fischer and Thatje, submitted)

Data for the resources of the coastal upwelling system model were far richer, and catch statistics are available as far back as the 1950s when the industrial fishery began to expand. Biomass data is available in the form of acoustic estimates for the four main small pelagic species (anchovy, sardine, horse mackerel, and mackerel) from about 1983 onward. Longer time series exist for a few main target species as reconstructed from VPA or other analyses of population dynamics (e.g. anchovy, hake, sardine, and bonito). The collaborations organized between IMARPE, Deutsche Gesellschaft für Techniche Zusammenarbeit (GTZ), and the International Center for Living Aquatic Resources Management (ICLARM) catalyzed the reworking and synthesis of data presented in two main books (Pauly and Tsukayama, 1987a; Pauly et al., 1989). At present, there is a need to standardize the excellent time series data of these works with newly created data of the past ca. 20 years. This presented model construction has already been incorporated by IMARPE as a starting platform for future explorations; specifically, a planned workshop for March, 2008, "Modeling management strategies for hake in the Northern Humboldt Current Ecosystem", will attempt to reconcile these long term data sets for use in management scenarios. Exploration of different multi-species harvesting strategies will be assessed against criteria of ecological, social and economic goals (Cochrane, 2002). These explorations may also benefit from the inclusion of idealized ENSO variability (e.g. forced changes to phytoplankton) to identify strategies of adaptive management.

Tables and Figures

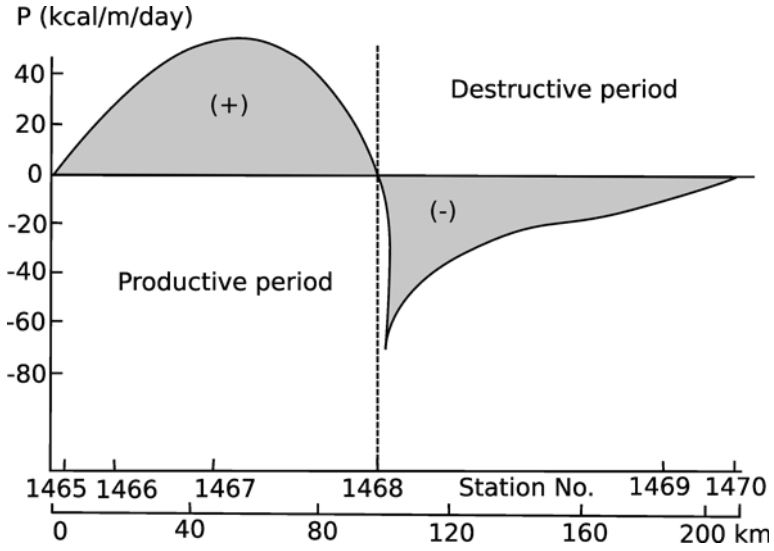

Figure VIII.1. Calculated plankton community net production along a transect crossing the Peruvian upwelling region (7°30'S) (modified from Shushkina et al., 1978).

References

Aguilar, P., 1999. Fórum El Fenómeno El Niño 1997-98: evolución, pronóstico y mitigación. Instituto del Mar del Perú, Lima.

Alamo, A., 1989. Stomach contents of anchoveta (Engraulis ringens), 1974-1982. In: Pauly, D., Muck, P., Mendo, J. ,Tsukayama, I. (Eds.), The Peruvian Upwelling Ecosystem: Dynamics and Interactions, Vol. 391. ICLARM, Manila, Philippines, pp. 105-108.

Alamo, A., Navarro, I., Espinoza, P., Zubiate, P., 1996a. Trophic relationships, alimentary spectrum and food ration of the main pelagic species during summer 1996. Informe. Instituto del Mar del Peru, Lima, Péru.

Alamo, A., Navarro, I., Espinoza, P., Zubiate, P., 1996b. Alimentary spectrum and food ration of Engraulis ringens and of Sardinops sagax sagax, and mortality of Peruvian anchoveta eggs by predation. Informe. Instituto del Mar del Peru, Lima (Peru).

Alamo, A., Espinoza, J., 1997a. Feeding spectrum of Peruvian hake during autumn 1997: Cruise RV Humboldt 9705-06, Callao to Puerto Pizarro. Informe. Instituto del Mar del Peru. Callao, 47-55.

Alamo, A., Espinoza, J., Zubiate, P., Navarro, I., 1997a. Feeding behaviour of the most important pelagic Peruvian resources during summer and early autumn 1997. Cruise 9702-04. Informe. Instituto del Mar del Peru, Callao.

Alamo, A., Espinoza, P., 1997b. Alimentary behaviour of Peruvian hake during winter 1996. Cruise RV SNP-1 9607-08. Informe. Instituto del Mar del Péru Lima, Péru.

Alamo, A., Espinoza, P., Zubiate, P., Navarro, I., 1997b. Alimentary behaviour of Peruvian anchovy Engraulis ringens during winter 1996. Cruise RV Humboldt 9608-09. Informe. Instituto del Mar del Péru, Lima, Péru.

Alamo, A., Espinoza, J., 1998. Alimentary variations in Engraulis ringens and other pelagic resources during 1997 winter-spring. Informe. Instituto del Mar del Peru. Callao, 45-52.

Alegre, A., Blaskovic, V., Castillo, R., Espinoza, P., Fernandez, F., Flores, R., Peraltilla, S., Tafur, R., Tam, J., Taylor, M., Yamashiro, C., 2005. Comportamiento alimentario del calamar gigante (*Dosidicus gigas*), enfatizando la depredacion ejercida sobre le merluza (*Merluccius gayi peruanus*). Instituto del Mar del Peru, Callao, Peru.

Alheit, J., Ñiquen, M., 2004. Regime shifts in the Humboldt Current ecosystem. Progress in Oceanography 60, 201-222.

Antezana, T., 2002a. Adaptive behavior of Euphausia mucronata in relation to the oxygen minimum layer of the Humboldt Current. In: Färber Lorda, J. (Ed.) Oceanography of the Eastern Pacific. CICESE, Ensenada, Mexico, pp. 29-40.

Antezana, T., 2002b. Vertical Distribution and Diel Migraion of Euphausia macronata in the Oxygen Minimum Layer of the Humboldt Current. In: Färber Lorda, J. (Ed.) Oceanography of the Eastern Pacific II. Editorial CICESE, pp. 13-28.

Arancibia, H., Neira, S., Christensen, V., Olson, R., Arreguín-Sanchez, F., Cubillos, L., Quinones, R., Gatica, C., Medina, M., 2003. Enfoque metodologico para el analysis ecosistemico en la administracion de pesquerias de la zona central de Chile. Concepcíon.

ARCH, 2006. ARCH Program Facility Core. Florida International University, University of Miami, Available from: http://www.rsmas.miami.edu/groups/niehs/arch/core.htm.

Argüelles, J., Tafur, R., Taipe, A., Villegas, P., Keyl, F., Dominguez, N., Salazar, M., in press. Changes in the population structure of jumbo flying squid *Dosidicus gigas* in Peruvian waters during 1989-2004. Progress in Oceanography.

Arias-González, J.E., Delesalle, B., Salvat, B., Galzin, R., 1997. Trophic functioning of the Tiahura reef sector, Moorea Island, French Polynesia. Coral Reefs 16, 231-246.

Arias Schreiber, M., 2003. Prey spectrum and feeding behaviour of two sympatric pinnipeds (*Arctocephalus australis* and *Otaria flavencens*) in relation to the 1997-98 ENSO in southern Peru. MSc., University of Bremen, Bremen, Germany, unpublished.

Arntz, W., Valdivia, E., 1985a. Visión integral del problema 'El Nino': introducción. In: Arntz, W., Landa, A. ,Tarazona, J. (Eds.), 'El Nino' y su impacto en la fauna marina. Instituto del Mar del Peru (special issue), Callao, Peru, pp. 91-101.

Arntz, W., Valdivia, E., 1985b. Incidencia del fenómeno 'El Nino' sobre los mariscos en el litoral peruano. In: Arntz, W., Landa, A. ,Tarazona, J. (Eds.), 'El Nino' y su impacto en la fauna marina. Instituto del Mar del Peru (special issue), Callao, Peru, pp. 91-101.

Arntz, W., Tarazona, J., 1990. Effects of El Niño on benthos, fish and fisheries off the South American Pacific coast. In: Glynn, P.W. (Ed.) Global ecological consequences of the 1982-83 El Niño-Southern Oscillation. Elsevier Oceanography Series, pp. 323-360.

Arntz, W.E., Valdivia, E., Zeballos, J., 1988. Impact of El Nino 1982-83 on the commercially exploited invertebrates (mariscos) of the Peruvian shore. Meeresforschung/Rep. Mar. Res. 32, 3-22.

Arntz, W.E., Fahrbach, E., 1991. El Nino-Klimaexperiment der Natur. Birkhaeuser Verlag, Basel (Switzerland).

Arntz, W.E., Tarazona, J., Gallardo, V.A., Flores , L.A., Salzwedel, H., 1991. Benthos communities in oxygen deficient shelf and upper slope areas of the Peruvian and Chilean Pacific coast, and changes caused by El Niño. Geological Society 58, 131-154.

Aronés, K., Ayón, P., Hirche, H.-J., Schwamborn, R., in press. Hydrographic structure and zooplankton abundance and diversity off Paita, northern Peru (1994 to 2004) - ENSO effects, trends and changes. Journal of Marine Systems.

Au, D.W., Smith, S.E., 1997. A demographic method with population density compensation for estimating productivity and yield per recruit of the leopard shark (Triakis semifasciata). Canadian Journal of Fisheries and Aquatic Sciences 54, 415-420.

Avaria, S., Muñoz, P., 1987. Effects of the 1982-1983 El Niño on the marine phytoplankton off northern Chile. Journal of Geophysical Research 92, 14369-14382.

Ayon Dejo, P., Arones Flores, K., 1997. Zooplankton and ichthyoplankton communities in front of Peruvian north-central coast. Cruise RV Humboldt 9705-06. Informe. Instituto del Mar del Peru. Callao, 70-79.

Ayon Dejo, P., Giron Gutierrez, M., 1997. Zooplankton and ichthyoplankton composition and distribution in front of the Peruvian coast during February to April 1997. Informe. Instituto del Mar del Peru. Callao, 49-55.

Ayón, P., Purca, S., Guevara-Carrasco, R., 2004. Zooplankton volume trends off Peru between 1964

and 2001. ICES Journal of Marine Science 61, 478-484.

Ayón, P., Swartzman, G., Bertrand, A., Gutierrez, M., Bertrand, S., in press. Relating the distribution and abundance of zooplankton in the Peruvian Humboldt Current System from 1983-2005 to environmental factors, including the proximity of major fish predators. Progress in Oceanography.

Baird, D., McGlade, J.M., Ulanowicz, R.E., 1991. The comparative ecology of six marine ecosystems. Philosophical Transactions: Biological Sciences 333, 15-29.

Baird, D., Luczkovich, J., Christian, R.R., 1998. Assessment of Spatial and Temporal Variability in Ecosystem Attributes of the St Marks National Wildlife Refuge, Apalachee Bay, Florida. Estuarine, Coastal and Shelf Science 47, 329-349.

Bakun, A., 1996. Patterns in the ocean. Ocean processes and marine population dynamics. University of California Sea Grant, California, USA, in cooperation with Centro de Investigaciones Biologicas de Noroeste, La Paz, Baja California Sur, Mexico.

Bakun, A., Broad, K., 2003. Environmental 'loopholes' and fish population dynamics: comparative pattern recognition with focus on El Nino effects in the Pacific. Fisheries Oceanography 12, 458-473.

Bakun, A., Weeks, S.J., 2006. The Marine Ecosystem off Peru: What are the secrets of its fishery productivity and what might its future hold? The Humboldt Current System: climate, ocean dynamics, ecosystem processes, and fisheries, Lima, Peru.

Bakun, A., Weeks, S.J., in press. The Marine Ecosystem off Peru: What are the secrets of its fishery productivity and what might its future hold? Progress in Oceanography.

Balech, E., 1988. Los Dinoflagelados del Atlantico Sudoccidental. Publicaciones Especiales Instituto Espanol de Oceanografia N 1, 310.

Ballón, M., Wosnitza-Mendo, C., Guevara-Carrasco, R., Bertrand, A., in press. Disentangling the relative effects of overfishing and environment on Peruvian hake Merluccius gayi peruanus biology and reproductive failure reveals a male affair. Progress in Oceanography.

Ballón, R.M., 2005. Comparative analysis of the community structure and trophic relations of the Peruvian hake Merluccius gayi peruanus and its by-catch of the years 1985 and 2001. Masters Thesis, University of Bremen, Bremen, Germany, unpublished.

Barber, R.T., Chavez, F.P., 1983. Biological consequences of El Nino. Science (Washington) 222, 1203-1210.

Barber, R.T., Chavez, F.P., Kogelschatz, J.E., 1985. Biological effects of El Nino. Bol. Erfen/Erfen Bull, 3-29.

Bello, R., Arias Schreiber, M., Sanchez, R., 1998. Distribution and relative abundance of Cetacea during the Cruise RV Humboldt 9709-10 from Matarani to Paita. Informe. Instituto del Mar del Peru. Callao, 78-85.

Benedetti-Cecchi, L., 2000. Variance in ecological consumer-resource interactions. Nature 407, 370-374.

Bertoglio, A., 2006. Available from: http://www.microthele.it.

Bertrand, A., Segura, M., Gutierrez, M., Vasquez, L., 2004. From small-scale habitat loopholes to decadal cycles: a habitat-based hypothesis explaining fluctuation in pelagic fish populations off Peru. Fish and Fisheries 5, 296-316.

Bidigare, R.R., Ondrusek, M.E., 1996. Spatial and temporal variability of phytoplankton pigment distributions in the Central Equatorial Pacific Ocean. Deep-Sea Research (Part II, Topical Studies in Oceanography) 43, 809-833.

Blaskovic, V., Torriani, F., Navarro, I., 1998. Caracteristicas troficas de las principales especies pelagicas durante el otono 1998. Crucero BIC Jose Olaya Balandra 9805-06 de Tacna a Mancora. Informe. Instituto del Mar del Peru. Callao 137, 72-79.

Blaskovic, V., Espinoza, P., Torriani, F., Navarro, I., 1999. Feeding behaviour of anchovy off Peruvian coast during spring 1998. Cruise R/V Jose Olaya Balandra 9811-12. Informe. Instituto del Mar del Peru. Callao, 77-84.

Bouchon, M., Cahuin, S., Ñiquen, M., 2001. Fluctuaciones de la ictiofauna pelágica en la región norte-centro del litoral peruano de 1994 a 1998. In: Tarazona, J., Arntz, W. ,Castillo, E. (Eds.), El Niño en América Latina: impactos biológicos y sociales. Consejo Nacional de Ciencia y Tecnología, Lima, pp. 73-79.

Brey, T., 2001. Population dynamics in benthic invertebrates. Available from: http://www.awi-bremerhaven.de/Benthic/Ecosystem/FoodWeb/Handbook/main.html.

Browman, H.I., Stergiou, K.I., 2004. Perspectives on ecosystem-based approaches to the management of marine resources. Marine Ecology Progress Series 274, 269-303.

Brown, P.C., Painting, S.J., Cochrane, K.L., 1991. Estimates of phytoplankton and bacterial biomass production in the northern and southern Benguela ecosystems. South African Journal of Marine Science 11, 537-564.

Brush, M.J., Brawley, J.W., Nixon, S.W., Kremer, J.N., 2002. Modeling phytoplankton production: Problems with the Eppley curve and an empirical alternative. Marine Ecology Progress Series 238, 31-45.

Calienes, R., Guillén, O., Lostanau, N., 1985. Variabilidad espacio-temporal de clorofila, producción primaria y nutrientes frente a la costa peruana. Boletin Instituto del Mar del Peru 10, 1-44.

Canby, T.Y., 1984. El Niño: Global Weather Disaster. National Geographic Magazine 165.

Cardoso, F., Tarazona, J., Paredes, C., 1998. Biological aspects of the Patagonian squid Loligo gahi (Cephalopoda: Loliginidae) in Huarmey, Peru. Revista Peruana de Biologia 5, 9-14.

Carr, M.E., 2002. Estimation of potential productivity in eastern boundary currents using remote sensing. Deep-Sea Research (Part II, Topical Studies in Oceanography) 49, 59-80.

Carr, M.E., 2003. Simulation of carbon pathways in the planktonic ecosystem off Peru during the 1997-1998 El Nino and La Nina. Journal of Geophysical Research. C. Oceans 108, [np].

Carre, M., Bentaleb, I., Blamart, D., Ogle, N., Cardenas, F., Zevallos, S., Kalin, R.M., Ortlieb, L., Fontugne, M., 2005. Stable isotopes and sclerochronology of the bivalve Mesodesma donacium: Potential application to Peruvian paleoceanographic reconstructions. Palaeogeography, Palaeoclimatology, Palaeoecology 228, 4-25.

Castillo, R., Juárez, L., Higginson, L., 1989. Predación y canibalísmo en la población de la merluza peruana en el área de Paita-Peru. Memorias del Simposio Internacional de los Recursos Vivos ylas Pesquerías en el Pacífico Sudeste, Viña del Mar, Chile, Rev. Pacífico Sur (Número Especial).

Chavez, F., Barber, R.T., 1985. La productividad de las aguas frente a la costa del Perú. Boletín ERFEN 15, 9-13.

Chavez, F.P., Barber, R.T., Sanderson, M.P., 1989. The potential primary production of the Peruvian upwelling ecosystem, 1953-1984. In: Pauly, D., Muck, P., Mendo, J. ,Tsukayama, I. (Eds.), The

Peruvian Upwelling Ecosystem: Dynamics and Interactions, Vol. 18. ICLARM conference proceedings, Manila, Philippines, pp. 50-63.
Chavez, F.P., Ryan, J., Lluch-Cota, S.E., Ñiquen, M., 2003. From anchovies to sardines and back: Multidecadal change in the Pacific Ocean. Science 299, 217-221.
Chen, D.G., Hare, S.R., 2006. Neural network and fuzzy logic models for pacific halibut recruitment analysis. Ecological Modelling 195, 11-19.
Christensen, V., Pauly, D., 1992. ECOPATH II - a software for balancing steady-state models and calculating network characteristics. Ecological Modelling 61, 169-185.
Christensen, V., Pauly, D., 1993a. Flow Characteristics of Aquatic Systems. In: Christensen, V. ,Pauly, D. (Eds.), Trophic models of aquatic systems, Vol. 26. ICLARM Conference Proceedings, pp. 338-352.
Christensen, V., Pauly, D., 1993b. Trophic models of aquatic ecosystems. ICLARM, MANILA (PHILIPPINES).
Christensen, V., 1994. On the Behaviour of some proposed goal functions for ecosystem development. Ecological Modelling 75/76, 37-49.
Christensen, V., 1995. Ecosystem maturity - towards quantification. Ecological Modelling 77, 3-32.
Christensen, V., Pauly, D., 1995. Fish production, catches and the carrying capacity of the world oceans. Naga, The ICLARM Quarterly July, 34-40.
Christensen, V., Walters, C.J., Pauly, D., 2000. Ecopath with Ecosim Version 4, Help system©.
Christensen, V., Walters, C.J., 2004. Ecopath with Ecosim: methods, capabilities and limitations. Ecological Modelling 172, 109-139.
Cloern, J.E., Dufford, R., 2004. Phytoplankton community ecology: principles applied in San Francisco Bay. Marine Ecology Progress Series 285, 11-28.
Cochrane, K.L., 2002. The use of ecosystem models to investigate ecosystem-based management strategies for capture fisheries: introduction. Fisheries Centre Research Reports 10, 5-10.
Cortez, T., Gonzalez, A.F., Guerra, A., 1999. Growth of Octopus mimus (Cephalopoda, Octopodidae) in wild populations. Fisheries Research 42, 31-39.
Csirke, J., 1989. Changes in the catchability coefficient in the Peruvian anchoveta (Engraulis ringens) fishery. In: Pauly, D., Muck, P., Mendo, J. ,Tsukayama, I. (Eds.), The Peruvian Upwelling Ecosystem: Dynamics and Interactions, Vol. 18. ICLARM conference proceedings, Manila, Philippines, pp. 207-219.
Csirke, J., Guevara Carrasco, R., Cardenas, G., Niquen, M., Chipollini, A., 1996. Situation of the Engraulis ringens and Sardinops sagax resources and perspectives to the fishing in the Peruvian waters, north and central regions of the Peru coast. Boletin. Instituto del Mar del Peru. Callao 15, 1-23.
Cupp, E.E., 1943. Marine Plankton Diatoms of the West Coast of North America. University of California Press, Berkeley, California.
Cury, P., Roy, C., 1989. Optimal environmental window and pelagic fish recruitment success in upwelling areas. Canadian Journal of Fisheries and Aquatic Sciences 46, 670-680.
Cury, P., Roy, C., Faure, V., 1998. Environmental constraints and pelagic fisheries in upwelling areas: the Peruvian puzzle. South African Journal of Marine Science/Suid-Afrikaanse Tydskrif vir Seewetenskap 19, 159-167.
Cury, P., Bakun, A., Crawford, R.J., Jarre, A., Quinones, R.A., Shannon, L.J., Verheye, H.M., 2000. Small pelagics in upwelling systems: patterns of interaction and structural changes in "wasp-waist" ecosystems. ICES Journal of Marine Science 57, 603-618.
Cushing, D.H., 1982. Climate and fisheries. Academic Press, London.
Daskalov, G., 1999. Relating fish recruitment to stock biomass and physical environment in the Black Sea using generalised additive models. Fisheries Research 41, 1-23.
Davis, J.P., Wilson, J.G., 1985. The energy budget and population structure of Nucula turgida in Dublin Bay. Journal of Animal Ecology 54, 557-571.
Deacon, E.L., Webb, E.K., 1962. Small-scale interactions. In: Hill, M.N. (Ed.) The sea: ideas and observations on progress in the study of the seas. Interscience, New York, pp.
Delgado, E., Villanueva, P., 1998. Peruvian coastal phytoplankton community during Cruise RV Humboldt 9803-05 from Tumbes to Tacna. Informe. Instituto del Mar del Peru. Callao, 114-120.
Delgado, E., Sánchez, S., Chang, F., Villanueva, P., Fernández, C., 2001a. El fitoplancton frente a la costa peruana durante el Niño 1997-98. In: Tarazona, J., Arntz, W.E. ,Castillo, E. (Eds.), El Niño en América Latina: impactos biológicos y sociales. CONCYTEC, Lima, pp. 29-38.
Delgado, E., Villanueva, P., Chang, F., Fernandez, C., 2001b. The Peruvian marine phytoplankton during Summer 2000. Informe. Instituto del Mar del Peru 159, 85-98.
DeMott, W.R., 1989. Optimal foraging theory as a predictor of chemically mediated food selection by selection by suspension-feeding copepods. Limnology and Oceanography 34, 140-154.
DeVries, T.J., Pearcy, W.G., 1982. Fish debris in sediments of the upwelling zone off central Peru: A late Quaternary record. Deep-Sea Research 29, 87-109.
DiSalvo, L.H., Alacron, E., Martinez, G., Uribe, E., 1984. Progress in the mass culture of *Argopecten purpuratus* with notes on its natural history. Rev. Chilena de Hist. Nat. 57, 33-45.
Drebes, G., 1974. Marines Phytoplankton. Georg Thieme Verlag, Stuttgart.
Dugdale, R.C., MacIsaac, J.J., 1971. A computational model for the uptake of nitrate in the Peru upwelling region. Investigación Pesquera 35, 299-308.
EDC, 2006. Environmental Data Center - Large Marine Ecosystems. Information Portal. Available from: http://woodsmoke.edc.uri.edu/Portal/ptk.
Edler, L., 1979. Phytoplankton and Chlorophyll: Recommendations on Methods for Marine Biological Studies in the Baltic Sea. Baltic Marine Biologists Publication.
Eppley, R.W., 1972. Temperature and phytoplankton growth in the sea. Fish Bulletin 70, 1063-1085.
Espinoza, J., Navarro, I., Torriani, F., 1998a. Variations in the alimentary spectrum of the main pelagic resources during autumn 1998. Cruise RV Humboldt 9803-05 from Tumbes to Tacna. Informe. Instituto del Mar del Peru. Callao, 134-142.
Espinoza, P., Blaskovic, V., Navarro, I., 1998b. Comportamiento alimentario de Engraulis ringens, a finales del invierno 1998. Crucero de evaluacion idroacustica de recursos pelagicos 9808-09. Informe. Instituto del Mar del Peru. Callao 141, 67-71.
Espinoza, P., Blaskovic, V., 2000. Changes in diet of Peruvian anchoveta Engraulis ringens and its influence on feeding dynamics. Boletin Instituto del Mar del Peru 19, 21-27.
Espinoza, P., Bertrand, A., in press. Revising previous hypothesis on the trophic position and ecological role of the Peruvian anchovy (Engraulis ringens). Progress in Oceanography.
FAO, 2003. Yearbook of Fishery Statistics.
Feldman, G.C., McClain, C.R., 2007. Ocean Color Web, SeaWifs. Available from: http://oceancolor.gsfc.nasa.gov/.

Field, J.C., Francis, R.C., Aydin, K., 2006. Top-down modeling and bottom-up dynamics: Linking a fisheries-based ecosystem model with climate hypotheses in the Northern California Current. Progress in Oceanography 68, 238-270.

Finn, J.T., 1976. Measures of ecosystem structure and function derived from analysis of flows. Journal of Theoretical Biology 56, 363-380.

Fischer, S., Thatje, S., submitted. Temperature-induced oviposition in the brachyuran crab Cancer setosus along a latitudinal cline: aquaria experiments and analysis of field-data.

Fréon, P., 2006. Interdecadal variability of anchovy abundance and overcapacity of commercial fleets in Peru. International Conference on The Humboldt Current System: Climate, ocean dynamics, ecosystem processes, and fisheries, Biblioteca Nacional del Perú / National Library of Peru Lima, Peru, November 27 - December 1, 2006.

Frisk, M.G., Miller, T.J., Dulvy, N.K., 2001. Life histories and vulnerability to exploitation of elasmobranchs: Inferences from elasticity, perturbation and phylogenetic analyses. Elasmobranch fisheries: Mangaging for sustainable use and biodiversity conservation, Dartmouth, NS (Canada), Northwest Atlantic Fisheries Organization.

Froese, R., Pauly, D., 2006. FishBase. Available from: www.fishbase.org.

Fukuyo, Y., 2006. Technical Guide for Dinoflagellate Study. Asian Natural Environmental Science Center, University of Tokyo, Available from: http://dinos.anesc.u-tokyo.ac.jp/.

Gonzales, E.I., Yépez , V.E., 2007. Estudio de línea base de la bahía de Sechura. Instituto del Mar del Perú, Lima.

Gonzalez, H., Hebbeln, D., Iriarte, J., Marchant, M., 2000. Sedimentation rates of faecal material, phytoplankton and microzooplankton at 2,300 m depth in the oceanic area off Coquimbo (30 degree S), Chile, during 1993-1995.

González, H., Daneri, G., Figueroa, D., Iriarte, J., Lefevre, G., Pizarro, G., Nones, R.Q., Sobrazo, M., Troncoso, A., 1998. Producción primaria y su destino en la trama trófica-pelágica y océano profundo e intercambio océano-atmósfera de CO_2 en la zona norte de la Corriente de Humboldt (23°S): Posibles efectos del evento El Niño, 1997–1998 en Chile. Revista Chilena de Historia Natural 71, 429–458.

González, H.E., Giesecke, R., Vargas, C.A., Pavez, A., Iriarte, J., Santibáñez, P., Castro, L., Escribano, R., Pagès, F., 2004a. Carbon cycling through the pelagic foodweb in the northern Humboldt Current off Chile (23 degrees S). ICES Journal of Marine Science 61, 572-584.

González, H.E., Hebbeln, D., Iriarte, J.L., Marchant, M., 2004b. Downward fluxes of faecal material and microplankton at 2300 m depth in the oceanic area off Coquimbo (30°S), Chile, during 1993-1995. Deep Sea Research Part II: Topical Studies in Oceanography 51, 2457-2474.

Guénette, S., Christensen, V., Pauly, D., in press. Trophic Modeling of the Peruvian Upwelling Ecosystem: Towards Reconciliation of Multiple Datasets. Progress in Oceanography.

Guevara-Carrasco, R., 2004. Peruvian hake overfishing: misunderstood lessons. Boletin Instituto del Mar del Peru 21, 27-32.

Guillén, V., 1990. Alimentación del pelícano o alcatraz (Pelecanus thagus) en la isla Macabí. Boletín de Lima 67, 85-88.

Gutiérrez, M., 2001. Efectos del evento El Niño 1997–98 sobre la distribución y abundancia de anchoveta (Engraulis ringens). In: Tarazona, J., Arntz, W.E. ,Castillo de Maruenda, E. (Eds.), El Niño en América Latina: impactos biológicos y sociales. Consejo Nacional de Ciencia yTecnología, Lima, Peru, pp. 55-72.

Gutierrez Torero, M., Herrera Almirón, N., 2002. An approach based on acoustic data to study the variability in distribution and abundance of small pelagics in the Humboldt ecosystem. In: Van der Lingen, C.D., Roy, C., Fréon, P., Barange, M., Castro, L., Gutierrez, M., Nykjaer, L. ,Shillington, F. (Eds.), GLOBEC-SPACC/ IDYLE/ ENVIFISH Workshop on Spatial Approaches to the Dynamics of Coastal Pelagic Resources and their Environment in Upwelling Areas. Instituto del Mar del Peru, Cape Town, South Africa.

Heimdal, B.R., 1993. Modern Coccolithophorids. In: Tomas, C.R. (Ed.) Marine Phytoplankton: a Guide to Naked Flagellates and Coccolithophorids. Academic Press, San Diego, pp. 147-249.

HELCOM, 2006. Biovolumes and Size-Classes of Phytoplankton in the Baltic Sea. Baltic Sea Environment Proceedings 106, 144.

Heymans, J.J., Baird, D., 2000. A carbon flow model and network analysis of the northern Benguela upwelling system, Namibia. Ecological Modelling 126, 9-32.

Heymans, J.J., Shannon, L.J., Jarre, A., 2004. Changes in the northern Benguela ecosystem over three decades: 1970s, 1980s, and 1990s. Ecological Modelling 172, 175-195.

Hilborn, R., Mangel, L.M., 1997. The Ecological Detective. Confronting Models with Data. Princeton University Press, Princeton, NJ.

Hillebrand, H., Duerselen, C.D., Kirschtel, D., Pollingher, U., Zohary, T., 1999. Biovolume calculation for pelagic and benthic microalgae. Journal of Phycology 35, 403-424.

Huebner, J.D., Edwards, D.C., 1981. Energy Budget of the Predatory Maine Gastropod Polinices duplicatus. Marine Biology 61, 221-226.

Humphreys, W.F., 1979. Production and Respiration in Animal Populations. The Journal of Animal Ecology 48, 427-453. doi:10.2307/4171.

Hutchings, L., Verheye, H.M., Mitchell-Innes, B.A., Peterson, W.T., Huggett, J.A., Painting, S.J., 1995. Copepod production in the southern Benguela system. ICES Journal of Marine Science 52, 439-455.

IOW, 2006. Galerie pelagischer Mikroalgen. Institut für Ostseeforschung Warnemünde, Available from: http://www.io-warnemuende.de/research/de_galerie.html.

IRI, 2008. The International Research Institute for Climate and Society: ENSO information page. Available from: http://iri.columbia.edu/climate/ENSO/.

Iriarte, J.L., González, H.E., 2004. Phytoplankton size structure during and after the 1997/98 El Nino in a coastal upwelling area of the northern Humboldt Current System. Marine Ecology Progress Series 269, 83-90.

IWC, 2004. International Whaling Commission report of the Modelling Workshop on Cetacean-Fishery Competition. J. Cetacean Res. Manage. 6 (Suppl.), 413-426.

Jahncke, J., Checkley, D.M., Hunt, G.L., 2004. Trends in carbon flux to seabirds in the Peruvian upwelling system: effects of wind and fisheries on population regulation. Fisheries Oceanography 13, 208-223.

James, A.G., 1987. Feeding ecology, diet and field-based studies on feeding selectivity of the Cape anchovy Engraulis capensis Gilcrist. In: Payne, A.I.L., Gulland, J.A. ,Brink, K.H. (Eds.), The Benguela and comparable ecosystems, Vol. 5. South African Journal of Marine Science, pp. 161-177.

James, A.G., Findlay, K.P., 1989. Effect of particle size and concentration on feeding behaviour, selectivity

and rates of food ingestion by the Cape Anchovy Engraulis capensis. Marine ecology progress series. Oldendorf 50, 275-294.
Jarre-Teichmann, A., 1992. Steady-state modelling of the Peruvian upwelling ecosystem. PhD thesis, University of Bremen, Bremen, Germany, unpublished.
Jarre-Teichmann, A., Pauly, D., 1993. Seasonal changes in the Peruvian upwelling ecosystem. In: Christensen, V. ,Pauly, D. (Eds.). ICLARM, Manila (Philippines), pp. 307-314.
Jarre-Teichmann, A., 1998. The potential role of mass balance models for the management of upwelling ecosystems. Ecological Applications 8, S93-S103.
Jarre-Teichmann, A., Christensen, V., 1998. Comparative modelling of trophic flows in four large upwelling ecosystems: global versus local effects. ORSTOM, Paris (France).
Jarre-Teichmann, A., Shannon, L.J., Moloney, C.L., Wickens, P.A., 1998. Comparing trophic flows in the southern Benguela to those in other upwelling ecosystems. South African Journal of Marine Science/Suid-Afrikaanse Tydskrif vir Seewetenskap 19, 391-414.
Jarre, A., Muck, P., Pauly, D., 1989. Interactions Between Fish Stocks in the Peruvian Upwelling Ecosystem. Multispecies Models Relevant to Management of Living Resources, Copenhagen, Denmark.
Jarre, A., Muck, P., Pauly, D., 1991. Two approaches for modelling fish stock interactions in the Peruvian upwelling ecosystem. ICES Mar. Sci. Symp. 193, 178-184.
JST, 2006. Soken-Taxa project - Microbial Digital Specimen Archives. Graduate University for Advanced Studies, Sokendai, Japan, and Japan Science and Technology Corporation, Available from: http://protist.i.hosei.ac.jp/PDB/Images/menuE.html.
Kaschner, K., 2004. Modelling and Mapping Resource Overlap between Marine Mammals and Fisheries on a Global Scale. PhD thesis, The University of British Columbia, Vancouver, BC (Canada), unpublished.
Kay, J.J., 1991. A non-equilibrium thermodynamic framework for discussing ecosystem integrity. Environmental Management 15, 483-495.
Keen, M.A., 1972. Sea Shells of Tropical West America - Marine Mollusks from Baja California to Peru. Stanford University Press, Stanford, California.
Konchina, Y., 1991. Trophic status of the Peruvian anchovy and sardine. Journal of Ichthyology 31, 59-72.
Kremer, J.N., Nixon, S.W., 1977. A coastal marine ecosystem. Simulation and analysis. Springer-Verlag, New York, USA.
Kuylenstierna, M., Karlson, B., 2006. Checklist of phytoplankton in the Skagerrak-Kattegat. Swedish Meteorological and Hydrological Institute, Available from: http://www.smhi.se/oceanografi/oce_info_data/plankton_checklist/ssshome.htm.
Landry, M.R., Kirshtein, J., Constantinou, J., 1996. Abundances and distributions of picoplankton populations in the Central Equatorial Pacific from 12 degree N to 12 degree S, 140 degree W. Deep-Sea Research (Part II, Topical Studies in Oceanography) 43, 871-890.
Lang, M., 2000. Populationsstruktur und Konsumverhaltung der decapoden Krebse *Cancer polydon* und *Cancer porteri* in der Independencia Bucht, Peru. Diplome thesis, Bremen University, Bremen, unpublished.
Lazareth, C.E., Lasne, G., Ortlieb, L., 2006. Growth anomalies in Protothaca thaca (Mollusca, Veneridae) shells as markers of ENSO conditions. Climate Research 30, 263-269.
Lazareth, C.E., Guzman, N., Poitrasson, F., Candaudap, F., Ortlieb, L., 2007. Nyctemeral variations of magnesium intake in the calcitic layer of a Chilean mollusk shell (Concholepas concholepas, Gastropoda). Geochimica et Cosmochimica Acta 71, 5369-5383.
Leon, R.I., Stotz, W.B., 2004. Diet and prey selection dynamics of Cancer polyodon in three different habitat types in Tongoy Bay, Chile. Journal of the Marine Biological Association of the United Kingdom 84, 751-756.
Libralato, S., Pranovi, F., Raicevich, S., Da Ponte, F., Giovanardi, O., Pastres, R., Torricelli, P., Mainardi, D., 2004. Ecological stages of the Venice Lagoon analysed using landing time series data. Journal of Marine Systems 51, 331-344.
Licea, J.L., Moreno, H., Santoyo, Figueroa, G., 1995. Dinoflageladas del Golfo de California. Universidad Autonoma de Baja California Sur, SEP-FOMES PROMARCO, La Paz, B.C.S., Mexico.
Lluch-Cota, D.B., Wooster, W.S., Hare, S.R., 2001. Sea surface temperature variability in coastal areas of the Northeastern Pacific related to the El Nino-Southern Oscillation and the Pacific Decadal Oscillation. Geophysical Research Letters 28, 2029-2032.
Macchiavello, J., Fonck, E., Edding, M., 1987. Antecedentes y perspectivas de1 Cultivo de Gracilaria en Coquimbo. In: Arana, P. (Ed.) Manejo y Desarollo Pesquero. Univ. Catolica de Valparaiso, Valparaiso, Chile, pp. 206-214.
Mace, P.M., 2004. In defence of fisheries scientists, single-species models and other scapegoats: Confronting the real problems. Marine Ecology Progress Series 274, 285-291.
Majluf, P., 1989. Reproductive ecology of South American fur seals in Peru. In: Pauly, D., Muck, P., Mendo, J. ,Tsukayama, I. (Eds.), The Peruvian upwelling ecosystem: dynamics and interactions, Vol. 18. ICLARM Conference Proceedings Lima, pp. 332-343.
Mann, K.H., 1982. Ecology of Coastal Waters. A Systems Approach. University of California Press, Berkeley, USA.
Martin, D., Grémare, A., 1997. Secondary production of Capitella sp. (Polychaeta: Capitellidae) inhabiting different organically enriched environments. Scientia Marina 61, 99-109.
Massuti, M., Margalef, R., 1930. Introducción Al Estudio Del Plancton Marino. Patronato Juan De La Cierva De Inves Tigacion Tecnica, Seccion De Biologica Marina, Barcelona.
Menden-Deuer, S., Lessard, E.J., Satterberg, J., 2001. Effect of preservation on dinoflagellate and diatom cell volume and consequences for carbon biomass predictions. Marine Ecology Progress Series 222, 41-50.
Mendo, J., Valdivieso, V., Yamashiro, C., Jurado, E., Morón, O., Rubio, J., 1987. Evaluación de la población de concha de abanico (*Argopecten purpuratus*) en la Bahía Independencia, Pisco, Peru, 17 de enero - 4 de febrero de 1987 Informe. Instituto del Mar del Peru (IMARPE), Callao, Peru.
Mendo, J., Valdivieso, V., Yamashiro, C., 1988. Cambios en densidad, numero y biomasa de la concha de abanico (*Argopecten purpuratus*) en la Bahia de Independencia (Pisco, Peru) durante 1984-1987. In: Salzwedel, H. ,Landa, A. (Eds.), Recursos y dinamica del ecosystema de afloramiento peruano, Vol. Extr. Bol. Inst. Mar Peru-Callao, Callao, pp. 382.
Mendo, J., Jurado, E., 1993. Length-based growth parameter estimates of the Peruvian scallop

(*Argopecten purpuratus*). Fisheries Research 15, 357-367.

Mendo, J., Tam, J., 1993. Multiple environmental states affecting penaeid shrimp production in Peru. Naga 16, 44-47.

Mendo, J., Wolff, M., 2002. Pesqueria y manejo de la concha de abanico (*Argopecten purpuratus*) en la Bahia de Independencia. In: Mendo, J. ,Wolff, M. (Eds.), Bases ecologicas y socioeconomicas para el manejo de los recursos vivos de la Reserva National de Paracas. Universidad Agraria La Molina, Lima, pp. 188-194.

Mendoza, J.J., 1993. A preliminary biomass budget for the northeastern Venezuela shelf ecosystem. In: Christensen, V. ,Pauly, D. (Eds.), Trophic Models of Aquatic Ecosystems, Vol. 26. ICLARM Conference Proceedings, pp. 285-297.

MIRACLE, 2006. Microfossil Image Recovery And Circulation for Learning and Education (MIRACLE). University College London Micropalaeontology Unit, Available from: http://www.ucl.ac.uk/GeolSci/micropal/index.html.

Moloney, C.L., Jarre, A., Arancibia, H., Bozec, Y.-M., Neira, S., Jean-Paul Roux, J.-P., Shannon, L.J., 2005. Comparing the Benguela and Humboldt marine upwelling ecosystems with indicators derived from inter-calibrated models. ICES Journal of Marine Science 62, 493-502.

Monaco, M.E., Ulanowicz, R.E., 1997. Comparative ecosystem trophic structure of three U.S mid-Atlantic estuaries. Marine Ecology Progress Series 161, 239-254.

Montecinos, A., Purca, S., Pizarro, O., 2003. Interannual-to-interdecadal sea surface temperature variability along the western coast of South America. Geophysical Research Letters 30, 1570-1573.

Morissette, L., . . , 2007. Complexity, cost and quality of ecosystem models and their impact on resilience: a comparative analysis, with emphasis on marine mammals and the Gulf of St. Lawrence. Ph. D. thesis, University of British Columbia, British Columbia, unpublished.

Muck, P., Fuentes, H., 1987. Sea lion and fur seal predation on the Peruvian anchoveta, 1953 to 1982. WorldFish Center studies and reviews. International Cent. for Living Aquatic Resour. Manage., Manila (Philippines).

Muck, P., Pauly, D., 1987. Monthly anchoveta consumption of guano birds, 1953 to 1982. In: Pauly, D. ,Tsukayama, I. (Eds.), The Peruvian anchoveta and its upwelling ecosystem: Three decades of change, Vol. 391. ICLARM, Manila, Philippines, pp. 219-233.

Muck, P., 1989. Major trends in the pelagic ecosystem off Peru and their implications for management. In: Pauly, D., Muck, P., Mendo, J. ,Tsukayama, T. (Eds.), The Peruvian upwelling ecosystem: dynamics and interactions, Vol. 18. ICLARM conference proceedings, Manila, Philippines, pp. 386-403.

Myers, R.A., 1998. When do environment-recruitment correlations work? Reviews in Fish Biology and Fisheries 8, 285-305.

Navarro, J.M., Gonzalez, C.M., 1998. Physiological responses of the Chilean scallop Argopecten purpuratus to decreasing salinities. Aquaculture 167, 315-327.

Neira, S., Arancibia, H., 2004. Trophic interactions and community structure in the upwelling system off Central Chile (33-39 degrees S). Journal of Experimental Marine Biology and Ecology 312, 349-366.

Neira, S., Arancibia, H., Cubillos, L., 2004. Comparative analysis of trophic structure of commercial fishery species off Central Chile in 1992 and 1998. Ecological Modelling 172, 233-248.

Nielsen, H.H., 2006. Southern Ocean diatoms. Vista, Available from: http://www2.npolar.no/~simon/f__kerguelensis.htm.

Nigmatullin, C.M., Nesis, K.N., Arkhipkin, A.I., 2001. A review of the biology of the jumbo squid Dosidicus gigas (Cephalopods: Ommastrephidae). Fisheries Research (Amsterdam) 54, 9-19.

Ñiquen, M., Bouchon, M., 2004. Impact of El Niño events on pelagic fisheries in Peruvian waters. Deep-Sea Research Part II-Topical Studies in Oceanography 51, 563-574.

Nishida, T., Chen, D.G., Mohri, M., 2007. Fuzzy logic analyses for spawner-recruitment relationship of bigeye tuna (Thunnus obesus) in the Indian Ocean incorporating the environmental regime shift. Ecological Modelling 203, 132-140.

Nixon, S., Thomas, A., 2001. On the size of the Peru upwelling ecosystem. Deep-Sea Research (Part I, Oceanographic Research Papers) 48, 2521-2528.

Nixon, S.W., 1982. Nutrient dynamics, primary production and fisheries yields of lagoons. Oceanologica Acta Special edition, 357-371.

NOAA, 2008. El Niño theme page - access to distributed informaion on El Niño. Available from: http://www.pmel.noaa.gov/tao/elnino/nino-home.html.

NODC, 2006. Phytoplankton of the Arctic Seas. The National Oceanographic Data Center, Available from: http://www.nodc.noaa.gov/OC5/BARPLANK/start.html.

Ochoa, N., Rojas de Mendiola, B., Gómez, O., 1985. Identificación del fenómeno El Niño a través de los organismos fitoplanctónicos. Boletin Instituto del Mar del Peru. Instituto del Mar del Perú (IMARPE), Callao, Peru.

Odum, E.P., 1969. The strategy of ecosystem development. Science 104, 262-270.

Ortiz, M., Wolff, M., 2002a. Trophic models of four benthic communities in Tongoy Bay (Chile): comparative analysis and preliminary assessment of management strategies. Journal of Experimental Marine Biology and Ecology 268, 205-235.

Ortiz, M., Wolff, M., 2002b. Spatially explicit trophic modelling of a harvested benthic ecosystem in Tongoy Bay (central northern Chile). Aquatic Conservation: Marine and Freshwater Ecosystems 12, 601-618.

Pacific Fisheries Environmental Laboratory, 2006. Upwelling Indices along the coast of South America. dataset, Available from: http://www.pfeg.noaa.gov/.

Parrish, R.H., Bakun, A., Husby, D.M., Nelson, C.S., 1983. Comparative climatology of selected environmental processes in relation to eastern boundary current pelagic fish reproduction. In: Sharp, G.D. ,Csirke, J. (Eds.), Proceedings of the expert consultation to examine changes in abundance and species composition of neritic fish resources, Vol. 291. FAO Fisheries Report, San Jose, Costa Rica, pp. 731-777.

Patterson, K.R., Zuzunaga, J., Cardenas, G., 1992. Size of the South American sardine (Sardinops sagax) population in the northern part of the Peru upwelling ecosystem after collapse of anchoveta (Engraulis ringens) stocks. Canadian Journal of Fisheries and Aquatic Sciences 49, 1762-1769.

Pauly, D., 1987. Managing the Peruvian upwelling ecosystem: A synthesis. WorldFish Center studies and reviews. 1987.

Pauly, D., Palomares, M.L., Gayanilo, F.C., 1987. VPA estimates of the monthly population length composition, recruitment, mortality, biomass and

related statistics of Peruvian anchoveta, 1953 to 1981. WorldFish Center studies and reviews. 1987.
Pauly, D., Tsukayama, I., 1987a. The Peruvian anchoveta and its upwelling ecosystem: Three decades of change. ICLARM, Manila, Philippines.
Pauly, D., Tsukayama, I., 1987b. On the implementation of management-oriented fishery research: The case of Peruvian anchoveta.
Pauly, D., Tsukayama, I., 1987c. On the implementation of management-oriented fishery research: The case of Peruvian anchoveta. In: Pauly, D. ,Tsukayama, I. (Eds.), The Peruvian Anchoveta and Its Upweling Ecosystem: Three Decades of Change, Vol. 391. ICLARM, Manila, Philippines, pp. 1-13.
Pauly, D., Muck, P., Mendo, J., Tsukayama, I., 1989. The Peruvian upwelling ecosystem: Dynamics and interactions. ICLARM conference proceedings, Manila, Philippines.
Pauly, D., Christensen, V., 1995. Primary production required to sustain global fisheries. Nature 374, 255-257.
Pauly, D., Christensen, V., Dalsgaard, J., Froese, R., Torres Jr, F., 1998. Fishing down marine food webs. Science 279, 860-863.
Peña, T.S., Johst, K., Grimm, V., Arntz, W., Tarazona, J., 2005. Population dynamics of a polychaete during three El Nino events: disentangling biotic and abiotic factors. Oikos 111, 253-258.
Pitcher, G.C., Brown, P.C., Mitchell-Innes, B.A., 1992. Spatio-temporal variability of phytoplankton in the southern Benguela Upwelling system. South African Journal of Marine Science/Suid-Afrikaanse Tydskrif vir Seewetenskap.
Plagányi, É.E., 2007. Models for an ecosystem approach to fisheries. FAO Technical Paper No. 477. University of Cape Town, Cape Town, South Africa.
Polovina, J.J., Ow, M.D., 1985. An approach to estimating an ecosystem box model. Fishery Bulletin 83, 457-460.
Pranovi, F., Libralato, S., Raicevich, S., Granzotto, A., Pastres, R., Giovanardi, O., 2003. Mechanical clam dredging in Venice lagoon: ecosystem effects evaluated with a trophic mass-balance model. Marine Biology 143, 393-403.
Purca, S., 2005. Variabilidad temporal de baja frecuencia en el Ecosistema de la Corriente de Humboldt frente a Perú. PhD. thesis, Universidad de Concepción, Concepción, Chile, unpublished.
Quigg, A., 2006. Phytoplankton Dynamics Laboratory. Department of Marine Biology, Texas A&M University Available from: http://www.marinebiology.edu/Phytoplankton/phyto.htm.
Quipuzcoa, L., Marquina, R., 2001. La estructura comunitaria del macrozoobentos en la plataforma continental del Peru: un analisis decadal. In: Espino, M., Samame, M. ,Castillo, R. (Eds.), Forum La merluza peruana (Merluccius gayi peruanus) biología y pesquería, Informe Instituto Mar Perú. IMARPE, pp. 46-49.
Richardson, A.J., Mitchell-Innes, B.A., Fowler, J.L., Bloomer, S.F., Verheye, H.M., Field, J.G., Hutchings, L., Painting, S.J., 1998. The effect of sea temperature and food availability on the spawning success of Cape anchovy Engraulis capensis in the southern Benguela. South African Journal of Marine Science/Suid-Afrikaanse Tydskrif vir Seewetenskap 19, 275-290.
Ricker, W.E., 1958. Maximum Sustained Yields from Fluctuating Environments and Mixed Stocks. Journal of the Fisheries Research Board of Canada 15, 991-1006.
Rines, J., 2006. Bacteriastrum. Thalassa, Available from: http://thalassa.gso.uri.edu/plankton/diatoms/genera/bacteria/genus/bacteria.htm.
Rippe, L., 1996. Gemeinschaftsanalyse des Küstennahen Mesoplanktons im Flachwassergebiet vor der Kolumbianischen Pazifikküste. Diplom thesis, Bremen University, Bremen, Germany, unpublished.
Rodhouse, P.G., Nigmatullin, C.M., 1996. The role of cephalopods in the world's oceans. Role as consumers. Philosophical Transactions: Biological Sciences 351, 1003-1022.
Rodriguez, J., Tintore, J., Allen, J.T., Blanco, J.M., Gomis, D., Reul, A., Ruiz, J., Rodriguez, V., Echevarria, F., Jimenez-Gomez, F., 2001. Mesoscale vertical motion and the size structure of phytoplankton in the ocean. Nature 410, 360-363.
Rojas de Mendiola, B., Gómez, O., Ochoa, N., 1985. Efectos del fenómeno El Niño sobre el fitoplancton. In: Arntz, W., Landa, A. ,Tarazona, J. (Eds.), El Niño: su impacto en la fauna marina. Intituto del Mar del Perú, Callao, Peru.
Rojas de Mendiola, S., 1981. Seasonal phytoplankton distribution along the Peruvian coast. In: Richards, F.A. (Ed.) Coastal Upwelling, Vol. 20. American Geophysical Union, Washington, D.C., pp. 348-356.
Rouillon, G., Mendo, J., Ochoa, N., 2002. Fitoplankton en el contenido estomacal de *Argopecten purpuratus* (Mollusca, Bivalvia) suspendida a differentes profundidades en Bahía Independencia. In: Mendo, J. ,Wolff, M. (Eds.), Memorias I Jornada "Bases Ecológicas y Socioeconómicas para el Manejo de los Recursos Vivos de la Reserva Nacional de Paracas". Universidad Nacional Agraria La Molina, Lima, pp. 60-67.
Rowe, S., Hutchings, J.A., 2003. Mating systems and the conservation of commercially exploited marine fish. Trends in Ecology & Evolution 18, 567-572.
Roy, C., Cury, P., Kifani, S., 1992. Pelagic fish recruitment success and reproductive strategy in upwelling areas: Environmental compromises.
Rybarczyk, H., Elkaim, B., Ochs, L., Loquet, N., 2003. Analysis of the trophic network of a macrotidal ecosystem: the Bay of Somme (Eastern Channel). Estuarine, Coastal and Shelf Science 58, 405-421.
Ryther, J.H., 1969. Photosynthesis and fish production in the sea. Science 166, 72-76.
Samamé, M., Benites, C., Valdivieso, V., Mendez, M., Yamashiro, C., Moron, O., 1985. Evaluacón del recurso concha de abanico (*Argopecten purpuratus*) en la Bahía Independencia, Pisco, en Octubre-Noviembre 1985. Instituto del Mar del Perú.
Sanchez, S., 1996. Composition, distribution and indicator organisms of phytoplanktonic community in the area Tambo de Mora to Paita. August and September 1995.
Santander, H., Luyo, G., Carrasco, S., Véliz, M., Castillo, O., 1981. Catálogo de zooplancton en el mar peruano. Boletin Instituto del Mar del Peru 6, 75.
Schetinnikov, A.S., 1989. Food spectrum of the squid Dosidicus gigas (Oegopsida) during ontegenesis. Zoologicheski Zhurnal 68, 28-39.
Schwinghamer, P., Hargrave, B., Peer, D., Hawkins, C.M., 1986. Partitioning of production and respiration size among size groups of organisms in an intertidalbenthic community. Marine Ecology Progress Series 31, 131-142.
Scott, B.E., Marteinsdottir, G., Begg, G.A., Wright, P.J., Kjesbu, O.S., 2006. Effects of population size/age structure, condition and temporal dynamics of spwaning on reprodictive output in Atlantic cod (Gadus morhua). Ecological Modelling 191, 383-415.
Sea Around Us, 2006. A global database on marine fisheries and ecosystems. Fisheries Centre, University British Columbia, Vancouver, Available from: www.seaaroundus.org.

SERC, 2006. Phytoplankton Guide - to the Chesapeake Bay and other regions. Smithsonian Environmental Research Center, Available from: http://www.serc.si.edu/labs/phytoplankton/guide/index.jsp.

Serra, J.R., 1983. Changes in the abundance of pelagic resources along the Chilean coast. Proceedings of the expert consultation to examine changes in abundance and species composition of neritic fish resources, a preparatory meeting for the FAO world conference on fisheries management and development, san jose, costa rica, FAO FISH. REP./FAO, INF. PESCA.

Serra, R., Tsukayama, I., 1988. A synopsis of biological and fishery data on the sardine, Sardina sagax (Jenyns 1842) in the Southeast Pacific.

Shannon, L.J., Jarre-Teichmann, A., 1999. A Model of trophic flows in the northern Benguela Upwelling system during the 1980s. South African Journal of Marine Science/Suid-Afrikaanse Tydskrif vir Seewetenskap 21, 349-366.

Shannon, L.J., Cury, P.M., Jarre, A., 2000. Modelling effects of fishing in the southern Benguela ecosystem. ICES Journal of Marine Science 57, 720-722.

Shannon, L.J., Moloney, C.L., Jarre, A., Field, J.G., 2003. Trophic flows in the southern Benguela during the 1980s and 1990s. Journal of Marine Systems 39, 83-116.

Shannon, L.J., Christensen, V., Walters, C.J., 2004a. Modelling Stock Dynamics in the Southern Benguela Ecosystem for the Period 1978–2002. African Journal of Marine Science 26, 179-196.

Shannon, L.J., Field, J.G., Moloney, C.L., 2004b. Simulating anchovy-sardine regime shifts in the southern Benguela ecosystem. Ecological Modelling 172, 269-281.

Shannon, L.J., Neira, S., Taylor, M.H., submitted. Comparing internal and external drivers in the southern Benguela, and the southern and northern Humboldt upwelling ecosystems. African Journal of Marine Science.

Shushkina, E.A., Vinogradov, M.Y., Sorokin, Y.I., Lebedeva, L.P., Mikheyev, V.N., 1978. Functional Characteristics of the Planktonic Communities in the Peruvian Upwelling Region. Marine Biology 18, 579-589.

Sinclair, M., 1988. Marine populations. An essay on population regulation and speciation. Washington Sea Grant, Seattle, WA.

Sinclair, M., Iles, T.D., 1988. Population richness of marine fish species. Aquat. Living Resour./Ressour. Aquat. Vivantes. 1, 71-83.

Sinclair, M., Iles, T.D., 1989. Population regulation and speciation in the oceans. J. Cons. Ciem. 45, 165-175.

Škaloud, P., 2006. Algae of the North Sea. Phycological research group at Department of Botany, Charles University of Prague, Available from: http://botany.natur.cuni.cz/skaloud/index_NorthSea.htm.

Sommer, U., Stibor, H., Katechakis, A., Sommer, F., Hansen, T., 2002. Pelagic food web configurations at different levels of nutrient richness and their implications for the ratio fish production:primary production. Hydrobiologia 484, 11-20.

Sommer, U., Hansen, T., Blum, O., Holzner, N., Vadstein, O., Stibor, H., 2005. Copepod and microzooplankton grazing in mesocosms fertilised with different Si:N ratios: no overlap between food spectra and Si:N influence on zooplankton trophic level. Oecologia 142, 274-283.

Sorokin, Y.I., Kogelschatz, J.E., 1979. Analysis of heterotrophic microplankton in an upwelling area. Hydrobiologia 66, 195-208.

Stotz, W., 2000. When aquaculture restores and replaces an overfished stock: Is the conservation of the Species assured? The case of the scallop Argopecten purpuratus in Northern Chile. Aquaculture International 8, 237-247.

Stotz, W.B., González, S.A., 1997. Abundance, growth, and production of the sea scallop Argopecten purpuratus (Lamarck 1819): bases for sustainable exploitation of natural scallop beds in north-central Chile. Fisheries Research 32, 173-183.

Strickland, J.D.H., Eppley, R.W., Rojas be Mendiola, B., 1969. Phytoplankton populations, nutrients and photosynthesis in Peruvian coastal waters. Bol. Inst. Mar. Peru 2, 4-45.

Sun, J., Liu, D., 2003. Geometric models for calculating cell biovolume and surface area for phytoplankton. Journal of Plankton Research 25, 1331-1346.

Tafur, R., Castillo, G., Crispin, A., Taipe, A., 2000. Evaluación Poblacional de la Concha de Abanico en la Bahía de Sechura e Isla Lobos de Tierra (Julio 1999). Informe Progresivo. IMARPE, Lima.

Tam, J., Purca, S., Duarte, L.O., Blaskovic, V., Espinoza, P., 2006. Changes in the diet of hake associated with El Niño 1997–1998 in the northern Humboldt Current ecosystem. Advances in Geosciences 6, 63-67.

Tarazona, J., Salzwedel, H., Arntz, W., 1988a. Oscillations of macrobenthos in shallow waters of the Peruvian central coast induced by El Nino 1982-83. Journal of Marine Research 46, 593-611.

Tarazona, J., Salzwedel, H., Arntz, W., 1988b. Positive effect of "El Nino" on macrozoobenthos inhabiting hypoxic areas of the Peruvian upwelling system. Oecologia 76, 184-190.

Tarazona, J., Canahuire, E., Salzwedel, H., Jeri, T., Arntz, W., Cid, L., 1991. Macrozoobenthos in two shallow areas of the Peruvian Upwelling ecosystem.

Tarazona, J., Arntz, W., Castillo, E., 2001. El Niño en América Latina: impactos biológicos y sociales. Consejo Nacional de Ciencia y Tecnología, Lima.

Taylor, M.H., Wolff, M., 2007. Trophic modeling of Eastern Boundary Current systems: a review and prospectus for solving the “Peruvian Puzzle”. Revista Peruana de Biologia 14, 87-100.

Taylor, M.H., Wolff, M., Mendo, J., Yamashiro, C., 2007a. Input-output parameters for the steady-state models of Independence Bay for the years 1996 and 1998 before application of the Ecoranger resampling routine. PANGAEA, Available from: http://www.pangaea.de.

Taylor, M.H., Wolff, M., Mendo, J., Yamashiro, C., 2007b. Diet matrix for the steady-state models of Independence Bay for the years 1996 and 1998 before application of the Ecoranger resampling routine. PANGAEA, Available from: http://www.pangaea.de.

Taylor, M.H., Wolff, M., Vadas, F., Yamashiro, C., 2007c. Input-output parameters for the steady-state model of Sechura Bay in 1996 before application of the Ecoranger resampling routine. PANGAEA, Available from: http://www.pangaea.de.

Taylor, M.H., Wolff, M., Vadas, F., Yamashiro, C., 2007d. Diet matrix for the steady-state trophic model of Sechura Bay in 1996 before application of the Ecoranger resampling routine. PANGAEA, Available from: http://www.pangaea.de.

Taylor, M.H., Wolff, M., Mendo, J., Yamashiro, C., in press. Comparative analysis of trophic flow structure between normal upwelling and El Niño periods for Bahía Independencia, Peru. Progress in Oceanography.

Thatje, S., 2008. Organismal biology joins Climate Research: the example of ENSO. Helgoland Marine Research 62 (suppl. 1). doi:10.1007/s10152-007-0098-z.

Throndsen, J., 1997. The planktonic marine flagellates. In: Tomas, C.R. (Ed.) Identifying Marine Phytoplankton. Academic Press, San Diego, pp. 7-146.

Tovar, H., Guillen, V., Nakama, M.E., 1987. Monthly population size of three guano bird species off Peru, 1953 to 1982. In: Pauly, D. ,Tsukayama, I. (Eds.), The Peruvian anchoveta and its upwelling ecosystem: Three decades of change, Vol. 391. ICLARM, Manila, Philippines, pp. 208-218.

Ulanowicz, R.E., 1986. Growth and development: ecosystem phenomenology. Springer-Verlag, New York.

Ulanowicz, R.E., Puccia, C.J., 1990. Mixed trophic impacts in ecosystems. Coenoses 5, 7-16.

Ulanowicz, R.E., 1997. Ecology, the ascendent perspective. Columbia University Press, New York.

Uriarte, A., Prouzet, P., Villamor, B., 1996a. Bay of Biscay and Ibero Atlantic anchovy populations and their fisheries. Scientia Marina 60, 237-255.

Uriarte, I., Farias, A., Munoz, C., 1996b. Cultivo en hatchery y preengorde del ostio del norte, *Argopecten purpuratus* (Lamarck, 1819), en el sur de Chile. Rev. Biol-Mar. Valparaiso 31, 81-90.

Van der Lingen, C.D., 1994. Effect of particle size and concentration on the feeding behaviour of adult pilchard *Sardinops sagax*. Marine Ecology Progress Series 109, 1-13.

Van der Lingen, C.D., 2002. Diet of sardine Sardinops sagax in the southern Benguela upwelling ecosystem. South African Journal of Marine Science/Suid-Afrikaanse Tydskrif vir Seewetenskap 24, 301-316.

Van der Lingen, C.D., Hutchings, L., Field, J.G., 2006. Comparative trophodynamics of anchovy Engraulis encrasicolus and sardine Sardinops sagax in the southern Benguela: are species alternations between small pelagic fish trophodynamically mediated. African Journal of Marine Science 28, 465-477.

Vega, R., Mendo, J., 2002. Consumo de alimento y crecimiento del pulpo *Octopus* spp. alimentado con *Argopecten purpuratus* en la Bahía de Paracas, Pisco. In: Mendo, J. ,Wolff, M. (Eds.), Memorias I Jornada "Bases Ecológicas y Socioeconómicas para el Manejo de los Recursos Vivos de la Reserva Nacional de Paracas". Universidad Nacional Agraria La Molina, Lima, pp. 212-220.

Villanueva, P., Fernandez, C., Sanchez, S., 1998. Biomasa planctonica como alimento disponible durante el crucero BIC Humboldt y BIC Jose Olaya Balandra 9808-09 de Paita a Los Paltos (Tacna). Informe. Instituto del Mar del Peru. Callao 141, 49-54.

Villegas, P., 2001. Growth, life cycle and fishery biology of Loligo gahi (d'Orbigny, 1835) off the Peruvian coast. Fisheries Research (Amsterdam) 54, 123-131.

Waller, T.R., 1969. The evolution of the Argopecten gibbus stock (Mollusca: Bivalvia), with emphasis on the tertiany and quartenary species of eastern North America. J. Paleontology 43, 125.

Walsh, J.J., Dugdale, R.C., 1971. A simulation model of the nitrogen flow in the Peruvian upwelling system. Investigación Pesquera 35, 309-330.

Walsh, J.J., 1981. A carbon budget for overfishing off Peru. Nature 290, 300-304.

Walters, C., Christensen, V., Pauly, D., 1997. Structuring dynamic models of exploited ecosystems from trophic mass-balance assessments. Reviews in Fish Biology and Fisheries 7, 139-172.

Walters, C., Pauly, D., Christensen, V., Kitchell, J.F., 2000. Representing Density Dependent Consequences of Life History Strategies in Aquatic Ecosystems: EcoSim II. Ecosystems 3, 70-83.

Walters, C.J., Martell, S.J.D., 2004. Fisheries ecology and management. Princeton University Press, Princeton, New Jersey.

Ware, D.M., 1992. Production characteristics of upwelling systems and the trophodynamic role of hake.

Warnke, K., 1999. Observations on Embryonic Development of *Octopus mimus* (Mollusca: Cephalopoda) from Northern Chile. The Veliger 42, 211-217.

Watters, G.M., Olson, R.J., Francis, R.C., Fiedler, P.C., Polovina, J.J., Reilly, S.B., Aydin, K.Y., Boggs, C.H., Essington, T.E., Walters, C.J., Kitchell, J.F., 2003. Physical forcing and the dynamics of the pelagic ecosystem in the eastern tropical Pacific: Simulations with ENSO-scale and global-warming climate drivers. Canadian Journal of Fisheries and Aquatic Sciences 60, 1161-1175.

Welch, H.E., 1968. Relationships between Assimiliation Efficiencies and Growth Efficiencies for Aquatic Consumers. Ecology 49, 755-759. doi:10.2307/1935541.

Westerhoff, P., 2006. Reducing Taste and Odor and Other Algae-Related: Problems for Surface Water Supplies in Arid Environments. Department of Civil and Environmental Engineering, Arizona State University, Available from: http://enpub.fulton.asu.edu/pwest/myweb/Taste%20and%20Odor%20Stuff/Taxonomic%20guide/Click_Here_To_Open_Taxonomic_Guide.html.

Wiff, R., Quiñones, R.A., 2004. Environmental Parameterization in Fisheries-Biology Models. A Review. Gayana 68, 76-92.

Wilson, J.G., Parkes, A., 1998. Network analysis of the energy flow through the Dublin ecosystem. Biology and Environment: Proceedings of the Royal Irish Academy 98B, 179-190.

Wolff, M., Wolff, R., 1983. Observations on the utilization and growth of the pectinid Agropecten purpuratus (L.) in the fishing area of Pisco, Peru. Boletin del Instituto del Mar del Per 7, 197-235.

Wolff, M., 1985. Fischerei, Oekologie und Populationsdynamik de Pilgermuschel *Argopecten purpuratus* (L) im Fischereigebiet von Pisco (Peru) unter dem Einfluss des El Nino 1982/1983. PhD thesis, Kiel University, Kiel, Germany, unpublished.

Wolff, M., 1987. Population dynamics of the Peruvian scallop Argopecten purpuratus during the El Nino phenomenon of 1983. Canadian Journal of Fisheries and Aquatic Sciences 44, 1684-1691.

Wolff, M., 1988. Spawning and recruitment in the Peruvian scallop Argopecten purpuratus. Marine Ecology Progress Series 42, 213-217.

Wolff, M., von Brand, E., Jollan, L., 1991. Temperature shock treatment for early larval selection in the Chilean scallop *Argopecten purpuratus* (Lamarck, 1819). In: Shumway, S.E. ,Sandifer, P.A. (Eds.), World Aquaculture Workshops, 1. An International Compendium of Scallop Biology and Culture - A Tribute to James Mason. Selected papers from the 7th International Pectinid Workshop. The World Aquaculture Society, Baton Rouge, pp. 357.

Wolff, M., Perez, H., 1992. Population dynamics, food consumption and gross conversion efficiency of Octopus mimus Gould, from Antofagasta, (northern Chile). ICES Council Meetings Papers. ICES, Copenhagen, Denmark, pp. 12.

Wolff, M., Soto, A., 1992. Population dynamics of Cancer polyodon in La Herradura Bay, northern Chile. Marine Ecology Progress Series 85, 70-81.

Wolff, M., Alarcon, E., 1993. Structure of a scallop Argopecten purpuratus (Lamarck, 1819)-dominated subtidal macro-invertebrate assemblage in northern Chile. Journal of Shellfish Research 12, 295-304.

Wolff, M., 1994. A trophic model for Tongoy Bay -- a system exposed to suspended scallop culture

(northern Chile). Journal of Experimental Marine Biology and Ecology 182, 149-168.

Wolff, M., Hartmann, H.J., Koch, V., 1996. A pilot trophic model for Golfo Dulce, a fjord-like tropical embayment, Costa Rica. Revista de biologia tropical 44, 215-231.

Wolff, M., Koch, V., Bautista Chavarria, J., Vargas, J.A., 1998. A trophic flow model of the Golfo de Nicoya, Costa Rica. Revista de Biologia Tropical 46, Supl. 6, 63-79.

Wolff, M., Mendo, J., 2000. Management of the Peruvian bay scallop (Argopecten purpuratus) metapopulation with regard to environmental change. Aquatic Conservation: Marine and Freshwater Ecosystems 10, 117-126.

Wolff, M., Mendo, J., 2002. Upwelling is the Disturbance, not El Niño: Insights from Modelling Community Organization and Flow Structure. Investigaciones Marinas 30, 166-167.

Wolff, M., Wosnitza-Mendo, C., Mendo, J., 2003. The Humboldt Current- Trends in exploitation, protection and research. In: Hempel, G. ,Sherman, K. (Eds.), Large Marine Ecosystems of the World. Elsevier, pp. 279-309.

Wolff, M., Taylor, M., Mendo, J., Yamashiro, C., 2007. A catch forecast model for the Peruvian scallop (*Argopecten purpuratus*) based on estimators of spawning stock and settlement rate. Ecological Modelling 209, 333-341. doi:10.1016/j.ecolmodel.2007.07.013.

Wosnitza-Mendo, C., Mendo, J., Guevara Carrasco, R., 2005. Políticas de gestión para la reducción de la capacidad excesiva de esfuerzo pesquero en Perú: el caso de la pesquería de la merluza. In: Agüero, M. (Ed.) Capacidad de pesca y manejo pesquero en Amèrica Latina y el Caribe, Vol. 461. FAO Technical Papers, pp. 343-372.

Yamashiro, C., Rubio, J., Jurado, E., Auza, E., Maldonado, M., Ayon, P., Antonietti, E., 1990. Evaluación de la población de Concha de Abanico (Argopecten purpuratus) en la Bahía de Independencia, Pisco, Perú 20 de febrero - 04 de marzo de 1988. Informe. Instituto del Mar del Péru, Callao, Peru.

Zuta, S., Tsukayama, I., Villanueva, R., 1983. El ambiente marino y las fluctuaciones de las principales poblaciones pelágicas de la costa peruana. FAO Fisheries Report 291, 179-253.

Appendix

Appendix 1. Phytoplankton biovolume database

Genus	species	sub-species (var.)	Group‡‡	Shape Code§§	Volume used (μm^3)	Own estimate (μm^3)	used	Direct value from lit. #1 (μm^3)	Lit. ID***	used	Direct value from lit. #2 (μm^3)	Lit. ID‡	used	Calculated from lit. #3(μm^3)†††	Lit. ID‡	used	Sun & Liu dimension (a) (µm)	Sun & Liu dimension (b) (µm)	Sun & Liu dimension (c) (µm)	Sun & Liu dimension (a1) (µm)	Sun & Liu dimension (a2) (µm)	Sun & Liu dimension (a3) (µm)	Sun & Liu dimension (a4) (µm)	Sun & Liu dimension (b1) (µm)	Sun & Liu dimension (b2) (µm)	Sun & Liu dimension (b3) (µm)
Acanthaires	sp		RADI.		2572441			2572441	30	x																
Actinocyclus	octonaris		DIAT.		97904			97904	36	x																
Actinoptychus	senarius		DIAT.	4	19856			19856	7	x																
Actlnoptychus	splendens		DIAT.	4	160761									160761	34	x	85.0		28.3							
Alexandrium	sp		DINO.		2810			2810	38	x																
Amphidinium	acutissimum		DINO.	3	1620			1620	38	x																
Amphidinium	sp		DINO.	3	30200																					
Amphiprora	sp		DIAT.	11	24300			24300	7	x																
Amphora	sp		DIAT.		359			359	7	x																
Anopiosolenia	brasiliensis		COCC.	13	861									861	50	x	85.0	4.5	4.5							
Asterionellopsis	sp		DIAT.		2498			2498	8	x																
Asterionellopsis	glacialis		DIAT.	22	1037			1037	7	x																
Asteromphalus	sp		DIAT.	4	11000			11000	7	x																
Asteromphalus	arachne		DIAT.	4	45497									45497	42	x	48.8		24.4							

‡‡ Taxonomic group abbreviations: Radiolarian (RADI.), Diatom (DIAT.), Dinoflagelate (DINO.), Coccolithophore (COCC.), Foraminifera (FORA.), Phytoflagelate (PHYT.)

§§ Refers to geometric model codes for the calculation of biovolume as described by Sun and Liu (2003)

*** Codes to references: 1(Ayon and Arones, 1997), 3(SERC, 2006), 7(SERC, 2006), 8(Kuylenstierna and Karlson, 2006), 9(IOW, 2006), 10(Quigg, 2006), 12(Rines, 2006), 13(Škaloud, 2006), 15(Kuylenstierna and Karlson, 2006), 16(Westerhoff, 2006), 17(Menden-Deuer et al., 2001), 18(Nielsen, 2006), 20(Fukuyo, 2006), 22(ARCH, 2006), 26(Cupp, 1943), 27(JST, 2006), 29(Massuti and Margalef, 1930), 30(MIRACLE, 2006), 34(Cupp, 1943), 35(Cloern and Dufford, 2004), 36(Strickland et al., 1969), 38(NODC, 2006), 40(Balech, 1988), 41(Licea et al., 1995), 44(Drebes, 1974), 46(Kuylenstierna and Karlson, 2006), 47(HELCOM, 2006), 48(JST, 2006), 49(Bertoglio, 2006), 50(Heimdal, 1993), 51(Throndsen, 1997)

††† Phytoplankton volume was calculated using dimensions from the literature and applied to the biovolume model of Sun and Liu (2003). When ranges were given, an average was applied to the dimension.

Genus	species	sub-species (var.)	Group‡‡	Shape Code§§	Volume used (µm³)	Own estimate (µm³)	used	Direct value from lit. #1 (µm³)	Lit. ID***	used	Direct value from lit. #2 (µm³)	Lit. ID‡‡‡	used	Calculated from lit. #3(µm³)†††	Lit. ID‡‡‡	used	Sun & Liu dimension (a) (µm)	Sun & Liu dimension (b) (µm)	Sun & Liu dimension (c) (µm)	Sun & Liu dimension (a1) (µm)	Sun & Liu dimension (a2) (µm)	Sun & Liu dimension (a3) (µm)	Sun & Liu dimension (a4) (µm)	Sun & Liu dimension (b1) (µm)	Sun & Liu dimension (b2) (µm)	Sun & Liu dimension (b3) (µm)
Asteromphalus	brookei		DIAT.	4	60134									60134	42	x	53.5		26.8							
Asteromphalus	heptactis		DIAT.	4	49087									49087	34	x	50.0		25.0							
Bacteriastrum	sp		DIAT.		295			295	12	x																
Bacteriastrum	hyalinum		DIAT.	28	3770									3770	34	x	12.0	20.0								
Biddulphia	alternans				91000			91000	7	x																
Bolivina	sp		FORA.		3908644			3908644	25	x																
Calciosolenla	murrayi		COCC.	2	663									663	50	x	62.5	4.5								
Carteria	marina		PHYT.	1	1023									1023	51	x	12.5									
Cerataulina	sp		DIAT.	28	41205			41205	7	x																
Cerataulina	pelagica		DIAT.	28	41205			41205	7	x																
Ceratium	sp		DINO.	25	3368			3368	7	x																
Ceratium	azoricum		DINO.	25	46797									46797	40	x				44.0	60.0	40.0	32.0	38.5	8.0	12.0
Ceratium	buceros		DINO.	25	144000			144000	38	x																
Ceratium	dens		DINO.	25	24838									24838	37	x										
Ceratium	furca		DINO.	25	3368			3368	7	x				3368	7	x										
Ceratium	fusus	v. fusus	DINO.	25	62500			62500	38	x																
Ceratium	fusus	v. seta	DINO.	25	62500			62500	38	x																
Ceratium	horridum		DINO.	25	222064									222064	40	x				63.7	127.3	122.5	126.0	49.0	17.5	17.5
Ceratium	kofoidii		DINO.	25	15765									15765	40	x				56.7	60.3	21.3	28.4	23.8	3.5	3.5
Ceratium	macroceros		DINO.	25	120000			120000	38	x																
Ceratium	massiliense		DINO.	25	689516									689516	40	x				147.7	334.8	184.8	192.7	66.0	18.5	18.5
Ceratium	pulchellum		DINO.	25	200533									200533	40	x				80.8	184.2	14.4	37.4	46.0	14.4	14.4
Ceratium	trichoceros		DINO.	25	99184									99184	40	x				54.1	310.9	405.6	410.1	40.5	9.0	13.5
Ceratium	tripos		DINO.	25	481932	481932	x							428177	37											
Ceratium	tripos	pulchellum	DINO.	25	200533									200533	40	x				80.8	184.2	14.4	37.4	46.0	14.4	14.4
Chaetoceros	sp		DIAT.		5616			5616		x																
Chaetoceros	affinis		DIAT.	29	1163	1163	x	2000	36					2799	37											
Chaetoceros	atlanticus		DIAT.	29	7930			7930	38	x							30.0	18.0	9.0							
Chaetoceros	breve		DIAT.		830									830	34	x	12.5	13.0	6.5							
Chaetoceros	compressus		DIAT.	29	5616									5616	37	x										
Chaetoceros	comvolutus		DIAT.	29	1794									1794	34	x	19.0	19.0	6.3							
Chaetoceros	constrictus		DIAT.	29	2380			2380	38	x							12.0	27.0	13.0							

Genus	species	sub-species (var.)	Group‡‡	Shape Code§§	Volume used (µm³)	Own estimate (µm³)	used	Direct value from lit. #1 (µm³)	Lit. ID***	used	Direct value from lit. #2 (µm³)	Lit. ID‡‡‡	used	Calculated from lit. #3(µm³)†††	Lit. ID‡‡‡	used	Sun & Liu dimension (a) (µm)	Sun & Liu dimension (b) (µm)	Sun & Liu dimension (c) (µm)	Sun & Liu dimension (a1) (µm)	Sun & Liu dimension (a2) (µm)	Sun & Liu dimension (a3) (µm)	Sun & Liu dimension (a4) (µm)	Sun & Liu dimension (b1) (µm)	Sun & Liu dimension (b2) (µm)	Sun & Liu dimension (b3) (µm)
Chaetoceros	costatus		DIAT.	29	1527									1527	34	x	12.0	18.0	9.0							
Chaetoceros	curvisetus		DIAT.	29	1601	1601	x																			
Chaetoceros	dadayi		DIAT.	29	900																					
Chaetoceros	danicus		DIAT.	29	1250			1250	38	x							20.0	10.0	5.0							
Chaetoceros	debilis		DIAT.	29	16000			16000	36	x																
Chaetoceros	decipiens		DIAT.		8838									8838	34	x	46.5	22.0	11.0							
Chaetoceros	diadema		DIAT.	29	3820			3820	38	x																
Chaetoceros	didymus		DIAT.	29	2714									2714	37	x	12.0	24.0	12.0							
Chaetoceros	eibenii		DIAT.	29	9945									9945	34	x	27.8	37.0	12.3							
Chaetoceros	lasciniosus		DIAT.		1074									1074	34	x	19.0	12.0	6.0							
Chaetoceros	lauderi		DIAT.	29	5195									5195	34	x	30.0	21.0	10.5							
Chaetoceros	lorenzianus		DIAT.	29	15863	15863	x	15000	36																	
Chaetoceros	peruvianus		DIAT.	29	14844	14844	x																			
Chaetoceros	radicans		DIAT.	29	700			700	38	x																
Chaetoceros	socialis		DIAT.	29	269	269	x	300	36		864	7														
Climacosphenia	sp		DIAT.		102206			102206	7	x																
Cocconeis	sp		COCC.		2356			2356	15	x																
Cocolito	sp		COCC.		140			140	36	x																
Codonella	sp		TINT.		256563			256563	29	x																
Corethron	sp		DIAT.		275806			275806	13	x																
Corethron	hystrix		DIAT.	5	36700			36700	38	x																
Coscinodiscus	sp		DIAT.		201629			201629	7	x																
Coscinodiscus	centralis		DIAT.	4	7971614	7971614	x							2042035	37		200.0		65.0							
Coscinodiscus	concinnus		DIAT.	4	11064297									11064297	37	x	350.0		115.0							
Coscinodiscus	curvatulus		DIAT.	4	49721									49721	34	x	57.5		19.1							
Coscinodiscus	excentricus		DIAT.	4	71825									71825	34	x	65.0		21.6							
Coscinodiscus	grani		DIAT.	4	756796									756796	34	x	142.5		47.5							
Coscinodiscus	marginatus		DIAT.	4	76913									76913	34	x	66.5		22.1							
Coscinodiscus	perforatus		DIAT.	4	370995	370995	x							259181	37		100.0		33.0							
Coscinodiscus	radiatus		DIAT.	4	254887			254887	7	x																
Coscinodiscus	wailessii		DIAT.	4	1525287									1525287	34	x	180.0		59.9							
Cyclotella	sp		DIAT.		2000			2000	38	x																

Genus	species	sub-species (var.)	Group‡‡	Shape Code§§	Volume used (µm³)	Own estimate (µm³)	used	Direct value from lit. #1 (µm³)	Lit. ID***	used	Direct value from lit. #2 (µm³)	Lit. ID‡‡‡	used	Calculated from lit. #3(µm³)†††	Lit. ID‡‡‡	used	Sun & Liu dimension (a) (µm)	Sun & Liu dimension (b) (µm)	Sun & Liu dimension (c) (µm)	Sun & Liu dimension (a1) (µm)	Sun & Liu dimension (a2) (µm)	Sun & Liu dimension (a3) (µm)	Sun & Liu dimension (a4) (µm)	Sun & Liu dimension (b1) (µm)	Sun & Liu dimension (b2) (µm)	Sun & Liu dimension (b3) (µm)
Cylindrotheca	closterium		DIAT.	2	2618									2618	37	x	200.0	5.0								
Cymbella	sp			17	1351									1351	48	x	52.0	10.0	7.0							
Dactyliosolen	fragilissimus			28	7563									7563	42	x	98.8	9.9								
Detonula	sp		DIAT.		7395			7395	4	x																
Detonula	confervacea		DIAT.	28	1710			1710	38	x																
Detonula	pumila		DIAT.	28	28274									28274	42	x	22.5	40.0								
Dictyocha	fibula		TINT.	1	4779	4779	x	3609	36																	
Dictyocha	speculum		TINT.	1	9744									9744	37	x	26.5									
Dictyocysta	sp		TINT.		256563			256563	29	x																
Dinophysis	sp		DINO.		3200			3200	7	x																
Dinophysis	acuminata		DINO.	3	3200			3200	7	x																
Dinophysis	caudata		DINO.	3	23965	23965	x	3217	7																	
Dinophysis	mitra		DINO.	3	50210									50210		x	56.5	46.5	36.5							
Dinophysis	ovum		DINO.	3	13832									13832		x	37.0	34.0	21.0							
Dinophysis	rotundata		DINO.	3	30811									30811		x	46.0	43.0	29.8							
Dinophysis	rotundatum		DINO.	3	30811									30811		x	46.0	43.0	29.8							
Dinophysis	tripos		DINO.	3	94245									94245		x	99.5	54.0	33.5							
Diploneis	sp		DIAT.		884			884		x																
Diplopelta	steinii			3	154844									154844		x	59.5	70.5	70.5							
Diplopeltopsis	minor				30500			30500		x																
Diplopsalis	sp		DINO.		21206			21206		x																
Diplopsalis	lenticula		DINO.		30500			30500		x																
Dissodium	sp		DINO.		19635			19635	8	x																
Dissodium	asymmetricum		DINO.	3	216327									216327	41	x	75.5	90.6	60.4							
Ditylum	sp		DIAT.		168491			168491	7	x																
Ditylum	brightwellii		DIAT.	30	168491			168491	7	x																
Dyctiocha	sp		SILI.		3609			3609	7	x																
Ebria	sp		SILI.		2160			2160	8	x																
Emiliania	huxleyi		COCC.	4	140			140	36	x																
Entomoneis	alata	v. alata		11	21350			21350	7	x																
Epithemia	sp		DIAT.		6833			6833	27	x																
Eucampia	sp		DIAT.		11100			11100	7	x																

Genus	species	sub-species (var.)	Group‡‡	Shape Code§§	Volume used (μm^3)	Own estimate (μm^3)	used	Direct value from lit. #1 (μm^3)	Lit. ID***	used	Direct value from lit. #2 (μm^3)	Lit. ID***	used	Calculated from lit. #3(μm^3)†††	Lit. ID***	used	Sun & Liu dimension (a) (µm)	Sun & Liu dimension (b) (µm)	Sun & Liu dimension (c) (µm)	Sun & Liu dimension (a1) (µm)	Sun & Liu dimension (a2) (µm)	Sun & Liu dimension (a3) (µm)	Sun & Liu dimension (a4) (µm)	Sun & Liu dimension (b1) (µm)	Sun & Liu dimension (b2) (µm)	Sun & Liu dimension (b3) (µm)
Eucampia	cornuta		DIAT.	29	4850									4850	34	x	32.5	19.0	10.0							
Eucampia	zoodiacus		DIAT.	29	8429	8429	x	11100	36																	
Eutintinnus	sp		TINT.		256563			256563	29	x																
Eutreptiella	gymnastica			6	538			538	38	x																
Exuviaella	marina				4850																					
Favella	sp		TINT.		256563			256563	29	x																
Fragilariopsis	sp		DIAT.		1750			1750	18	x																
Fragilariopsis	doliolus		DIAT.	29	1167									1167	39	x	50.7	7.7	3.8							
Fragiliaria	crotonensis			29	166									166	40	x	62.5	2.3	1.5							
Gephyrocapsa	oceanica		COCC.	1	524									524	50	x	10.0									
Glenodinium	sp			3	4647									4647	7	x	24.0	21.5	17.2							
Gonyaulax	sp		DINO.		22619			22619	7	x				21370	40											
Gonyaulax	polygramma		DINO.	8	37500			37500	38	x																
Gonyaulax	spinifera		DINO.	8	16965									16965	37	x	50.0	36.0								
Grammatophora	sp		DIAT.	11	1000			1000	15	x																
Grammatophora	angulosa		DIAT.	11	342									342	37	x	29.0	5.0	3.0							
Grammatophora	marina		DIAT.	11	1210									1210	37	x	55.0	7.0	4.0							
Grammathophora	oceanica		DIAT.	11	6725									6725	49	x										
Guinardia	sp		DIAT.		64403			64403	9	x																
Guinardia	delicatula		DIAT.	28	1172	1172	x																			
Guinardia	flaccida		DIAT.		282743									282743	44	x	100.0	60.0								
Guinardia	striata		DIAT.	28	42000			42000	37	x																
Gymnodinium	sp		DINO.		3181			3181	7	x																
Gymnodinium	lohmanni		DINO.	3	809			809	38	x																
Gymnodinium	sanguineum		DINO.	3	22468	22468	x	79201	7	x																
Gymnodinium	sp		DINO.	3	135000			135000	36	x							111.0	40.0	25.0							
Gymnodinium	splendens		DINO.		79201			79201	7	x																
Gyrodinium	sp				66881			66881	38	x																
Gyrosigma	sp		DIAT.		5184			5184	16	x																
Gyrosigma	balticum		DIAT.		10400									10400	9	x	130.0	20.0	8.0							
Halopappus	vahseli			2	436									436	50	x	17.0	7.0								
Helicosphaera	carteri			2	4725									4725	50	x	25.0	19.0								

Genus	species	sub-species (var.)	Group[‡‡]	Shape Code[§§]	Volume used (μm^3)	Own estimate (μm^3)	used	Direct value from lit. #1 (μm^3)	Lit. ID[***]	used	Direct value from lit. #2 (μm^3)	Lit. ID[*]	used	Calculated from lit. #3(μm^3)[†††]	Lit. ID[*]	used	Sun & Liu dimension (a) (µm)	Sun & Liu dimension (b) (µm)	Sun & Liu dimension (c) (µm)	Sun & Liu dimension (a1) (µm)	Sun & Liu dimension (a2) (µm)	Sun & Liu dimension (a3) (µm)	Sun & Liu dimension (a4) (µm)	Sun & Liu dimension (b1) (µm)	Sun & Liu dimension (b2) (µm)	Sun & Liu dimension (b3) (µm)
Helicostomella	sp		TINT.		256563			256563	29	x																
Helicotheca	tamesis			10	73656									73656	45	x	88.0	93.0	9.0							
Hemiaulus	sp		DIAT.		21279			21279	7	x																
Hemiaulus	sinensis		DIAT.	29	2403									2403	34	x	25.5	12.0	10.0							
Lauderia	sp		DIAT.		50265			50265	7	x																
Lauderia	annulata			4	9880			9880	38	x																
Leptocylindrus	sp		DIAT.		3464			3464	7	x																
Leptocylindrus	danicus				739	739	x																			
Leptocylindrus	mediterraneus		DIAT.	28	2545									2545	34	x	40.0	9.0								
Leptocylindrus	minimus				95			95	38	x	156	7														
Leucocryptos	marina			9	449			449	38	x																
Licmophora	sp		DIAT.		7290			7290	7	x																
Licmophora	abbreviata		DIAT.	21	22500			22500	38	x				26315	34		100.0	60.0	40.0							
Lioloma	sp		DIAT.	10	25000			25000	24	x																
Lioloma	delicatulum		DIAT.	10	14440									14440	34	x	1520.0	2.0	4.8							
Lioloma	mediterranea		DIAT.	10	6032									6032	34	x	754.0	2.0	4.0							
Lithodesmium	sp		DIAT.		16917			16917	17	x																
Lithodesmium	undulatum		DIAT.	30	57440									57440	34	x	51.0	51.0								
Melosira	sp		DIAT.		20309			20309	7	x																
Melosira	moniliformis		DIAT.		12831			12831	7	x																
Melosira	sulcata		DIAT.	28	136			136	7	x																
Monadas	sp				900			900	36	x																
Navicula	sp		DIAT.		5060			5060	7	x																
Navicula	membranacea				1140																					
Nitzschia	longissima		DIAT.	13	5875			5875	7	x																
Octactis	sp		SILI.		12174			12174	23	x																
Odontella	sp		DIAT.		822333			822333	7	x																
Olisthodiscus	luteos		PHYT.	3	6283									6283	51	x	40.0	30.0	10.0							
Ophiaster	hydroideus		COCC.	2	48									48	50	x	4.5	4.5								
Oxyphysis	sp		DINO.		11879			11879	20	x																
Oxyphysis	oxytoxoides		DINO.	8	528									528	40	x	56.0	6.0								
Oxytoxum	longiceps		DINO.	2	4562									4562	41	x	64.0	16.5								

Genus	species	sub-species (var.)	Group‡‡	Shape Code§§	Volume used (μm^3)	Own estimate (μm^3)	used	Direct value from lit. #1 (μm^3)	Lit. ID***	used	Direct value from lit. #2 (μm^3)	Lit. ID‡	used	Calculated from lit. #3(μm^3)†††	Lit. ID‡	used	Sun & Liu dimension (a) (µm)	Sun & Liu dimension (b) (µm)	Sun & Liu dimension (c) (µm)	Sun & Liu dimension (a1) (µm)	Sun & Liu dimension (a2) (µm)	Sun & Liu dimension (a3) (µm)	Sun & Liu dimension (a4) (µm)	Sun & Liu dimension (b1) (µm)	Sun & Liu dimension (b2) (µm)	Sun & Liu dimension (b3) (µm)
Planktoniella	sp		DIAT.		353429			353429	26	x																
Planktoniella	sol		DIAT.	4	11545									11545	37	x	35.0		12.0							
Pleurosigma	sp		DIAT.		43081			43081	7	x																
Podolampas	sp		DINO.		226195			226195	20	x																
Podolampas	palmipes		DINO.	7	19375									19375	40	x	88.0	29.0								
Polykrikos	sp				74113																					
Proboscia	alata	f. gracillima		28	120000			120000	7	x																
Pronoctiluca	pelagica			1	4310			4310	38	x																
Prorocentrum	gracile		DINO.	3	1497	1497	x							7760	37		57.0	20.0	13.0							
Prorocentrum	micans		DINO.	3	18889	18889	x	5678	7																	
Protoperidinium	sp		DINO.	8	306613			306613	7	x																
Protoperidinium	brevipes		DINO.	8	9650			9650	38	x																
Protoperidinium	brochii		DINO.	8	82318									82318	41	x	68.0	68.0								
Protoperidinium	claudicans		DINO.	8	70686									70686	37	x	75.0	60.0								
Protoperidinium	conicoides		DINO.	8	62500			62500	38	x																
Protoperidinium	conicum		DINO.	8	125173									125173	37	x	85.0	75.0								
Protoperidinium	crassipes		DINO.	8	101788									101788	37	x	75.0	72.0								
Protoperidinium	depressum		DINO.	8	869000			869000	7	x																
Protoperidinium	diabolus		DINO.	8	110964									110964	41	x	86.5	70.0								
Protoperidinium	divergens		DINO.	8	215305									215305	41	x	112.5	85.5								
Protoperidinium	excentricum		DINO.	8	32044									32044	37	x	34.0	60.0								
Protoperidinium	granii		DINO.	8	18000			18000	38	x																
Protoperidinium	leonis		DINO.	8	259000			259000	7	x																
Protoperidinium	longipes		DINO.	8	72859									72859	40	x	92.0	55.0								
Protoperidinium	longispinum		DINO.	8	82896			82896	47	x																
Protoperidinium	minutum		DINO.	8	13888									13888	41	x	34.0	39.5								
Protoperidinium	oblongum		DINO.	8	120162									120162	41	x	117.5	62.5								
Protoperidinium	obtusum		DINO.	8	129015									129015	40	x	77.0	80.0								
Protoperidinium	oceanicum		DINO.	8	155476	155476	x	18000	37					445059	38		170.0	100.0								
Protoperidinium	pedunculatum		DINO.	8	44259									44259	41	x	35.0	69.5								
Protoperidinium	pellucidum		DINO.	8	78000			78000	7	x																
Protoperidinium	pentagonum		DINO.	8	569195			569195	7	x																

Genus	species	sub-species (var.)	Group[‡‡]	Shape Code[§§]	Volume used (μm^3)	Own estimate (μm^3)	used	Direct value from lit. #1 (μm^3)	Lit. ID[***]	used	Direct value from lit. #2 (μm^3)	Lit. ID[*]	used	Calculated from lit. #3(μm^3)[†††]	Lit. ID[*]	used	Sun & Liu dimension (a) (µm)	Sun & Liu dimension (b) (µm)	Sun & Liu dimension (c) (µm)	Sun & Liu dimension (a1) (µm)	Sun & Liu dimension (a2) (µm)	Sun & Liu dimension (a3) (µm)	Sun & Liu dimension (a4) (µm)	Sun & Liu dimension (b1) (µm)	Sun & Liu dimension (b2) (µm)	Sun & Liu dimension (b3) (µm)
Protoperidinium	punctulatum		DINO.	8	39340									39340	41	x	52.5	53.5								
Protoperidinium	quarnerense		DINO.	9	53721									53721	40	x	57.0	60.0								
Protoperidinium	steinii		DINO.	8	23765			23765	7	x				23765	37		54.0	41.0								
Protoperidinium	subinerme		DINO.	8	131000			131000	38	x																
Protoperidinium	tenuissimum		DINO.	8	2363									2363	41	x	25.0	19.0								
Protoperidinium	tristylum		DINO.	8	77500									77500	41	x	69.0	65.5								
Pseudonitzschia	sp		DIAT.		450			450	7	x																
Pseudo-nitzschia	delicatissima		DIAT.	13	82									82	34	x	58.5	2.1	1.4							
Pseudo-nitzschia	pacifica		DIAT.	13	1038									1038	34	x	86.5	6.0	4.0							
Pseudo-nitzschia	pungens		DIAT.	13	489									489	34	x	116.5	3.6	2.4							
Pyrocystis	sp		DINO.		19635			19635	22	x																
Pyrocystis	lunula		DINO.	3	356047									356047	37	x	170.0	80.0	50.0							
Pyrophacus	sp		DINO.		34600			34600	7	x																
Pyrophacus	horologicum		DINO.	3	74616									74616	40	x	25.0	75.5	75.5							
Rhizosoienia	robusta		DIAT.		1872389	1872389	x																			
Rhizosolenia	sp		DIAT.		42000			42000	7	x																
Rhizosolenia	bergonii		DIAT.	28	616566									616566	34	x	371.0	46.0								
Rhizosolenia	calcar	avis	DIAT.	28	478445									478445	34	x	700.0	29.5								
Rhizosolenia	chunii		DIAT.	28	457707	457707	x																			
Rhizosolenia	imbricata		DIAT.	28	70686									70686	34	x	400.0	15.0								
Rhizosolenia	pungens		DIAT.	28	19007									19007	7	x	200.0	11.0								
Rhizosolenia	robusta		DIAT.	28	3885340	3885340	x																			
Rhizosolenia	setigera		DIAT.	28	16286									16286	34	x	144.0	12.0								
Rhizosolenia	stylitormis		DIAT.	28	199327	199327	x																			
Schroderella	sp		DIAT.		3142			3142	26	x																
Scrippsielia	trochoidea		DINO.	3	8350									8350	40	x	34.5	21.5	21.5							
Scripsiella	sp		DINO.		11069			3910	38		11069	7	x													
Skeletonema	sp		DIAT.		177			177	7	x																
Skeletonema	costatum		DIAT.	5	239	239	x	400	36		177	7														
Stephanopyxis	sp		DIAT.		540000			540000	7	x																
Stephanopyxis	turris		DIAT.	5	47713									47713	37	x	45.0	45.0								
Tetraselmis	sp		PHYT.	2	300			300	10	x				251	51	x	11.0	6.6								

Genus	species	sub-species (var.)	Group[‡‡]	Shape Code[§§]	Volume used (μm^3)	Own estimate (μm^3)	used	Direct value from lit. #1 (μm^3)	Lit. ID[***]	used	Direct value from lit. #2 (μm^3)	Lit. ID[*]	used	Calculated from lit. #3(μm^3)[†††]	Lit. ID[*]	used	Sun & Liu dimension (a) (µm)	Sun & Liu dimension (b) (µm)	Sun & Liu dimension (c) (µm)	Sun & Liu dimension (a1) (µm)	Sun & Liu dimension (a2) (µm)	Sun & Liu dimension (a3) (µm)	Sun & Liu dimension (a4) (µm)	Sun & Liu dimension (b1) (µm)	Sun & Liu dimension (b2) (µm)	Sun & Liu dimension (b3) (µm)
Thalassionema	sp		DIAT.		495			495	7	x																
Thalassionema	frauenfeldii		DIAT.	10	945									945	34	x	105.0	3.0	3.0							
Thalassionema	nitzschioides		DIAT.	10	3080	3080	x																			
Thalassiosira	sp		DIAT.		39270			39270	7	x																
Thalassiosira	angulata		DIAT.		3370			3370	38	x																
Thalassiosira	anguste-lineata		DIAT.	4	23856			20900	38					23856	37	x	45.0		15.0							
Thalassiosira	gravida		DIAT.		29100			29100	38	x																
Thalassiosira	minima		DIAT.	4	471									471	46	x	10.0		6.0							
Thalassiosira	nordenskioldii		DIAT.		3310			3310		x																
Thalassiosira	rotula		DIAT.		20475	20475	x																			
Thalassiosira	subtilis		DIAT.	4	25032	25032	x							3927	37		25.0		8.0							
Thalassiothrix	longissima		DIAT.	10	56250									56250	37	x	2250.0	5.0	5.0							
Tintinnopsis	sp		TINT.		256563			256563	29	x																
Xystonella	sp		TINT.		256563			256563	29	x																

Appendix 2. Calculated mean cell biovolumes for 26 species of phytoplankton collected in Ancon Bay, Peru. Biovolumes were calculated for individually measured cells (> 25 when possible) assuming a geometric form as described by Sun and Liu (2003). Mean biovolumes (vertical dashed line of histogram, upper graphs) were recorded in the database of Appendix 1. Cumulative standard error (as % of mean volume, lower graphs) was used to gauge the confidence level of the mean value. Ideally, sampling should be conducted until the standard error is low for a large proportion of additional samples (reference of 10% indicated by the horizontal line.

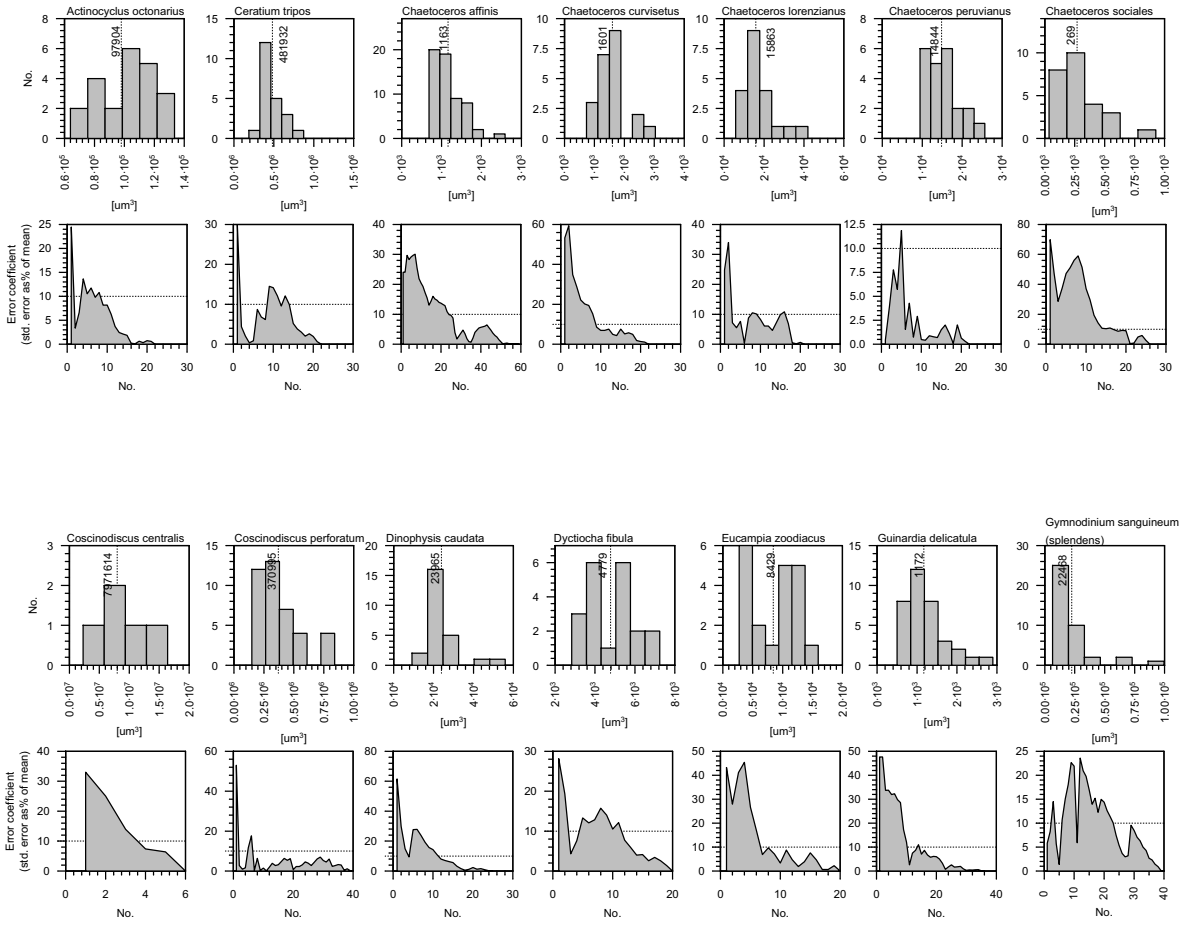

Appendix 2 (cont.).